Density Functional Theory Studies on (*S*)-Proline and *N*-Heterocyclic Carbene (NHC) Mediated Organocatalytic Reactions

Thesis submitted to the

University of Kerala

for the award of Degree of

Doctor of Philosophy

in Chemistry under the Faculty of Science

By

Ajitha M. J.

Computational Modeling and Simulation Section

Process Engineering and Environmental Technology Division

National Institute for Interdisciplinary Science and Technology (CSIR)

Thiruvananthapuram – 695 019

Kerala, India

2012

DEDICATED TO...

MY BELOVED PARENTS, BROTHERS,

TEACHERS AND FRIENDS

DECLARATION

I hereby declare that the Ph.D. thesis entitled "**Density Functional Theory Studies on (*S*)-Proline and *N*-Heterocyclic Carbene (NHC) Mediated Organocatalytic Reactions**" is an independent work carried out by me at the Computational Modeling and Simulation Section, Process Engineering and Environmental Technology Division, National Institute for Interdisciplinary Science and Technology (NIIST-CSIR), Trivandrum, under the supervision of Dr. C. H. Suresh and it has not been submitted elsewhere for any other degree, diploma or title.

Ajitha M. J.

National Institute for Interdisciplinary Science & Technology
(Formerly Regional Research Laboratory)
(Council of Scientific & Industrial Research) India

Industrial Estate P.O., Pappanamcode, Trivandrum – 695 019

Dr. Cherumuttathu H. Suresh
Senior Scientist

E-Mail: sureshch@gmail.com
Phone: 0471 – 2515264, 9446552294

August 30, 2012

CERTIFICATE

This is to certify that the work embodied in the thesis entitled "**Density Functional Theory Studies on (*S*)-Proline and *N*-Heterocyclic Carbene (NHC) Mediated Organocatalytic Reactions**" has been carried out by Ms. Ajitha M. J. under my supervision and guidance at the Computational Modeling and Simulation Section, Process Engineering and Environmental Technology Division, National Institute for Interdisciplinary Science and Technology (NIIST-CSIR), Trivandrum and this work has not been submitted elsewhere for a degree.

Dr. C. H. Suresh

(Thesis Supervisor)

ACKNOWLEDGEMENT

"How numerous, Oh Lord, my God, you have made your wondrous deeds!

And in your plans for us there is none to equal you.

Should I wish to declare or tell them, too many are they to recount."

<div align="right">

[Psalm 40:5]

</div>

I am truly grateful to everyone who has directly or indirectly inspired and encouraged me for the successful realization of this thesis.

I have immense pleasure in placing on record my deep sense of gratitude to Dr. C. H. Suresh, my thesis supervisor for suggesting the research problem and also for his encouragement, inspiring advice and timely guidance throughout the course of this work.

I owe my sincere thanks to Dr. Suresh Das, Director, NIIST-CSIR and former directors, Prof. T. K. Chandrashekar and Dr. B. C. Pai for having given me an opportunity to carry out my doctoral work in this institution.

I take huge pleasure to offer my special thanks to Dr. Roschen Sasikumar, Dr. Elizabeth Jacob and Dr. S. Savithri for their valuable encouragement.

I also extend my special thanks to Dr. K. P. Vijayalakshmi for her constant encouragement and support that have been valuable throughout the research.

I would like to thank the whole scientific as well as non scientific staffs of NIIST for supporting my thesis directly or indirectly.

I thank all the members of the Computational Modeling and Simulation section and in particular, Dr. Panneerselvam R., Dr. Jijoy Joseph, Mr. Alex Andrews, Dr. Manju M. S., Dr. Jomon Mathew, Mr. Manoj M., Ms. Neetha Mohan, Mr. Sajith P.K., Ms. Ali Fathima Sabirneeza A., Mr. Fareed Basha, Ms. Shaija P. B., Ms. Rejitha John, Ms.

Sandhya K. S., Ms. Remya K., Ms. Lincy T. L. and Ms. Rakhi R. for their help and cooperation. I also thank members of other Divisions of NIIST.

I would like to appreciate the love, affection and care extended by my friends, Julie, Flowerin, Parvathy, Roshni, Anoop, Deepthy, Faseela, Swapna, Reshmi, Sangeetha, Remani, Anju, Gowri, Neenu, Saumya, Sreena, Rijo, Divya, Antu, Gigi and Rohini.

I am obliged to all my teachers for their help and encouragement at different stages of my life.

My Family and friends have been a constant source of support and encouragement. Words are insufficient to express my heartfelt thanks for their constant love, care and support.

Ajitha M. J.

Contents

List of Tables

List of Figures

List of Schemes

List of Abbreviations

DFT   : Density Functional Theory

MM   : Molecular Mechanics

MD   : Molecular Dynamics

MC   : Monte Carlo

QM/MM   : Hybrid Quantum Mechanics/Molecular Mechanics

QM   : Quantum Mechanics

ONIOM   : Our N-layered Integrated Molecular Orbital + Molecular Mechanics

HF   : Hartree-Fock

HK   : Hohenberg-Kohn

SCF   : Self-Consistent-Field

LCAO   : Linear Combination of Atomic Orbital

CI   : Configuration Interaction

CC   : Coupled Cluster

CIS   : Configuration Interaction Single-excitation

LDA   : Local-Density Approximation

CCSD   : Coupled Cluster Single and Double

GGA   : Generalized Gradient Approximation

AO   : Atomic Orbital

DZ   : Double Zeta

XC   : Exchange Correlation

STO   : Slater-Type Orbital

GTO   : Gaussian-Type Orbital

MESP   : Molecular Electrostatic Potential

PES   : Potential Energy Surface

SCRF   : Self-Consistent Reaction Field

PCM   : Polarizable Continuum Model

UAHF   : United Atom Topological Model for Hartree-Fock

EDA   : Energy Decomposition Analysis

TS   : Transition State

IRC   : Intrinsic Reaction Coordinates

ee   : Enantiomeric Excess

MP   : Moller-Plesset Perturbation Theory

NHC   : *N*-Heterocyclic Carbene

DBU   : 1,8-DiazaBicyclo[5.4.0]Undec-7-ene

TBD   : 1,5,7-TriazaBicyclo[4.4.0]Dec-5-ene

TDI   : Turnover Frequency Determining Intermediate

TDTS   : Turnover Frequency Determining Transition State

ZPE   : Zero Point Energy

TEP   : Tolman Electronic Parameter

PAH   : Polycyclic Aromatic Hydrocarbon

NICS   : Nucleus Independent Chemical Shift

HOMA   : Harmonic Oscillator Model of Aromaticity

Preface

Asymmetric organocatalysis has been an intense area of research where the main aim is to introduce one or more chiral domains in molecular systems through catalytic activity of small organic molecules. The history and development of organocatalysis and its classification, a brief account of various mechanistic aspects of such reactions, especially (*S*)-proline and *N*-heterocyclic carbene (NHC) mediated reactions, are summarized in the first part of Chapter 1. Nowadays quantum chemistry has become one of the most important tools to study structural parameters, energetic details, orbital interactions and effect of external perturbations to understand the reactivity of organic molecules. The second part of Chapter 1 describes various computational methods and their theoretical basis. As this approach includes detailed analysis of structural and energetic features of all the transition states and intermediates associated with each elementary step in the catalytic cycles of the reactions, the research could have larger implications towards understanding and developing improved catalysts.

The first part of Chapter 2 deals with the detailed mechanistic investigation of sixteen possible diastereomeric pathways for the C-C bond formation step in the (*S*)-proline catalyzed Mannich reaction to understand how stereoelectronic features invoke enantioselectivity of the final product. In addition, the elucidation of complete reaction mechanisms of (*S*)-proline catalyzed aldol reaction of acetone with acetaldehyde in DMSO solvent has also been described in the second part of Chapter 2. It is observed that a higher energy conformer of the catalyst is the active form to carry out the reaction rather than its most stable conformer.

The first part of Chapter 3 deals with the mechanistic studies on the NHC catalyzed Stetter reaction between benzaldehyde with cyclopropene and Michael acceptor (*N*-

acylamido acrylate) and the role of water or bases such as 1,8-diazabicyclo[5.4.0]undec-7-ene (DBU) and 1,5,7-triazabicyclo[4.4.0]dec-5-ene (TBD) in the reaction mechanism. It is observed that the presence of water or base significantly lower the activation barrier for the formation of Breslow intermediate. The second part of Chapter 3 deals with the elucidation of actual pathway for the NHC mediated CO_2 transformation reaction of epoxide to cyclic carbonate.

The first part of Chapter 4 introduces NHC-CO_2 adduct as a simple and efficient organic model to assess the steric and electronic effects in NHC. We have used molecular electrostatic potential minimum, observed at the carbene lone pair region of NHC (V_{min1}) as well as at the carboxylate region of the NHC-CO_2 adduct (V_{min2}) to characterise the electronic and steric properties of the N- and C-substituents. Furthermore, several multi-topic NHC ligands with up to four carbene centers are designed on the basis of Clar's aromatic sextet theory and are discussed in second part of Chapter 4. Annelation of NHC to a benzenoid moiety as well as branching through C_{sp3} linkage is highly recommended for the synthesis of stable multi-topic architectures.

Introduction

Part A - Organocatalysis
&
Part B - Computational Chemistry
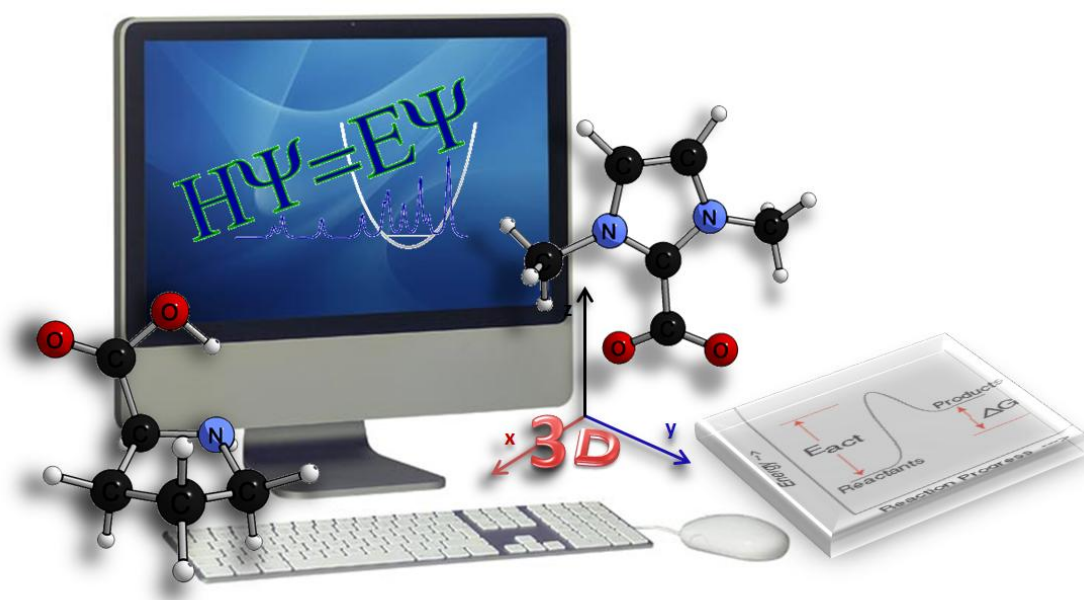
"Computational chemistry simulates chemical structures and reactions numerically, based in full or in part on the fundamental laws of physics"

[Foresman and Frisch 1996]

Part A - Organocatalysis

The term "organocatalysis" describes the acceleration of chemical reactions through the use of small organic molecules as catalysts [Ahrendt *et al.* 2000; MacMillan 2008]. The concept of organocatalysis is a relatively new and popular field within the domain of chiral molecule (or enantioselective) synthesis and is emerged as a discrete strategy only in the past decade [Jacobsen and MacMillan 2010]. The rapid progress in the field of asymmetric organocatalysis is due to the result of both the novelty of the concept and, more significantly, the fact that the productivity and selectivity of many organocatalytic reactions meet the standards of established organic reactions [Enders *et al.* 2007; Pellissier 2007; Melchiorre *et al.* 2008; Bertelsen and Jørgensen 2009]. The operational simplicity, ready availability of the catalysts, and the low toxicity of organocatalysts makes it an attractive field for the construction of complex molecular skeleton in a highly stereo controlled manner [Dalko and Moisan 2001; Dalko and Moisan 2004; Gaunt *et al.* 2007].

1.1 Historical Background

Despite the recent introduction of this type of catalysis to synthetic chemistry, organocatalytic reactions are believed to have a very rich historical past during the evolution of life [Dalko and Moisan 2004; Barbas III 2008]. Evidence has been found that this kind of catalysis could have played a significant role in the origin of homochirality in living organisms by transferring their asymmetry to other prebiotic building blocks, such as sugars [Pizzarello and Weber 2004; Weber and Pizzarello 2006; Pizzarello and Weber 2010; Burroughs *et al.* 2012]. Enantiomerically augmented amino acids such as L-alanine and L-isovaline, at ranks of catalyst enantiomeric excess (*ee*) in

carbonaceous meteorites, were able to catalyze the aldol-type dimerization of glycolaldehyde as well as the reaction between glycolaldehyde and formaldehyde generating sugar derivatives. Proline, the most efficient natural amino acid catalyst in aldol-type condensation reactions is barely present in meteorites. However, unprompted generation of proline and other aminoacids in the interstellar medium is likely [Muñoz Caro *et al.* 2002; Meierhenrich *et al.* 2002; Meinert *et al.* 2011], supporting the suggestion that prebiotic molecules might be delivered to the early earth by cometary dust, meteorites or interplanetary dust particles. The formation of sugars was amplified in a number of well-designed de-novo constructions of differentiated carbohydrates in the racemic prebiotic world [Northrup and MacMillan 2004; [a]Córdova *et al.* 2005; [b]Córdova *et al.* 2005; Hayashi *et al.* 2006; Klussmann *et al.* 2006; Córdova *et al.* 2006; Ramasastry *et al.* 2007; Burroughs *et al.* 2010]. It is likely, therefore, that these aldol products were the precursor of complex molecules such as RNA and DNA [Orgel 2004; Oberhuber and Joyce 2005; Kamioka *et al.* 2010]. Prebiotic RNA most likely played a substantial role in orchestrating a number of vital biochemical transformations essential for life, in which sugars performed as chiral templates [Joyce *et al.* 1984; Bolli *et al.* 1997].

1.2 The Advent and Development of Organocatalysis

Organic molecules have been used as catalysts since the beginning of synthetic chemistry. The discovery of the first organocatalytic reaction is attributed to Justus von Liebig's synthesis of oxamide from dicyan [von Liebig 1860] in the presence of an aqueous solution of acetaldehyde (Scheme 1.1).

The discovery of enzymes and their functions had an important impact on the development of asymmetric catalytic reactions. As early as 1858, Louis Pasteur
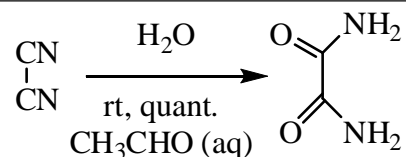
Scheme 1.1 Von Liebig's oxamide synthesis.

introduced the revolutionary concept of "dissymmetry" after he carried out the first enzymatic kinetic resolution [Pasteur 1858]. Starting from racemic ammonium tartrate, the organism *Penicillium glauca* selectively metabolized (*d*)-ammonium tartrate. In 1908, Georg Bredig was interested to find the chemical origin of enzyme activity observed in living organisms and re-examined non-enzymatic asymmetric decarboxylation reactions where he showed that enantiomeric enrichment in the thermal decarboxylation of optically active camphorcarboxylic acid in (*d*) and (*l*) limonenes, respectively [Bredig and Balcom 1908]. As an extension of this work, he studied the same decarboxylation reaction in the presence of natural alkaloids like nicotine or quinidine [Bredig and Fajans 1908]. Subsequently, the first example of enantioselective C-C bond forming reaction under metal-free conditions (Scheme 1.2) was reported by Bredig and Fiske [Bredig and Fiske 1913] where the addition of HCN to benzaldehyde in the presence of quinine or quinidine afforded optically active cyanohydrins (<10% ee).

In the same line with these pioneering works, Wolfgang Langenbeck made several significant contributions to the field, particularly, identifying and explaining the enzymatic processes by using simple aminoacids or small peptides in order to mimic the behavior of natural enzymes [Langenbeck 1928; Langenbeck 1949]. He also coined the term ''Organic Catalysts'' (''Organische Katalysatoren'') to define those reactions promoted solely by organic compounds [Langenbeck 1932]. Breding's asymmetric cyanohydrin synthesis was reinvented by Prelog [Prelog and Wilhelm 1954] which paved the way to more efficient asymmetric synthesis. The advent of synthetically useful levels
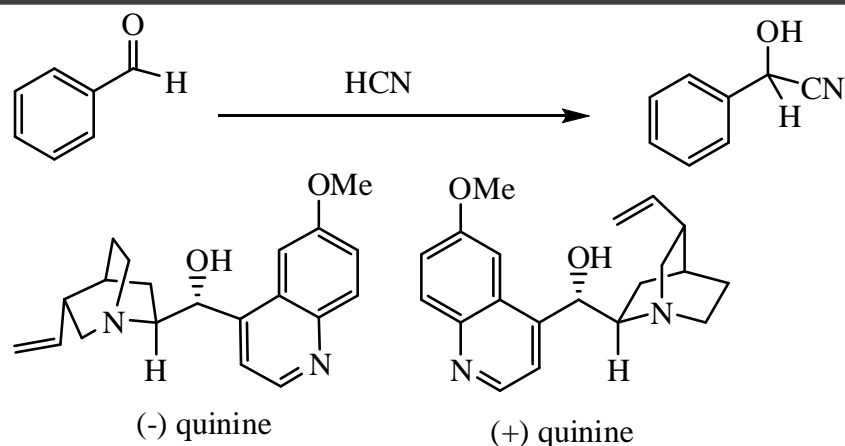
Scheme 1.2 Bredig's synthesis of optically active cyanohydrins.

of enantioselectivity can be dated to the early 1960s, when Pracejus described the use of

O-acetylquinine as an organocatalyst to enable the enantioselective methanolysis of

methyl phenyl ketene to (-)-α-phenyl methylpropionate (Scheme 1.3) [Pracejus 1960].
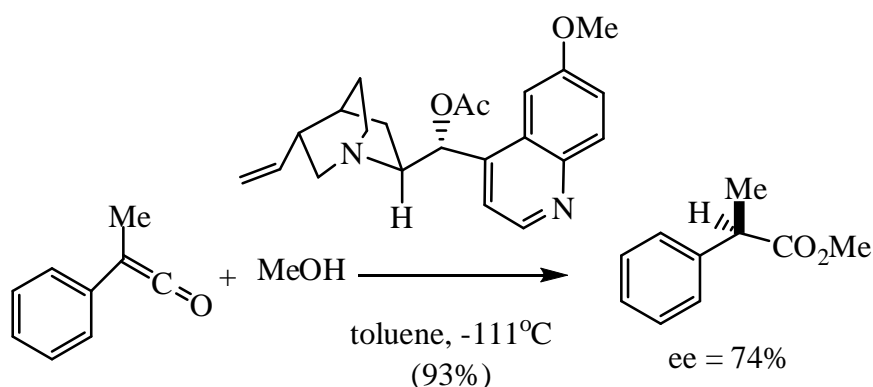
Scheme 1.3 Pracejus' enantioselective ester synthesis from methyl ketene.

Another important event in the history of organocatalytic reaction was the

discovery of the proline catalyzed asymmetric intramolecular aldol reaction

independently by two industrial groups. Hajos and Parrish at the Hoffmann La Roche

[Hajos and Parrish 1971; Hajos and Parrish 1974] reported proline catalyzed

intramolecular aldol reactions to give aldols in good yields and *ee*s followed by acid

catalyzed dehydration to yield aldol condensation products (Eq. (*i*) and (*ii*); Scheme
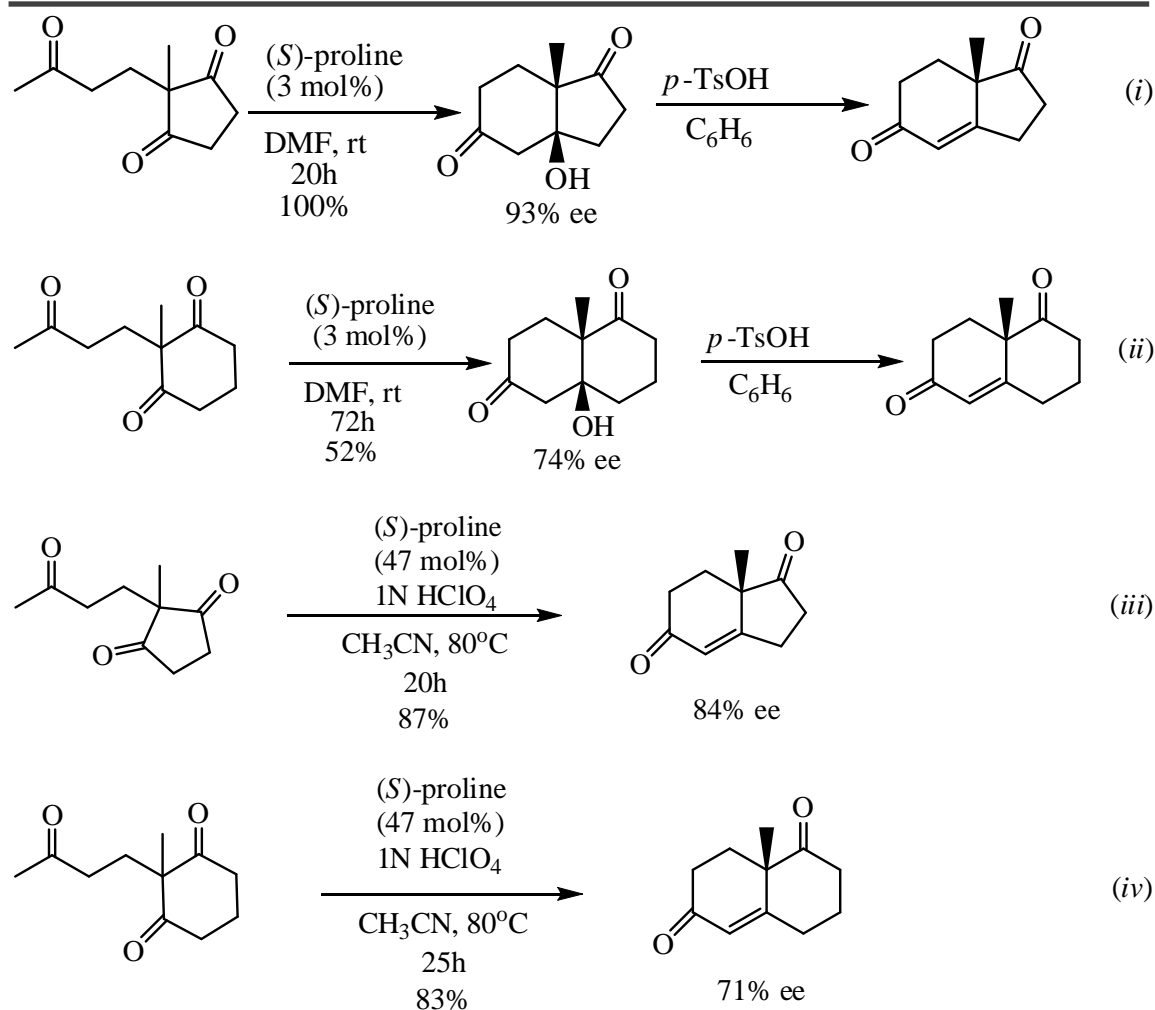
Scheme 1.4 Hajos-Parrish-Eder-Sauer-Wiechert reactions.

1.4). The aldol condensation products can also be obtained directly from triketones if the cyclization is performed in the presence of proline and an acid co-catalyst (Eq. (*iii*) and (*iv*); Scheme 1.4) as shown by Eder, Sauer and Wiechert at the Schering [Eder *et al.* 1971].

The late 1970s and early 1980s marked a clear turning point, with the advent of more general and efficient asymmetric organocatalysts and organocatalytic reactions [Dalko 2007]. During this period, a number of reactions which proceeded *via* ion-pairing mechanisms were uncovered. Inoue and co-workers developed chiral diketopiperazines as chiral Brønsted acids for the asymmetric hydrocyanation reactions [Jacobsen *et al.* 1999], thereby paving the way for the efficient hydrocyanation reactions of aldimines

developed some years later by the groups of Lipton and Jacobsen [Iyer *et al.* 1996; Sigman and Jacobsen 1998]. The advent of efficient phase-transfer reactions dates back to the mid-1980s, when researchers at Merck reported that substituted 2-phenyl-1-indanone systems could be alkylated with remarkably high enantioselectivity (up to 94%) in the presence of catalytic amounts of substituted *N*-benzylcinchoninium halides (50% NaOH/toluene) [Dolling *et al.* 1984; Hughes *et al.* 1987]. The chiral amine mediated cycloaddition reactions, which were pioneered by Kagan [Kagan and Riant 1992], as well as the earliest examples of the enantioselective oxidation of chalcones using polyamino or resin bonded polyamino acid under tri- and bi-phasic conditions, the so called Juliá reaction [Juliá *et al.* 1980; Juliá *et al.* 1982] were also striking. Reinvestigation of the Hajos-Parrish-Eder-Sauer-Wiechert reaction by List and co-workers [List *et al.* 2000] also opened an avenue for a number of related transformations such as the enantioselective intermolecular cross-aldol, Mannich, Michael and Diels-Alder type transformations and the application of these transformations in multistep (domino) reactions [Zhu and Bienayme 2004; Berkessel and Gröger 2005; Ramachary *et al.* 2006; Guo and Ma 2006]. Rising from a small collection of chemically unique and unusual, mechanistically inadequately understood reactions, organocatalysis has highly developed at a truly spectacular pace, which today represents the third pillar of asymmetric catalysis besides metal and biocatalysis [Dalko and Moisan 2001; Berkessel and Gröger 2005; Dalko 2007; MacMillan 2008; Dondoni and Massi 2008].

1.3 Classification of Organocatalysis

According to Seayad and List [Seayad and List 2005], most but not all organocatalysts can be broadly classified as Lewis bases, Lewis acids, Brønsted bases, and Brønsted acids and the simplified form of the corresponding catalytic cycles are shown in Scheme 1.5. In Lewis base catalysis, the catalyst (B:) initiate the catalytic cycle
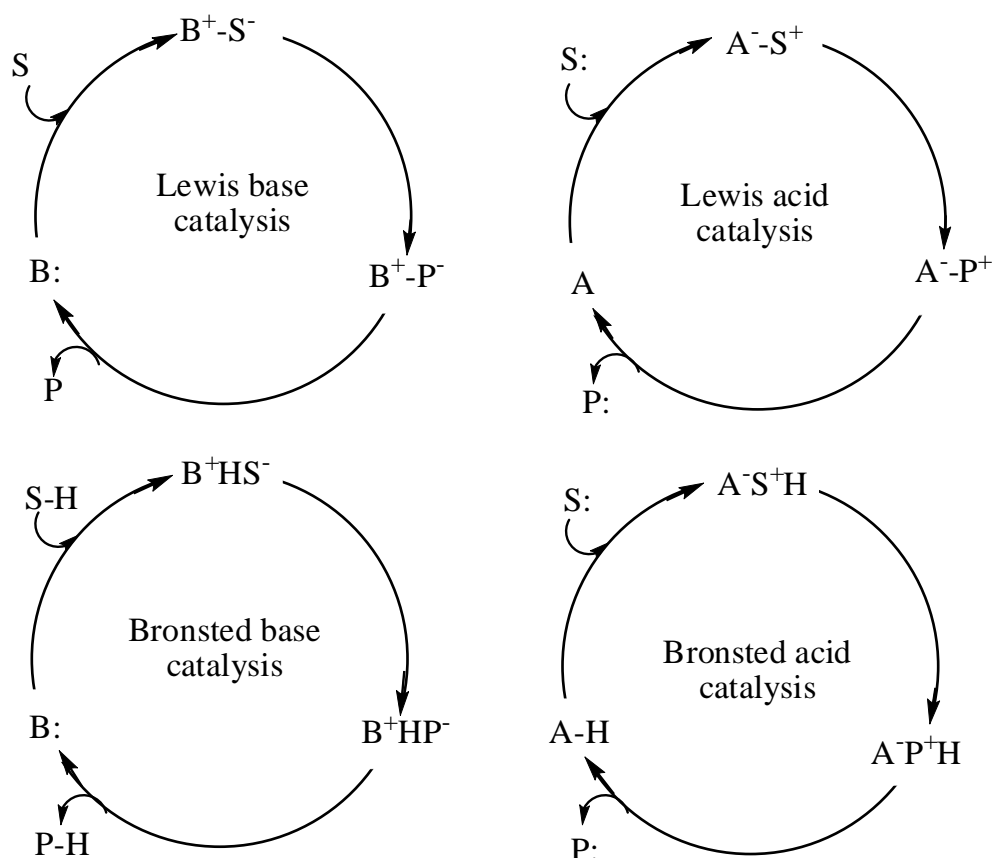
Scheme 1.5 Organocatalytic cycles [Seayad and List 2005].

via nucleophilic addition to the substrate (S) followed by subsequent reactions to release the final product (P) with the regeneration of the catalyst for further turnover. In Lewis acid catalysis, the catalyst (A) activates nucleophilic substrates (S:) in a similar manner to give the product. Brønsted base and acid catalytic cycles are initiated *via* a partial deprotonation or protonation, respectively (Scheme 1.5). A major limitation of the mechanistic classification approach is the typical lack of information on the mechanisms of most organocatalytic reactions, in particular kinetic data [Clemente and Houk 2004; Allemann *et al.* 2004; Cheong and Houk 2004].

The majority of organocatalysts are N-, C-, O-, P-, and S-based Lewis bases that operate through diverse mechanisms and convert the substrates either into activated nucleophiles or electrophiles. Some of the examples for O-, S-, and P-based Lewis base catalysts are shown in Figure 1.1.
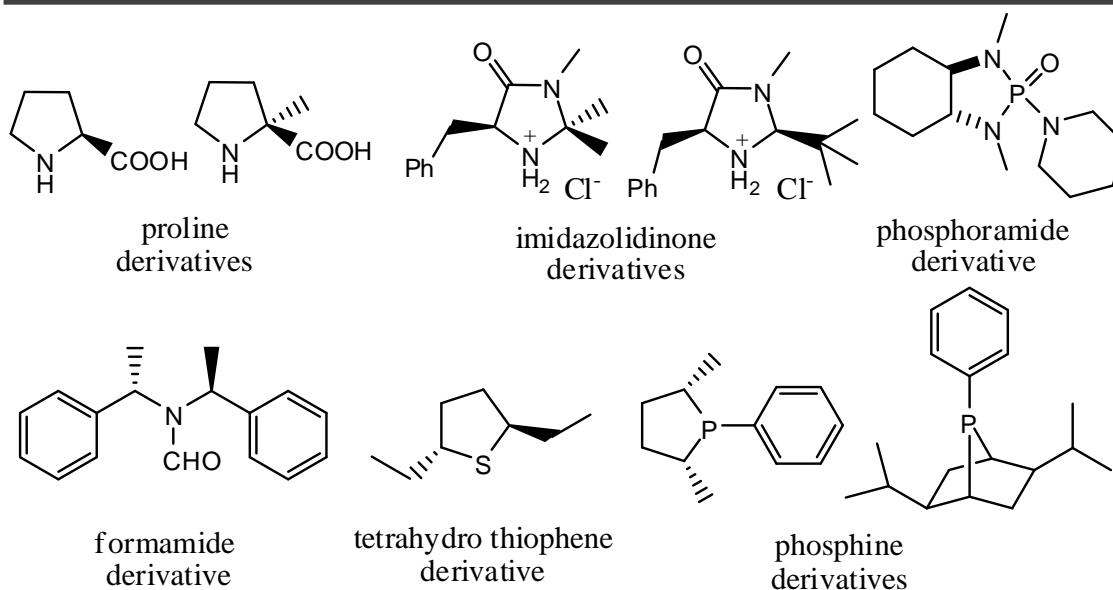
Figure 1.1 Examples for O-, S-, and P- based chiral Lewis base catalysts.

Typical reactive intermediates in organocatalytic reactions are iminium ions, enamines, ammonium enolates, carbenes *etc.* (Scheme 1.6). In iminium catalysis, the active species is an iminium ion formed by the reversible reaction of an amine catalyst with a carbonyl substrate. The higher reactivity of the iminium ion compared to the carbonyl species is utilized to facilitate reactions such as Knoevenagel condensations, cyclo and nucleophilic additions and cleavage of σ-bonds adjacent to the *α*-carbon [Guthrie and Jordan 1972; Trost 1991; Ahrendt *et al.* 2000; Jen *et al.* 2000]. Enamine catalysis involves a catalytically generated enamine intermediate that is formed *via* deprotonation of an iminium ion and that reacts with various electrophiles or undergoes pericyclic reactions. This concept has also been extended to highly enantioselective *α*-functionalizations of aldehydes and ketones such as aldol [List *et al.* 2000; Notz and List 2000; List *et al.* 2001; Bahmanyar *et al.* 2003; Pidathala *et al.* 2003], Mannich [List 2000; List *et al.* 2002; [b]Hayashi *et al.* 2003; [a]Hayashi *et al.* 2003; Notz *et al.* 2003; Notz *et al.* 2004], aminations [List 2002; Bøgevig *et al.* 2002; Kumaragurubaran *et al.* 2002], hydroxylations [Brown *et al.* 2003; [c]Hayashi *et al.* 2003; Zhong 2003; Hayashi *et al.*

2004], alkylations [Vignola and List 2004], chlorinations [Brochu *et al.* 2004; Halland *et*

al. 2004], and intramolecular Michael reactions [Fonseca and List 2004]. In the case of

ammonium enolate catalysis, a ketene interacts with a nucleophilic amine catalyst

(typically a quinine or quinidine derivative) forming an ammonium enolate intermediate

which reacts with electrophiles [Wynberg and Staring 1982; Wynberg and Staring 1985;

Iwabuchi *et al.* 1999; Calter *et al.* 2003; France *et al.* 2004; Papageorgiou *et al.* 2004;

Bremeyer *et al.* 2004; Miller 2004]. In carbene catalysis, the carbene reacts with the

aldehyde forming the nucleophilic Breslow intermediate, facilitating addition to an

electrophile (Scheme 1.6). Typical examples of carbene catalysis include reactions that

take advantage of umpolung aldehyde reactivity, wherein an acyl anion equivalent
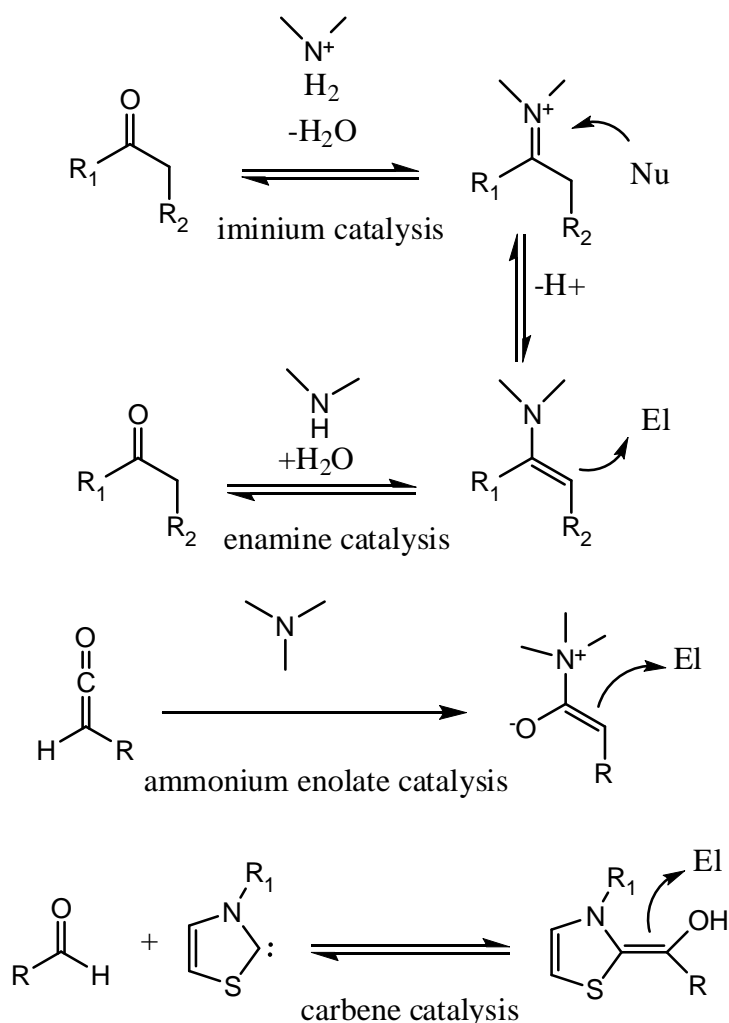
Scheme 1.6 Examples of Lewis base organocatalysis.

reacts with an electrophile [Enders and Kallfass 2002; Kerr *et al.* 2002; Kerr and Rovis 2003; Enders and Balensiefer 2004; Johnson 2004].

An important class of organic catalysts that can be considered as Lewis acids are phase-transfer catalysts which includes cinchonine and cinchonidine catalysts [Dolling *et al.* 1984]. Recently, Maruoka and co-workers developed highly efficient and enantioselective C_2 symmetric chiral spiro-ammonium salt catalysts derived from commercially available (*S*)- or (*R*)-1,1-bi-2-naphthol (Figure 1.2), and successfully applied them to enantioselective α-alkylations as well as aldol and Michael reactions [Ooi *et al.* 1999; Ooi *et al.* 2002; Maruoka and Ooi 2003; [b]Ooi *et al.* 2003; [a]Ooi *et al.* 2003; Ooi and Maruoka 2004]. Another important example of Lewis acid catalysis is the epoxidation of olefins using chiral dioxiranes generated *in situ* from chiral ketone catalysts and Oxone (potassium peroxomonosulfate) as oxidant [Curci *et al.* 1984; Curci *et al.* 1995; Denmark *et al.* 1995; Shi 2004; Yang 2004].

N-benzyl cinchoninium salt

spiro ammonium salt

N-anthracenyl cinchonidium salts
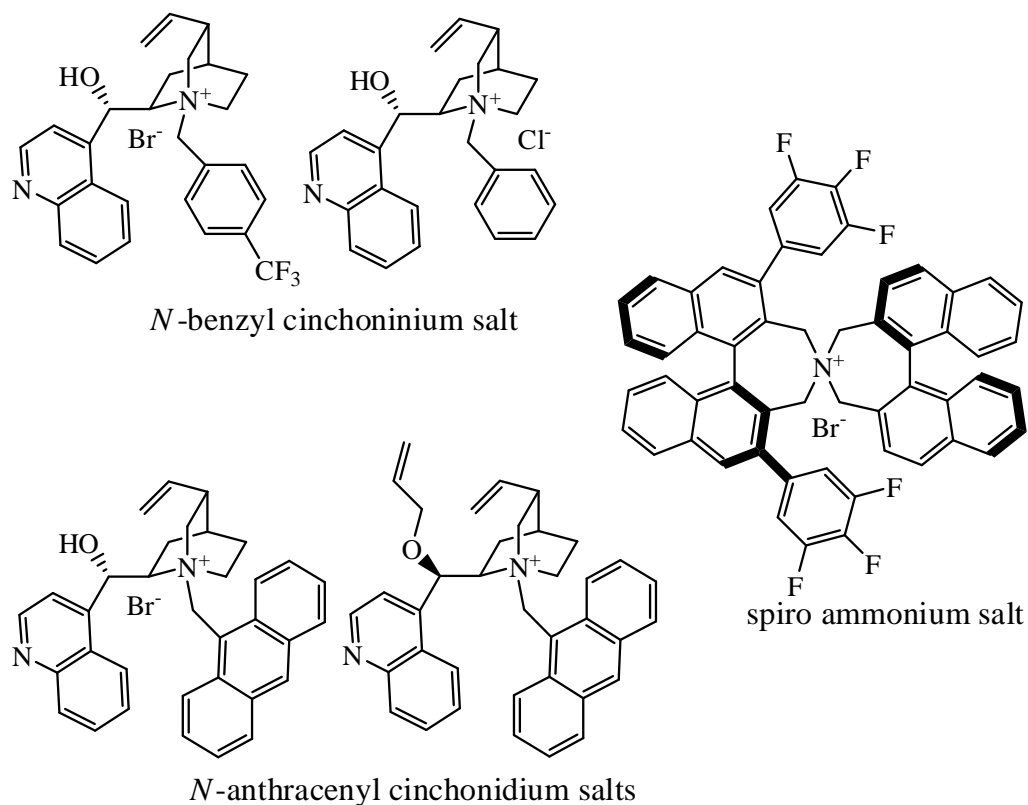
Figure 1.2 Examples for chiral Lewis acid catalysts.

Typical examples of organic Brønsted base catalysis in asymmetric synthesis are hydrocyanation reactions (*e.g.* cyanohydrins synthesis and the Strecker reaction). Inoue and co-workers studied the addition of HCN to various aldehydes using cyclopeptide (Figure 1.3), achieving high asymmetric inductions. Lipton and co-workers used a similar cyclopeptide for the Strecker reaction of various *N*-benzhydryl imines to α-aminonitriles (Figure 1.3) [Iyer *et al.* 1996]. Corey and Grogan reported the Strecker reaction using a synthetic chiral C_2 symmetric guanidine derivative (Figure 1.3) [Corey and Grogan 1999]. In these cases, hydrogen cyanide interacts with the nitrogen base by hydrogen bonding to form a cyanide ion, which can then add to the carbonyl compound or the imine coordinated with the peptide/guanidine hydrogen through hydrogen bonding. Another example of Brønsted base catalysis is the Michael reaction of a prochiral glycine derivative tert-butyl diphenyliminoacetate in the presence of a modified guanidine under solvent free conditions [Ishikawa *et al.* 2001].

cyclopeptide derivatives

guanidine derivatives
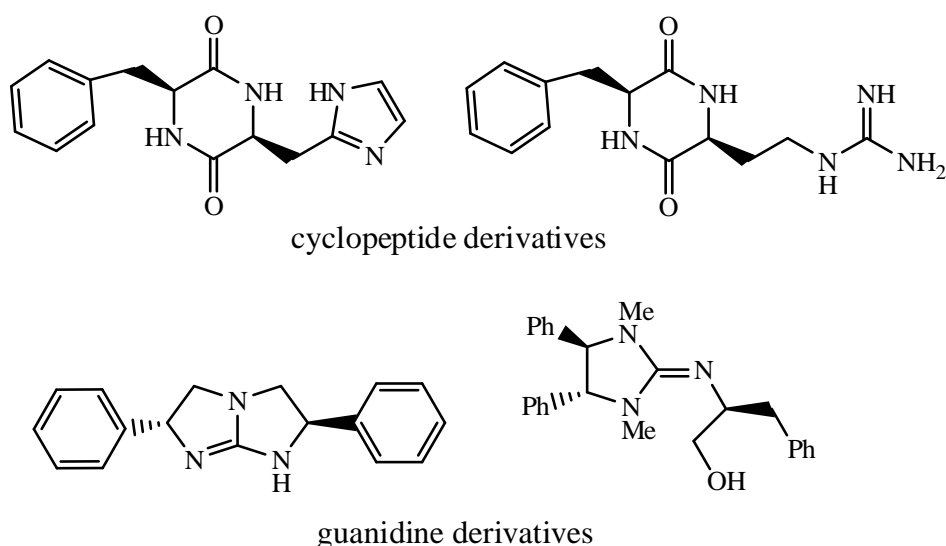
Figure 1.3 Examples for organic Brønsted base catalysts.

Recently, catalysis through hydrogen bonding [Schreiner 2003; Pihko 2004] has been introduced as a powerful methodology for asymmetric catalysis. For example, Jacobsen and co-workers developed enantioselective Strecker [Sigman and Jacobsen

1998; Sigman *et al.* 2000], Mannich [Wenzel and Jacobsen 2002], hydrophosphonylation

[Joly and Jacobsen 2004] and Pictet–Spengler [Taylor and Jacobsen 2004] reactions of

imines, using urea and thiourea catalyst-motifs (Figure 1.4). These catalysts seem to

activate the imine substrate by forming hydrogen bonds from the urea hydrogens to the

imine nitrogen in a bridging mode. This catalysis is described as general acid catalysis,

as it is somewhat related to the enzymatic catalysis where H-bonding to a transition state

occurs. Very recently, Mannich reactions and aza-Friedel-Crafts alkylations of aldimines

using chiral Brønsted acid catalysts have also been reported [Uraguchi *et al.* 2004;

Uraguchi and Terada 2004; Akiyama *et al.* 2004].
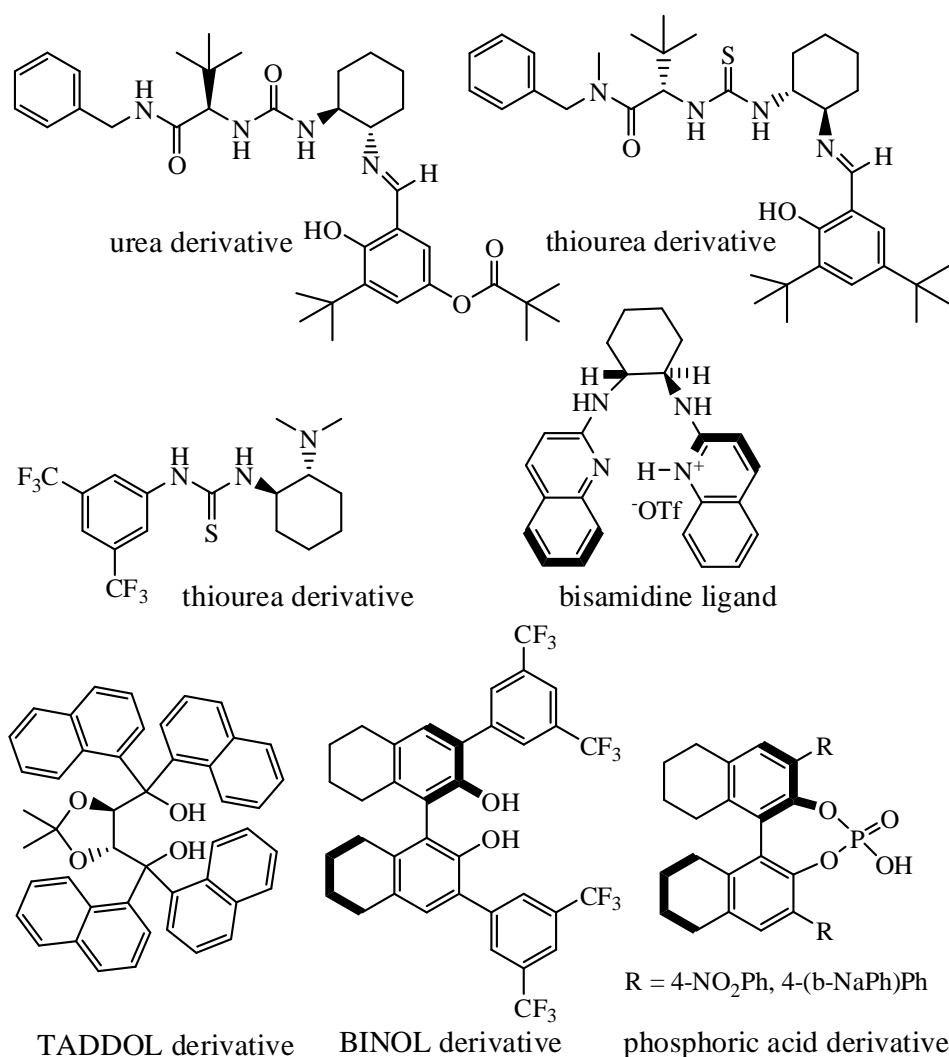
Figure 1.4 Examples for chiral Brønsted acid catalysts.

1.4 Asymmetric Organocatalytic Domino Reactions

The possibility to tie two or more organocatalytic reactions has become a challenging goal for chemists. To circumvent the costly protection/deprotection processes as well as the purification of intermediates, the synthetic potential of multicomponent domino reactions has been developed for the efficient and stereoselective construction of complex molecules from simple precursors in a single process. Organocatalytic domino reactions are, in a manner biomimetic, as the similar principles are often seen in the biosynthesis of natural products. They often proceed with excellent stereoselectivities and are environment friendly. The efficiency of asymmetric domino reactions can be judged by the number of bonds formed, the number of newly created stereocenters and the increase in molecular complexity [Enders *et al.* 2007].

The application of organocatalyzed cascade reactions in natural product synthesis was impressively revealed for the first time by Terashima and co-workers in 1998 when the field of organocatalysis was just in its infancy [Kaneko *et al.* 1998]. Chiral amine catalysts and their derivatives offer a highly controlled, efficient and robust means of accessing molecules with dense stereochemistry and functionality in a simple synthetic format. In 2004, Jorgensen and co-workers published two reports of organocatalyzed enantioselective Michael-aldol cascade reactions. The reaction of α,β-unsaturated ketones with β-ketoesters, β-diketones, or β-ketosulfones yield cyclohexanones with up to four contiguous stereocenters [Pulkkinen *et al.* 2004; Halland *et al.* 2004]. In 2005, MacMillan and co-workers reported enantioselective domino nucleophilic addition-electrophilic addition reactions of α,β-unsaturated aldehydes using imidazolidinone catalysts [Huang *et al.* 2005]. Very recently, chiral Brønsted acid catalysts have created widespread application in organocatalysis particularly in the field of pharmaceutical industry. A Brønsted acid catalyzed asymmetric domino transfer hydrogenation of

quinolines was recently presented by Rueping and co-workers [Rueping *et al.* 2006]. Hayashi and co-workers have developed a powerful one-pot reaction for the rapid construction of the Tamiflu core [Ishikawa *et al.* 2009] which is a neuramidase inhibitor recommended by World Health Organisation (WHO) for swine flu (H1N1).

1.5 Mechanistic Aspects of Organocatalytic Reactions

A complete mechanism of any chemical reaction describes the actual process by which a reaction takes place; which bonds are broken and which bonds are formed and in what order, the geometry and the electronic structure of each reactive intermediate, activated complex, and transition state (TS), the number of steps involved, the relative rates of each step, *etc.* The reaction intermediates are chemical species, often unstable and short-lived, which are temporary products and act as reactants for the next step. Reaction intermediates are often free radicals or ions. TSs are commonly molecular entities involving unstable bonds and/or unstable geometry. They correspond to maxima of the reaction coordinate on the potential energy surface (PES) for the reaction. A complete mechanism must also account for all the reactants used, the function of a catalyst, stereochemistry, all products formed and the amount of each. Reactions may proceed by different mechanisms under different conditions. In some cases there are several proposed mechanisms, each of which completely explains all the data. In order to state a mechanism completely, positions of all atoms including those of solvent molecules and energy of the systems at every point in the process have to be specified.

There are different aspects to the characterization of an organic chemical reaction. The determination of thermodynamic parameters such as the equilibrium constant at a specified temperature, the enthalpy and entropy of reaction; still on the same macroscopic scale, the measurements of rate constants and activation parameters, *etc.* are some of them. Alternatively, it could involve learning how reactants are transformed into

products at the molecular level. Computational chemistry is becoming increasingly important to analyze mechanisms even though most of the evidence about the molecular reaction mechanism is gleaned from experimental measurements on the macroscopic scale. However, advancement in computational methods in quantum mechanics (QM), density functional theory (DFT) and molecular mechanics (MM) and the rapid increase in computer power have opened up a new avenue for understanding various mechanistic possibilities besides conventional experimental observations.

The amino acid proline, is a remarkable molecule from the beginning of asymmetric catalysis (Scheme 1.4). It is a secondary, cyclic, pyrrolidine-based amino acid. It is an abundant chiral molecule that is inexpensive and available in both enantiomeric forms. The two functional groups (a carboxylic acid and an amine portion) make proline bi-functional and assist chemical transformations in concert similar to enzymatic catalysis. The most important difference when compared to other amino acids is proline's effective aminocatalysis - a Lewis base type catalysis that facilitates iminium- and enamine-based transformations (Figure 1.5). The immediate consequence of proline's pyrrolidine portion is the bicyclo[3.3.0]octane ring system of its metal complexes. Hence proline can be a ligand in asymmetric transition-metal catalysis, a chiral
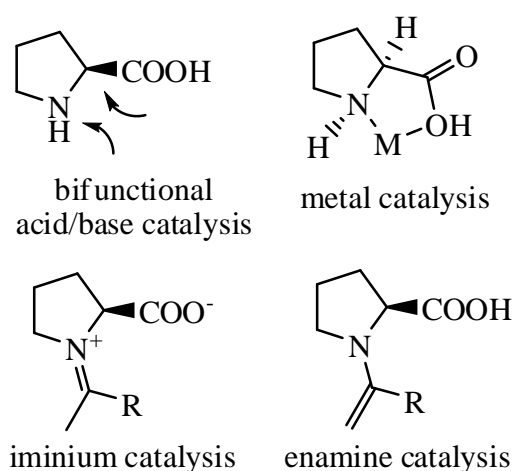
Figure 1.5 Modes of action in proline catalysis.

modifier in heterogeneously catalyzed hydrogenations and most importantly, proline itself can be an effective soluble organocatalyst of several powerful asymmetric transformations such as Mannich reaction, Michael addition, α-oxidation, α-amination, α-sulfenylation/selenylation, α-halogenation, cycloaddition reactions *etc.* [List 2004; Notz *et al.* 2004; [b]Kotsuki *et al.* 2008; [a]Kotsuki *et al.* 2008].

There have been experimental as well as computational studies aimed at interpreting the role of key intermediates such as iminium ions or enamines in proline catalysis [Bock *et al.* 2010; Jacobsena and MacMillanb 2010; Hein *et al.* 2011; Cheong *et al.* 2011; Verma *et al.* 2011; Sharma and Sunoj 2011; Schmid *et al.* 2011]. The synergy between experimental and theoretical studies has contributed to the appraisal of the mechanism of proline catalyzed asymmetric reactions [List *et al.* 2002; Bahmanyar and Houk 2003; Brown *et al.* 2003; Vignola and List 2004]. The last decade has witnessed increasing activities toward identifying improved proline catalysts for asymmetric catalysis [Sakthivel *et al.* 2001; Notz *et al.* 2004; Halland *et al.* 2004; Miller 2004; Shinisha and Sunoj 2007]. However our interest in organocatalysis, more specifically in the conformational flexibility of the catalyst and its high enantioselectivity prompted us to perform some theoretical studies on these types of reactions.

Recently, the chemistry surrounding *N*-heterocyclic carbenes (NHC) is also becoming a prominent area of research due to versatile utilization of these ligands in producing a large variety of metal complexes, uses as reagents in organic reactions as well as identification of these molecules as efficient organocatalysts [Arduengo III 1999; Garber *et al.* 2000; Stauffer *et al.* 2000; Fürstner *et al.* 2001; Trnka and Grubbs 2001; Connor *et al.* 2002; Enders and Balensiefer 2004; Enders *et al.* 2007; Hahn and Jahnke 2008; De Frémont *et al.* 2009; Radius and Bickelhaupt 2009; Alcarazo *et al.* 2010; Dröge and Glorius 2010; Kirmse 2010]. A large variety of NHCs with structural and electronic

diversities have been reported by several groups [Nemcsok et al. 2004; Tonner et al. 2007; Hahn and Jahnke 2008; Tonner and Frenking 2008; Radius and Bickelhaupt 2009; Poyatos et al. 2009; Prades et al. 2011].

Initially considered as simple tertiary phosphine mimics in organometallic chemistry [Green et al. 1997], there is increasing experimental substantiation that NHC-metal catalysts surpass their phosphine based counterparts in both activity and scope. Among the advantages associated with replacing a tertiary phosphine with an NHC are (*i*) the reduced need for excess ligand in a catalytic reaction due to the stronger NHC binding to the metals compared to PR_3 ligands, (*ii*) improved air and moisture stability of metal-NHC complexes compared to metal-phosphine analogues, stemming from the tendency for the phosphine to frequently oxidize in air, and (*iii*) the remarkable activity in catalysis, generally attributed to the unique combination of strong σ-donor, poor π-acceptor, and steric properties of NHCs. Their interesting features of structure and bonding come up from the combined effect of electronic stabilization by mesomeric interaction of lone pairs of electrons on nitrogen atoms with the vacant p orbital of sp^2 hybridized carbene center and as a consequence of shielding by sterically demanding substituents on the ring. NHCs are electron rich and strong σ donors and form strong bonds with majority of metals. Their π back-bonding ability in various metal complexes is a source of debate. The exceptional stability of NHCs was later shown to arise from the combined π-donating and σ-withdrawing properties of nitrogen, which increase the HOMO-LUMO (HOMO = highest occupied molecular orbital and LUMO = lowest unoccupied molecular orbital) gap of the molecule [Heinemann *et al.* 1996; Boehme and Frenking 1996]. Further, the ability to tune the stereoelectronic features of the ligand through substituents on C_4 and C_5 positions as well as N-centers make them attractive for the design of homogeneous catalysts [Dröge and Glorius 2010]. Minor structural

differences can have a remarkable effect on catalytic activity and selectivity of carbenes. However, detailed insights on the mechanisms and the associated energetics are not readily available even for some of the typical NHC-organocatalytic reactions. Our interest in organocatalysis, more specifically in the participation of NHCs as catalysts prompted us to perform some theoretical studies on the molecular mechanisms of these types of reactions. A comprehensive study of the stereoelectronic parameters associated with NHCs [Bourissou et al. 2000; Díez-González and Nolan 2007] appears vital and is fundamental to understand the factors governing their reactivity, as well as necessary for the development of even more active NHC-containing catalytic systems. Interestingly, the properties of tertiary phosphine ligands were first characterized in terms of electronic effects, until Tolman reported the importance of steric factors [Tolman 1977]. Contrary to tertiary phosphines, studies on NHC ligands have focused principally on steric properties, because of the analogy with phosphines and/or the possible formation of dimeric species.

Computational approaches to the understanding of the mechanism of chemical reactions generally begin by establishing the relative energies of the starting materials, TSs and products as the stationary points on the potential energy surface of the reaction complex. Examining the intervening species *via* the intrinsic reaction coordinate (IRC) offers additional insights into the destiny of the reactants by delineating, step-by step and the energetics involved along the reaction path between the stationary states and thus provides a better understanding on 'why does a reaction choose a particular pathway'. Today, computational methods for modeling molecules and reactions attain results at more or less any accuracy desired, as long as sufficient computer resources are accessible. These methods are proving to be particularly useful for modeling catalytic reactions. Indeed, a theoretical approach is sometimes faster than an experimental one and is often the only way to achieve the level of detail that chemists seek. Small chiral

catalysts are ideal for computational modeling, because their size makes accurate

simulations feasible, allowing detailed results to be generated and can be used to design

new catalysts [Houk and Cheong 2008].

Part B - Computational Chemistry

The underlying physical laws necessary for the mathematical theory of a large part of physics and the whole of chemistry are thus completely known, and the difficulty is only that exact application of these laws leads to equations much too complicated to be soluble.

[Dirac 1929]

A number of experimental observations in the late 1800s and early 1900s forced physicists to look beyond Newton's laws of motion (classical mechanics) for a more general theory to understand the fundamental nature of molecules [Kümmel 2002; Cramer 2004]. In 1900, Planck illustrated that electromagnetic radiation was emitted and absorbed from a black body in discrete quanta, each having energy proportional to the frequency of radiation. In 1904, Einstein invoked these quanta to explain the photo-electric effect and it had become increasingly clear that electromagnetic radiation had particle-like properties in addition to its wave-like nature such as diffraction and interference. In 1924, de Broglie declared that matter also had this dual nature (particle-wave duality). This led to the formulation of Schrödinger's wave equation for matter [Schrödinger 1926] which is the basic governing equation to predict the behavior of matter at microscopic level (quantum mechanics). The electronic Schrodinger equation is a many-body problem in its exact form whose computational complexity propagates exponentially with the number of electrons, and hence, an exact solution is intractable. Physicists and chemists developed methods that can solve, in principle, the time-independent Schrödinger equation for many electron systems, albeit with drastic approximations and the errors associated with them. Hartree-Fock theory and electron

correlation methods are important in this regard. The introduction of computers and the accessibility of a variety of software have aided to deal with the complex mathematical problems. The advances in supercomputers, or the vector/parallel machines, powerful workstations, and desktop computers have widened the scope for running the electronic structure programs for the systems of more than 100 atoms. Now quantum chemistry calculations are relevant to a broad range of chemical problems such as thermochemistry, reaction mechanisms, material science, cluster science, catalysis, and enzymology.

Computational chemistry, as the term says, is a branch of chemistry that uses computer science to simulate chemical structures and reactions numerically, based in full or in part on the fundamental laws of physics [Foresman and Frisch 1996]. It helps chemists to study chemical phenomena by running calculations on computer rather than by probing reactions and compounds experimentally. Gaussian, Gauss-View, GAMESS, MOPAC, TURBOMOLE, CHARMM, TINKER, VASP, Spartan, Sybyl, Hyperchem, ADF, CASTEP *etc.* are some of the packages that are available with varying capabilities, ease of use, and performance. Some methods can be used to model not only stable molecules, but also short lived, unstable intermediates, and even transition states. Computational chemistry methods range from highly accurate methods (typically feasible only for small systems) to very approximate methods. For computational quantum chemical calculations one may employ different methods based on (*i*) *ab initio* quantum chemical methods, (*ii*) density functional theory (DFT) methods, (*iii*) semi-empirical quantum chemical methods, (*iv*) molecular mechanics (MM), (*v*) molecular dynamics (MD) and Monte Carlo (MC) simulations, or (*vi*) hybrid quantum mechanics/molecular mechanics (QM/MM) methods. All these methods perform the same basic types of calculations such as computing the lowest energy of a particular molecular structure (based on the first derivative of energy with respect to the atomic

positions) and computing vibrational frequencies and other properties (based on the second derivative of energy with respect to the atomic structure).

Ab initio (Latin term for "from the beginning" or "from first principle") methods provide a mathematical description of the chemical system by solving the Schrödinger equation. It employs rigorous mathematical approximations, without employing any empirical data but the universal constants such as the speed of light, the masses, and charges of electrons and nuclei, Planck's constant *etc.* Hence, the results are known to be accurate and generally are in good agreement with the experimental results [Szabo and Ostlund 1996], and these methods claim high computational effort and normally used for small systems.

In DFT, one works with the electron probability density ($\rho(\boldsymbol{r})$) instead of the molecular wave function, based on the Hohenberg-Kohn [Hohenberg and Kohn 1964] and Kohn-Sham [Kohn and Sham 1965] formalisms which states that the physical observables of a system in its ground state can be expressed as functionals of the electron density [Parr and Yang 1989]. DFT methods include the effects of electron correlation which account for the instantaneous interactions of opposite spin. Thus, DFT results are more accurate for some type of systems and can provide the benefits of some more expensive *ab initio* methods at essentially Hartree-Fock cost and are presently the most successful approach to compute the electronic structure of matter.

Semi-empirical techniques are much faster, use approximations from empirical (experimental) data to provide the input into the mathematical models, and are generally applicable to very large molecular systems. They solve an approximate form of the Schrödinger equation, use empirical data to assign values to some of the integrals that occur in the calculation and neglect some of the integrals. Semi-empirical quantum methods [Pople and Beveridge 1970; Stewart 1990] represent a middle way between the

highly expensive quantitative results from *ab initio* methods and the mostly qualitative results available from Molecular Mechanics.

The MM methods [Weiner and Kollman 1981; Boyd and Lipkowitz 1982; Bowen and Allinger 1991; Dinur and Hagler 1991] does not use a Hamiltonian or wave function. Instead, they perform computations based upon interactions among the nuclei and the electronic effects are implicitly included in force fields through parametrizations. The molecule is viewed as atoms held together by bonds and the molecular electronic energy is expressed as the sum of bond-stretching, bond bending, and other kinds of energies. Hence in molecular mechanics, computations are quite inexpensive, while it can handle chemical systems containing many thousands of atoms such as proteins, enzymes, and other macromolecular systems.

The MD and MC methods are the two most widely used methods for atomic-level modeling of fluids [Doll and Freeman 1994]. MD uses Newton's laws of motion to examine the time-dependent behavior of systems, including vibrations or Brownian motion, using a classical mechanical description [Schlick 2002; Rapaport 2004]. MD simulations have provided ample information on the fluctuations and conformational changes of proteins and nucleic acids, and these methods now regularly used to investigate the structure, dynamics and thermodynamics of biological molecules and their complexes. For MC, a new configuration is selected on Metropolis sampling algorithm and Boltzmann-weighted averages for structure and thermodynamic properties. MC methods are exclusively useful for simulating systems with many coupled degrees of freedom, such as fluids, disordered materials, strongly coupled solids, and cellular structures.

The hybrid QM/MM approach combines the strength of both QM (accuracy) and MM (speed) calculations, generally applicable for the calculation of ground and excited state properties like molecular energies and structures, atomic charges, reaction

pathways *etc.* [Warshel and Levitt 1976; Singh and Kollman 1986; Field *et al.* 1990; Gao 1996; Mordasini and Thiel 1998]. The ONIOM (our N-layered integrated molecular orbital + molecular mechanics) method developed by Morokuma and co-workers is one of the more general QM/MM methods that allows to combine a variety of quantum mechanical methods as well as a molecular mechanics method in multiple layers [Maseras and Morokuma 1995; Humbel *et al.* 1996; [a]Svensson *et al.* 1996; [b]Svensson *et al.* 1996; Dapprich *et al.* 1999; Vreven and Morokuma 2000; Vreven *et al.* 2001].

1.6 Theoretical Background

1.6.1 The Schrödinger Equation

Quantum mechanics explains how entities like electrons have both particle-like and wave-like characteristics. All quantum chemical methods describe the electronic structure of matter in terms of Schrödinger equation. The Schrödinger equation describes the wave function of a particle:

$$\left\{ \frac{-\text{h}^2}{8\pi^2\text{m}} \nabla^2 + \mathbf{V} \right\} \Psi(\boldsymbol{r_i},\text{t}) = \frac{i\text{h}}{2\pi} \frac{\partial \Psi(\boldsymbol{r_i},\text{t})}{\partial \text{t}} \qquad \text{(Eq. 1.1)}$$

where, Ψ is the wave function, m is the mass of the particle, h is Planck's constant, and $\mathbf{V}$ is the potential field in which the particle is moving. The product of Ψ with its complex conjugate (Ψ^*) is interpreted as the probability distribution of the particle ($|\Psi|^2$).

If $\mathbf{V}$ is not a function of time, the Schrödinger equation can be simplified using the mathematical technique known as separation of variables. The wave function can be written as the product of a spatial function and time function:

$$\Psi\ (\boldsymbol{r_i},\ \text{t}) = \Psi\ (\boldsymbol{r_i})\ \tau\ (\text{t}) \qquad \text{(Eq. 1.2)}$$

By substituting Eq. 1.2 in Eq. 1.1, two equations will be obtained, one of which depends on the position of the particle independent of time and the other of which is a function of

time alone. Since most of the chemical phenomena are due to the time-independent interactions, one may write time-independent Schrödinger equation, which in its simplest form:

$$\mathbf{H}\Psi\,(\boldsymbol{r}_i) = \mathrm{E}\Psi\,(\boldsymbol{r}_i) \qquad\qquad \text{(Eq. 1.3)}$$

where **H** is the Hamiltonian operator comprising of the nuclear and electronic kinetic energy operators and the potential energy operators corresponding to the nuclear-nuclear, nuclear-electron, and electron-electron interactions. The many-particle wave function Ψ describes the system, while E is the energy Eigen value of the system. The Hamiltonian operator for N electron and M nucleus can be written as:

$$\mathbf{H} = -\sum_{i=1}^{N}\frac{1}{2}\nabla_i^2 - \sum_{A=1}^{M}\frac{1}{2\mathrm{M}_A}\nabla_A^2 - \sum_{i=1}^{N}\sum_{A=1}^{M}\frac{Z_A}{\boldsymbol{r}_{iA}} + \sum_{i=1}^{N}\sum_{j>i}^{N}\frac{1}{\boldsymbol{r}_{ij}} + \sum_{A=1}^{N}\sum_{B>A}^{M}\frac{Z_A Z_B}{\boldsymbol{R}_{AB}} \qquad \text{(Eq. 1.4)}$$

Here, the indices i and j run over the N electrons whereas A and B run over the M nuclei. The distance between the ith electron and A^{th} nucleus is $\boldsymbol{r}_{iA}$; the distance between i^{th} and j^{th} electron is $\boldsymbol{r}_{ij}$ and the distance between the Ath nucleus and B^{th} nucleus is $\boldsymbol{R}_{AB}$. M_A is the ratio of the mass of the nucleus A to the mass of an electron and Z_A is the atomic number of nucleus A.

Schrödinger equation can be solved by applying several approximation, Born-Oppenheimer (BO) approximation [Born and Oppenheimer 1927] being the first among them. It is based on the concept that the nuclear and electronic motions take place at different time scales and it is reasonable since the mass of a typical nucleus is thousands of times greater than that of an electron. Thus, an electron in motion sees relatively static nuclei, while a moving nucleus feels averaged electronic motion. From this, the separation of the electronic and nuclear Hamiltonians is possible and to make their corresponding wave functions as well. Hence, the full Hamiltonian for the molecular system can be written as:

$$\mathbf{H} = \mathbf{T}^{elec}(r_i) + \mathbf{T}^{nucl}(\mathbf{R}_A) + \mathbf{V}^{nucl-elec}(r_i,\mathbf{R}_A) + \mathbf{V}^{elec}(r_i) + \mathbf{V}^{nucl}(\mathbf{R}_A) \qquad \text{(Eq. 1.5)}$$

The molecular wave function can then be represented as a product of electronic and nuclear counterparts:

$$\Psi(r_i,\mathbf{R}_A) = \Phi^{elec}(r_i,\mathbf{R}_A)\Phi^{nucl}(\mathbf{R}_A) \qquad \text{(Eq. 1.6)}$$

where r_i and $\mathbf{R}_A$ are the positions of electrons and nuclei, respectively. This allows the two parts of the problem to be solved independently and hence the kinetic energy term for the nuclei can be neglected to construct an electronic Hamiltonian. The Eigen value equation for the electronic case is then written as:

$$\mathbf{H}^{elec}\Phi^{elec}(r_i,\mathbf{R}_A) = \mathbf{E}^{eff}(\mathbf{R}_A)\Phi^{elec}(r_i,\mathbf{R}_A) \qquad \text{(Eq. 1.7)}$$

The electronic Hamiltonian depends explicitly on the electronic coordinates and parametrically on nuclear coordinates. Since the chemical phenomena occur primarily due to various interactions between electrons of the systems, explicit treatment of the electronic Hamiltonian generally suffices to investigate chemical properties and reactions. Accordingly, $\mathbf{E}^{eff}$ is also used as the effective potential for the nuclear Hamiltonian. Thus Eq. 1.5 can be written as:

$$\mathbf{H}^{nucl} = \mathbf{T}^{nucl}(\mathbf{R}_A) + \mathbf{E}^{eff}(\mathbf{R}_A) \qquad \text{(Eq. 1.8)}$$

This Hamiltonian is used in the Schrödinger equation for nuclear motion, describing the vibrational, rotational, and translational states of the nuclei. Solving the nuclear Schrödinger equation is necessary for predicting the vibrational spectra of molecules.

The system of atomic units (a.u.), also referred as Hartree units, has been conveniently adopted as a convention in QM wherein the mass of an electron, Planck's constant, charge of a proton, the length corresponding to radius of first Bohr orbit in hydrogen atom and 4π times the permittivity in free space (ε_0) are all set to unity. Coordinates can be transformed to *bohrs* by dividing them by a_0. Energies are measured in *hartrees* which is defined as the Coulomb repulsion between two electrons separated

by one *bohr*:

$$1\,hartree = \frac{e^2}{a_0} \qquad \text{(Eq. 1.9)}$$

where a_0 is the *bohr radius*:

$$a_0 = \frac{h^2}{4\pi m_e e^2} = 0.5291772\ \text{Å} \qquad \text{(Eq. 1.10)}$$

The acceptable solutions of Eq. 1.3 need to be necessarily well-behaved. Therefore, Ψ must be finite, single valued, continuous, quadratically integrable, and obeying the appropriate boundary conditions:

$$\int \Psi^*(\boldsymbol{r}_1,\boldsymbol{r}_2......,\boldsymbol{r}_N)\Psi(\boldsymbol{r}_1,\boldsymbol{r}_2......,\boldsymbol{r}_N)d^3\boldsymbol{r}_1 d^3\boldsymbol{r}_2...d^3\boldsymbol{r}_N = 1 \qquad \text{(Eq. 1.11)}$$

1.6.2 Hartree-Fock Theory

Hartree devised an approximate wave function of many-electron systems (Hartree product (HP) function) which is a product of the one-electron functions and generally referred as orbitals [Hartree 1928]. In this function, the spatial distribution of electrons has been defined in terms of spatial orbitals. Thus, the HP function can be written as:

$$\Psi^{HP}(X_1,X_2,.....,X_N) = \chi_i(X_1)\chi_j(X_2).....\chi_k(X_N) \qquad \text{(Eq. 1.12)}$$

These spatial orbitals are functions of the position vectors of electrons. The concept of electronic spin is also introduced in the one-electron function (orbital) by means of the spin functions $\alpha(\omega)$ and $\beta(\omega)$ that correspond to the up and down spin electrons, respectively. This leads to the spin orbitals, $\{\chi_j\}$ defined below:

$$\begin{aligned}\chi_{2i-1}(X) &= \psi_i(\boldsymbol{r})\alpha(\omega) \\ \chi_{2i}(X) &= \psi_i(\boldsymbol{r})\beta(\omega)\end{aligned} \qquad \text{(Eq. 1.13)}$$

where each electron is defined in terms of combined spatial and spin coordinates, *X*.

According to the Pauli's exclusion principle [Pauli 1925], no two electrons of an

atom shall have identical value of all the four quantum numbers *viz.* n, l, m, and s. Since the HP function is an independent-electron wave function, it do not satisfy the antisymmetry principle. Slater [Slater 1930] and Fock [Fock 1930] independently proposed that an antisymmetrized sum of all the permutations of HP functions would solve this problem for many-electron systems. Thus, an N-electron wave function within the HF formulation can be written as:

$$\Psi(X_1, X_2, \ldots, X_N) = \frac{1}{\sqrt{N!}} \begin{vmatrix} \chi_i(X_1) & \chi_j(X_1) & \cdots & \chi_N(X_1) \\ \chi_i(X_2) & \chi_j(X_2) & \cdots & \chi_N(X_2) \\ . & . & \cdots & . \\ \chi_i(X_N) & \chi_j(X_N) & \cdots & \chi_N(X_N) \end{vmatrix} \qquad \text{(Eq. 1.14)}$$

This determinant mixes all of the possible orbitals of all of the electrons in the molecular system to form the wave function. The factor $1/\sqrt{N!}$ is a normalization factor. The spin orbitals are denoted as χ's, while X_1, X_2...*etc.* represent the combined spatial and spin coordinates of the respective electrons. The simplest antisymmetric wave function which can be used to describe the ground state of an N-electron system is a single Slater determinant:

$$\left| \Psi_0 \right\rangle = \left| \chi_i \chi_j \cdots \chi_N \right\rangle \qquad \text{(Eq. 1.15)}$$

Sometimes the term restricted Hartree-Fock (RHF) is used to accentuate that the wave function is restricted to be a single determinantal function for a configuration wherein electrons of α-spin as well as of β-spin occupy the same space orbitals. When this restriction is relaxed, and different orbitals are allowed for electrons with different spins, we have an unrestricted Hartree-Fock (UHF) calculation. This refinement is most likely to be important when the numbers of α- and β-spin electrons vary.

According to variation principle, the exact wave function serves as a lower bound to the energies calculated by any other normalized antisymmetric function:

$$E_0 = \left\langle \psi_o \,|\, \mathbf{H} \,|\, \psi_o \right\rangle$$

(Eq. 1.16)

where $\mathbf{H}$ is the full electronic Hamiltonian. By minimizing E_0 with respect to the choice of spin orbitals, one can derive an equation called the Hartree–Fock (HF) equation which determines the optimal spin orbitals. Hartree-Fock equation is an Eigen value equation of the form:

$$f(i)\chi(X_i) = \varepsilon\chi(X_i)$$

(Eq. 1.17)

where $f(i)$ is a one electron operator called the Fock operator of the form:

$$f(i) = -\frac{1}{2}\nabla_i^2 - \sum_{A=1}^{M}\frac{Z_A}{r_{iA}} + V^{HF}(i)$$

(Eq. 1.18)

where $V^{HF}(i)$ is the Hartree-Fock potential which is the average potential experienced by the ith electron due to the presence of other electrons. Thus, the HF approximation replaces the complicated many electron problem by a one electron problem where electron-electron repulsion is treated in an average way. The procedure of solving the Hartree-Fock equation is called the self-consistent-field (SCF) method and is given below.

An initial guess at the spin orbital is made to calculate the average field ($V^{HF}(i)$) seen by each electron and then solve the Eigen value equation (Eq. 1.17) for a new set of spin orbitals. These new spin orbitals are used to obtain new fields and repeat the procedure until the self-consistency is reached (until fields no longer change and the spin orbitals used to construct the Fock operator are same as its Eigen functions). The solution of HF Eigen value problem yields a set $\{\chi_k\}$ of orthonormal HF spin orbitals with orbital energies $\{\varepsilon_k\}$. The N-spin orbitals with the lowest energies are called the occupied orbitals and the remaining members of the set $\{\chi_k\}$ are called virtual or unoccupied orbitals. For the electron (1):

$$V^{HF}(1) = \sum_{j}^{N} \left(J_j(1) - K_j(1) \right) \qquad \text{(Eq. 119)}$$

Coulomb operator, $J_j(1) = \int \chi_j(2) \dfrac{1}{\boldsymbol{r}_{12}} \chi_j(2) dx_2 \qquad \text{(Eq. 1.20)}$

And the exchange operator can only be written through its effect when operating on a spin orbital:

$$K_j(1) \chi_i(1) = \left[\int \chi_j(2) \dfrac{1}{\boldsymbol{r}_{12}} \chi_i(2) dx_2 \right] \chi_j(1) \qquad \text{(Eq. 1.21)}$$

Roothaan and Hall [Roothaan 1951; Hall 1951] proposed the derivation of the HF equations for the closed shell systems. The HF equation Eq. 1.17 may be rewritten by substituting Eq. 1.22, where the spin orbital is expressed as the linear combination of basis functions, leads to Eq. 1.23.

$$\psi_i = \sum_{\mu=1}^{K} C_{\mu i} \phi_\mu \qquad i = 1, 2, \ldots, K \qquad \text{(Eq. 1.22)}$$

where ϕ_μ are the basis functions corresponding to atomic orbitals and $C_{\mu i}$ are the coefficients of ϕ_μ and K is the total number of basis functions.

$$f_{(i)} \sum_{\mu=1}^{K} C_{\mu i} \phi_\mu = \varepsilon \sum_{\mu=1}^{K} C_{\mu i} \phi_\mu \qquad \text{(Eq. 1.23)}$$

Premultiplying on both sides of Eq.1.23 by $\phi_\mu{}^*$ and integrating gives the Roothaan Hall equation:

$$FC = SC\varepsilon \qquad \text{(Eq. 1.24)}$$

where ε are orbital energies, S is the overlap matrix and F is the Fock matrix. The Fock matrix F is the matrix representation of the Fock operator (Eq. 1.18) in the basis ϕ_μ.

The Fock matrix must be diagonalized to find out the unknown molecular orbital coefficients in order to determine the Eigen values from Roothaan Hall equation (Eq. 1.24). The MO coefficients of the Fock matrix are determined by the SCF procedure,

where first we guess the orbital coefficients (*e.g.* from an effective Hamiltonian method) and then we iterate to convergence.

Other than exchange, all electron correlations are ignored in Hartree-Fock theory constructed using the Roothaan approach which stems from the one-electron nature of Fock operator. Further, the choice of basis set was challenging to early computational chemists. Even though the linear combination of atomic orbital (LCAO) approach using hydrogenic orbitals remains attractive, this basis set requires numerical solution of the four index integrals appearing in the Fock matrix elements which is a tedious process. Since each index runs over the total number of basis functions, there are in principle N^4 total integrals to be evaluated, and this quartic scaling behavior with respect to basis set size proves to be a bottleneck in HF theory applied to essentially any molecules.

Historically, two philosophies began to emerge at this stage, one utilizes some approximations by some sort of parametrization to reproduce key experimental quantities which underlies the motivation for so called 'semi-empirical' MO theories and the other essentially views HF theory as a stepping stone on the way to exact solution of the Schrödinger equation. HF theory provides a very well defined energy, one which can be converged in the limit of an infinite basis set, and the difference between that converged energy and reality is the electron correlation energy. It was anticipated that developing the technology to achieve the HF limit with no further approximations would not only permit the evaluation of the chemical utility of the HF limit, but also probably enable moving on from that low-altitude base camp to the Schrödinger equation summit. Such was the foundation for further research on "*ab initio*" HF theory [Cramer 2004]. However, Hartree-Fock theory in its pure form does not include a full treatment of the effects of electron correlation (energy contribution arising from electrons interacting with one another).

1.6.3 Post Hartree-Fock Methods

Post Hartree-Fock methods are the set of methods developed to improve the Hartree–Fock (HF), or self-consistent field (SCF) method. The post-HF methods try to obtain the correlation energy E_{corr}, defined as the difference between the exact *ab initio* energy and exact (complete basis) HF energy [[b]Boys 1950], *viz.*

$$E_{corr} = \varepsilon_0 - E_0 \qquad \text{(Eq. 1.25)}$$

where, ε_0 is the exact Eigen value of H_{elec} and E_0 is the "best" HF energy with the basis set extrapolated to completeness. The popular approaches that try to compute E_{corr} are the configuration interaction [Pople *et al.* 1976; Foresman *et al.* 1992], coupled cluster (CC) [Kümmel 2002; Cramer 2004] and many body perturbation theory (MBPT) [Brillouin 1934; Kelly 1969] methods.

In configuration interaction (CI) the excited states are also included in the description of an electronic state and in principle CI provides an exact solution for the many electron problems. The HF wave function is used as the reference determinant and the energy is minimized variationally with respect to the determinant expansion coefficients. If only one electron has been moved from each determinant, it is called a configuration interaction single-excitation (CIS) calculation. CIS calculations give an approximation to the excited states of the molecule, but do not change the ground-state energy. Single and double excitation (CISD) calculations yield a ground state energy that has been corrected for correlation. Triple-excitation (CISDT) and quadruple-excitation (CISDTQ) calculations are done only when very high accuracy results are desired. The configuration interaction calculation with all possible excitations is called a full CI. The full CI calculation using an infinitely large basis set will give an exact quantum mechanical result but is highly expensive.

The coupled cluster method is one of the most important practical advancement over the CI method [Čizek 1966]. It is the more mathematically refined technique for estimating the electron correlation energy. The coupled cluster correlation energy is determined completely by the singles and doubles coefficients and the two electron MO integrals. The cost of including single excitations in addition to doubles is worth to increase in accuracy and this defines CCSD models. Inclusion of connected triple excitations defines CCSDT and if the singles/triples coupling term is included then it is called CCSD(T).

Möller-Plesset perturbation theory improves the Hartree-Fock method by adding electron correlation effects by means of Rayleigh-Schrodinger perturbation theory (RSPT) [Bartlett and Silver 1975; Krishnan and Pople 1978], usually to second (MP2), third (MP3), and fourth (MP4) order. They are at present the most popular way to incorporate electron correlation in molecular quantum mechanical calculations, especially at the MP2 level. Möller-Plesset calculations are computationally exhaustive and so their use is often restricted to single point calculations at geometry obtained using a lower level of theory.

1.6.4 Density Functional Theory (DFT)

The basic idea of DFT is to describe an interacting system of electrons *via* its density ($\rho(r)$) which is the probability density of finding any of the N electrons within the volume element dr while the other N-1 electrons have arbitrary positions. Further, the density $\rho(r)$ is an observable, subject to a measurement experimentally while the many-particle wave function is an intangible entity and the density is a very conventional parameter for a collective description of many-electron system wherein single particle co-ordinates lose their identity.

The key variable in DFT, $\rho(r)$ can be given as:

$$\rho(\boldsymbol{r}) = N \int d^3\boldsymbol{r}_2 \int d^3\boldsymbol{r}_3 \dots \int d^3\boldsymbol{r}_N \psi^*(\boldsymbol{r}_1, \boldsymbol{r}_2 \dots \boldsymbol{r}_N) \psi(\boldsymbol{r}_1, \boldsymbol{r}_2 \dots \boldsymbol{r}_N) \qquad \text{(Eq. 1.26)}$$

Hohenberg and Kohn proved that the energy is a unique functional of the electron density [Hohenberg and Kohn 1964]. In this theory, the electron density plays the role of basic variable. The Hohenberg-Kohn (HK) theorems may be stated as (*i*) the external potential and hence the total energy is a unique functional of electron density and (*ii*) the ground state energy can be obtained variationally: the density that minimizes the total energy is the exact ground state density. DFT is distinguished by having fewer variables; the electron density with three spatial coordinates compares to the N-electron wave function with 3N spatial coordinates (or four including spin). The goal of DFT methods is to design a functional connecting the electron density with the energy $E[\rho]$. The energy functional could be divided into three parts, kinetic energy of electrons, $T[\rho]$, nuclear-electron interaction, $E_{ne}[\rho]$, and electron-electron interaction, $E_{ee}[\rho]$:

$$E[\rho] = T[\rho] + E_{ne}[\rho] + E_{ee}[\rho] \qquad \text{(Eq. 1.27)}$$

The electron-electron interaction is composed of Coulomb, $J[\rho]$, and Exchange, $K[\rho]$, parts. From all terms, only $E_{ne}[\rho]$ and $J[\rho]$ can be derived from their classical terms as Eq. 1.28 and Eq. 1.29, respectively:

$$E_{ne}[\rho] = \sum_A \int \frac{Z_A \rho(\boldsymbol{r})}{|\boldsymbol{R}_A - \boldsymbol{r}|} \mathrm{d}\boldsymbol{r} \qquad \text{(Eq. 1.28)}$$

$$J[\rho] = \frac{1}{2} \int \int \frac{\rho(\boldsymbol{r})\rho(\boldsymbol{r}')}{|\boldsymbol{r} - \boldsymbol{r}')} \mathrm{d}\boldsymbol{r}\mathrm{d}\boldsymbol{r}' \qquad \text{(Eq. 1.29)}$$

To obtain the kinetic energy part, Kohn and Sham [Kohn and Sham 1965] introduced the noninteracting reference system. Then, the Hamiltonian does not contain electron-electron interaction. Like the Hartree-Fock method, the ground state wave function corresponds to a Slater determinant constructed of the spin orbitals called Kohn-Sham (KS) orbitals (ϕ) that are the Eigen functions of Kohn-Sham operator (f^{KS}), where

$V_S(r)$ is the effective potential:

$$f^{KS} = -\frac{1}{2}\nabla^2 + V_S(r) \tag{Eq. 1.30}$$

To connect this non-interacting system with the real system, the effective potential is chosen such that the electron density from non-interacting system, $\rho_s(r)$, is equal to the one in real system. *i.e.*

$$\rho(r) \equiv \rho_S(r) = \sum_i^N \left|\phi_i(r)\right|^2 \tag{Eq. 1.31}$$

Now, the major part of the exact kinetic energy can be calculated accurately for the non-interacting electrons, T_S:

$$T_S = \sum_i^N \left\langle \phi_i \left| -\frac{1}{2}\nabla^2 \right| \phi_i \right\rangle \tag{Eq. 1.32}$$

Thus Eq. 1.27 can be modified in terms of known functionals and the unknown exchange-correlation term, $E_{xc}[\rho]$:

$$E[\rho] = T_S[\rho] + E_{ne}[\rho] + J[\rho] + E_{XC}[\rho] \tag{Eq. 1.33}$$

$$E_{XC}[\rho] = (T[\rho] - T_S[\rho]) + (E_{ee}[\rho] + J[\rho]) \tag{Eq. 1.34}$$

The first term in Eq. 1.34 is the correction term for the kinetic energy, which is considered as the kinetic correlation energy whereas the second term contains exchange and potential correlation energy. The different DFT methods have different choices of the functional forms of the unknown exchange-correlation term. If the exact $E_{xc}[\rho]$ was known, DFT would provide the exact total energy, including electron correlation. The $E_{xc}[\rho]$ is often split into exchange and correlation contributions, in which the kinetic energy correlation is somewhat hidden:

$$E_{XC}[\rho] = E_X[\rho] + E_C[\rho] \tag{Eq. 1.35}$$

Even the HK and KS formalisms do not lead to the exact form of exchange-correlation functional E_{XC}, much of it is left to a systematic search and guesswork.

Therefore approximations are required for the calculation of physical quantities. The most widely used approximation in physics is local density approximation (LDA) where the functional depends only on the density at the coordinate where the functional is evaluated:

$$E_{XC}[\rho] \equiv \int \varepsilon_{XC}(\rho) d^3 \boldsymbol{r} \qquad \text{(Eq. 1.36)}$$

The local spin density approximation (LSDA) is a straight forward generalization of LDA to include electron spin:

$$E_{XC}[\rho_\uparrow, \rho_\downarrow] \equiv \int \varepsilon_{XC}(\rho_\uparrow, \rho_\downarrow) d^3 \boldsymbol{r} \qquad \text{Eq. 1.37)}$$

Highly accurate formulae for the exchange-correlation energy density $\varepsilon_{XC}(\rho_\uparrow, \rho_\downarrow)$ have been constructed from simulations of a free electron gas. This had been the most successful method for decades until newer functionals within KS formalism were introduced. A notable difference came with the generalized gradient approximation (GGA) where, in addition to the density values, the functionals are dependent on the gradient of densities. GGA are local but also take into account the gradient of the density at the same coordinate:

$$E_{XC}[\rho_\uparrow, \rho_\downarrow] \equiv \int \varepsilon_{XC}(\rho_\uparrow, \rho_\downarrow, \vec{\nabla}\rho_\uparrow, \vec{\nabla}\rho_\downarrow) d^3 \boldsymbol{r} \qquad \text{(Eq. 1.38)}$$

The most widely used exchange functionals are Slater's X_α [Slater 1951] and B88 [Becke 1988] (Becke's 1988 functional that includes Slater's exchange with gradient corrections) having the form:

$$E_{XC}^{Becke88} = E_{XC}^{LDA} - \gamma \int \frac{\rho^{4/3} X^2}{(1 + 6\gamma \sinh^{-1} X)} d^3 \boldsymbol{r} \qquad \text{(Eq. 1.39)}$$

where $x = \rho^{-4/3|\nabla\rho|}$ and γ is a parameter chosen to fit the exchange energy of inert gas atoms (0.0042 a.u. as defined by Becke). Similarly, there exist local and gradient-corrected correlation functionals. Amongst the other functionals, widely used are P86

and PW91 by Perdew and Wang [Perdew *et al.* 1992] *etc.*

There also exists another type of functional, which offers some improvement over the corresponding pure DFT functional. This includes a mixture of HF and DFT exchange along with DFT correlation. The popular functional BLYP is obtained by coupling of Becke's generalized gradient corrected exchange functional with the gradient corrected correlation functional of Lee, Yang, and Parr [Lee *et al.* 1988]. A popular hybrid functional is B3LYP, Becke-3 parameters non-local exchange functional, with the non-local correlation functional of Lee and co-workers, functional having the form [Lee *et al.* 1988; Becke 1993]:

$$E_{xc}^{B3LYP} = (1-a)E_x^{LSDA} + aE_x^{HF} + b\Delta\Delta_x^{B88} + E_c^{VWN3} + (1-c)E_c^{LSDA} + cE_c^{LYP} \quad \text{(Eq. 1.40)}$$

The meta GGA functional - M06-L [Zhao and Truhlar 2006], hybrid meta GGA functional - MPWB1K [Zhao and Truhlar 2004], M06-2X [[b]Zhao and Truhlar 2008], Grimme's gradient corrected functional - B97D [Grimme 2006], *etc.* are some of the other important density functionals used in this thesis. For M06-L, the exchange functional is given by (Eq. 1.41):

$$E_x^{M06-L} = \sum_\sigma \int d\boldsymbol{r} \left[F_{X\sigma}^{PBE}\left(\rho_\sigma, \nabla_{\rho\sigma}\right) f(w_\sigma) + \varepsilon_{X\sigma}^{LSDA} h_X(x_\sigma, z_\sigma) \right] \quad \text{(Eq. 1.41)}$$

and the correlation functional is given by (Eq.1.42):

$$E_C^{\alpha\beta} = \int e_{\alpha\beta}^{UEG} [g_{\alpha\beta}(x_\alpha, x_\beta) + h_{\alpha\beta}(x_{\alpha\beta}, z_{\alpha\beta})] d\boldsymbol{r} \quad \text{(Eq. 1.42)}$$

Zhao and Truhlar [Zhao and Truhlar 2004] used Adamo and Barone's mPW exchange functional [Adamo and Barone 1998] for F^{GCE} and the Becke95 functional [Becke 1996] for F^{Corr} in the following equation (Eq. 1.42) to derive MPWB1K functional:

$$F = F^H + (X/100)F^{HFE} + [1 - (X/100)](F^{SE} + F^{GCE}) + F^{Corr} \quad \text{(Eq. 1.42)}$$

where, F^H is the Hartree operator (*i.e.*, the nonexchange part of the Hartree-Fock

operator), F^{HFE} is the Hartree-Fock exchange operator, X is the percentage of Hartree-Fock exchange, F^{SE} is the Dirac-Slater local density functional for exchange, F^{GCE} is the gradient correction for the exchange functional and F^{Corr} is the total correlation functional including both local and gradient-corrected parts and a dependence on kinetic energy density.

For M06-2X exchange functional, the term $h_X(x_\sigma, z_\sigma)$ in Eq. 1.41 is 0. In this special case, the M06 functional form for exchange reduces to M05 functional form for exchange. The functional form of the M06-2X correlation functionals is the same as the functional form of the M06-L functionals.

B97D is a semi empirical GGA-type density functional constructed with a long-range dispersion correction where the total energy is given by:

$$E_{DFT-D} = E_{KS-DFT} + E_{disp} \qquad \text{(Eq. 1.43)}$$

where E_{KS-DFT} is the usual self-consistent Kohn–Sham energy as obtained from the chosen density functional and E_{disp} is an empirical dispersion correction given by:

$$E_{disp} = -S_6 \sum_{i=1}^{N_{at}-1} \sum_{j=i+1}^{N_{at}} \frac{C_6^{ij}}{R_{ij}^6} f_{dmp}(\boldsymbol{R}_{ij}) \qquad \text{(Eq. 1.44)}$$

Here, N_{at} is the number of atoms in the system, C_6^{ij} denotes the dispersion coefficient for atom pair *ij*, S_6 is a global scaling factor that only depends on the DF used, and $\boldsymbol{R}_{ij}$ is an interatomic distance. The selection of a particular density functional for a calculation can be made on the basis of the desired accuracy of energy parameters and of the acceptable computational effort.

In summary, DFT provides an economical alternative for treating molecules at correlated level of theory. However, disadvantage of DFT is the exchange correlation functional, which cannot be derived meticulously from first principles. As of today, DFT remains an attractive alternative to more rigorous methods, such as CI.

1.6.5 Basis Sets

The Basis set refers to the set of mathematical functions from which non-orthogonal one-particle wave functions are constructed. These are used to build molecular orbitals, which are expanded as a linear combination of atomic orbitals with the weights or coefficients to be determined (Eq. 1.23). Since it is not possible to obtain the exact AOs for many-electron atoms, Slater type orbitals (STOs) [Allen and Karo 1960] were used to mimic AOs in the early days [Clementi 1964]:

$$\chi_{\zeta,\text{n,l,m}}(r,\theta,\varphi) = NY_{l,m}(\theta,\varphi)r^{n-1}e^{-\zeta r} \quad \text{(Polar coordinates)} \qquad \text{(Eq. 1.45)}$$

where, ζ is the orbital exponent and n, l, and m are the quantum numbers, N is the normalization constant and $Y_{l,m}(\theta,\varphi)$ is the spherical harmonics.

Due to the difficulty in computing two- and other multi-center integrals using STOs, Francis S. Boys suggested the use of standard Gaussian functions centered on atoms (Gaussian type orbitals (GTO)) [[a]Boys 1950; Feller and Davidson 1990]. A Cartesian Gaussian function used in electronic structure calculations has the form:

$$\chi_{\zeta,\text{n,l,m}}(r,\theta,\varphi) = NY_{l,m}(\theta,\varphi)r^{2n-2-l}e^{-\zeta r^2} \quad \text{(Polar coordinates)} \qquad \text{(Eq. 1.46)}$$

$$\chi_{\zeta,l_x,l_y,l_z}(x,y,z) = Nx^{l_x}y^{l_y}z^{l_z}r^{2n-2-l}e^{-\zeta r^2} \quad \text{(Cartesian coordinates)} \qquad \text{(Eq. 1.47)}$$

where x, y and z are the Cartesian components.

The GTOs have several advantages over STOs; a) the GTO has a zero slope whereas the STO has a cusp at the nucleus. b) GTOs diminish too rapidly with distance. c) the extra d-, f-, g-, *etc.* functions may lead to linear dependence of the basis set. They are usually dropped when large basis sets are used. The computational advantage of GTOs over STOs is primarily due to the Gaussian product theorem [Shavitt 1963], *viz.* the product of two GTOs is also a Gaussian function centered at the weighted midpoint of the two functions. In addition, the resulting integrals can be evaluated analytically.

However, for the sake of computational convenience, it is a common practice [Stewart 1970] to bunch together a set of GTOs with fixed coefficients, a_i (contraction coefficients). Such a linear combination is termed the contracted GTO (CGTO):

$$\chi^{\mathrm{CGTO}}(\zeta, l_x, l_y, l_z) = \sum_i^k a_i \chi^{\mathrm{PGTO}}(\alpha_i, \zeta, l_x, l_y, l_z)$$ (Eq. 1.48)

The orbital exponent and contraction coefficients are determined from appropriate atomic calculations. There are varieties of Gaussian basis sets available now, which have been incessantly improved over the years. The single-zeta Gaussian basis sets (minimal basis sets) are the simplest GTOs [Hehre *et al.* 1969]. A double zeta (DZ) basis set doubles the number of functions in the minimal basis set and the split valence basis sets are produced when the doubling or tripling is restricted only to valence orbitals. Pople and coworkers designed the split valence basis sets of type 'k-nlmG' where 'k' indicates the number of primitive Gaussian type orbitals (PGTOs) used for representing the core orbitals and 'nlm' indicates the number of functions the valence orbitals are split into and the number of PGTOs used for their representation [Ditchfield *et al.* 1971]. 3-21G, 6-31G and 6-311G basis sets are some of the examples of split valence basis sets [Hehre *et al.* 1972; Binkley *et al.* 1980]. In most cases the higher angular momentum functions called polarization functions are added to make a better description of chemical bond; for example, the p-orbital can introduce a polarization to the s-orbital for a bound hydrogen atom. This is important when considering accurate representations of bonding between atoms, because the very presence of the bonded atom creates the energetic environment of the electrons spherically asymmetric. To spread the electron density over the molecule, diffuse functions are also added to the basis set which are denoted by + or ++ signs. These are very shallow Gaussian basis functions, which more accurately represent the tail portion of the atomic orbitals, which are distant from the atomic nuclei. These additional basis functions can be important when considering

anions and other large, soft molecular systems. Pople's split valence basis sets (6-31G(d,p), 6-311++G(2d,2p), 6-311+G(2df,2p) *etc.*) and Dunning's correlation consistent basis sets [Dunning Jr. 1970; Woon and Dunning Jr. 1993] [Dunning Jr. 1989] (cc-pvdz, cc-pvtz *etc.*) are some of the most frequently used basis functions. The choice of basis set determines how many functions (*i.e.* Gaussian curves) will be used to express the molecule in a particular computation, depending on the number of atoms of each type present and is directly related to the computation time required.

1.6.6 Molecular Electrostatic Potential (MESP)

The molecular electrostatic potential of a molecule, $V(r)$ is a real physical property, and that can be determined experimentally by X-ray diffraction techniques or calculated rigorously from the electron density, $\rho(r)$, distribution using Eq. 1.49, where Z_A is the charge on nucleus A located at R_A and r' is a dummy integration variable [Gadre and Shirsat 2000]:

$$V(r) = \sum_{\alpha}^{N} \frac{Z_A}{|r - R_A|} - \int \frac{\rho(r')\,\mathrm{d}^3 r'}{|r - r'|}$$
(Eq. 1.49)

The two terms refer to the bare nuclear potential and the electronic contributions, respectively. Balancing of these two terms brings about effective localization of electron–rich regions in the molecular system. Eq. 1.49 indicates that the value of $V(r)$ in any particular region depends on whether the effect of nuclei or electrons is dominant there and the electrostatic potential is certainly specific to a given molecular geometry. Thus MESP is positive in the region close to nuclei and negative in the electron-rich region. In Figure 1.6, the electrostatic potential on the molecular surface of a simple *N*-heterocyclic carbene is depicted where the electron density is indicated by red color to blue color from lowest to highest points respectively.
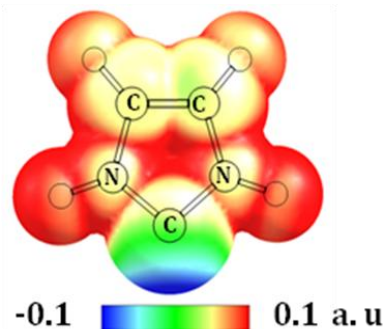
Figure 1.6 3D molecular electrostatic potential contour maps of *N*-heterocyclic carbene molecule computed at B3LYP/6-311++G(d,p) level of theory.

The MESP, $V(\boldsymbol{r})$ can attain positive, zero or negative values. This is in contrast to the behavior of electron densities in position, which can attain only non-negative values [Politzer and Parr 1974]. The MESP at a nucleus of A molecule $V_{0,A}$ can be give as:

$$V_{0,A} = \sum_{B \neq A} \frac{Z_B}{\left| \boldsymbol{R}_B - \boldsymbol{R}_A \right|} - \int \frac{\rho(\boldsymbol{r}')\mathrm{d}^3\boldsymbol{r}'}{\left| \boldsymbol{r} - \boldsymbol{r}' \right|} \qquad \text{(Eq. 1.50)}$$

Nevertheless, every atom is considered to possess a MESP maximum at its center [Gadre and Pathak 1990; Pathak and Gadre 1990; Gadre *et al.* 1992; Shirsat *et al.* 1992; Gadre and Shirsat 2000]. All chemical notations such as lone pairs, bonds, and π-bonds (aromatic, delocalized, and localized) have their topographical expressions in MESP. The topography of molecular electrostatic potential can be characterized in terms of critical point *viz.* minima, saddle and maxima. MESP brings out electron rich regions like lone-pairs of electrons and π-bonds in the form of a negative valued (3, +3) minima. Any bonding (covalent/weak) interaction between atoms is featured by the presence of a positive valued (3, -1) bond critical point (BCP) and while ring structures show always a positive valued (3, +1) ring critical point. The absence of non-nuclear maxima is a main feature of MESP topography over other scalar fields in the interpretation of electronic mechanisms. Similar to the molecular electron density (MED) topography, BCPs bring out the strain in bonds by deviating from the line joining the corresponding atoms. The

significance of the negative-valued MESP and their critical points in molecules and their

anionic species have been broadly addressed in the literature [Politzer and Truhlar 1981;

Gadre and Shrivastava 1993; Luque *et al.* 1994; Gadre *et al.* 1996].

1.6.7 Potential Energy Surface (PES)

A potential energy surface is a mathematical function that gives the energy of a

molecule as a function of its geometry. Potential energy surface is generally used to

model chemical reactions and interactions in simple chemical and physical systems. The

PES arises upon the application of the BO approximation to the solution of the

Schrodinger equation. Considering the general Hamiltonian:

$$H = T_r + T_R + V(r,R) \tag{Eq. 1.51}$$

where T_r is the operator for the kinetic energy of electronic motion, T_R is the operator for

the kinetic energy of nuclear motion, and $V(r,R)$ is the potential energy due to

electrostatic interactions between all of the charged particles (electrons and nuclei). On

applying the BO approximation the nuclear kinetic energy term, T_R in the molecular

Hamiltonian vanishes and the electronic and nuclear degrees of freedom can be

separated. This yields the time-independent Schrödinger equation for the electronic

degrees of freedom:

$$\left[T_r + V(r,R)\right]\psi(r;R) = E(R)\psi(r;R) \tag{Eq. 1.52}$$

In Eq. (1.52), $\psi(r;R)$ is the electronic wave function which depends parametrically on

the nuclear positions, and the energy of the system, $E(R)$, is a function of the nuclear

degrees of freedom. A plot of E versus R gives the PES.

The study of most chemical processes and properties by computational chemists

begins with the optimization of one or more structures to find minima on PESs, which

correspond to equilibrium geometries. A simplified PES can be represented as a

topographic surface with valleys and saddle points as in Figure 1.7. A common analogy
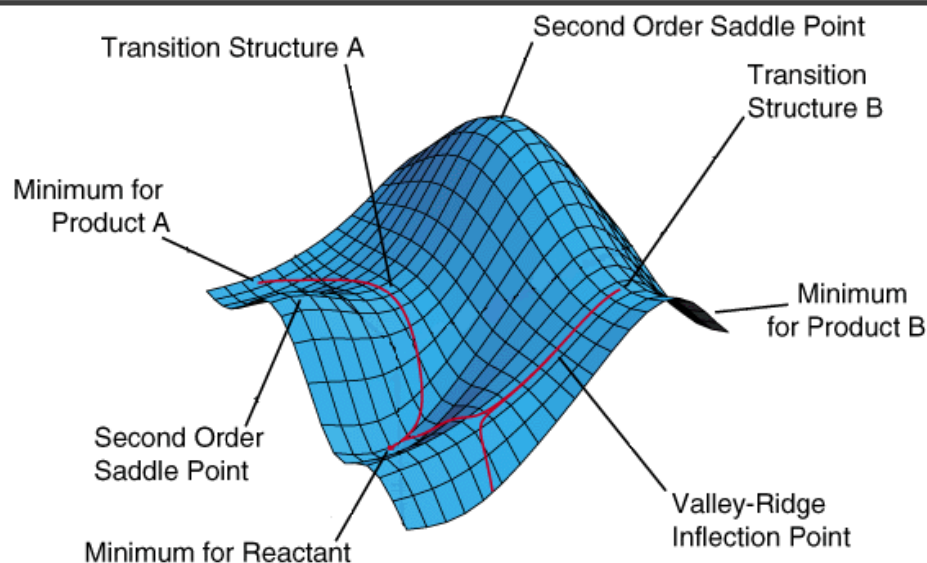
Figure 1.7 Representation of a 3D-model potential energy surface.

compares the topology of PESs to mountainous landscapes. Molecular structures correspond to the positions of minima in the valleys. Reaction rates can be determined from the height and profile of the pathway connecting reactant and product valleys. From the shape of a valley, the vibrational spectrum of a molecule can be computed, and the response of the energy to electric and magnetic fields determines molecular properties such as dipole moment, polarizability, NMR shielding, *etc.* [Jørgensen and Simons 1986; Dykstra 1988; Pulay 1995; Jensen 1999].

To obtain reaction barriers and to calculate reaction rates using transition state theory (TST), it is necessary to locate first-order saddle point on the PES, which correspond to TS. A transition structure is the highest point on the reaction path that requires the least energy to get from the reactant to the product. In other words, it is a stationary point that is an energy maximum in one direction and a minimum in all others. For a point to be considered, to be a TS structure, the first derivatives must be zero and the energy must be a maximum along the reaction path connecting the valley of reactants with the valley of products on the PES.

An alternative and more advanced procedure to trace the path of a chemical

reaction is provided by the intrinsic reaction coordinate (IRC) method. The basic idea is to start at a transition state and slide down the hill towards the adjacent local minimum, at either side of the transition state, by determining the minimum on the local sphere around a given point along the path, with as radius the chosen step length. IRC uses mass weighted Cartesian coordinates even if the geometry is provided in terms of internal coordinates.

The different aspects to the characterization of the PES is the analysis of thermodynamic parameters such as contributions to entropy, energy, and heat capacity resulting from translational, electronic, rotational and vibrational motion. The starting point in each case is the partition function q(V,T) for the corresponding component of the total partition function. The partition function from any component can be used to determine the entropy contribution S from that component, using the relation (Eq. 1.53):

$$S = NK_B + NK_B \ln\left(\frac{q(V,T)}{N}\right) + NK_B T\left(\frac{\partial \ln q}{\partial T}\right)_V \qquad \text{(Eq. 1.53)}$$

The internal thermal energy E can also be obtained from the partition function and is used to obtain the heat capacity:

$$E = NK_B T^2\left(\frac{\partial \ln q}{\partial T}\right)_V \qquad \text{(Eq. 1.54)}$$

$$C_V = \left(\frac{\partial E}{\partial T}\right)_{N,V} \qquad \text{(Eq. 1.55)}$$

where, T = temperature, V = volume, Nk_B = Boltzmann constant = $1.380662*10^{-23}$ J/K, and N = number of moles. These three equations will be used to derive the final expressions used to calculate the different components of the thermodynamic quantities. The translational entropy (Eq. 1.56) is calculated from translational partition function (Eq. 1.57):

$$S_t = R\left(\ln(q_t e) + T\left(\frac{3}{2T}\right)\right) \qquad \text{(Eq. 1.56)}$$

where, R = gas constant = 8.31441 J/(mol K) = 1.987 kcal/(mol K), m = mass of the

molecule, S_t = entropy due to translation and q_t = translational partition function which is

given by:

$$q_t = \left(\frac{2\pi m K_B T}{h^2} \right)^{3/2} V \qquad \text{(Eq. 1.57)}$$

The entropy due to electronic motion is given by:

$$S_e = R \left(\ln(q_e) + T \left(\frac{\partial \ln q_e}{\partial T} \right) V \right) \qquad \text{(Eq. 1.58)}$$

where, S_e = entropy due to electronic motion and q_e = electronic partition function which

is given by (Eq. 1.59): $q_e = \omega_0 e^{-\varepsilon 0/K_B T} + \omega_1 e^{-\varepsilon 1/K_B T} + \omega_2 e^{-\varepsilon 2/K_B T} + ...$ (Eq. 1.59)

The contribution of rotation to the entropy is given by:

$$S_r = R \left(\ln q_r + T \left(\frac{\partial \ln q_r}{\partial T} \right) \right)_V \qquad \text{(Eq. 1.60)}$$

where, S_r = entropy due to rotational motion and q_r = rotational partition function which

is given by:

$$q_r = \frac{1}{\sigma_r} \left(\frac{T}{\Theta_r} \right) \qquad \text{(Eq. 1.61)}$$

where, σ_r = symmetry number for rotation and Θ_r = characteristic temperature for

rotation. The total entropy contribution from the vibrational partition function is given

by:

$$S_v = R \left(\ln(q_v) + T \left(\frac{\partial \ln q}{\partial T} \right)_v \right) \qquad \text{(Eq. 1.62)}$$

Where, S_v = entropy due to vibrational motion and q_v = vibrational partition function

which is given by:

$$q_v = \prod_K \frac{1}{1 - e^{-\Theta_{v,K}/T}} \qquad \text{(Eq. 1.63)}$$

where, $\Theta_{v,K}$ = characteristic temperature for vibration K. The usual way to calculate

enthalpies of reaction is to calculate heats of formation, and take the appropriate sums and difference (Eq. 1.64).

$$\Delta_r H^o(298K) = \sum_{products} \Delta_f H^o_{prod}(298K) - \sum_{reactants} \Delta_f H^o_{react}(298K)$$ (Eq. 1.64)

However, since Gaussian provides the sum of electronic and thermal enthalpies, there is a short cut: namely, to simply take the difference of the sums of these values for the reactants and the products. Calculation of the Gibbs free energy of a reaction is similar, except we have to add the entropy term (Eq. 1.65):

$$\Delta_f G^o(298K) = \Delta_f H^o(298K) - T(S^o(M, 298K) - \sum S^o(X, 298K))$$ (Eq. 1.65)

1.6.8 Solvent effects

Even though gas phase predictions are appropriate for many purposes, the properties of molecules and transition states are considerably affected by their surrounding environment. It is found that solvent environment influences structure, energies, spectra, and other properties of solute. The supermolecule approach, molecular mechanics, and recently appeared various hybrid constructions are some of the methods used to treat solvent effects. In supermolecule approach solvent molecules are explicitly added to the solute in the QM calculation, require large number of solvent molecules for obtaining quantitative results and hence highly expensive. Molecular mechanics methods use atomic force field but do not allow an adequate description of many processes, such as bond breaking in chemical reaction. The hybrid QM/MM methods use QM for the solute and MM for the solvent molecules, but not easy to setup and they are costly.

Self-consistent reaction field (SCRF) methods are another family of models for systems in non-aqueous solutions. In these methods, the solvent is modeled as a continuum of uniform dielectric constant ε (the reaction field). The solute is placed into cavity within the solvent. For easy understanding of the solvation process and separation

of effects of different nature, it is convenient in the continuum theory to split the solvation process in three imaginary steps: *i*) creation of the cavity, *ii*) turning on dispersion-repulsion forces and, then *iii*) electrostatic forces. Dispersion-repulsion forces and cavitation contribution to the energy normally comes with opposite signs, therefore, reducing the total contribution. In many cases, specifically for the case of charged or highly polar solutes, electrostatic forces play the dominant role. Additionally, during the chemical reaction, cavitation and repulsion forces do not change much, and therefore, if we are concerned with the effect of solvent on reaction, they may be neglected. SCRF methods vary with how they define the cavity and the reaction field [Foresman and Frisch 1996].

Onsager reaction field model is the simplest SCRF model wherein the solute occupies a fixed spherical cavity of radius within the solvent field. A dipole in the molecule will induce a dipole in the medium, and the electric field applied by the solvent dipole will in turn interact with the molecular dipole, leading to net stabilization. However the systems having a dipole moment of '0' will not exhibit solvent effects for the Onsager SCRF model (SCRF=dipole) and therefore Onsager model calculations performed on them will give same results as that of gas phase calculations. This is an inherent limitation of Onsager model.

Tomasi's polarized continuum model (PCM) defines the cavity as the union of a series of interlocking atomic spheres (Figure 1.8). The effect of polarization of the solvent continuum is represented numerically. It is computed by numerical integration rather than by an approximation to the analytical form used in the Onsager model. The two isodensity surface-based SCRF models also use a numerical representation of the solvent model.
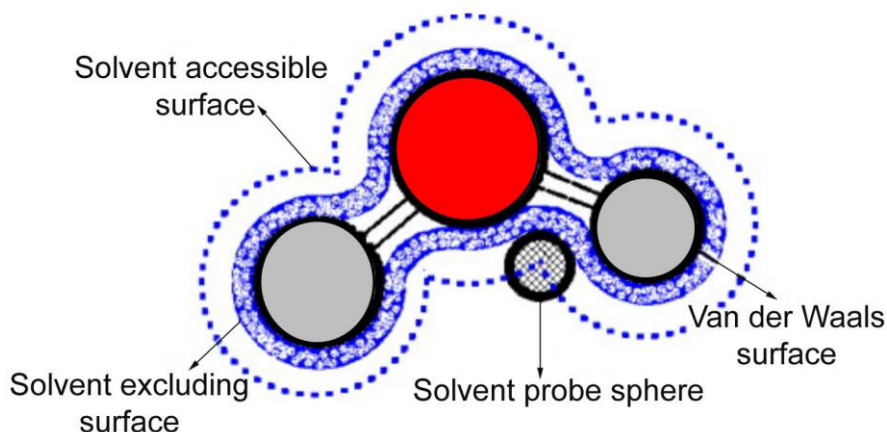
Figure 1.8 Polarized continuum model.

The isodensity PCM (IPCM) model defines the cavity as an isodensity surface of the molecule. This isodensity is determined by an iterative process in which an SCF cycle is performed and converged using the current isodensity cavity. The resultant wave function is then used to compute an isodensity surface, and the cycle is repeated until the cavity shape no longer changes upon completion of the SCF. An isodensity surface is a very natural, intuitive shape for the cavity since it corresponds to the reactive shape of the molecule to as great a degree as is possible.

However, a cavity defined as an isosurface and the electron density are necessarily coupled. The self-consistent isodensity polarized continuum model (SCI-PCM) was designed to take this effect fully into account. It includes the effect of solvation in the solution of the SCF problem. This procedure solves for the electron density which minimizes the energy, including the solvation energy which itself depends on the cavity which in turn depends on the electron density. SCF-PCM thus accounts for the full coupling between the cavity and the electron density and includes coupling terms that IPCM neglects.

1.6.9 Energy Decomposition Analysis (EDA)

The energy decomposition analysis which was developed by Morokuma [Morokuma 1977] and by Ziegler and Rauk [Ziegler and Rauk 1977] is a powerful method, which connects the gap between elementary quantum mechanics and a conceptually simple interpretation of the nature of the chemical bond. The EDA considers the formation of a molecule A-B as a result of interactions between corresponding fragments A and B in their electronic and geometric ground states. The energy required to activate the A and B fragments from the equilibrium state to their united form in A-B (ΔE_{AB}) can be written as a sum of two components (Eq. 1.66):

$$\Delta E_{AB} = \Delta E_{int} + \Delta E_{prep} \qquad \text{(Eq. 1.66)}$$

where interaction energy ΔE_{int} corresponds to the energy difference between the transition state and its frozen fragments in A-B. ΔE_{prep} is the energy required to promote the fragments A and B from their most stable electronic ground state to the electronic ground state which they possess in A-B. The ΔE_{int} is made up of three components (Eq. 1.67):

$$E_{int} = \Delta E_{ele} + \Delta E_{Pauli} + \Delta E_{orb} \qquad \text{(Eq. 1.67)}$$

where the term ΔE_{ele} is the electrostatic interaction energy between the fragments which are calculated with a frozen density distribution in the geometry of A-B molecule. ΔE_{Pauli} is the destabilizing Pauli repulsion, from interactions between electrons on either fragment with the same spin and is responsible for the steric repulsion. The stabilizing orbital interaction term ΔE_{orb} is calculated in the final step of the analysis when the orbitals relax to their final form. The latter term can be decomposed into contributions of orbitals with different symmetry, which makes it possible to distinguish between σ, π, and δ bonding. These terms are defined by assigning intermediate states of the total system during the course of bond formation, which are calculated by applying the laws of

quantum mechanics. Thus, the EDA provides a bridge between the physical laws of quantum mechanics and the heuristic bonding models of chemistry and can be used to analyze chemical bonds in molecules and to translate results of quantum chemical calculations into terms like covalency, ionicity, aromaticity, donation and back donation, or hybridization [Uddin and Frenking 2001; Velde *et al.* 2001; Lein *et al.* 2003; Bickelhaupt and Baerends 2003; Frenking *et al.* 2003; Nemcsok *et al.* 2004; Esterhuysen and Frenking 2004; Lein and Frenking 2005; Jacobsen 2005; Kovacs *et al.* 2005; Krapp *et al.* 2006; Suresh and Frenking 2010; Hopffgarten and Frenking 2012].

Summary

The part A of Chapter 1 gives a brief introduction about the history and development of organocatalysis and the classification of organocatalysis into Lewis base catalysis, Lewis acid catalysis, Brønsted base catalysis and Brønsted acid catalysis. Enantioselective organocatalysis has emerged as a powerful synthetic strategy that is complementary to metal-catalyzed transformations and has accelerated the progress of new methods to make diverse chiral molecules. The newly emerging field of asymmetric organocatalytic domino reactions has also been introduced.

The part B of Chapter 1 deals with the theoretical background of computational methods which are commonly used in computational chemistry calculations. This part includes a brief account on the Schrödinger equation and the major approximations used to solve it, the Hartree-Fock theory which is the fundamental of much of the electronic structure methods, the post HF methods, the density functional theory, the polarized continuum model and some specific electronic properties. Today computational chemistry plays an important role in the detailed analysis of structural and energetic features of the transition states and intermediates in the catalytic cycle and offers valuable information on understanding and developing improved catalysts. Computational chemistry simulates chemical structures and reactions numerically, by incorporating the results of theoretical chemistry with the aid of efficient computer programs.

Mechanistic Studies on (*S*)-Proline Catalyzed Mannich and Aldol Reactions

acetaldehyde   *N*-acetyl benzaldimine   *β*-aminoketone

Mannich reaction

CH$_3$CN

1.72 (*S*)- proline   2.13
(catalyst)

conformational preferences

DMSO

aldol reaction

acetone   acetaldehyde   *β*-hydroxyketone
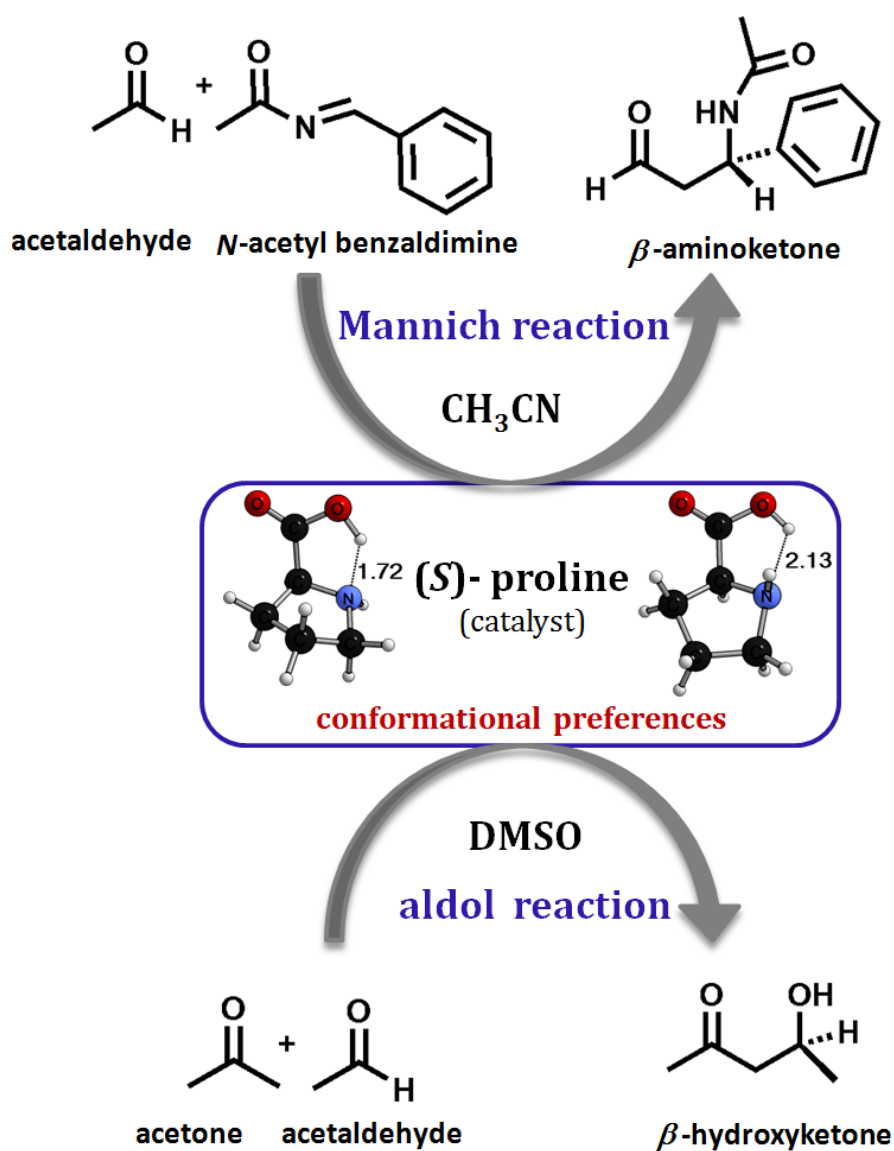
Abstract

In Part A of this chapter, a detailed mechanistic investigation of the C-C bond formation step in (S)-proline catalyzed Mannich reaction of acetaldehyde with N-acetyl protected benzaldimine in acetonitrile solvent has been described. Sixteen possible diastereomeric pathways have been analyzed to understand how stereoelectronic features invoke enantioselectivity of the final product. Both kinetic and thermodynamic factors of the reaction obtained using various DFT methods point out that si-enantiofacial nucleophilic attack of anti-enamine on the iminium carbon of the E, s-cis N-acetyl protected imine is the stereoselective pathway. Structural features of the transition states predicted that enamine in anti conformation attacks the imine through a Burgi-Dunitz trajectory to yield the stereocenter. Computations at B3LYP-PCM/6-311++G(3df,2p)//B3LYP-PCM/6-31G(d,p) level showed a strong linear correlation between Burgi-Dunitz angle and activation energy when anti-enamine is used as nucleophile to react with all the configurations of the imine. Further, energy decomposition analysis (EDA) has been carried out at B3LYP/TZ2P+ level for all the transition states, which revealed that the most dominant factor that control the enantioselectivity of the (S)-proline catalyzed Mannich reaction is steric effect. Though the less favored transition states showed high amount of stabilizing orbital interaction, the destabilizing steric effects from both Pauli repulsion and preparation energy for the reactant molecules are very high and overshadowed the stabilizing effects. However, in the most favored transition state, a balanced outcome of electronic

and steric effects was observed. Solvation effect was nearly the same for all the transition states and electrostatic effects showed no correlation to the rank order of the energy of the transition states.

*In part B of this chapter, the full catalytic cycle of the stereoselective (S)-proline catalyzed aldol reaction of acetone and acetaldehyde in dimethyl sulfoxide (DMSO) solvent has been described using three different DFT methods, viz. B3LYP, MPWB1K, and B97D in conjunction with the PCM method. At all the levels of theory, one of the higher energy conformers of the catalyst, **1b** showed higher activity than the most stable conformer, **1a**. On the basis of $\Delta G^{\#}$ of 39.8 kcal/mol (B97D-PCM level) observed for the reaction of **1a** with acetone, **1a** is considered to be inactive in the catalytic cycle while the same reaction with **1b** showed 22.7 kcal/mol lower value of $\Delta G^{\#}$ than **1a**. All the possibilities for enamine formation and C-C bond formation step have been considered for describing the most appropriate stereoselective catalytic cycle which showed that the full cycle is made up of a relay of eight proton transfer steps and the reaction is categorized under hydrogen bond catalysis. The hydration across the iminium bond of the second nucleophilic adduct – an intermediate formed subsequent to the aldehyde addition to the enamine – is the rate limiting step of the reaction with $\Delta G^{\#} = 21.7$ kcal/mol (B97D-PCM level).*

Part A: (*S*)-Proline Catalyzed Mannich Reaction

2.1 Introduction

(*S*)-proline catalyzed asymmetric synthesis [Bui and Barbas III 2000; Córdova *et al.* 2002; Kofoed *et al.* 2003; Bøgevig *et al.* 2004; Córdova 2004; Hayashi 2005; Enders *et al.* 2005; Cabrera *et al.* 2008; Enders and Narine 2008; Hahn *et al.* 2008] remains a powerful method for the generation of optically active chiral domains in a number of biologically active and pharmaceutically important compounds [Mukherjee *et al.* 2007]. Although Hajos and co-workers [Hajos and Parrish 1974] and Wiechert and co-workers [Eder *et al.* 1971] independently reported the first highly enantioselective organocatalytic reactions in the early 1970s, the use of small organic molecules in asymmetric catalysis came out as a dazzling area only after three decades [List *et al.* 2000]. The (*S*)-proline catalyzed Mannich reaction received much attention for the synthesis of chiral nitrogen containing molecules [List 2000; List 2001; Sakthivel *et al.* 2001]. The three-component Mannich reaction of ketones, aldehydes, and amines gave *β*-amino ketones in good yields and high enantioselectivities. Various *anti*-Mannich reactions have also been investigated using pipecolic acid and pyrrolidine derivatives as catalysts [Cheong *et al.* 2006; Mitsumori *et al.* 2006; Zhang *et al.* 2008]. However, the use of unmodified carbonyl compounds led to unfavorable side reactions and resulted in low quantitative yield of enantiomeric products. To overcome this drawback, indirect Mannich variants [List *et al.* 2002] have been developed that assign specific role for each carbonyl compound in the reaction mixture. The treatment of acetaldehyde [Alcaide and Almendros 2008] with the aliphatic and aromatic *N*-Boc imines in presence of (*S*)-proline gives *β*-amino aldehydes in moderate yield and good enantioselectivity [Yang *et*

al. 2008]. Similar methods are also applied to different types of Mannich reactions such as double Mannich and cross Mannich reactions [Yang *et al.* 2007; Tanaka *et al.* 2008; Chandler *et al.* 2009].

Houk and co-workers theoretically showed that stereochemistry of the C-C bond formation in (*S*)-proline catalyzed Mannich reaction follows *si*-enantiofacial attack of the enamine on the carbonyl compound whereas it is *re*-enantiofacial attack in (*S*)-proline catalyzed aldol reaction even though both the reactions followed a metal free Zimmerman-Traxler-like transition states [Bahmanyar and Houk 2003; Allemann *et al.* 2004]. Their studies demonstrated that a proton transfer from the carboxylic acid moiety of the proline to the developing alkoxide ion is essential for the C-C bond formation [^aBahmanyar and Houk 2001; Bahmanyar and Houk 2003; Clemente and Houk 2004]. Alternative mechanism involving oxazolidinone intermediate is also extensively studied by several groups [Seebach *et al.* 2007; Schmid *et al.* 2010; Blackmond *et al.* 2010; Sharma and Sunoj 2010]. Fu and co-workers explained the stereoselectivities of the direct *anti-* and *syn*-Mannich reactions catalyzed by different amino acids [Fu *et al.* 2008]. Theoretical investigation of the stereocontrolling step of (*S*)-proline catalyzed Mannich reaction of cyclohexanone, formaldehyde, and aniline were also carried out recently [Parasuk and Parasuk 2008]. Uchimaru and co-workers studied conformational behavior of imine and enamine molecules for the C-C bond formation and showed that protonation of the Mannich product preferentially occurs at the nitrogen atom [Hayashi *et al.* 2008]. Theoretical investigation on the stereoselectivities of direct organocatalytic Mannich reactions involving ketimines was also reported recently [Li *et al.* 2009].

The aim of the present study is to understand the rationale behind good yield and very high enantioselectivity (enantiomeric ratio 99:1) of (*S*)-proline catalyzed Mannich reaction of acetaldehyde with *N*-Boc imines in acetonitrile solvent [Yang *et al.* 2008]. To achieve this, rigorous transition state modeling is carried out to locate all possible

diastereomeric C-C bond formation pathways of the reaction. This study will also focus on how the stereoelectronic factors around the reaction center affect the enantioselectivity of the reaction. The insights obtained from this study may find applications in the rational design of new organocatalysts with considerable structural and stereochemical complexity.

2.2 Computational Methods

All the geometries including the transition state structures were optimized using the standard B3LYP functional [Lee *et al.* 1988; Becke 1993] and 6-31G(d,p) basis set together with PCM [Mennucci *et al.* 1999; Cossi *et al.* 2002]. B3LYP is a hybrid generalized gradient approximation (GGA) method which incorporates the exact Hartree-Fock exchange and built with the Becke's three-parameter exchange functional (B3) in conjunction with the Lee–Yang–Parr correlation functional (LYP) [Lee *et al.* 1988; Becke 1993]. The selected solvent is acetonitrile (dielectric constant = 36.64) and additional input keywords, (radii = UAHF) and scfvac were specified for the PCM calculations [Barone *et al.* 1997]. The united atom topological model for Hartree Fock (UAHF) keyword is specified to build the cavity for PCM calculation which is automatically set by the program according to the molecular topology, hybridization, formal charge, *etc.* [Cossi *et al.* 2002]. Gaussian 03 suite of programs [Frisch *et al.* 2004] was used for all the calculations. The *N*-Boc (*N*-protecting tert-butoxy carbonyl) group of the benzaldimine in this reaction [Yang *et al.* 2008] was replaced by acetyl group to reduce the computational cost. The transition states were located using QST3 method [Peng and Schlegel 1993; Peng *et al.* 1996] as implemented in Gaussian 03 and were ascertained by first order saddle points pertaining to the desired reaction coordinates. Further, intrinsic reaction coordinate (IRC) calculations were carried out with B3LYP-PCM/6-31G(d,p) level to authenticate the result [Gonzalez and Schlegel 1989; Gonzalez

and Schlegel 1990]. Energetics of the reactions were also tested by doing single point PCM calculations with GGA functionals PBE [Perdew *et al.* 1996] and BP86 [Perdew 1986; Becke 1988], meta GGA functional TPSS [Tao *et al.* 2003], hybrid GGA functionals B3LYP [Lee *et al.* 1988; Becke 1993], and hybrid meta GGA functional MPWB1K [Lynch *et al.* 2000; Lynch *et al.* 2003] using 6-311++G(3df,2p) basis set on the B3LYP-PCM/6-31G(d,p) level optimized geometries. Throughout this paper the energetics of the reaction is discussed on the basis of the B3LYP-PCM/6-311++G(3df,2p)//B3LYP-PCM/6-31G(d,p) level zero-point energy (ZPE) corrected SCF energy (ΔE_{rel}) and Gibbs free energy (ΔG_{rel}) values with respect to the infinitely separated reactants, unless otherwise specified. The activation energies, $\Delta E^{\#}$ and $\Delta G^{\#}$ are respectively the difference in ZPE-corrected electronic energy and Gibbs free energy between a transition state and the corresponding reactants. Energy decomposition analysis (EDA) was performed at B3LYP/TZ2P+ level [Barone *et al.* 1994; Boese *et al.* 2005] on all the transition states using the decomposition scheme as implemented in ADF program [Bickelhaupt and Baerends 2000; Velde *et al.* 2001], which is based on Morokuma's energy decomposition scheme [Morokuma 1977] to Kohn-Sham molecular orbitals and the extended transition state partitioning scheme of the orbital interactions developed by Ziegler and Rauk [Ziegler and Rauk 1977]. The ADF basis set TZ2P+ for all the elements have triple-ξ quality and augmented by two sets of polarization functions [Huzinaga 1965; Dunning Jr 1971; Dunning Jr 1989]. For all EDA calculations, the B3LYP-PCM/6-31G(d,p) level optimized geometries have been used and the use of triple-ξ quality basis set in EDA assures reliable results [[a]Fernandez *et al.* 2010; [b]Fernandez *et al.* 2010].

2.3 Stereoelectronic Features of Imine and Enamine in C-C Bond Formation

The most attractive feature of the (*S*)-proline catalyzed Mannich reaction between acetaldehyde and benzaldimine in acetonitrile solvent [Yang *et al.* 2008] is the high enantioselectivity of the reaction (enantiomeric ratio 99:1). A plausible catalytic cycle for this reaction is depicted in Scheme 2.1 in which the catalyst attacks the acetaldehyde to form an iminium ion-water complex and then rearranges to form an enamine with the release of one water molecule. In the subsequent step, the enamine promotes a nucleophilic attack on benzaldimine to form a C-C bond with the generation of one stereocenter. The water molecule present in the medium may add at this stage to the developed iminium bond (C=N) to give the final product with the regeneration of catalyst. Enantioselectivity of the reaction can be envisaged by exploring different possibilities for the C-C bond formation step.
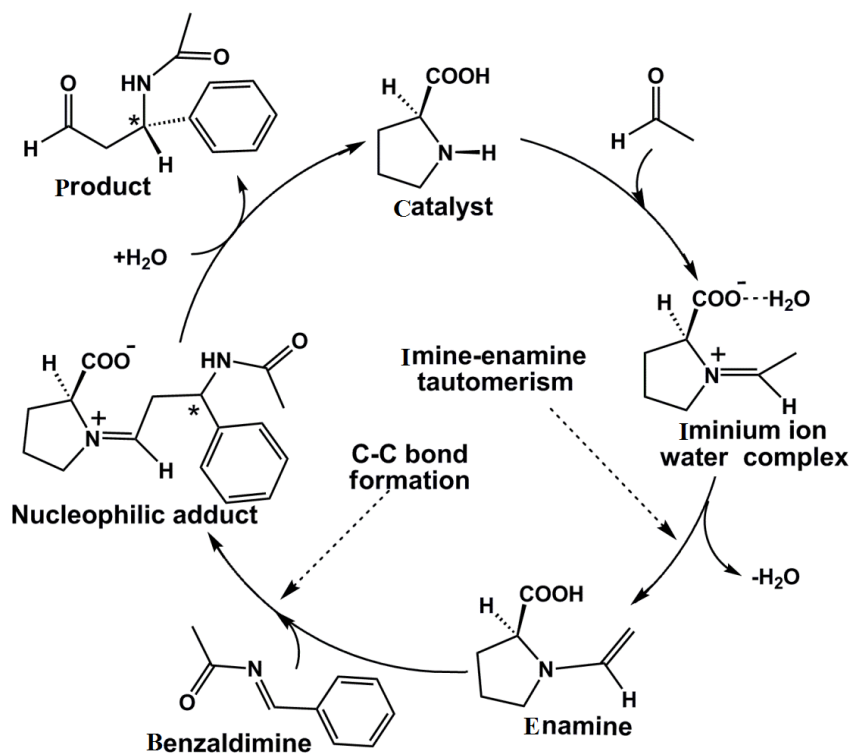
Scheme 2.1 Plausible mechanism of the (*S*)-proline catalyzed Mannich reaction.

Proline mediated enamine formation is well established in the literature [Allemann *et al.* 2004; Parasuk and Parasuk 2008] and therefore this stage of the reaction will not be discussed in detail. Our results also supported the earlier results that direct pathway leading to *syn*-enamine (CC double bond and COOH are in the same side of the molecule) is highly favored (15.5 kcal/mol) than other pathways. However, *syn*- to *anti*-enamine conversion is possible due to easy C-N bond rotation ($\Delta G^{\#}$ = 9.5 kcal/mol). Both *syn*- and *anti*-enamine forms are nearly isoenergetic as the former is more stable than the latter by only 0.1 kcal/mol.

To understand the diastereoselective C-C bond formation step, both *syn*- and *anti*-enamine forms are reacted with the possible conformations of *N*-acetyl benzaldimine. *N*-acetyl benzaldimine can have four geometrical isomers as shown in Figure 2.1 where the *E* and *Z* notations are used in accordance with the arrangements of priority groups around the iminium C=N bond while the *s-cis* and *s-trans* notations are used with respect to the iminium C=N bond and the C=O bond of acetyl group. Both *E*-isomers are more stable than the *Z*-isomers.
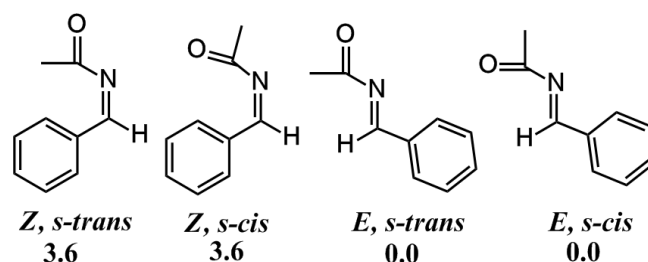
Figure 2.1 Four geometrical isomers of *N*-acetyl benzaldimine. Relative energies (ZPE corrected) are given in kcal/mol.

The *syn*-enamine can attack the different isomers of benzaldimine either in *re*-enantiofacial mode or in *si*-enantiofacial mode resulting in eight different transition states for the C-C bond formation (Figure 2.2). Similarly the *si*- and *re*-enantiofacial attack of *anti*-enamine on the iminium carbon of the *N*-acetyl benzaldimine can result in another

eight different transition states (Figure 2.3). For the calculation of energetics reported in Figures 2.2 and 2.3, the combination of most stable form of enamine (*syn*) and benzaldimine (*E,s-trans*) is used as the reference.

In Figure 2.2, **TS$_a$**, **TS$_b$**, **TS$_c$**, and **TS$_d$** are the transition states in the diastereomeric pathways for the *si*-enantiofacial attack of the *syn*-enamine whereas **TS$_e$**, **TS$_f$**, **TS$_g$**, and **TS$_h$** are the transition states in the diastereomeric pathways for the *re*-enantiofacial attack of the *syn*-enamine. The $\Delta E^{\#}$ and $\Delta G^{\#}$ values depicted in Figure 2.2 suggest that *si*-enantiofacial mode of attack of enamine in a particular transition state is preferred over the corresponding *re*-enantiofacial mode of nucleophilic attack. It is also
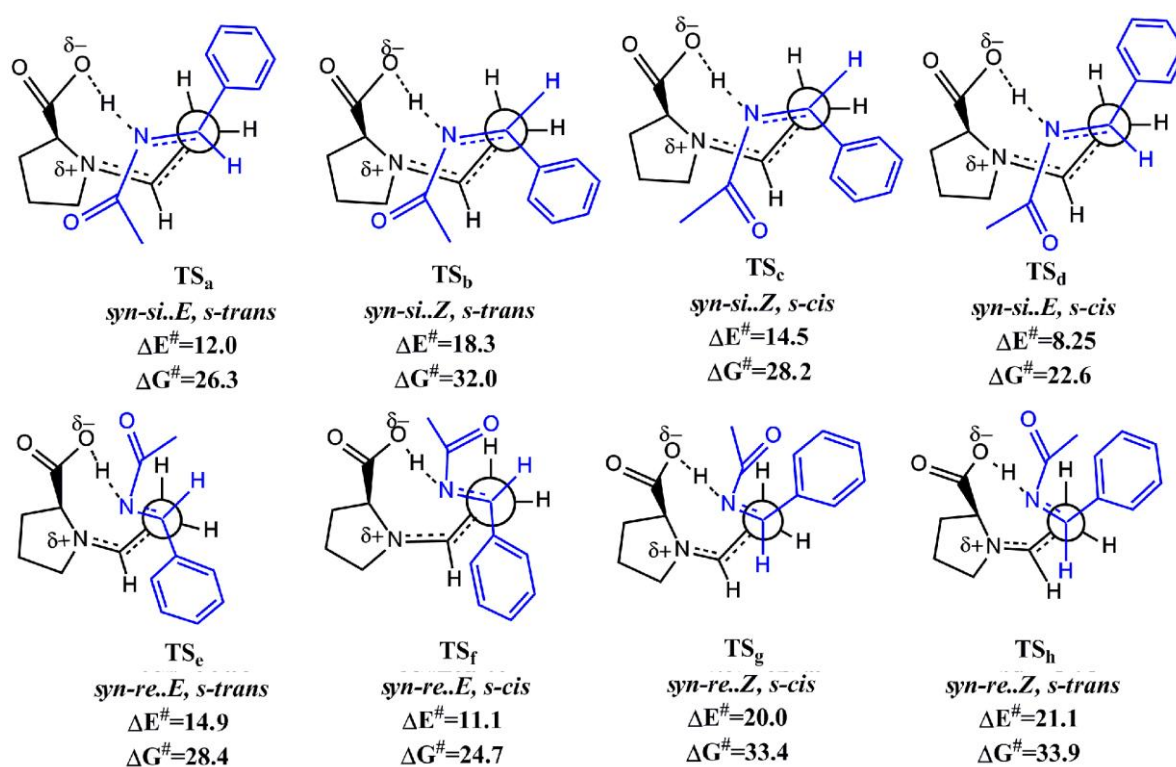
Figure 2.2 Transition states corresponding to different diastereomeric pathways for the formation of C-C bond between *syn*-enamine and *N*-acetyl benzaldimine. Activation parameters ($\Delta E^{\#}$ and $\Delta G^{\#}$) are reported with respect to the infinitely separated reactants. All values are in kcal/mol at B3LYP-PCM/6-311++G(3df,2p)//B3LYP-PCM/6-31G(d,p) level.

interesting to note that the transition states showing the *E*-form of benzaldimine are more stable than their *Z*-form counterparts and the reason for this can be attributed to the inherent destabilizing effect of *Z*-configuration in these structures. Similarly geometrical arrangement of *s-cis* form of benzaldimine is preferred over the corresponding *s-trans* arrangement. However it is clear from the energetics given in Figure 2.2 that the configuration that *N*-acetyl benzaldimine (*E* or *Z*) adopts in the transition state is more important than the mode of nucleophilic attack of the enamine (*si* or *re*) for reaching a lower energy transition state. The *si*-enantiofacial attack of *syn*-enamine on the *E, s-cis* imine gives the most stable **TS$_d$** ($\Delta G^{\#}$ = 22.7 kcal/mol) and in this case too, the destabilizing steric and lone pair effects are very small compared to other transition states.

Among the eight different diastereomeric pathways for the *si*- and *re*-enantiofacial attack of the *anti*-enamine on the benzaldimine (Figure 2.3), the most stable is **TS$_l$** and it corresponds to the *si*-facial nucleophilic attack of *anti*-enamine on benzaldimine in *E, s-cis* configuration ($\Delta G^{\#}$ = 18.9 kcal/mol). The $\Delta G^{\#}$ of all other modes of reaction will fall in the range of 21.7 to 30.2 kcal/mol. The energetics of all the sixteen pathways (**TS$_a$** to **TS$_p$**) can be related with the preferred mode of orientation of the enamine and benzaldimine fragments in the respective transition states. The enamine in *anti* conformation always yields lower energy pathway than its *syn* conformation. The *E*-configuration (based on the priority groups around the CN double bond) of the benzaldimine is always better than the *Z*-configuration for diastereoselectivity. The *s-cis* configuration (based on the orientation of the CN and CO double bonds) of the benzaldimine is always preferred than the corresponding *s-trans* configuration. The *si*-enantiofacial nucleophilic attack of *anti*-enamine is always less energy demanding than the corresponding *re*-enantiofacial attack. These observation thus justify that the *anti-si...E, s-cis* mode of attack (**TS$_l$**) is most favorable. Further, in all the sixteen transition
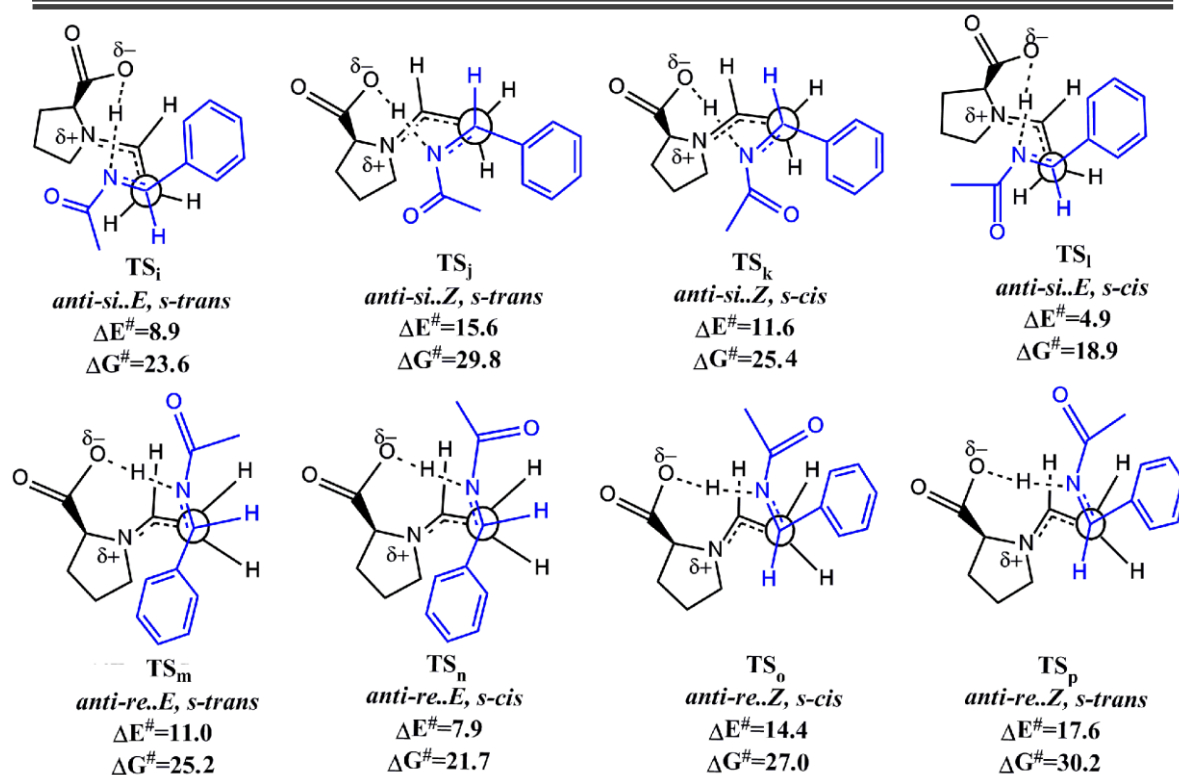
Figure 2.3 Transition states corresponding to different diastereomeric pathways for the formation of C-C bond between *anti*-enamine and *N*-acetyl benzaldimine. Activation parameters ($\Delta E^{\#}$ and $\Delta G^{\#}$) are reported with respect to the infinitely separated reactants. All values are in kcal/mol at B3LYP-PCM/6-311++G(3df,2p)//B3LYP-PCM/6-31G(d,p) level.

states described herein, the formation of intermolecular hydrogen bond between acidic hydrogen of the proline and nitrogen atom of the benzaldimine is necessary for the maximum stabilization of negative charge developed at the iminium nitrogen along with the nucleophilic attack which subsequently led to the C-C bond formation as noted previously [Arno and Domingo 2002]. The energetics of the diastereomeric pathways of the C-C bond formation step obtained using other DFT functionals are very similar to that of the B3LYP. Pure GGA and meta GGA functionals have slightly lowered the activation energies compared to the hybrid GGA and hybrid meta GGA functionals. All methods agree to the conclusion that the most favorable pathway for the C-C bond

formation is a nucleophilic attack of the *anti*-enamine on the iminium carbon of the *E, s-cis N*-acetyl protected imine *via* the transition state **TS$_l$**.

In Figure 2.4(a), a general mode of approach of a nucleophile (Nu) to the electrophilic carbon of a carbonyl system is presented with a good choice for the probable Nu-C=O angle and this angle is known as Burgi-Dunitz angle [Burgi *et al.* 1973; Burgi *et al.* 1974; Burgi and Dunitz 1983]. The Burgi-Dunitz description of the nucleophilic attack can be extended to rationalize the Nu-C=C angle of enolates and Nu-C=N angle of related electrophiles. In light of this argument, the structure of **TS$_l$** is depicted in Figure 2.4(b) where the C-C=N angle of 99.2° is the Burgi-Dunitz angle since the C-C bond formation can be considered as the outcome of a nucleophilic attack by the terminal carbon of the C=C bond of the enamine to the electrophilic carbon of the imine. The preferred pathway explained the enantiomeric excess (98%) observed in the experiment *via* the Curtin-Hammett principle (Eq. 2.1). According to Curtin-Hammett principle,

$$ee = \frac{e^{(-\delta\Delta G/RT)}-1}{e^{(-\delta\Delta G/RT)}+1} \qquad \text{(Eq. 2.1)}$$

where, $-\delta\Delta G$=2.71 kcalmol^{-1} , R=1.987*10^{-3} kcalK^{-1}mol^{-1} and T=298.15 K.

In Figure 2.5, the Burgi-Dunitz angle of all the transition states is plotted against the activation energy ($\Delta E^{\#}$) of the C-C bond formation step. A strong linear correlation exists between the two quantities when the enamine reacts in the *anti* conformation with the benzaldimine (correlation coefficient = 0.966) and the transition state showing the smallest Burgi-Dunitz angle (**TS$_l$**) yields the most preferred pathway. Five of the transition states from *syn*-enamine conformation may also strictly follow the Burgi-Dunitz pathway as they fit well on the correlation line while the deviated points **TS$_e$**, **TS$_f$**, and **TS$_h$** may be considered as exceptions. The correlation also suggests that the
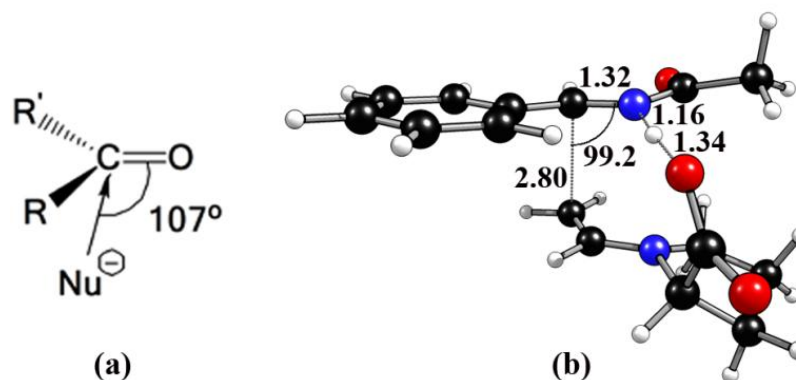
Figure 2.4 (a) Definition of Burgi-Dunitz angle for the nucleophilic attack on carbonyl systems and (b) geometry of the most preferred transition state. Bond lengths are given in Å and angles in degrees.
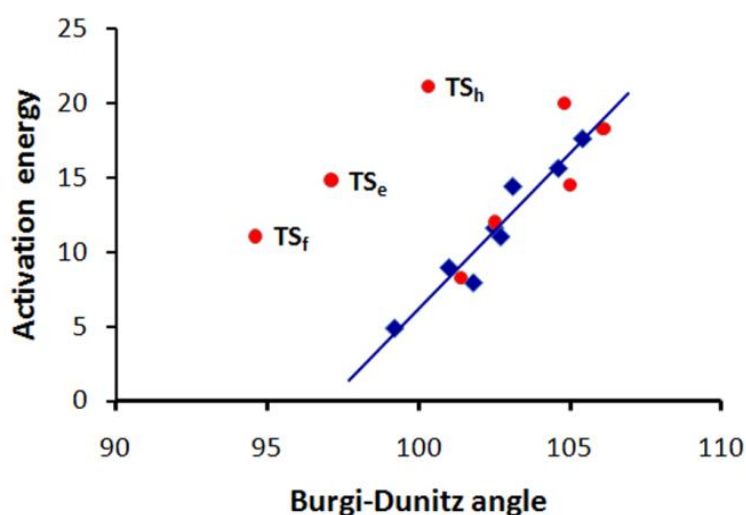
Figure 2.5 Correlation between Burgi-Dunitz angle (in degrees) and activation energy (in kcal/mol). Red circles represent the transition states showing *syn* conformation of the enamine whereas blue squares represent *anti* conformation of the enamine. The correlation line is for the blue squares.

stereocenter formation in (*S*)-Proline catalyzed Mannich reaction of acetaldehyde is controlled by a Burgi-Dunitz trajectory.

In Table 2.1, the C-C, N-H, and O-H distances of all the sixteen transition states are presented along with the Burgi-Dunitz angle. Interestingly, the most favorable **TS**ₗ

has the longest C-C interaction distance as well as the shortest O-H distance. It means that only a mild activation of the C=N bond is enough to transfer the proton to the carboxylate group if the approach of the imine is in *E, s-cis* form and the enamine is in *anti-si* form.

Table 2.1 Bond distances and Burgi-Dunitz angle of diastereomeric transition states for the C-C bond formation step of the (*S*)-proline catalyzed Mannich reaction of acetaldehyde and *N*-acetyl benzaldimine.

Transition states	C-C bond distance (Å)	N-H bond distance (Å)	O-H bond distance (Å)	Burgi-Dunitz angle (°)
TS$_a$	2.520	1.121	1.419	102.5
TS$_b$	2.347	1.096	1.476	106.1
TS$_c$	2.460	1.105	1.428	105.0
TS$_d$	2.572	1.126	1.390	101.4
TS$_e$	2.512	1.145	1.374	97.1
TS$_f$	2.663	1.140	1.378	94.6
TS$_g$	2.195	1.496	1.063	104.8
TS$_h$	2.410	1.119	1.407	100.3
TS$_i$	2.614	1.127	1.411	101.0
TS$_j$	2.420	1.124	1.418	104.6
TS$_k$	2.684	1.155	1.350	102.5
TS$_l$	2.802	1.162	1.343	99.2
TS$_m$	2.658	1.086	1.516	102.7
TS$_n$	2.755	1.091	1.483	101.8
TS$_o$	2.784	1.094	1.466	103.1
TS$_p$	2.648	1.078	1.522	105.4

2.4 An Energy Decomposition Analysis

In the case of transition states given in Figure 2.2 and Figure 2.3, the EDA method (Chapter 1-Part B; Section 1.6.9) can be applied because each transition state can

be considered as made up of a benzaldimine fragment (A) and an enamine fragment (B). The analysis of ΔE_{int} and the four terms (ΔE_{Pauli}, ΔE_{ele}, ΔE_{orb}, and ΔE_{prep}) that contribute to the ΔE_{AB} provides a convenient way to assess the stereoelectronic aspects of the reaction. It may be noted that ΔE_{AB} (Table 2.2) and the $\Delta E^{\#}$ reported in the previous sections are very similar quantities. $\Delta E^{\#}$ is computed from the ZPE and solvation energy corrected total energies of the transition state and the corresponding weak complex of bezaldimine and enamine whereas for ΔE_{AB}, the difference between the total energy of the transition state and the sum of the total energies of the most stable states of benzaldimine and enamine are used. Therefore, excluding the correction terms and the

Table 2.2 Energy-decomposition analysis (B3LYP/TZ2P+) of the sixteen transition states (all energies are in kcal/mol).

TS	ΔE_{int}	ΔE_{ele}	ΔE_{orb}	ΔE_{Pauli}	ΔE_{prep}	ΔE_{AB}
TS$_a$	-58.9	-79.5	-142.5	163.2	75.3	16.5
TS$_b$	-68.2	-88.1	-167.7	187.7	91.9	23.7
TS$_c$	-63.4	-84.9	-147.5	169.0	79.9	16.5
TS$_d$	-54.6	-79.0	-133.2	157.6	63.9	9.3
TS$_e$	-49.5	-78.9	-129.6	158.9	69.4	19.9
TS$_f$	-51.5	-77.2	-124.51	150.3	63.3	11.8
TS$_g$	-17.8	-66.7	-68.70	117.6	35.7	17.9
TS$_h$	-54.8	-79.3	-145.63	170.1	81.0	26.2
TS$_i$	-57.2	-76.8	-135.50	155.1	71.3	14.1
TS$_j$	-57.9	-79.3	-144.75	166.1	78.7	20.8
TS$_k$	-49.0	-69.9	-115.72	136.7	63.2	14.2
TS$_l$	-46.5	-71.4	-112.67	137.5	53.5	7.0
TS$_m$	-71.4	-89.4	-163.85	181.9	89.6	18.3
TS$_n$	-69.5	-86.1	-151.93	168.5	79.2	9.7
TS$_o$	-71.0	-85.3	-146.07	160.3	87.5	16.5
TS$_p$	-73.3	-87.0	-164.36	178.1	99.4	26.1

complexation energy, ΔE_{AB} and $\Delta E^{\#}$ should behave similarly and indeed they show a good correlation (correlation coefficient = 0.942).

In Figure 2.6, the EDA terms ΔE_{int}, ΔE_{Pauli}, ΔE_{ele}, ΔE_{orb}, and ΔE_{prep} are plotted against the ΔE_{AB}. None of these quantities show a strong correlation to ΔE_{AB}. However, except the case of **TS$_g$**, a linear trend can be found for the plots of (ΔE_{Pauli}, ΔE_{AB}),
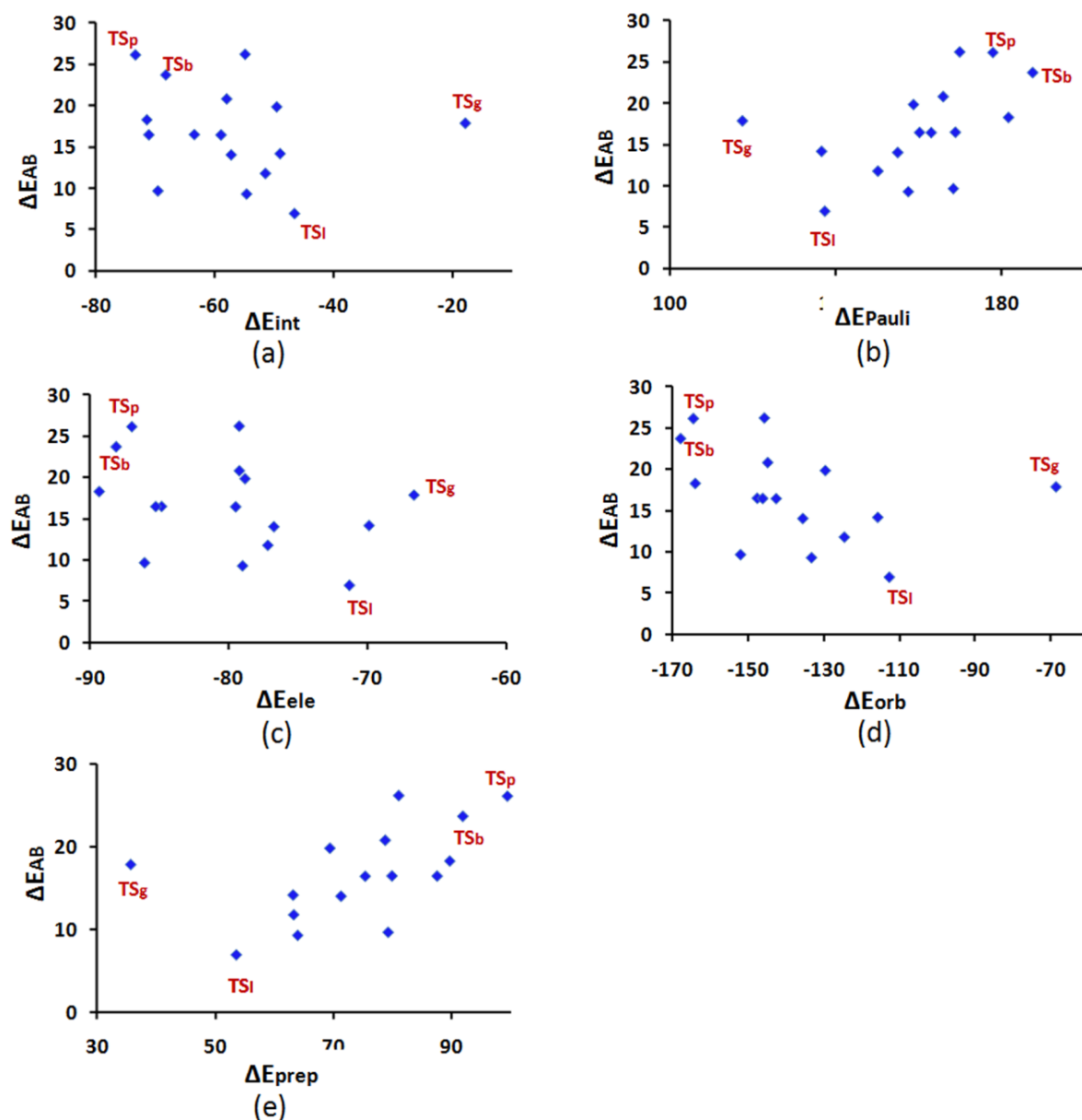
Figure 2.6 Plots showing comparison of the energy contributions of (a) ΔE_{int} (b) ΔE_{Pauli} (c) ΔE_{ele} (d) ΔE_{orb}, and (e) ΔE_{prep} to the ΔE_{AB} of various transition states. Some representative systems are depicted with labels.

(ΔE_{prep}, ΔE_{AB}), and (ΔE_{orb}, ΔE_{AB}) where the first two cases show an increase in the ΔE_{AB} with respect to an increase in the corresponding destabilizing energy terms while in the last case, the ΔE_{AB} increases with an increase in the stabilizing orbital interaction. Interestingly, the stabilizing ΔE_{int} is the lowest for the most stable transition state **TS$_l$** while high values of ΔE_{int} are observed for more unstable transition states **TS$_b$**, **TS$_h$**, and **TS$_p$**. The ΔE_{orb}, the main contributor to the stabilizing part of ΔE_{int} follows a trend similar to ΔE_{int}. **TS$_g$** is clearly an exception to these trends because only in this case the O-H bond of the COOH moiety of the enamine is retained while this bond is broken in all other cases (Table 2.1). In **TS$_g$**, the magnitude of ΔE_{orb}, ΔE_{Pauli}, and ΔE_{prep} are significantly smaller than the rest while its ΔE_{ele} is comparable to the rest. Therefore in **TS$_g$** the electrostatic effect would play a significant role in the activation process whereas in all other cases, this effect does not show any dependency to the rank order of the activation energies (Figure 2.6(c)).

In general, high values of ΔE_{AB} is observed for those transition states showing high amount of stabilization from ΔE_{orb}, which is counterintuitive as one would expect a decrease in the activation energy with an increase in the stabilizing interactions. It means that the stabilizing electronic effects are overshadowed by the destabilizing steric effects, which comes from the ΔE_{prep} and ΔE_{Pauli}. The contributions of ΔE_{prep} is considered mostly steric in nature due to the fact that it describes mainly the structural reorganization of the substituents around the activated region of the transition state, *viz.* the COOH moiety of the enamine and the CHO and phenyl moieties of benzaldimine.

Thus the EDA analysis clearly suggests that the most dominant factor that control the enantioselectivity of the (*S*)-proline catalyzed Mannich reaction is the steric effect. The electrostatic effects are not significant except the case of **TS$_g$** while the orbital interactions contribute more for those transition states showing high activation energies.

2.5 Concluding Remarks on Mannich reaction

For an unbiased approach to stereoselectivity, all possible pathways for the C-C bond formation step of the Mannich reaction are modeled by considering both *syn-* and *anti*-enamine conformers as well as four possible geometrical isomers of *N*-acetyl benzaldimine. Results from various DFT methods converged to the same conclusion that the *si*-facial nucleophilic attack of the *anti*-enamine on the benzaldimine in the *E, s-cis* configuration through **TS$_l$** is the most preferred diastereomeric pathway. In general it can be said that for similar transition states, enamine in *anti* conformation is preferred over *syn* conformation, *si*-facial nucleophilic attack of enamine is preferred over *re*-enantiofacial nucleophilic attack, *E*-configuration of benzaldimine is preferred over the *Z*-configuration and *s-cis* form of benzaldimine is preferred over the *s-trans* form. All these requirements are fulfilled in the most preferred transition state **TS$_l$**. Irrespective of the mode of reaction, geometrical features of the majority of the transition states followed a clear Burgi-Dunitz trajectory for the C-C bond formation step which is supported by the fact that $\Delta E^{\#}$ correlates linearly with the Burgi-Dunitz angle. The solvation effect is nearly the same for all the transition states and thus not a deciding factor for the stereoselectivity.

Further, the observed enantioselectivity of the Mannich reaction is opposite to that of inter and intramolecular aldol reaction catalyzed by (*S*)-proline. EDA analysis is applied for the first time to understand the stereoselectivity of an organocatalytic reaction which clearly showed that steric effect is the most dominant factor that controls the enantioselectivity of (*S*)-proline catalyzed Mannich reaction. In the most favored transition state (**TS$_l$**), the reactants undergo only small amount of structural deformation whereas in the highly disfavored transition states, drastic structural changes occurred. Though the orbital interactions were strong in difficult transition states, the high amount

of preparation energy worked against the corresponding pathways. On the other hand, a balanced effect of ΔE_{int} and ΔE_{prep} were in favor of the **TS₁**. Thus, EDA showed that minimization of the destabilizing steric effects is very important for obtaining enantioselectivity in (*S*)-proline catalyzed Mannich reaction. Since the focus of the study is on the stereoelectronic aspects that control the C-C bond formation step, full mechanism of the Mannich reaction is not considered for a discussion. The predicted enantiomeric excess using Curtin-Hammett principle on the preferred pathway is in good agreement with the experimental results and the product showed an (*S*) configuration which also agreed with the experiment.

Part B: (*S*)-Proline Catalyzed Aldol Reaction

2.6 Introduction

The naturally occurring amino acid (*S*)-proline is extensively used as a catalyst for both intramolecular and intermolecular stereoselective aldol reactions [Hoffmann *et al.* 1998; List *et al.* 2000; List 2002; List *et al.* 2004; Gruttadauria *et al.* 2008] and in fact, (*S*)-proline catalyzed Hajos-Parrish reaction [Eder *et al.* 1971; Hajos and Parrish 1974] discovered in the 1970s is considered as a prototype of asymmetric catalysis. The high stereoselectivity of (*S*)-proline catalyzed aldol reactions is attributed mainly to the formation of hydrogen bonded transition states [Sakthivel *et al.* 2001; Lacoste 2006]. Mainly four mechanistic pathways have been proposed for the C-C bond formation step of Hajos-Parrish reaction (Figure 2.7), (*i*) the Hajos-Parrish mechanism involving a carbinolamine intermediate (nucleophilic substitution mechanism), (*ii*) the Hajos-Parrish mechanism involving an enamine intermediate (enaminium-catalyzed mechanism), (*iii*) the Agami's mechanism [Agami *et al.* 1985; Agami *et al.* 1986] involving two proline molecules, and (*iv*) the List's mechanism [List 2002] involving assistance from carboxylic acid of the proline (carboxylic acid catalyzed enamine mechanism). Transition state modeling at density functional theory (DFT) level by Houk and co-workers supported mechanism (*iv*) [Li *et al.* 1988; [a]Bahmanyar and Houk 2001; [b]Bahmanyar and Houk 2001; Hoang *et al.* 2003; Clemente and Houk 2004; Cheong and Houk 2005; Clemente and Houk 2005], originally put forward by Jung [Jung 1976] as the most favorable pathway. Further, detailed mechanistic investigation at DFT level has been done by Boyd and co-workers [Rankin *et al.* 2002; Ban *et al.* 2002]. Arno and Domingo studied different possibilities for the diastereoselective C-C bond formation for

Nucleophilic substitution
mechanism

Enaminium-catalyzed
mechanism

Dual proline
enaminium-catalyzed
mechanism

Carboxylic acid-catalyzed
enamine mechanism
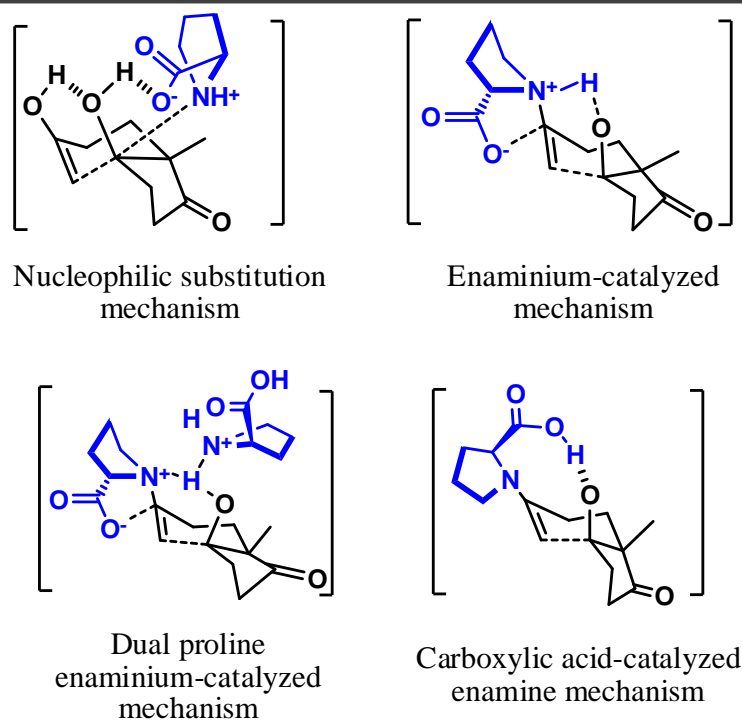
Figure 2.7 Mechanisms proposed for the proline catalyzed intramolecular aldol reactions.

the intermolecular aldol reaction between acetone and propanaldehyde and found that the *anti-re* attack of the catalyst gives the desired product [Arno and Domingo 2002]. Houk and co-workers established the stereoselectivity and elucidated the complete mechanism of (*S*)-proline catalyzed intramolecular aldol reaction of an achiral triketone [Hoang *et al.* 2003; Bahmanyar and Houk 2003; Allemann *et al.* 2004].

Using experimental set up with LA-MB-FTMW spectrometer, very recently Alonso and co-workers reported extensive conformational studies on (*S*)-proline and identified eight different minimum energy conformers [Lesarri *et al.* 2002; Mata *et al.* 2009]. The geometrical structures of those conformers are given in Figure 2.8. This proves that (*S*)-proline possesses considerable conformational flexibility due to the ring flipping and different orientation of the -COOH moiety with respect to the ring nitrogen. Therefore, for a systematic and unbiased approach to organocatalytic reactions, conformational study of the catalyst becomes important to discover the most favorable

pathway [Pidun and Frenking 1998]. Previous mechanistic studies have not addressed this issue of conformational behaviour of the catalytically active regions. In this chapter, we make such an attempt to describe full mechanistic pathways using different (*S*)-proline conformers and also unambiguously bring out the active role played by a high energy conformation of (*S*)-proline in the reaction between acetone and acetaldehyde. Further, we will show that the full catalytic cycle can be visualized in terms of a chain of proton transfer pathways involving eight different steps in terms of Gibbs energy profile. The proposed complete proton transfer mechanism is expected to be relevant in the study of aldol reactions catalyzed by enzymes in biological system [Rothlisberger *et al.* 2008].

2.7 Computational Methods

All geometries including the transition state structures were optimized at three different density functional theory (DFT) methods, *viz.* B3LYP/6-31G(d,p), MPWB1K/6-31++G(d,p) and B97D/6-311+G(d,p). B3LYP is a hybrid generalized gradient approximation (GGA) method which incorporates the exact Hartree-Fock exchange and built with the Becke's three-parameter exchange functional (B3) in conjunction with the Lee–Yang–Parr correlation functional (LYP) [Lee *et al.* 1988; Becke 1993]. Although this method is good for main group chemistry [Suresh *et al.* 2007; Krishnan *et al.* 2008; Pillai *et al.* 2008], recent studies pointed out the shortcomings in estimating the barrier heights and modeling noncovalent interactions [Wodrich *et al.* 2006; [a]Zhao and Truhlar 2008]. MPWB1K is a hybrid meta-GGA method formulated by Truhlar and co-workers [Zhao and Truhlar 2004] which has been recently used for making good predictions on thermochemistry, thermochemical kinetics, hydrogen bonding, and weak interactions [Suresh *et al.* 2009; Mohan *et al.* 2010]. B97D is a recently developed DFT method by Grimme [Grimme 2006] which includes a semiempirical correction for the treatment of van der Waals (dispersion) interaction.

Very recently, this method has been successfully applied for some mechanistic investigations [Peverati and Baldridge 2008; Moss *et al.* 2010; Ducháčková *et al.* 2010; Kadlčíková *et al.* 2010]. In all the three DFT methods, solvent effects were also included by applying the PCM method of the self consistent reaction field for full optimization [Mennucci *et al.* 1999; Cossi *et al.* 2002]. To indicate the PCM option, the DFT methods are named as B3LYP-PCM, MPWB1K-PCM and B97D-PCM. Solvent parameters of dimethyl sulfoxide (DMSO) are used in the calculation. The B3LYP-PCM, MPWB1K-PCM calculations were performed using Gaussian 03 [Frisch *et al.* 2004] and B97D-PCM calculations were performed using Gaussian 09 [Frisch *et al.* 2009] suites of quantum chemical programs. The UAHF keyword is specified to build the cavity for PCM calculation which is routinely set by the program according to the molecular topology, hybridization, formal charge, *etc.* [Cossi *et al.* 2002]. The transition states (TSs) were located using synchronous transit-guided *quasi*-Newton method (QST3) [Peng and Schlegel 1993; Peng *et al.* 1996]. TSs were characterized by only one imaginary frequency (first order saddle points) relevant to the desired bond-breaking/bond-forming reaction coordinates. Further, IRC calculations were performed to verify the connectivity of transition states to the proper reactants and products. Always the relative Gibbs free energy (ΔG_{rel}) is reported with respect to infinitely separated reactants (the most stable (*S*)-proline conformation, acetone and acetaldehyde) in the solvent unless otherwise specified.

2.8 Elucidation of complete catalytic cycle

2.8.1 Selection of (*S*)-Proline Conformations

Different conformations of (*S*)-proline are depicted in Figure 2.8 along with relative free energy at the three different DFT levels. The most stable conformation is **1a** which is in agreement with the LA-MB-FTMW experimental results [Lesarri *et al.* 2002;

Mata *et al.* 2009]. Close proximity of the acidic proton and the N-lone pair in **1a**, **1b,** and

1d would bring in bi-functionality to the catalyst towards an approaching carbonyl

compound by simultaneous attack through N-lone pair on the carbonyl carbon and

interaction of the acidic proton on the developing alkoxide moiety. Such a bi-

functionality nature is not possible with other conformations. Since **1a** and **1d** differ

only in the orientations of the methylene moieties, both would show very similar

behavior in mechanistic studies. Hence, we have considered only **1a** and **1b** for detailed

mechanistic studies. Further, the transition state search for the nucleophilic adduct from

conformers **1e**, **1f**, **1g**, and **1h** failed and the reason is attributed to their inability to

	1a	**1b**	**1c**	**1d**
ΔG_{rel}	0.0, *0.0*, **0.0**	5.9, *6.3*, **5.9**	8.2, *8.2*, **7.6**	0.3, *0.5*, **0.5**

	1e	**1f**	**1g**	**1h**
ΔG_{rel}	3.4, *3.8*, **4.8**	3.5, *3.7*, **4.5**	4.7, *5.2*, **6.1**	4.7, *5.0*, **5.4**
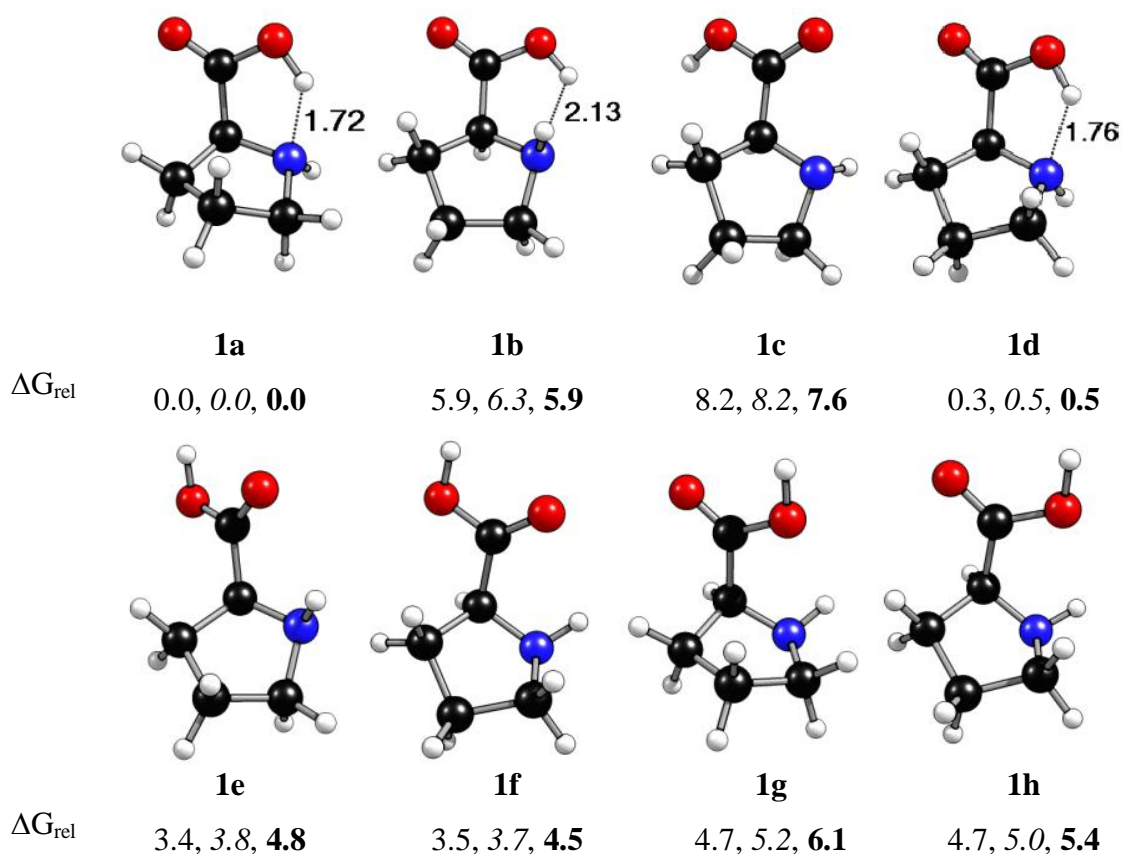
Figure 2.8 Different conformers of (*S*)-proline. Numerical values in regular, italics, and bold fonts are the relative Gibbs energies (ΔG_{rel}) with respect to the most stable conformer (**1a**) in kcal/mol at B3LYP-PCM, MPWB1K-PCM, and B97D-PCM levels respectively. B97D-PCM level structures are given.

transfer the carboxylate proton to the developing alkoxide moiety of the approaching carbonyl compound and a transition state search from **1c** is converged to that from **1b**. **1a** is more stable than **1b** by 5.9 kcal/mol at B97D-PCM/6-311+G(d,p) level and possesses a *syn*-orientation for C-H bond of the chiral carbon and the N-H bond of the ring nitrogen, whereas the C-H and the N-H bonds of **1b** exhibit anti orientation. Higher stability of **1a** can be attributed to the intramolecular O-H**...**N hydrogen bond of distance 1.72 Å. The zwitterionic form of the catalyst **1a** (more stable than the neutral **1a** by 0.9 kcal/mol in DMSO solvent) is also modeled which is expected to be catalytically inactive due to the quaternization of the nitrogen centre. Since quaternization removes the nucleophilicity of the nitrogen, this tautomer is not considered for the mechanistic studies.

2.8.2 Initial Nucleophilic Attack: Active Form of the Catalyst

Using the *(S)*-proline conformations **1a** and **1b**, the nucleophilic attack of the N-lone pair on the carbonyl carbon of acetone is investigated. Acetone is preferred rather than aldehyde for the initial reaction and hence in intermolecular aldol reaction, aldehyde is added slowly to the performed solution of proline and ketone [Calderon *et al.* 2008] to overcome the side reactions arising from the inability of the catalyst to differentiate between the aldehyde and ketone for the initial nucleophilic attack. The free energy profiles for the (**1a** + acetone) and (**1b** + acetone) reactions are presented in Figure 2.9 and Figure 2.10, respectively. In the case of **1a**, the pre-reacting complex of the proline and acetone (**2a**) has to pass through the transition state TS_{1a} (ΔG_{rel} = 20.3 kcal/mol) to reach the zwitterionic intermediate **3a**. The zwitter ion to neutral form (**3a** → TS_{2a} →**4a**) generates the highest point TS_{2a} in the free energy profile (ΔG_{rel} = 39.8 kcal/mol). The activation free energy barrier ($\Delta G^{\#}$) for this step is 19.3 kcal/mol. On the whole, the reaction is endergonic by 30.0 kcal/mol of energy. It is thus clear that this highly endergonic reaction requiring a high value of ΔG_{rel} for TS_{2a} may not occur at specified
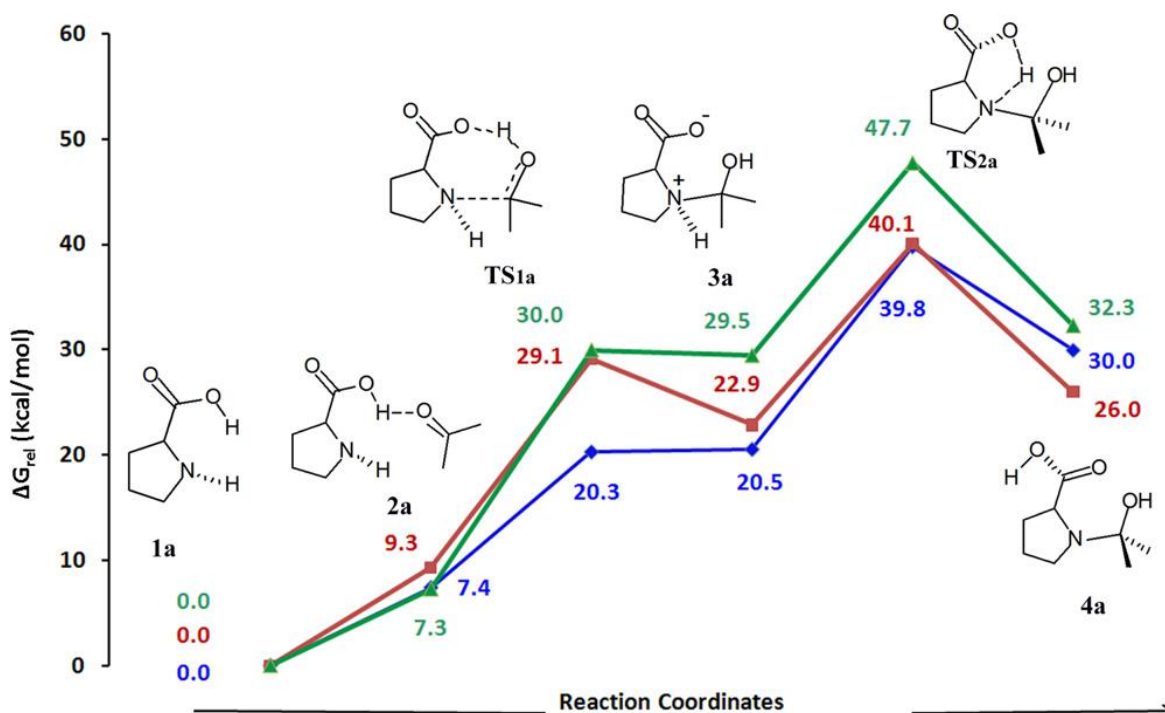
Figure 2.9 Energy profile diagram for the initial nucleophilic attack by **1a**. Numerical values are the relative Gibbs energies (ΔG_{rel}) in kcal/mol (B3LYP-PCM values in green, MPWB1K-PCM in red, and B97D-PCM in blue colors) with respect to **1a**.

reaction conditions. The ΔG_{rel} values point out that the structures calculated with dispersion-corrected method are substantially more stable than those with other methods.

Enhancement in catalytic activity is expected when the N-lone pair in (*S*)-proline is readily available for the initial nucleophilic attack on the carbonyl carbon. Among all the conformations, the N-center has maximum degree of pyramidalization in **1b** (23.2^0) which indicate higher nucleophilic character from the localized N-lone pair than the other conformations. In **1a**, the lone pair is partially shielded by the O-H**···**N hydrogen bond while **1b** has a more exposed N-lone pair. If **1a** can be converted easily to **1b** *via* a pyramidal inversion at the ring nitrogen, **1b** would play a more active role in the catalysis. The $\Delta G^{\#}$ for **1a** to **1b** conformational change *via* **TS$_{ab}$** is only 11.0 kcal/mol (Figure 2.10). The reaction of **1b** with acetone, passing through a van der Waals complex
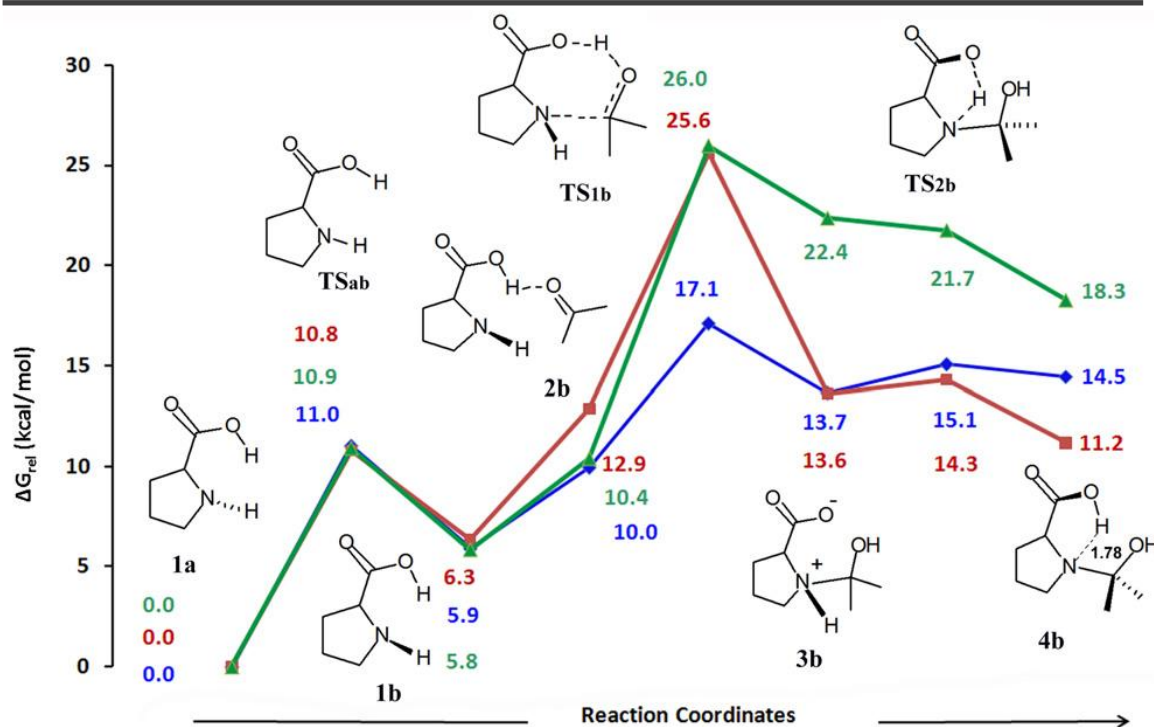
Figure 2.10 Energy profile diagram for the initial nucleophilic attack by **1b**. Numerical values are the relative Gibbs energies (ΔG_{rel}) in kcal/mol (B3LYP-PCM values in green, MPWB1K-PCM in red, and B97D-PCM in blue colors) with respect to **1a**.

(**2b**) can yield the zwitterionic intermediate **3b**. This step requires ΔG_{rel} of 17.1 kcal/mol and the associated transition state is **TS$_{1b}$**. The geometries of **2b** and **TS$_{1b}$** agree well with the recent report given by Yang and co-workers [Yang *et al.* 2010]. The next step of the reaction is nearly barrier less ($\Delta G^{\#} = 1.4$ kcal/mol). Thus, even with **1a** as the reference point for proline, the ΔG_{rel} between **1a** and **TS$_{1b}$** is only 17.1 kcal/mol (B97D-PCM) which is 22.7 kcal/mol smaller than the pathway described in Figure 2.9 using the transition state **TS$_{2a}$**. Further, the pathway passing through the intermediacy of **1b** is endergonic by 14.5 kcal/mol which is 15.5 kcal/mol lower in energy than that of the pathway exclusively *via* **1a**. However, one may argue that **4a** and **4b** are readily interconvertible due to rotation of the carboxylate group on the pyrrolidine ring, suggesting that pathways in Figure 2.9 and Figure 2.10 will have the same endergonic

character. Thus it is clear that pathway in Figure 2.9 can be discarded on the basis of the high $\Delta G^{\#}$ of 39.8 kcal/mol observed for **TS$_{2a}$** while pathway in Figure 2.10 is the right choice to carry out the reaction which also suggests that **1b** must be the active form of the catalyst and not **1a**. Hence, hereafter we have considered only the subsequent reactions from **4b** (Figure 2.10).The higher stability of **4b** than **4a** is due to a strong intramolecular N…H hydrogen bond of distance 1.78 Å in **4b** (Figure 2.10).

2.8.3 Formation of the Iminium Ion and Conversion to Enamine

Elimination of a water molecule takes place from **4b** (1-(2-hydroxypropan-2-yl)pyrrolidine-2-carboxylic acid) when it passes through **TS$_{3b}$** and forms the zwitter ionic iminium ion-water complex **5b** (Figure 2.11). At the B97D-PCM level, this step requires $\Delta G^{\#}$ of 3.5 kcal/mol of free energy while at MPWB1K-PCM level and at B3LYP-PCM levels; the $\Delta G^{\#}$ is 12.9 and 7.5 kcal/mol, respectively. At MPWB1K-PCM and B97D-PCM levels, the product system shows higher stabilization than the reactant while at B3LYP-PCM level, the product and reactant systems show nearly equal free energy. Further, the binding energy of water in **5b** is 3.6 kcal/mol at B97D-PCM level and 1.6 kcal/mol at MPWB1K-PCM level. At both these levels, the dissociation of water to **6b** is favored due to gain in entropy on the ΔG_{rel} scale. On the other hand, at the B3LYP-PCM level, the dissociation of water molecule is slightly disfavored.

(*S*)-proline catalysis is widely accepted to undergo enamine pathway [Spencer *et al.* 1965; Molines and Wakselman 1976]. Iminium ion formed can be converted to enamine in four different pathways; two water-assisted and two direct pathways which may give either *syn*-enamine or *anti*-enamine. Hence, we have considered both **5b** and **6b** for further mechanistic investigations. Although the energetics in Figure 2.11 is in favor of **6b**, pathway from **5b** also will be useful to verify the role of water. In Figure 2.12, the ΔG_{rel} of all the four diastereomeric transition states are depicted. The $\Delta G^{\#}$ for
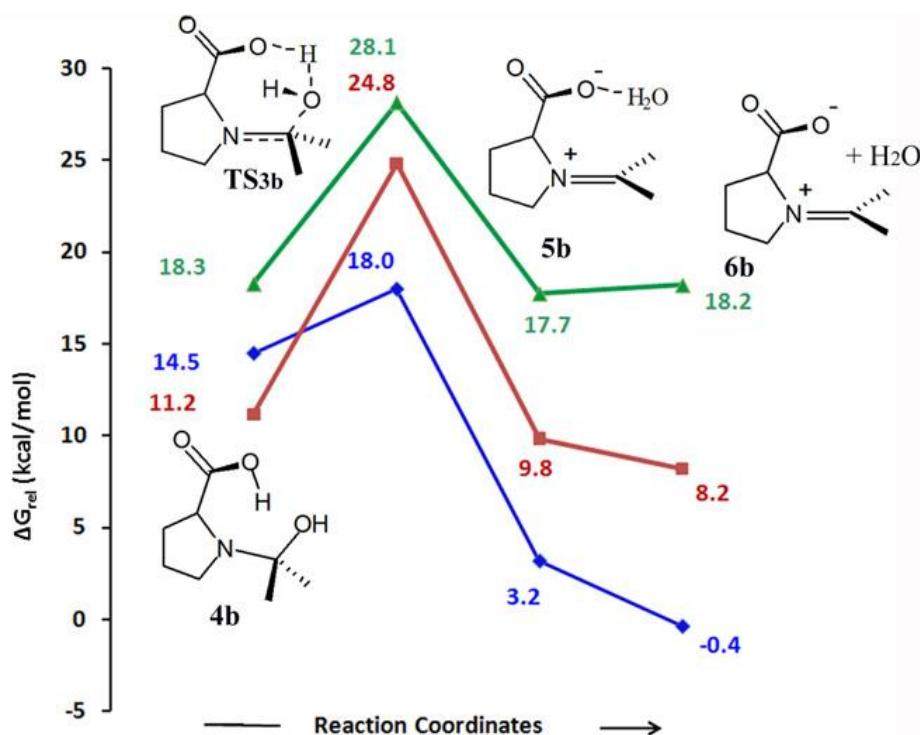
Figure 2.11 Energy profile diagram for the formation of iminium ion. The numerical values are the relative Gibbs energies (ΔG_{rel}) in kcal/mol (values of B3LYP-PCM in green, MPWB1K-PCM in red, and B97D-PCM in blue colors) with respect to **1a**.

the formation of water- assisted-*syn* enamine *via* **TS₄ₐ**, water-assisted-*anti* enamine *via* **TS₄c**, direct-*syn* enamine *via* **TS₄b** and direct-*anti* enamine *via* **TS₄d** are 23.9, 22.5, 16.2 and 28.0 kcal/mol, respectively (Figure 2.12). In general MPWB1K-PCM level $\Delta G^{\#}$ is slightly higher than B97D-PCM values while B3LYP-PCM values are slightly smaller and on the whole, all the three levels agree that the formation of *syn*-enamine (**7b**) without the assistance of water *via* **TS₄b** is the most preferred pathway. The product from **TS₄ₐ, TS₄b, TS₄c,** and **TS₄d** are respectively **7a** (*syn*-enamine water complex), **7b**, **8a** (*anti*-enamine water complex) and **8b** (*anti*-enamine). All the levels also agree that *anti*-enamine is thermodynamically the most stable structure. Though the preferred pathway leads to **7b**, formation of *anti*-enamine **8b** can be easily achieved by the N-C bond

rotation. The $\Delta G^{\#}$ for the rotation is only 5.2 kcal/mol at B97D-PCM/6-311+G(d,p) level of theory.

	TS$_{4a}$	**TS$_{4b}$**	**TS$_{4c}$**	**TS$_{4d}$**
ΔG_{rel}	35.4, *33.7*, **23.2**	30.0, *24.5*, **15.9**	35.6, *32.8*, **22.1**	44.5, *36.9*, **27.6**
$\Delta G^{\#}$	17.2, *25.5*, **23.9**	11.8, *16.3*, **16.2**	17.4, *24.6*, **22.5**	26.3, *28.6*, **28.0**

	7a	**7b**	**8a**	**8b**
ΔG_{rel}	25.5, *18.6*, **16.2**	22.1, *13.8*, **10.7**	23.3, *17.9*, **13.2**	21.1, *13.3*, **9.6**
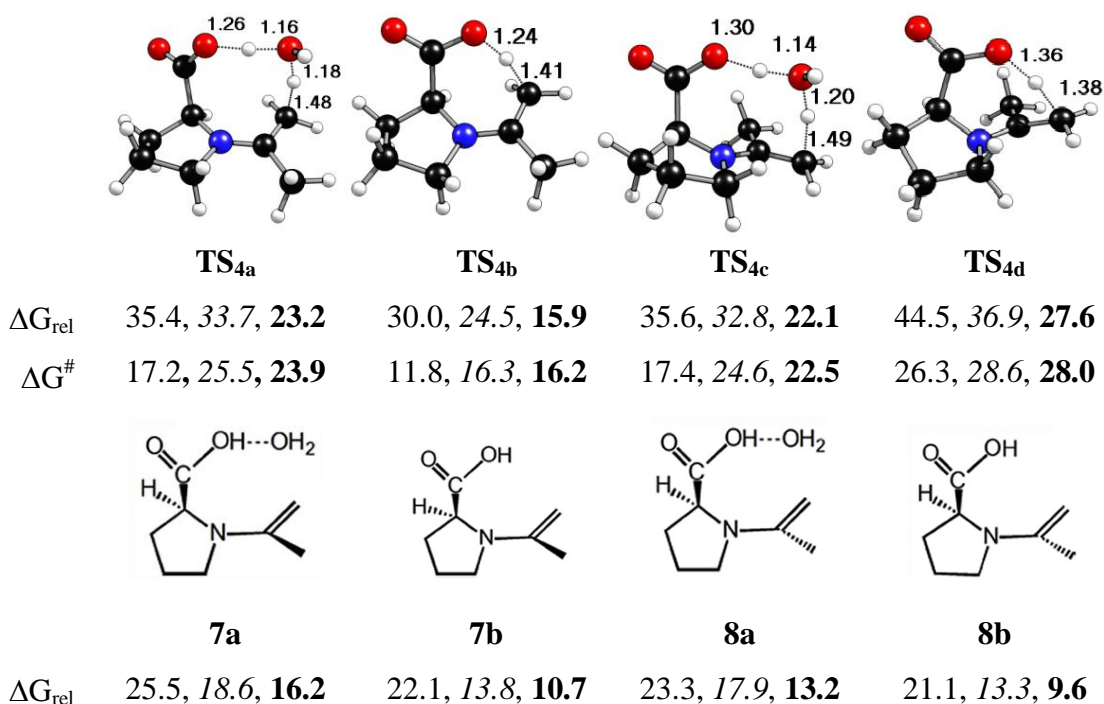
Figure 2.12 Transition states for water-assisted and direct pathways of enamine formation and the ensuing products. Numerical values are the relative Gibbs energies (ΔG_{rel}) and activation Gibbs energy barrier ($\Delta G^{\#}$) in kcal/mol (regular, italics, and bold fonts are at B3LYP-PCM, MPWB1K-PCM, and B97D-PCM levels respectively). **7a** and **7b** are *syn*-enamines and **8a** and **8b** are *anti*-enamines. B97D-PCM level structures are given.

2.8.4 Second Nucleophilic Attack (C-C Bond Formation Step)

The second nucleophilic attack of enamine on acetaldehyde is accountable for the C-C bond formation step. Since **7b** and **8b** are nearly iso-energetic and easily interconvertible, both were considered for modeling *si-* and *re-* facial nucleophilic attack on the carbonyl carbon of the approaching electrophiles. Accordingly, four different diastereomeric pathways for the C-C bond formation is considered *viz.* the *anti-si via* **TS$_{5a}$,** *anti-re via* **TS$_{5b}$,** *syn-si via* **TS$_{5c}$,** and *syn-re via* **TS$_{5d}$** (Figure 2.13) which account

	TS$_{5a}$	**TS$_{5b}$**	**TS$_{5c}$**	**TS$_{5d}$**
ΔG_{rel}	36.9, *31.2*, **20.4**	37.1, *29.6*, **19.9**	39.6, *32.8*, **22.5**	39.2, *31.9*, **21.5**
$\Delta G^{\#}$	15.8, *17.9*, **10.8**	16.0, *16.3*, **10.4**	17.5, *19.1*, 11.8	17.1, *18.1*, **10.8**

	10a	**10b**	**10c**	**10d**
ΔG_{rel}	24.3, *8.9*, **8.3**	22.1, *6.5*, **6.8**	22.7, *7.5*, **7.2**	25.1, *9.5*, **10.0**
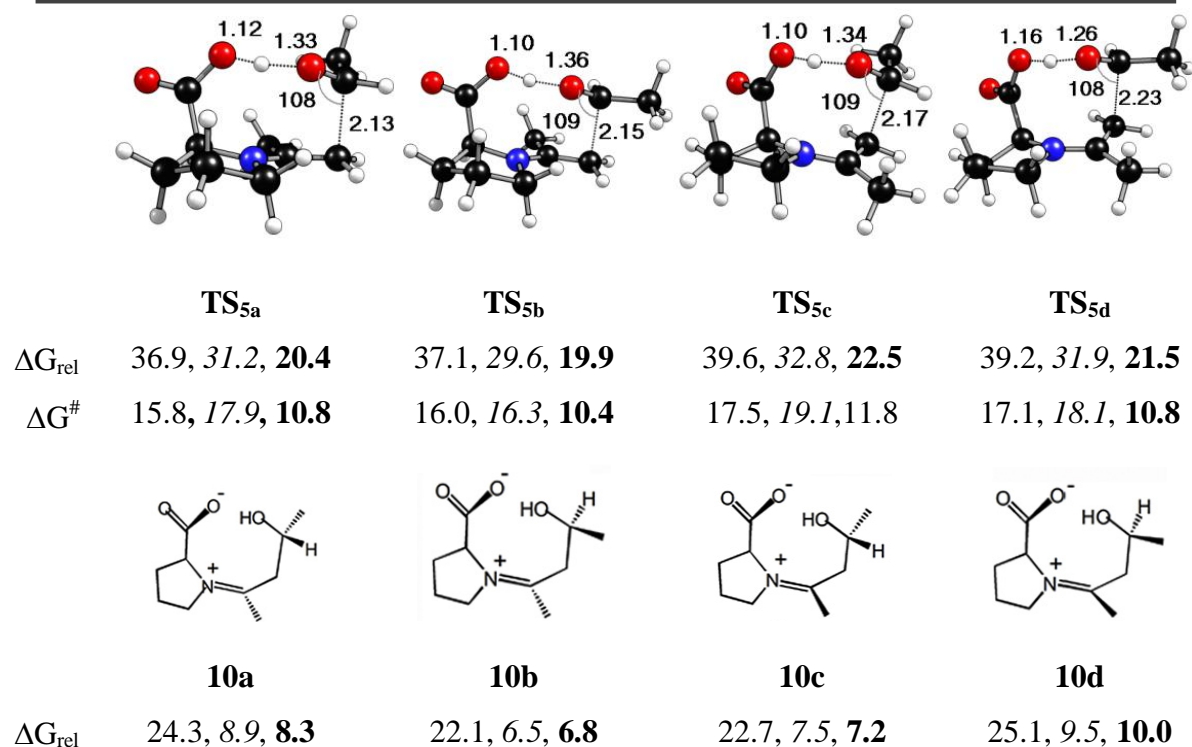
Figure 2.13 Transition states for C–C bond formation and the ensuing products. Numerical values are the relative Gibbs energies (ΔG_{rel}) and activation Gibbs energy barrier ($\Delta G^{\#}$) in kcal/mol (regular, italics, and bold fonts are at B3LYP-PCM, MPWB1K-PCM, and B97D-PCM levels respectively). B97D-PCM level structures are given.

for the stereocontrolling step of the reaction. It is interesting to note that all the pathways are Burgi-Dunitz type [Burgi *et al.* 1973; Burgi *et al.* 1974; Burgi and Dunitz 1983] where the nucleophile will attack the carbonyl carbon, forming an angle in the range of 108° to 109°. Among them, the attack of the acetaldehyde by the *anti*-enamine in a *re*-fashion *via* **TS$_{5b}$** is the most preferred one ($\Delta G^{\#}$ = 10.4 kcal/mol) which leads to the formation of the product **10b** in the (*S*)-configuration. According to Curtin-Hammett principle, the enantiomeric excess of the (*S*)-isomer is found to be 39.86 %.

2.8.5 Regeneration of the Catalyst

The product **10b** is zwitterionic and it is expected that the water molecule eliminated from **5b** can re-enter into the reaction to form the zwitterionic water complex

11b (Figure 2.14). This leads to the addition of water across the carboxylate group and the unsaturated carbon to form **12b** ($\Delta G^{\#}$ = 21.7 kcal/mol). In the next two consecutive steps, rearrangement of protons in COOH and OH moieties occur (**12b** → **TS$_{7b}$** → **13b** → **TS$_{8b}$** → **14b**) giving rise to the formation of **14b** which is a weak complex of the desired product (*S*)-β-hydroxy ketone (**15b**) and (*S*)-proline. Regeneration of the active form of the catalyst (**1b**) takes place with the release of 4.2 kcal/mol of energy. The regenerated catalyst **1b** is active to keep the catalytic cycle alive (Scheme 2.2).
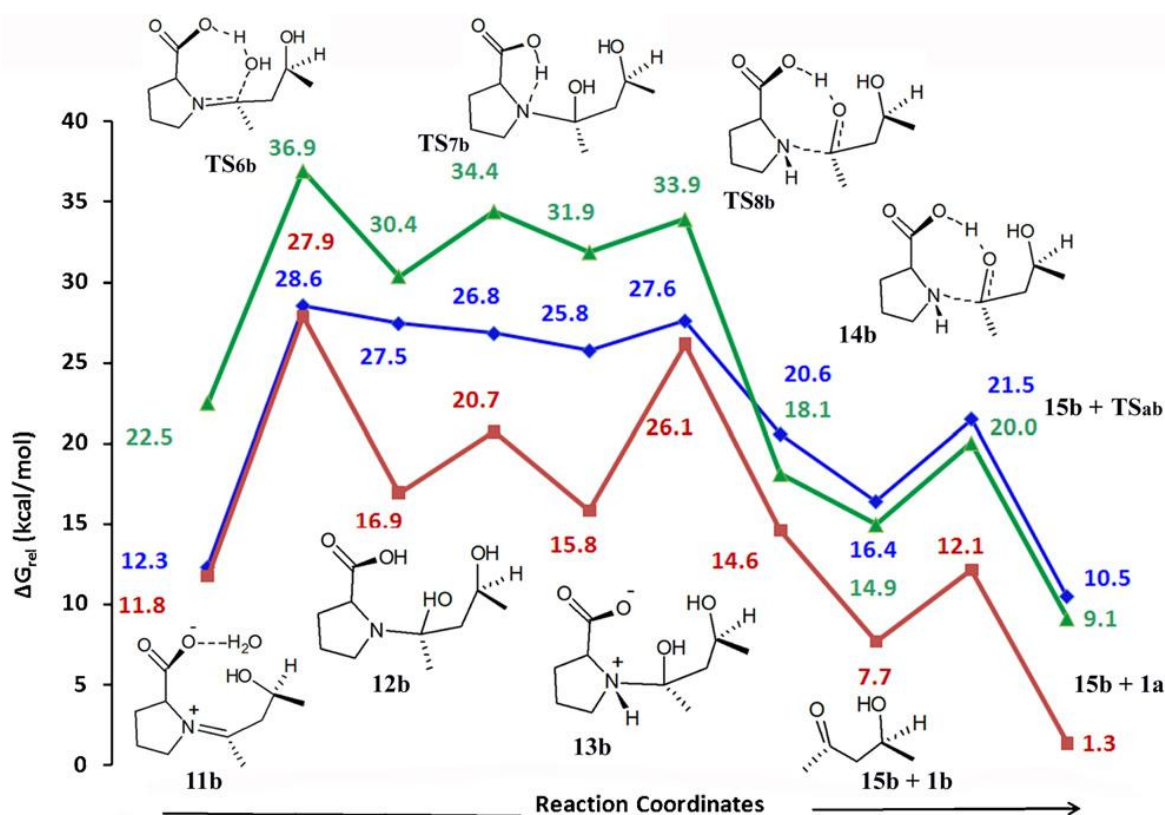
Figure 2.14 Energy profile diagram for the regeneration of (*S*)-proline catalyst. The numerical values are the relative Gibbs energies (ΔG_{rel}) in kcal/mol (values of B3LYP-PCM in green, MPWB1K-PCM in red and B97D-PCM in blue colors) with respect to **1a**.

The complete catalytic cycle of the most probable mechanism described herein passes through eight proton transfer transition states (**TS$_{1b}$, TS$_{2b}$, TS$_{3b}$, TS$_{4b}$, TS$_{5b}$, TS$_{6b}$, TS$_{7b}$,** and **TS$_{8b}$**) and they all describe proton transfer from reactant side to product side

(Scheme 2.2). The well defined hydrogen bonded frameworks in the transition states provide the driving force for the shuttling of acidic proton from COOH to ketonic/aldehydic CO and also to secondary amine functionality.
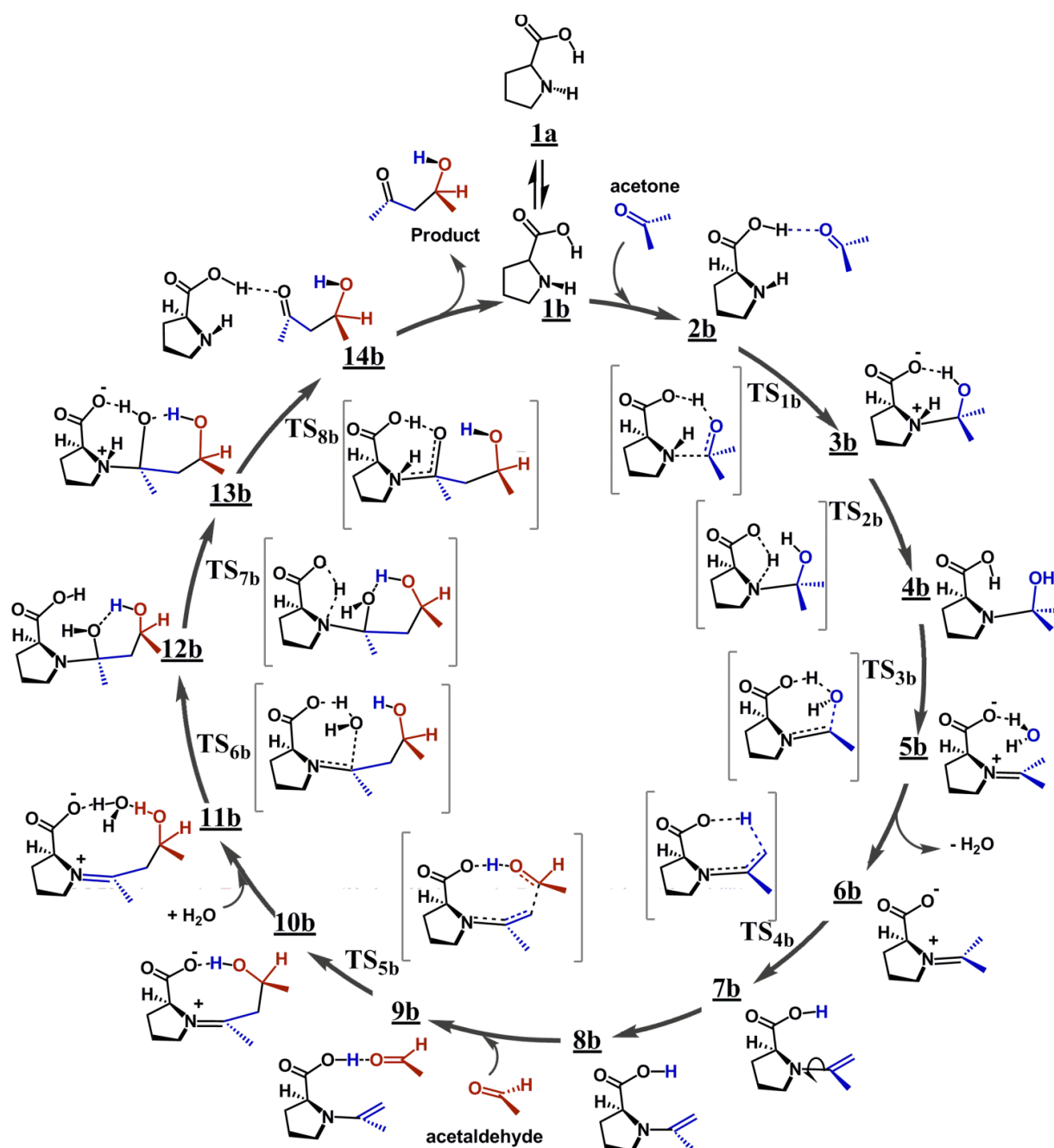
Scheme 2.2 The catalytic cycle of (*S*)-proline catalyzed intermolecular aldol reaction between acetone and acetaldehyde

2.9 Concluding Remarks on Aldol Reaction

The intermolecular aldol reaction of acetone and acetaldehyde catalyzed by (*S*)-proline have been reinvestigated by different DFT-PCM methods (B3LYP-PCM/6-31G(d,p), MPWB1K-PCM/6-31++G(d,p) and B97D-PCM/6-311+G(d,p) basis sets) and the full catalytic cycle of the reaction yielding the stereoselective product is established on the basis of dispersion-corrected B97D-PCM/6-311+G(d,p) level of theory. All the DFT methods agreed to the conclusion that a higher energy conformation of (*S*)-proline is the active form of the catalyst and not the most stable conformation. Further, the possibility of different diastereomeric transition states was investigated on the basis of relative Gibbs free energies. On the basis of the energetics obtained using the three DFT methods, the full catalytic cycle suggested five important steps, *viz.* (*i*) first nucleophilic addition between catalyst and acetone *via* **TS$_{1b}$**, (*ii*) iminium ion formation *via* **TS$_{3b}$**, (*iii*) imine-enamine conversion *via* **TS$_{4b}$**, (*iv*) C-C bond formation *via* **TS$_{5b}$**, (*v*) water addition *via* **TS$_{6b}$**. The ΔG_{rel} values indicate that structures calculated with dispersion-corrected method are substantially more stable than those with other methods. On the other hand, the B3LYP-PCM method clearly underestimates the stability of the intermediates and transition states. On the basis of the $\Delta G^{\#}$ values obtained at B97D-PCM and MPWB1K-PCM levels, it can be said that the water addition (**TS$_{6b}$**) is the most difficult step of the catalytic cycle. According to the B97D-PCM results, the second most difficult step of the catalytic cycle has to be the imine to enamine conversion (**TS$_{4b}$**). The C-C bond formation and imine to enamine conversion steps have nearly equal $\Delta G^{\#}$ at MPWB1K-PCM level while the B97D-PCM results showed that C-C bond formation is a relatively easy step.   Previous studies supported the imine to enamine conversion as the rate determining step in proline catalyzed intramolecular aldol reaction [Zhu *et al.* 2009]. On the other hand, kinetic and mechanistic studies of intermolecular aldol reaction by

Blackmond and co-workers [Zotova *et al.* 2009] suggested that the rate limiting step is the C-C bond formation. The results presented herein suggest that water addition is the most difficult step of the catalytic cycle which supports the experimental finding by Pihko and co-workers [Nyberg *et al.* 2004; Pihko *et al.* 2006]. A noteworthy feature of the reaction is that the amine and carboxylate functionalities operated in tandem for the proton migration in almost every step of the reaction through the formation of hydrogen bonds, and thus the (*S*)-proline catalyzed aldol reaction may be categorized under the hydrogen bond catalysis. In fact, it is felt that this type of hydrogen bond catalysis can play an important role in certain enzymatic reactions, particularly when carboxyl functionality of the amino acids concentrates in the active region [Rothlisberger *et al.* 2008]. This study adds new insights into our understanding of aldol reaction in terms of the conformational choice of the proline catalyst, free energy profile, proton relay mechanism and the determination of the rate limiting steps.

Summary

The part A of this chapter deals with the stereoelectronic features of imine and enamine in the diastereoselective C-C Bond Formation step of (*S*)-proline catalyzed Mannich reaction between acetaldehyde and *N*-Boc benzaldimine. The mechanistic study presented herein proves that the *si*-facial nucleophilic attack of the *anti*-enamine on the benzaldimine in the *E, s-cis* configuration is the most preferred diastereomeric pathway for the stereocontrolling step in (*S*)-proline catalyzed Mannich reaction. EDA analysis has been applied for the first time to understand the stereoselectivity of an organocatalytic reaction which clearly showed that steric effect is the most dominant factor that controls the enantioselectivity of (*S*)-proline catalyzed Mannich reaction.

The part B of this chapter deals with the elucidation of complete catalytic cycle of (*S*)-proline catalyzed aldol reaction between acetone and acetaldehyde. A higher energy conformer of (*S*)-proline is found to be the active catalyst in intermolecular aldol reaction and not the most stable conformation. The results presented herein suggest that water addition is the most difficult step in the reaction. A prominent feature of the catalytic cycle is that the amine and carboxylate functionalities operated in tandem for the proton migration in almost every step of the reaction through the formation of hydrogen bonds.

Mechanistic Studies on

NHC Catalyzed Stetter and

CO_2 Fixation Reactions

NHC mediated Stetter reaction

Benzaldehyde + Cyclopropene

Ph H + Ph

H_2O/DBU/TBD
THF-Solvent

Product

Proton transfer *via* assisted pathway

NHC mediated CO_2 fixation reaction

$\Delta G^{\#}$ = 40.4 kcal/mol
$\Delta E^{\#}$ = 39.5 kcal/mol

$\Delta G^{\#}$ = 25.6 kcal/mol
$\Delta E^{\#}$ = 24.7 kcal/mol

Energy

Reaction Coordinates
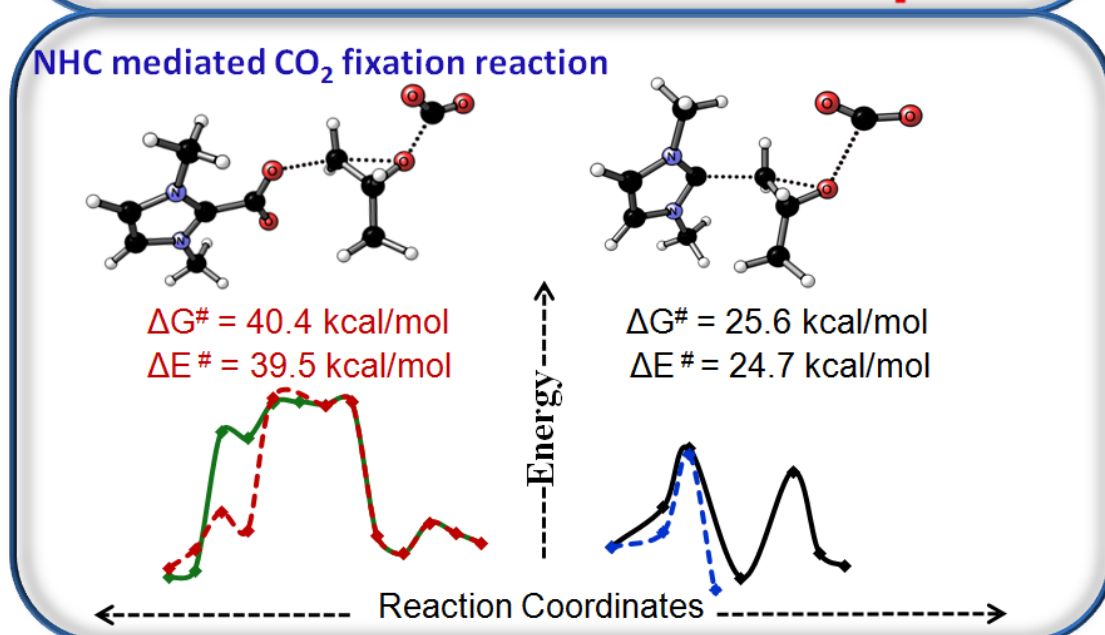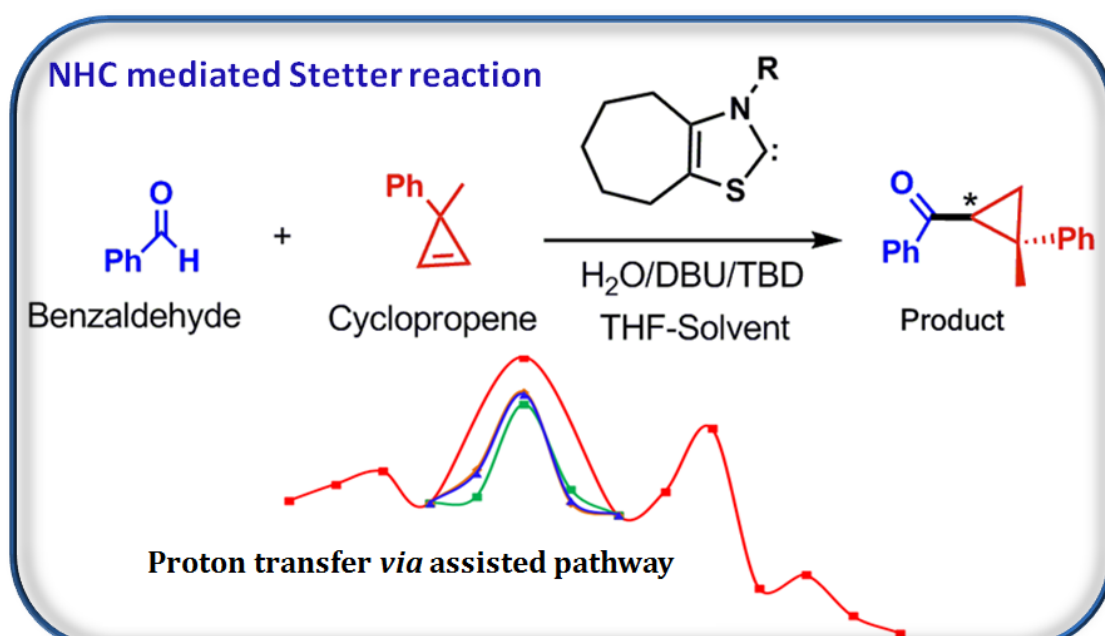
Abstract

In part A of this chapter, NHC catalyzed intermolecular Stetter reaction between benzaldehyde and cyclopropene has been described using M06-2X/6-311++G(3df,2p)//M06-2X/6-31+G(d,p) level of theory. Different mechanistic possibilities have been proposed and discussed, by identifying the key intermediates for each elementary step and the corresponding transition states interconnecting them on the respective potential energy surfaces. This analysis clearly reveals that water or bases such as DBU or TBD play an important role in the proton transfer process to form the Breslow intermediate where these species significantly lower the activation barriers (ΔG$^{\#}$ = 28.4, 23.8, and 24.3 kcal/mol respectively for 5TS-H$_2$O, 5TS-DBU, and 5TS-TBD) which otherwise will be quite high (44.8 kcal/mol) for the reaction to occur at room temperature. The nucleophilic attack of Breslow intermediate on cyclopropene with simultaneous proton transfer is the stereocontrolling step of the reaction. An early transition state (8TS; 19.5 kcal/mol) is located for the initial nucleophilic attack which is followed by the regeneration of catalyst (10TS; 4.0 kcal/mol) to get the final product. The zwitterionic intermediate formed after the C-C bond formation (9) is found to be turnover frequency determining intermediate (TDI) and subsequent transition state for regeneration of the catalyst (10TS) is identified as turnover frequency determining transition state (TDTS). Overall, the reaction is exergonic by 40.6 kcal/mol of Gibbs energy.

In part B of this chapter, six different pathways for the NHC-mediated CO_2 transformation reaction of epoxide to cyclic carbonate were discussed with DFT method at MPWB1K/6-311++G(3df,2p) level. On the basis of the computed energetics and comparison with the reported experimental results, we propose that the nucleophilic attack of NHC on the least substituted carbon of the epoxide can take place if the developing alkoxide moiety is stabilized by interaction from a CO_2. This will yield a stable zwitterionic acyclic carbonate intermediate, **15**. Formation of **15** as well as the subsequent step leading to the formation of **18** in Pathway VI are found to be ter molecular in nature. Therefore, the feasibility of this reaction can be expected only in presence of excess CO_2 under drastic experimental conditions. The most stable intermediate **18** in pathway VI may serve as the role of turnover frequency determining intermediate (TDI) and the subsequent transition state **TS$_{11}$** may act as the turnover frequency determining transition state (TDTS). The ter molecular pathway suggested for this reaction provides the role of free NHC and CO_2 in the reaction mechanism and thus contributes toward the improved design and application of this reaction.

Part A: NHC Catalyzed Intermolecular Stetter Reaction

3.1 Introduction

Since the first report of *N*-heterocyclic carbenes (NHCs) in the early sixties [Wanzlick 1962; Wanzlick 1962], and later the seminal discoveries of NHC-transition metal complexes [Öfele 1968; Wanzlick and Schönherr 1968; Öfele 1970], the development and applications of NHCs has seen great activity, to reach now a status of 'privileged' ligands in organometallic chemistry [Herrmann 2002; Nolan 2006; Glorius 2007]. In addition, NHCs are found to be efficient organocatalysts in their own right [Arduengo III 1999; Garber *et al.* 2000; Stauffer *et al.* 2000; Fürstner *et al.* 2001; Trnka and Grubbs 2001; Connor *et al.* 2002; Enders *et al.* 2007; Hahn and Jahnke 2008; De Frémont *et al.* 2009; Radius and Bickelhaupt 2009; Alcarazo *et al.* 2010; Dröge and Glorius 2010; Kirmse 2010] which represents an attractive alternative and, in some cases, offers transformations unparalleled in metal catalysis.

The phenomenal success of NHCs in organocatalysis can be attributed primarily to their electronic properties leading to different modes of action in catalysis [Biju *et al.* 2011]. The different modes of action of NHCs in organocatalysis are given in Figure 3.1. The nucleophilicity of NHCs allows its addition to electrophiles such as aldehydes (**a**). The electron-withdrawing nature of azolium moiety can acidify the R-position (**e**). Alternatively, the same tetrahedral intermediate formed in **a** can undergo hydride transfer in the presence of easily reducible substrates like activated carbonyl compounds giving acyl azolium species and a reduced reaction partner (**h**). The enaminol moiety (Breslow intermediate) formed in mode **e** is highly nucleophilic and acts as an acylating agent (**b**,

Electron-donor properties

a) nucleophilicity   b) enamine reactivity I   c) enamine reactivity II   d) enamine reactivity III
                          (external electrophile)   (conjugate)   (internal leaving group)
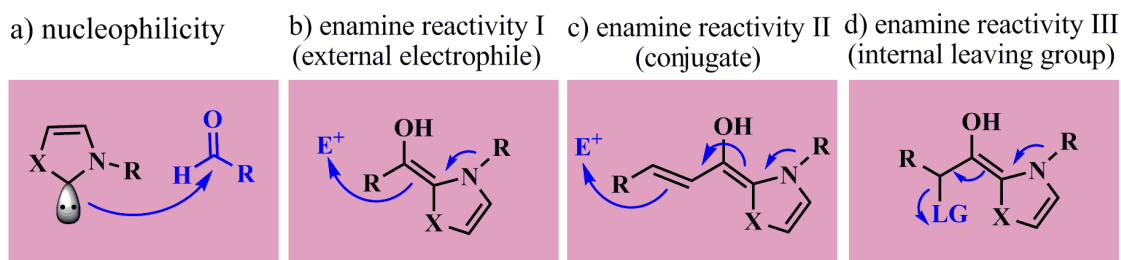
Electron-acceptor properties

e) α-acidity   f) leaving group I   g) leaving group II
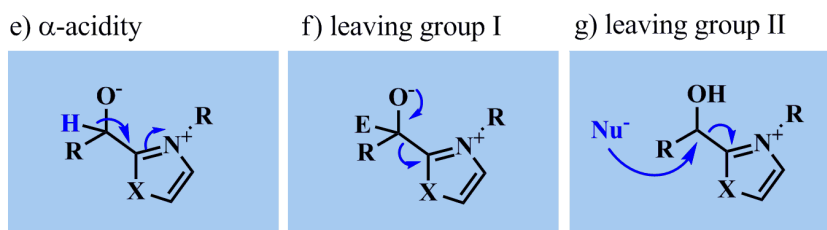
Azolium moiety as bystander

h) hydride transfer   i) enol(ate) reactivity
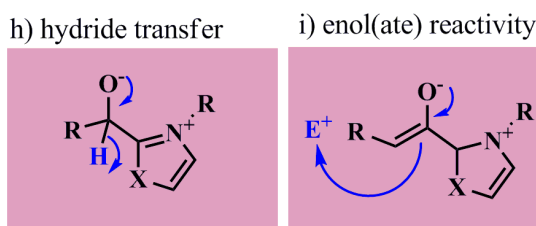
Dual mode

j) dual activation
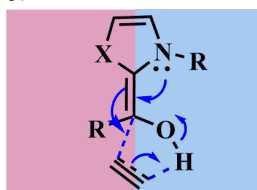
Figure 3. 1 Modes of action in NHC-organocatalysis [Biju *et al.* 2011].

then **f**). Furthermore, the addition of NHC to α,β-unsaturated aldehydes can lead to a dienaminol intermediate, rendering the α-carbon atom nucleophilic (**c**). Additionally, the enaminol can trigger elimination, if there is a leaving group at the R-position of the aldehyde (**d**). In this process, a nucleophilic enol(ate) can form, in which the attached azolium species acts as a bystander (**i**). Moreover, the catalyst can increase the

electrophilicity in acyl azolium species and act as a good leaving group, re-entering the catalytic cycle (**g**). A variety of NHC catalyzed redox processes lead to the formation of acyl azolium species using an oxidant. Finally, the Breslow intermediate can also act in a dual push-pull fashion: the positively polarized proton of the enaminol can interact with the reaction partner and withdraw electron density from it, activating it for the attack of the enamine part of the Breslow intermediate (**j**).

The electronic and steric properties of NHCs can be tuned over a broad range by choosing various nitrogen heterocycles as well as by the suitable choice of substituents on the ring carbon and nitrogen atoms. Minor structural differences can have a remarkable effect on catalytic activity and selectivity of carbenes. However, detailed insights on the mechanisms and the associated energetics are not readily available even for some of the typical NHC-organocatalytic reactions. Our interest in organocatalysis, more specifically in the participation of NHCs as catalysts prompted us to perform some theoretical studies on the molecular mechanisms of these types of reactions. In this chapter, various mechanistic possibilities involved in NHC catalyzed asymmetric Stetter reaction as well as CO_2 fixation reaction using epoxide are addressed by exploring the corresponding PES.

Recently, the use of NHCs as organocatalysts offers a unique activation mode of aldehydes, reversing their intrinsic reactivity by rendering the carbonyl carbon nucleophilic [Breslow 1958; Teles *et al.* 1996; Chiang *et al.* 2007; Nair *et al.* 2008; Cardinal-David *et al.* 2010; Berkessel *et al.* 2010; Cohen *et al.* 2011; Nair *et al.* 2011]. The corresponding nucleophilic acyl anion generated *via* this umpolung strategy can react with various electrophiles, like aldehydes, ketones, imines, polarized C=C bonds *etc*. [Burstein and Glorius 2004; Sohn and Bode 2006; Marion *et al.* 2007; Kayaki *et al.* 2009; Jousseaume *et al.* 2011; Mahatthananchai *et al.* 2011; Piel *et al.* 2011]. In the benzoin condensation and the Stetter reaction, the two conventional umpolung reactions,

there are some selectivity issues correspond to significant challenges, especially in intermolecular variants of these reactions. In intermolecular cross-benzoin reactions, high levels of selectivity were recently achieved, even in the hydroxymethylation of aldehydes with formaldehyde. The key to success was careful selection of the NHC catalyst and reaction conditions [Biju *et al.* 2011]. NHC catalyzed Stetter reaction between an aldehyde and a cyclopropene to generate acylcyclopropanes has been investigated very recently by Glorius and co-workers [Bugaut *et al.* 2011; Liu *et al.* 2011]. In Scheme 3.1, a plausible catalytic cycle of the NHC catalyzed Stetter reaction between benzaldehyde and a cyclopropene is depicted in which the catalyst attacks the benzaldehyde to form a zwitterion (*i*) and then the positively charged azolium ring acidifies the α-CH bond derived from the aldehyde to form an enamine species (*ii*). In the subsequent step, Breslow intermediate promotes a nucleophilic attack on cyclopropene to form a C-C
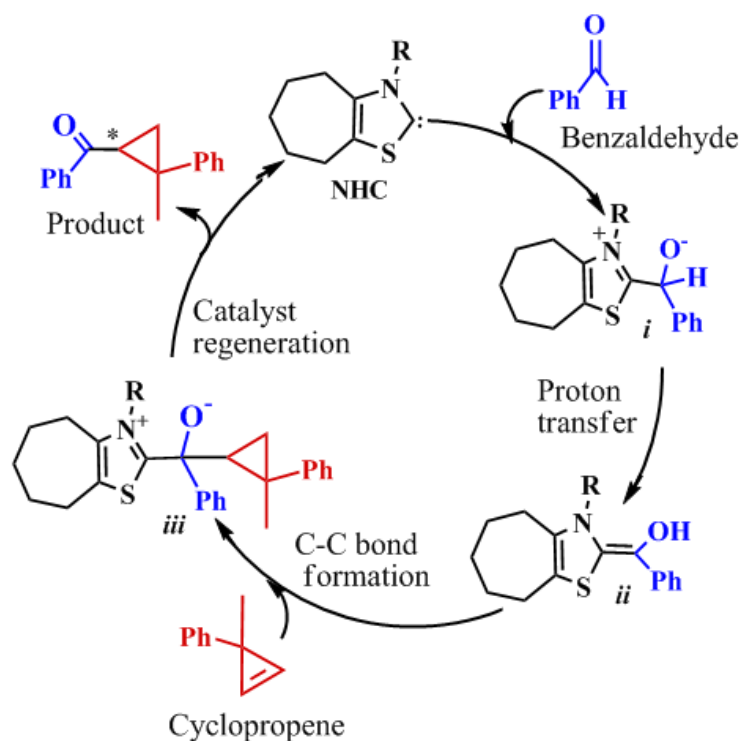
Scheme 3.1 Plausible mechanism of NHC catalyzed Stetter reaction between benzaldehyde and a cyclopropene.

bond with the generation of one stereocenter. The nucleophilic adduct formed after the C-C bond formation undergoes regeneration of the catalyst with the liberation of final product (Scheme 3.1). This reaction is attractive for the formation of Breslow intermediate and the subsequent C−C bond formation between *ii* and the cyclopropene.

It is reported that addition of water or base such as 1,8-diazabicyclo[5.4.0]undec-7-ene (DBU) and 1,5,7-triazabicyclo[4.4.0]dec-5-ene (TBD) enhances the reaction rate [Jousseaume *et al.* 2011; Chiang and Bode 2011; Biju *et al.* 2011; Padmanaban *et al.* 2011]. The role of base assisted proton transfer in NHC- catalyzed cycloannulation reaction of the homoenolate derived from butenal with pentenone has been reported recently by Sunoj and co-workers [Verma *et al.* 2011]. Many theoretical and experimental studies have indicated that a trace amount of water existing in the system also plays a critical role in assisting the proton transfer process in certain reactions [Xia *et al.* 2007; Song *et al.* 2010; Sherman *et al.* 2010; Gonzalez *et al.* 2011]. Hence, further studies on the role of water/base in the NHC catalyzed Stetter reaction between an aldehyde and a cyclopropene to generate acylcyclopropanes should be worthwhile.

3.2 Computational Methods

All the geometries including the transition state structures were optimized at the density functional theory (DFT) using the standard M06-2X functional [[b]Zhao and Truhlar 2008] together with 6-31+G(d,p) basis set for all the atoms. Further refinement of all energies were done with single point calculation using M06-2X/6-311++G(3df,2p) method together with self consistent reaction field polarizable continuum model (PCM) [Mennucci *et al.* 1999; Cossi *et al.* 2002]. M06-2X functionals is a high-nonlocality functional with double the amount of nonlocal exchange (2X) [[b]Zhao and Truhlar 2008]. It is parametrized only for nonmetals and is recommended for a combination of main group thermochemistry, kinetics, and noncovalent interactions. The selected solvent is

tetrahydrofuran (dielectric constant = 7.43) and additional input keywords (radii = UAHF) and scfvac were specified for the PCM calculations [Barone *et al.* 1997]. Gaussian 03 suites of programs [Frisch *et al.* 2009] were used for all the calculations. The transition states were located using synchronous transit-guided *quasi*-Newton method (QST3) [Peng and Schlegel 1993; Peng *et al.* 1996] as implemented in Gaussian 03 and were ascertained by only one imaginary frequency (first order saddle points) pertaining to the desired reaction coordinates. Throughout this paper the energetics of the reaction is discussed on the basis of the PCM-M06-2X/6-311++G(3df,2p)//M06-2X/6-31+G(d,p) level Gibbs energy (ΔG_{rel}) values with respect to the infinitely separated reactant system, unless otherwise specified. Energies from these PCM single point calculations were combined with the thermodynamic corrections in the gas phase to obtain the ΔE_{rel}, $\Delta H_{rel,}$ and the ΔG_{rel} in tetrahydrofuran. The activation energy, $\Delta G^{\#}$ is the difference in Gibbs energy between a transition state and the corresponding reactants.

3.3 Elucidation of Complete Reaction Pathway

3.3.1 Formation of Breslow Intermediate-Role of Water or Base

The nucleophilic attack of NHC on the benzaldehyde is preferred since Michel acceptor is added successively to the performed solution of the catalyst and benzaldehyde. At first the catalyst, NHC (**1**) forms a weak van der Waals complex (**2**) with benzaldehyde which then undergoes a nucleophilic attack of carbene lone pair on the carbonyl carbon of the benzaldehyde (*via* **3TS**; 9.1 kcal/mol) to form a zwitterionic intermediate (**4**; -0.7 kcal/mol). It is expected that the formation of Breslow intermediate is necessary for further reaction. A three membered cyclic transition state (**5TS**; 44.1 kcal/mol) is located for the formation of Breslow intermediate with $\Delta G^{\#}$ of 44.8 kcal/mol (Figure 3.2). The activation barrier for **5TS** is very high under the experimental conditions. Hence, we have also checked the role of DBU, TBD, and water in the proton
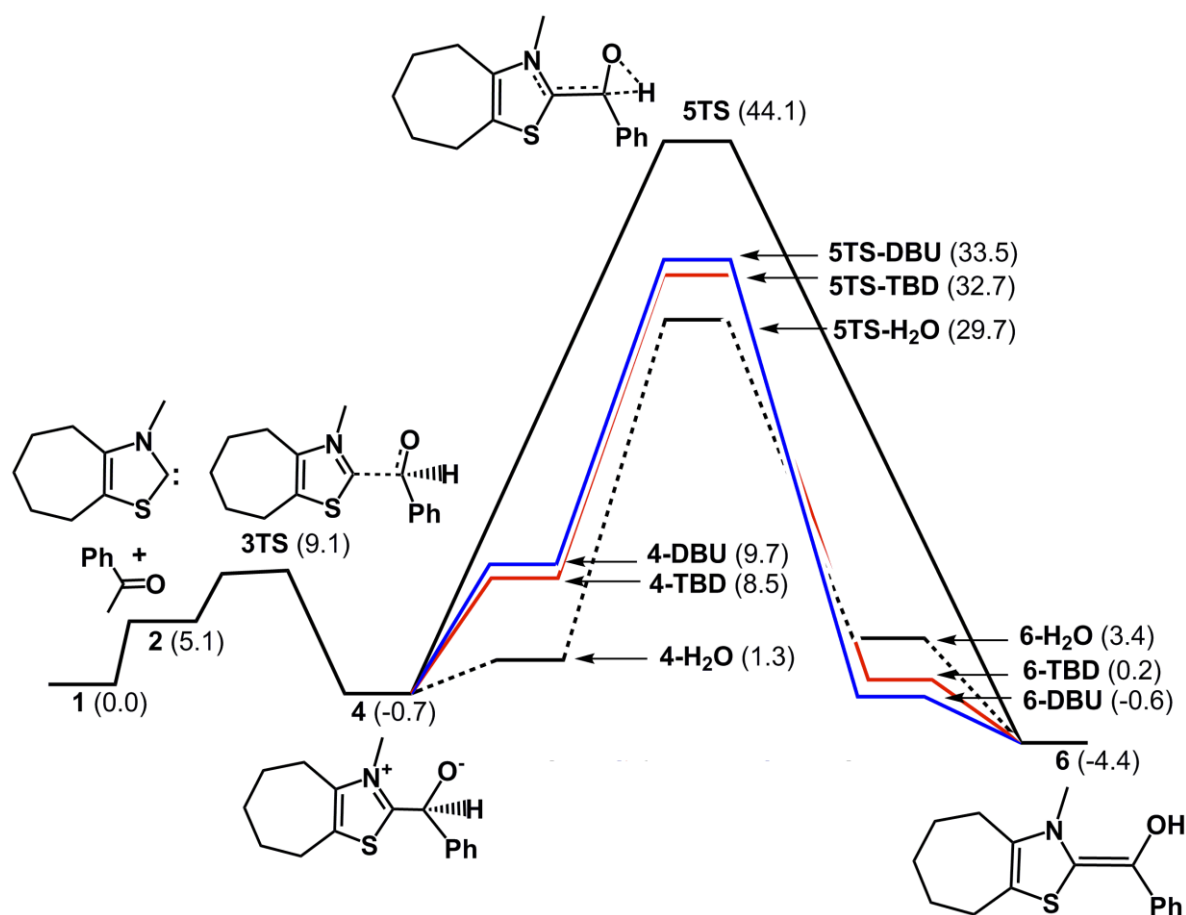
Figure 3.2 Reaction profile for the formation of Breslow intermediate from the nucleophilic attack of NHC on benzaldehyde followed by proton transfer. Black solid lines represent direct, black dotted lines represent H_2O assisted, blue lines represent DBU assisted, and red lines represent TBD assisted proton transfer step. Gibbs energies are reported in kcal/mol with respect to the infinitely separated reactants.

transfer step leading to the formation of Breslow intermediate, **6**. It is found that **5TS** assisted by DBU substantially reduces the activation barrier ($\Delta G^{\#}$) to 23.8, water to 28.4, and TBD to 24.3 kcal/mol (Figure 3.3) suggesting that water and base plays an important role in promoting the formation of Breslow intermediate. The geometric structures of the direct proton transfer (**5TS**), water assisted (**5TS-H₂O**), DBU assisted (**5TS-DBU**), and TBD assisted (**5TS-TBD**) proton transfer transition states are given in Figure 3.3.
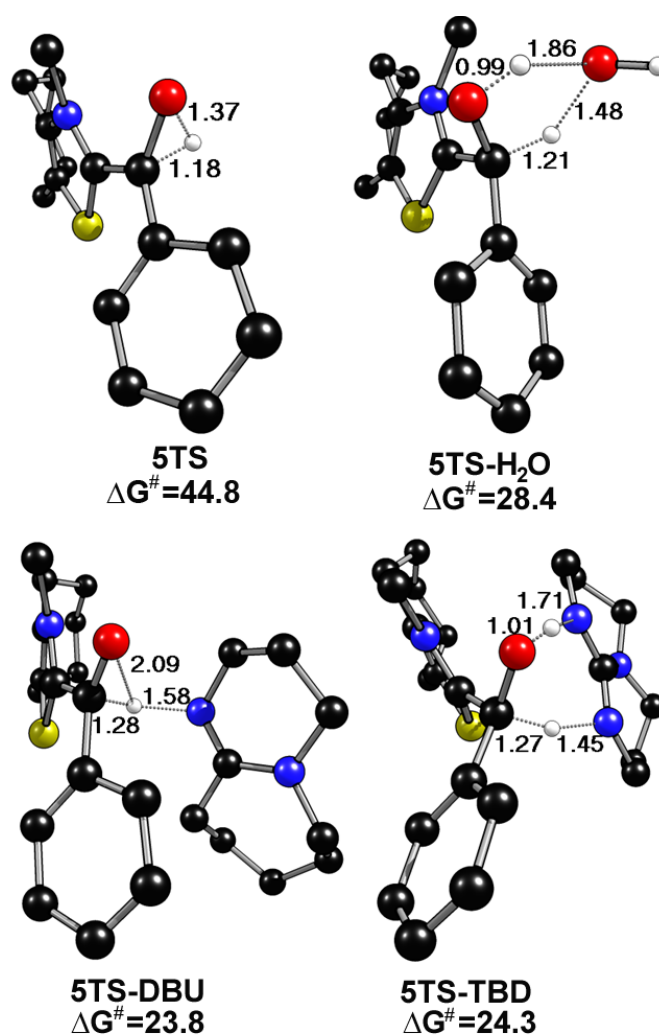
Figure 3.3 Possible TSs for direct proton transfer (**5TS**), water assisted (**5TS-H$_2$O**), DBU assisted (**5TS-DBU**), and TBD assisted (**5TS-TBD**) proton transfer processes. Energies in kcal/mol and distances in Å. Color code: black—C, ivory—H, blue—N, and red—O.

3.3.2 C-C Bond Formation Step and Regeneration of the Catalyst

Breslow intermediate **6** undergoes a nucleophilic addition reaction with the cyclopropene to form C-C bond. Enantioselectivity of the reaction can be envisaged by exploring different possibilities for the C-C bond formation step. The possibilities of concerted and stepwise transition states have been checked for the C-C bond formation,

but only the concerted nucleophilic addition with simultaneous proton transfer to the olefinic double bond has been observed. Different diastereomeric transition states between Breslow intermediate and cyclopropene is shown in Figure 3.4.
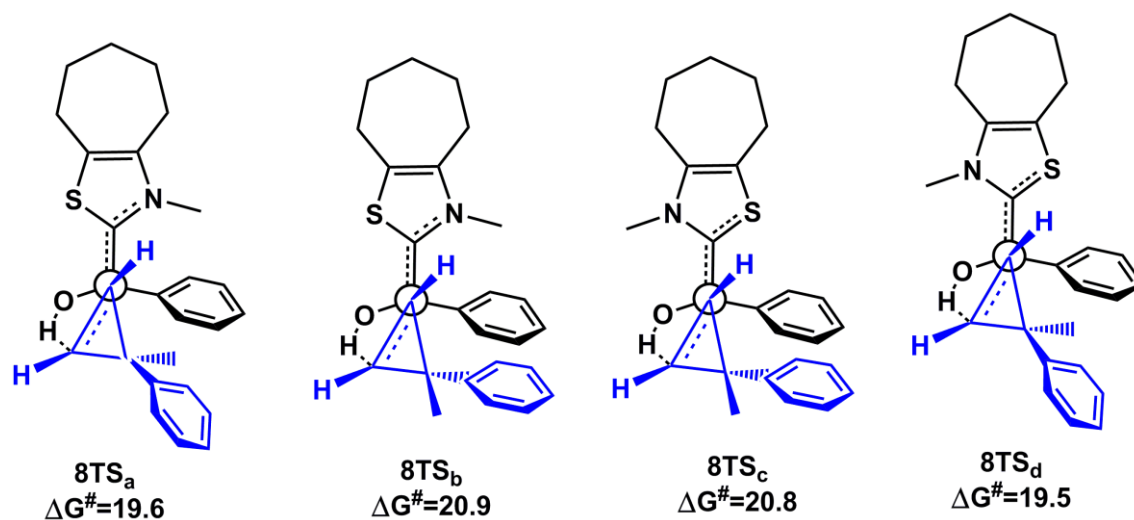
Figure 3.4 Transition states corresponding to different diastereomeric pathways for the formation of C-C bond between Breslow intermediate and cyclopropene. Activation barriers ($\Delta G^{\#}$) are reported in kcal/mol.

The phenyl groups from Breslow intermediate and cyclopropene have an *anti* orientation (**8TS$_a$** and **8TS$_d$**) than a *syn* orientation (**8TS$_b$** and **8TS$_c$**) for the preferred diastereomeric C-C bond formation. The energy profile diagram for the C-C bond formation followed by regeneration of the catalyst is given in Figure 3.5. The zwitterionic intermediate (**9**) formed after the nucleophilic attack of Breslow intermediate on the cyclopropene will undergo regeneration of the catalyst with an activation barrier of 4.1 kcal/mol (*via* **10TS**; $\Delta G_{rel} = -22.8$ kcal/mol) to get a stable van der Waals complex **11** ($\Delta G_{rel} = -35.3$ kcal/mol). The 3D structures of **8TS$_d$** and **10TS** is given in Figure 3.6. Overall the reaction is exergonic by 40.6 kcal/mol of Gibbs energy. ΔE_{rel} and ΔG_{rel} values are given in Table 3.1.
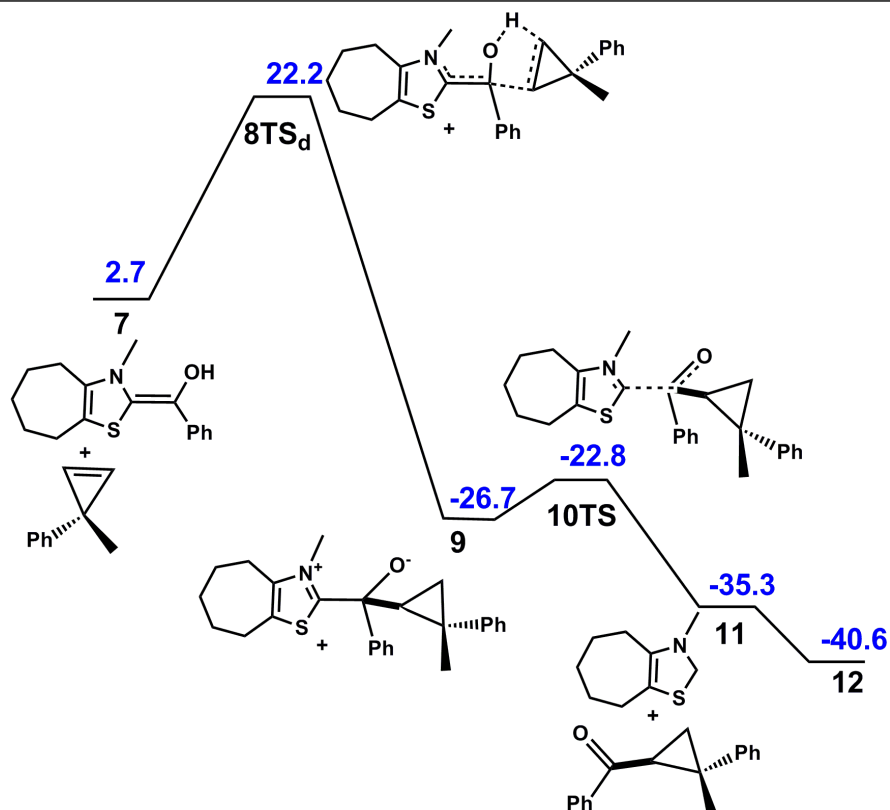
Figure 3.5 Reaction profile for the C-C bond formation step followed by catalyst regeneration. ΔG_{rel} (kcal/mol) are reported with respect to the separated reactants.
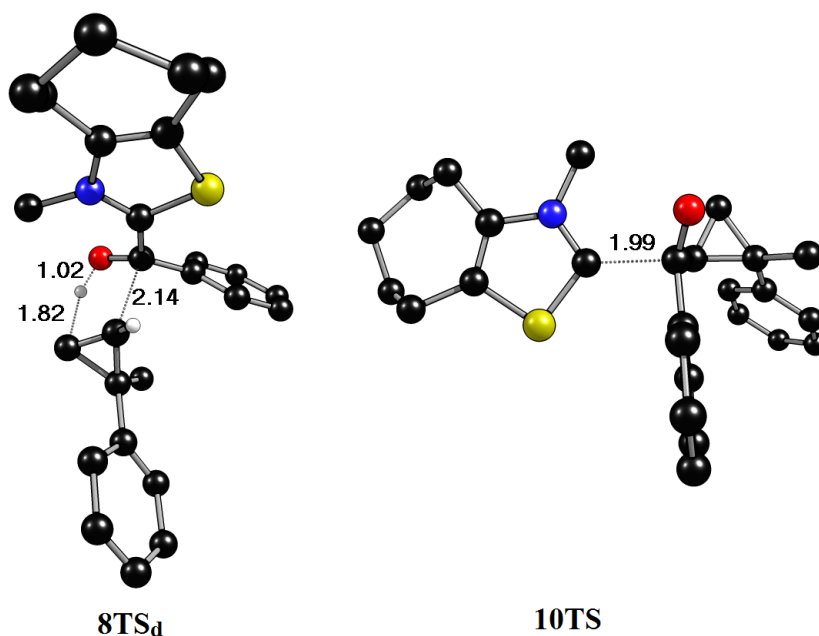
Figure 3.6 3D structures of **8TS$_d$** and **10TS** with important bond length parameters. Bond lengths are given in Å. Only selected hydrogen atoms are shown. Color code: black—C, ivory—H, blue—N, and red—O.

Table 3.1 ΔE_{rel} and ΔG_{rel} energies in Kcal/mol.

System	ΔE_{rel}	ΔG_{rel}
1	0.0	0.0
2	-7.1	5.1
3TS	-2.9	9.1
4	-13.2	-0.7
5TS	31.8	44.1
6	-17.1	-4.4
7	-20.6	2.7
8TS$_d$	-4.3	22.2
9	-54.1	-26.7
10TS	-47.7	-22.8
11	-60.8	-35.3
12	-53.5	-40.6
4-H$_2$O	-19.8	1.3
5TS-H$_2$O	6.6	29.7
6-H$_2$O	-17.9	3.4
4-DBU	-14.2	9.7
5TS -DBU	7.9	33.5
6-DBU	-26.8	-0.6
4-TBD	-16.6	8.5
5TS -TBD	6.1	32.7
6-TBD	-25.8	0.2

3.4 Concluding Remarks on Stetter Reaction

Several mechanistic possibilities of NHC catalyzed Stetter reaction have been proposed and discussed, by identifying the key intermediates for each elementary step and the corresponding transition states interconnecting them on the respective PES. This analysis clearly reveals the role of H$_2$O or bases such as DBU or TBD in the proton transfer process to form the Breslow intermediate as they significantly lower the activation barriers by $16.4 - 21.0$ kcal/mol which otherwise will be insurmountable at the

room temperature. The nucleophilic attack of Breslow intermediate on the cyclopropene with simultaneous proton transfer is the stereocontrolling step of the reaction. The initial nucleophilic attack of the NHC on the carbonyl carbon is a less energy demanding step to generate a stable zwitter ionic intermediate (**4**). An early transition state (**8TS$_d$**; 19.5 kcal/mol) is located for the C-C bond formation step which is followed by the regeneration of catalyst (**10TS**; 4.0 kcal/mol) to get the final product **12** (((1*S*,2*S*)-2-methyl-2-phenylcyclopropyl)(phenyl)methanone). The zwitterionic intermediate formed after the C-C bond formation (**9**) is found to be turnover frequency determining intermediate (TDI) and subsequent transition state for regeneration of the catalyst (**10TS**) is identified as turnover frequency determining transition state (TDTS) [Stegelmann *et al.* 2009; Kozuch and Shaik 2011]. Overall, the reaction is exergonic by 40.6 kcal/mol of Gibbs energy.

Part B: NHC Catalyzed CO$_2$ Fixation Using Epoxides

3.5 Introduction

Recently, *N*-heterocyclic carbenes (NHCs) [Cutler *et al.* 1988; Hahn and Jahnke 2008; Díez-González *et al.* 2009; Vougioukalakis and Grubbs 2010; Phan *et al.* 2010] have been employed as CO$_2$ transformation catalysts [Zhou *et al.* 2008; Riduan *et al.* 2009; Zhou *et al.* 2009; Kayaki *et al.* 2009; Nair *et al.* 2010; Gu and Zhang 2010; Huang *et al.* 2010] with epoxides and provided a new approach on the potential use of CO$_2$ as C$_1$ chemical feed stock [Sakakura *et al.* 2007; Aresta and Dibenedetto 2007] for the synthesis of cyclic carbonate [Bhanage *et al.* 2001; Luinstra *et al.* 2005; Ma *et al.* 2010]. Chemical fixation of CO$_2$ has become an important area of research with the onset of global warming [Zachos *et al.* 2001; Banerjee *et al.* 2008]. NHCs show good affinity to CO$_2$ and yield stable NHC-CO$_2$ adducts. These adducts have been identified as convenient precursors to deliver NHC to transition metal complexes under mild reaction conditions [Holbrey *et al.* 2003; Tommasi and Sorrentino 2005; Voutchkova *et al.* 2005; Voutchkova *et al.* 2007]. The presence of excess amount of CO$_2$ can significantly inhibit the decomposition of NHC-CO$_2$ while the addition of epoxide or substrate such as propargylic alcohol has a negative effect in stabilizing these adducts [Duong *et al.* 2004; Van Ausdall *et al.* 2009]. Lu and co-workers reported that the ability of NHC-CO$_2$ adducts to undergo decarboxylation increases with increase in steric bulkiness on the N-substituent and decreases with increase in electron density on the imidazolium ring [Zhou *et al.* 2008; Kayaki *et al.* 2009]. They also studied thermal stability of NHC-CO$_2$ adducts by means of *in situ* FTIR method and intuitively analyzed various possibilities of

NHC catalyzed cyclic carbonate synthesis in presence of CO_2 and epoxide. NHC-mediated cyclic carbonate syntheses are reported under drastic experimental conditions (4.5 - 10MPa CO_2 pressure and 40 - 100°C) [Zhou *et al.* 2008; Kayaki *et al.* 2009] and mechanistic details are yet to be unraveled for such reactions. This work will show that NHC and not NHC-CO_2 adduct is the active catalytic component in cyclic carbonate synthesis. Further, the role of CO_2 as Lewis acid to epoxide and its stabilizing effect on an important transition state to cleave the epoxide ring will be unraveled.

3.6 Computational Methods

All calculations were performed with Gaussian 03 suite quantum chemical programs [Frisch *et al.* 2004]. Full geometry optimizations followed by frequency calculations of all the stationary points were carried out with MPWB1K/6-31++G(d,p) level of theories [Zhao and Truhlar 2004] to ascertain the nature of the stationary points as minima or transition states on the respective PES [Lynch *et al.* 2000; Lynch *et al.* 2003]. MPWB1K is a hybrid meta-GGA method formulated by Truhlar and co-workers which has been recently used for making good predictions on thermochemistry, thermochemical kinetics, hydrogen bonding, and weak interactions [Suresh *et al.* 2009; Mohan *et al.* 2010]. All the calculations were done in the gas phase at 298 K. The transition states were ascertained by one and only one imaginary frequency (first order saddle points) pertaining to the desired reaction coordinates. The intrinsic reaction coordinate (IRC) calculations are carried out at the MPWB1K/6-31++G(d,p) level to further authenticate the result [Gonzalez and Schlegel 1989; Gonzalez and Schlegel 1990]. Each transition state is connected to the corresponding reactant and product by using rigorous optimization condition with the "opt=calcfc" option available in the program. Further, refinement of the energies has been carried out with single point calculation at MPWB1K/6-311++G(3df,2p) level. Zero point energy (ZPE) corrected

electronic energy (ΔE_{rel}) and Gibbs energy (ΔG_{rel}) obtained at MPWB1K/6-311++G(3df,2p)//MPWB1K/6-31++G(d,p) level is used to discuss the energetics of the reaction mechanisms and all the values are relative with respect to infinitely separated reactants (0.0 kcal/mol), unless otherwise specified. ZPE values and thermal correction to Gibbs energy is obtained from MPWB1K/6-31++G(d,p) optimized geometries. Activation barriers ($\Delta E^{\#}$ and $\Delta G^{\#}$) correspond to the respective energy difference between transition state and pre-reactant complex. Evaluation of the performance of different DFT methods have been carried out by single point energy calculations on MPWB1K/6-31++G(d,p) optimized geometries using different density functionals and 6-311++G(3df,2p) basis set, *viz.* generalized gradient approximation (GGA) functional BP86 [Perdew 1986; Becke 1988], meta-GGA functional TPSS [Tao *et al.* 2003], hybrid GGA functionals B3LYP [Lee *et al.* 1988; Becke 1993] and PBE0 [Adamo and Barone 1999], and hybrid meta-GGA functionals M05 [Zhao *et al.* 2005]. Pure GGA and meta-GGA functionals have slightly lower energy barriers compared to hybrid GGA and hybrid meta-GGA functionals.

3.7 Elucidation of the Actual Catalytic Pathway

3.7.1 NHC-CO$_2$ Mediated Pathways

Three possible mechanisms for NHC-mediated coupling of CO_2 with epoxide is shown in Figure 3.7 where NHC-CO$_2$ adduct is shown as the active catalytic component and the corresponding energy profiles are given in Figure 3.8. At first NHC (**1**) and CO_2 form a weak van der Waals complex **2$_{vdW}$**. The ΔE_{rel} of **2$_{vdW}$** is -3.6 kcal/mol, indicating thermal stabilization while ΔG_{rel} is positive (4.3 kcal/mol) due to loss of entropy in the association process. **2** immediately undergoes a nucleophilic addition *via* **TS$_1$** (Figure 3.9) to yield **3**, the zwitterionic covalent adduct NHC-CO$_2$. Activation energy ($\Delta E^{\#}$) of 2.6 kcal/mol and activation Gibbs free energy ($\Delta G^{\#}$) of 4.1 kcal/mol are observed for this
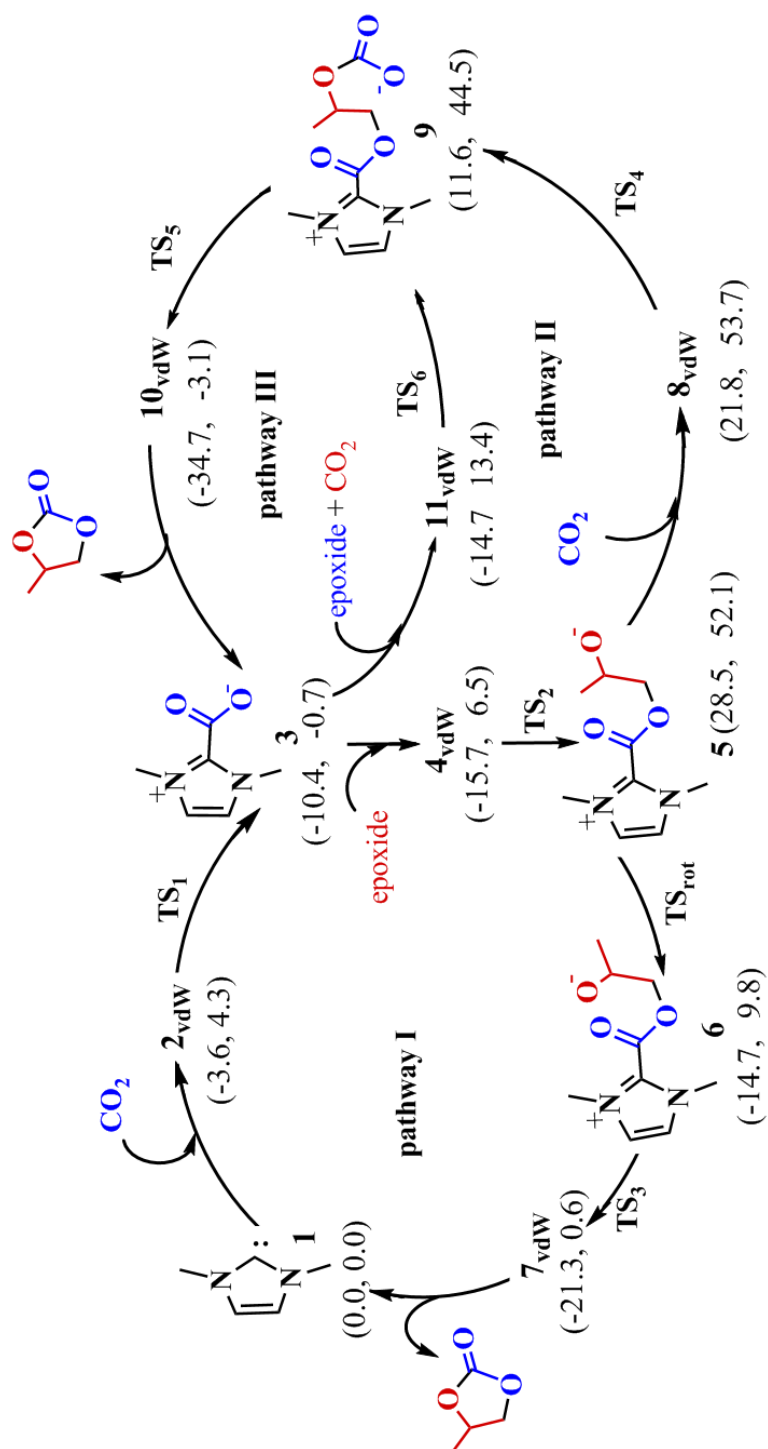
Figure 3.7 Three possible mechanisms (pathway I, II, and III) for cyclic carbonate synthesis. Values in parenthesis are

(ΔE_{rel}, ΔG_{rel}) in kcal/mol.

step. **3** is stabilized by 10.4 kcal/mol and the reaction is slightly exergonic ($\Delta\Delta G_{rel}$ = -0.7 kcal/mol). **3** forms a weak complex $\mathbf{4_{vdw}}$ with epoxide and subsequently undergoes S_N2 type epoxide ring opening *via* $\mathbf{TS_2}$ ($\Delta E^{\#}$ = 45.9 kcal/mol and $\Delta G^{\#}$ = 47.1 kcal/mol) to yield the zwitterion **5**. $\mathbf{TS_2}$ is formed by the attack of the nucleophile on the least substituted electron deficient carbon of the epoxide (C_1) through an approach *anti* with respect to the leaving epoxy oxygen (Figure 3.9). **5** can be converted to the more stable rotamer **6** *via* $\mathbf{TS_{rot}}$, the transition state for the C_1-C_2 bond rotation ($\Delta E^{\#}$ = 2.2, $\Delta G^{\#}$ = 2.7 kcal/mol). **6** undergoes an intramolecular nucleophilic attack of the alkoxide moiety on the carbon of the ester functionality *via* $\mathbf{TS_3}$ ($\Delta E^{\#}$ = 6.8 kcal/mol; $\Delta G^{\#}$ = 5.6 kcal/mol) and yields the cyclic carbonate with the regeneration of active catalyst **1** (pathway I).

Reaction of CO_2 with zwitterion **5** (pathway II) as well as a ter molecular reaction of CO_2, epoxide, and zwitterion **3** (pathway III) is considered as probable modes of carbonate formation (Figure 3.7). The ter molecular pathway is considered because this type of reactions is carried out under very high CO_2 pressure (4.5 - 10MPa) [Zhou *et al.* 2008; Kayaki *et al.* 2009]. Since pathway II bypasses the ter molecular pathway, it can
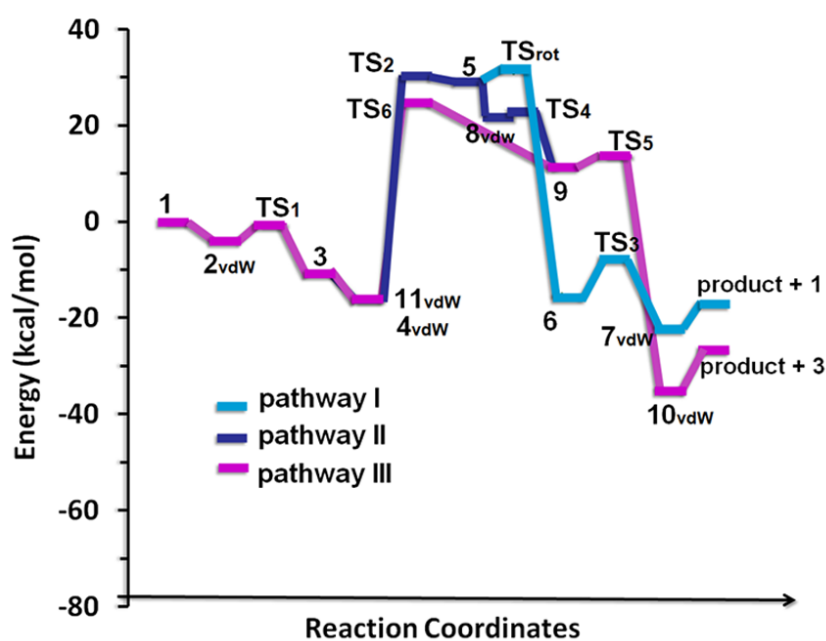
Figure 3.8 ZPE-corrected energy profiles. Structures of TSs are given in Figure 3.9.

be used to assess the role of excess CO_2. If 8_{vdw} is formed, formation of a zwitterionic carbonate intermediate **9** can take place by passing through a nearly barrier less transition state **TS$_4$** (pathway II). From **9**, the product formation occurs when the carboxylate oxygen attacks the methylene carbon *via* **TS$_5$** ($\Delta E^{\#} = 1.6$ kcal/mol; $\Delta G^{\#} = 2.0$ kcal/mol).

Thus for pathways I and II, the rate determining transition state is **TS$_2$**. In pathway III, **9** is formed *via* **TS$_6$** ($\Delta E^{\#} = 39.5$ kcal/mol; $\Delta G^{\#} = 44.4$ kcal/mol). Compared to **TS$_2$**, **TS$_6$** is 5.4 kcal/mol more stabilized as a result of additional interaction between the partially cleaved C-O bond of the epoxide and the CO_2 (Figure 3.9). In other words, CO_2 acts as a Lewis acid to the developing alkoxide ion.
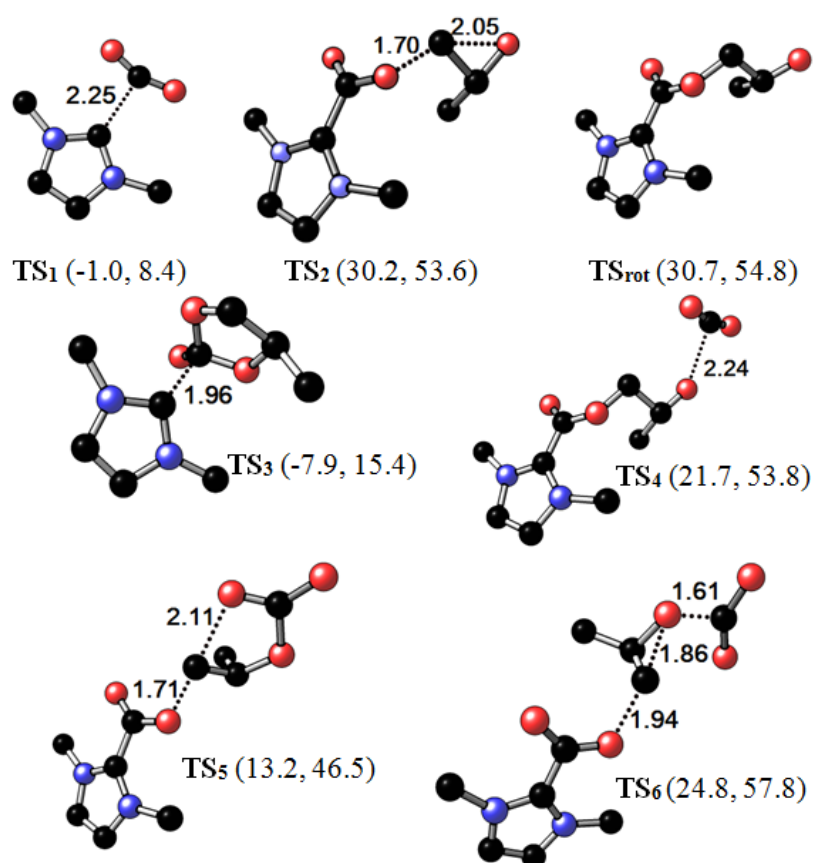
Figure 3.9 Possible TSs for NHC-CO_2 mediated coupling of CO_2 with epoxide to form carbonate. Hydrogen atoms are omitted for clarity. The ordered pair in parenthesis is (ΔE_{rel}, ΔG_{rel}). Energies in kcal/mol and distances in Å. Color code: black —C, blue —N, and red —O.

3.7.2 NHC Mediated Pathways

If we invoke a condition that free NHC reacts with epoxide first, the formation of NHC-epoxide complex 12_{vdw} has to be considered or the decarboxylation of NHC-CO_2 adduct must occur to release free NHC to carry out the reaction. However, S_N2 type ring opening of the epoxide in 12_{vdw} *via* TS_7 ($\Delta E^{\#}$ = 29.5 kcal/mol and $\Delta G^{\#}$ = 32.6 kcal/mol) will not yield the cyclic carbonate (Pathway IV; Figure 3.10) and instead converts to 1,3-dimethyl-2-methylene-2,3-dihydro-1H-imidazole and acetaldehyde, and destroys the catalytic activity of NHC. In fact, among all the vdW complexes obtained in this work, 12_{vdW} has the lowest binding energy (2.2 kcal/mol) and suggest that the formation of such a complex is less likely and therefore pathway IV may not operate. For the epoxide ring opening mechanism to be effective, the negative charge accumulated on the alkoxide moiety must be delocalized to attain stability which can happen *via* interaction with additional substrate molecule. This theory gets support from the fact that certain Lewis acids such as SalenAlEt can play the role of intermolecular cooperative catalyst to enhance the reaction rate [Zhou *et al.* 2008] through stabilizing interaction with alkoxide moiety. Since excess CO_2 is used under high pressure, NHC attack on epoxide has been modeled in the presence of CO_2 (pathway V). The *anti* attack of NHC on least substituted carbon atom of the epoxide takes place with simultaneous nucleophilic attack of the developing alkoxide oxygen on CO_2 *via* TS_8 ($\Delta E^{\#}$ = 24.7 kcal/mol; $\Delta G^{\#}$ = 25.6 kcal/mol). It is clear that the interaction of CO_2 improves the catalytic activity by reducing the activation barrier from 29.5 kcal/mol in TS_7 to 24.7 kcal/mol in TS_8. Pathway V is energetically more favorable (highly exothermic and exergonic) than the nucleophilic attack of the NHC-CO_2 adduct on the epoxide through pathways I, II, and III. Therefore, formation of the highly stable zwitterion **15** can occur and it may further
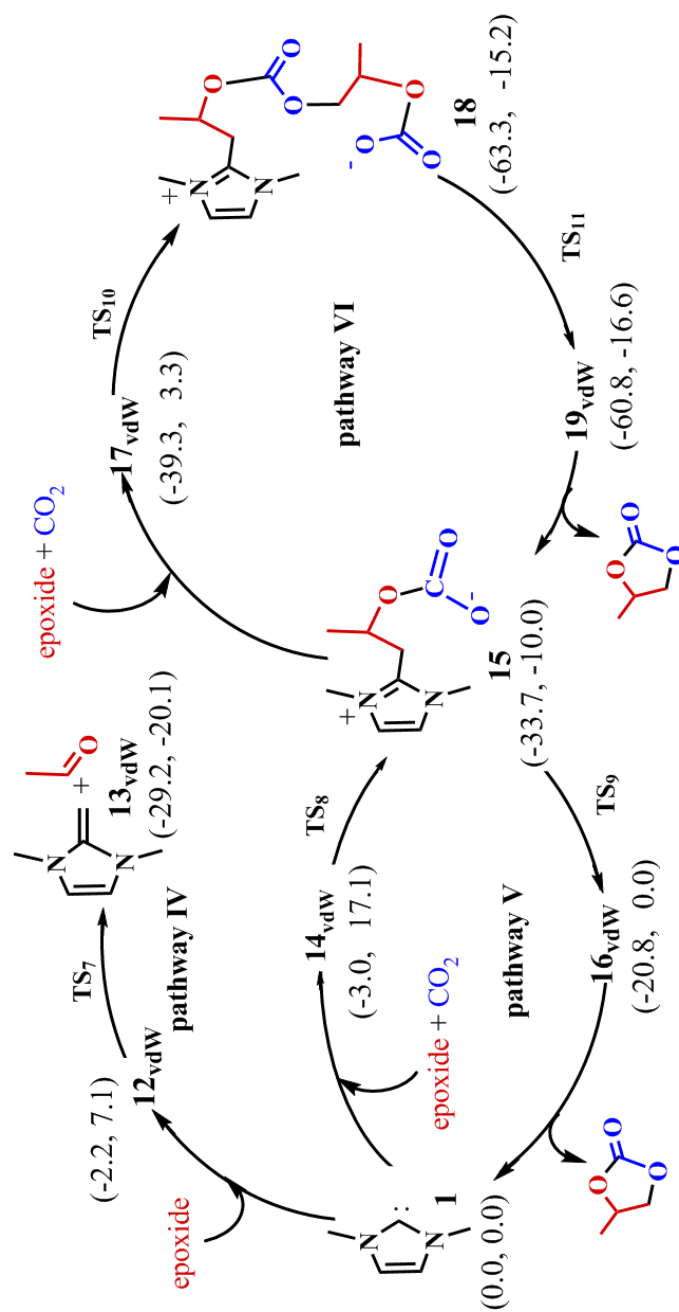
Figure 3.10 Three possible mechanisms (pathway IV, V, and VI) for cyclic carbonate synthesis. Values in parenthesis are (ΔE_{rel}, ΔG_{rel}) in kcal/mol.

undergo cyclization *via* **TS$_9$** to yield the product with the regeneration of the catalyst. However, the step involving **TS$_9$** needs a high $\Delta E^{\#}$ of 46.3 kcal/mol ($\Delta G^{\#}$ = 44.9 kcal/mol) and determines the rate of the reaction. Structures of all the transition states located for pathways IV, V, and VI are depicted in Figure 3.12.

Since **15** is very stable and NHC-mediated reactions are carried out under excess CO_2 at very high pressure, the possibility of another ter molecular pathway (pathway VI) is explored wherein **15** reacts with one more epoxide and CO_2. In this mechanism, formation of **17$_{vdW}$** is feasible and further activation of this complex *via* **TS$_{10}$** can yield another stable intermediate **18** (ΔE_{rel} = -63.3 kcal/mol; ΔG_{rel} = -15.2 kcal/mol). The $\Delta E^{\#}$ of 27.8 kcal/mol and $\Delta G^{\#}$ of 30.6 kcal/mol are relatively low compared to other pathways. The product formation occurs when **18** passes through **TS$_{11}$** ($\Delta E^{\#}$ = 41.6 kcal/mol and $\Delta G^{\#}$ = 40.5 kcal/mol) to yield **19$_{vdW}$**. Overall, pathway VI is highly exothermic ($\Delta\Delta E_{rel}$ = -50.2 kcal/mol) as well as exergonic ($\Delta\Delta G_{rel}$ = -16.0 kcal/mol). The ΔE_{rel} values of NHC-CO_2-mediated pathways (I, II, and III) obtained using other DFT functionals are given in Table 3.2 and those of NHC-mediated pathways (IV, V, and VI) are given in Table 3.3.

The energetics of the various pathways obtained using other DFT functionals were very similar to that of MPWB1K and the conclusions on pathway VI remained the same (Table 3.2 and Table 3.3). Pure GGA and meta-GGA functionals have slightly lowered the energy barriers compared to hybrid GGA and hybrid-meta-GGA functionals. For instance, the observed $\Delta E^{\#}$ values for **TS$_{11}$** at BP86, TPSS, B3LYP, PBE0, MPWB1K and M05 levels are 34.0, 32.7, 39.1, 41.4, 41.6, and 43.3 kcal/mol, respectively.
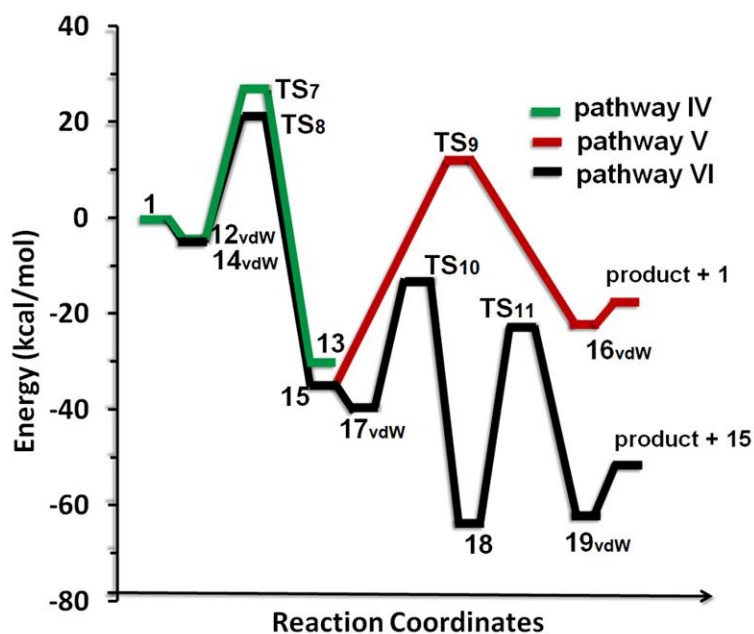
Figure 3.11 ZPE-corrected energy profiles for the three pathways. Structures of TSs are given in Figure 3.12.
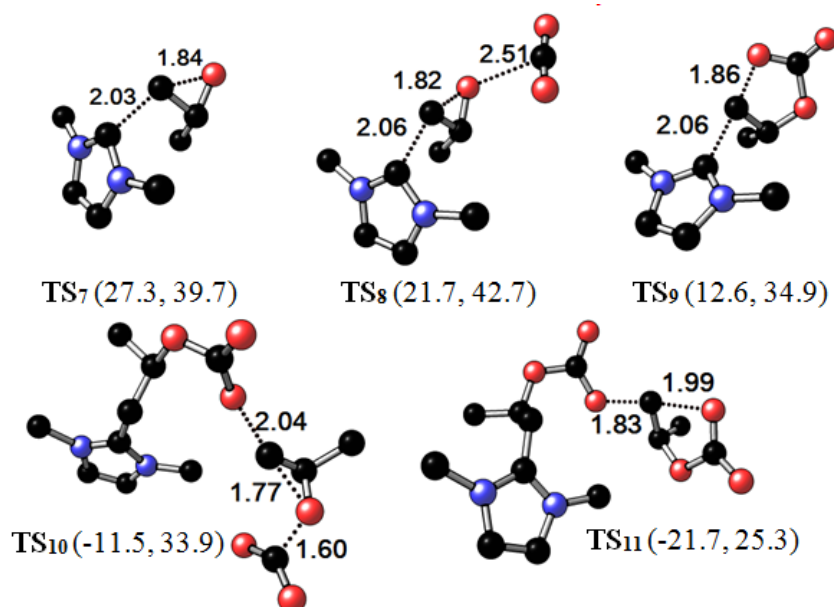
Figure 3.12 Possible TSs for NHC-CO_2 mediated coupling of CO_2 with epoxide to form carbonate. Hydrogen atoms are omitted for clarity. The ordered pair in parenthesis is (ΔE_{rel}, ΔG_{rel}). Energies in kcal/mol and distances in Å. Color code: black —C, blue —N, and red —O.

Table 3.2 ZPE-corrected SCF energies of pathway I, II, and III in kcal/mol with respect to the infinitely separated reactants (NHC + CO_2 + epoxide) at six different DFT functionals using 6-311++G(3df,2p) basis set (single point calculation of MPWB1K/6-31++G(d,p) optimized geometries).

geometry	BP86	TPSS	B3LYP	PBE0	M05
pathway I					
1	0.0	0.0	0.0	0.0	0.0
2$_{vdW}$	-2.2	-2.9	-2.7	-2.8	-3.7
TS$_1$	-0.7	-0.7	0.8	-1.6	2.1
3	-7.6	-6.1	-5.4	-11.1	-1.9
4$_{vdW}$	-8.2	-8.2	-6.5	-13.9	-5.9
TS$_2$	24.6	26.4	31.9	28.5	41.1
5	23.5	26.1	31.4	25.1	39.5
TS$_{rot}$	23.7	26.6	31.8	26.8	40.5
6	-2.3	-0.4	0.7	-12.8	6.1
TS$_3$	1.2	2.4	4.3	-7.5	9.7
7$_{vdW}$	-8.5	-8.6	-9.6	-18.2	-5.8
product	-8.2	-7.3	-9.1	-15.6	-2.9
pathway II					
8$_{vdW}$	22.0	23.9	28.4	20.4	34.9
TS$_4$	21.9	23.8	27.9	20.1	35.2
9	20.8	21.9	29.1	12.4	35.1
TS$_5$	21.1	20.8	25.3	13.2	36.9
10$_{vdW}$	-18.4	-17.6	-18.2	-31.7	-10.7
pathway III					
11$_{vdW}$	-4.8	-7.1	-5.9	-13.1	-5.0
TS$_6$	27.4	25.4	31.4	22.6	41.7

Table 3.3 ZPE-corrected SCF energies of pathway IV, V, and VI in kcal/mol with respect to the infinitely separated reactants (NHC + CO_2 + epoxide) at six different DFT functionals using 6-311++G(3df,2p) basis set (single point calculation of MPWB1K/6-31++G(d,p) optimized geometries).

geometry	BP86	TPSS	B3LYP	PBE0	M05
pathway IV					
12_{vdW}	-1.4	-1.9	-1.6	-1.6	-3.1
TS_7	19.2	20.1	25.0	23.8	29.1
13_{vdW}	-30.1	-26.9	-32.1	-29.7	-27.3
pathway V					
14_{vdW}	4.1	2.4	2.3	-0.1	-2.3
TS_8	17.1	17.2	22.0	19.8	24.5
15	-23.6	-20.8	-22.0	-32.2	-17.5
TS_9	14.8	15.3	19.5	11.5	28.7
16_{vdW}	-9.6	-9.6	-10.6	-18.5	-6.2
pathway VI					
17_{vdW}	-23.2	-20.4	-24.1	-36.3	-23.6
TS_{10}	-1.6	-0.5	2.0	-11.8	12.1
18	-35.5	-32.5	-37.9	-56.5	-29.5
TS_{11}	-1.5	0.2	1.2	-15.1	13.8
19_{vdW}	-37.6	-35.1	-38.4	-56.3	-29.8

3.8 Concluding Remarks on NHC Catalyzed CO_2 Fixation

On the basis of the computed energetics and comparison with the reported experimental results, we propose that the nucleophilic attack of NHC on the least substituted carbon of the epoxide can take place if the developing alkoxide moiety is stabilized by interaction from a CO_2. This will yield a stable zwitterionic acyclic carbonate intermediate **15**. The formation of **15** as well as the step leading to **18** is ter molecular in nature. Therefore, the feasibility of this reaction can be expected only in

presence of excess CO_2 under drastic experimental conditions. The previous experiments are conducted at CO_2 atmosphere of 4.5-10 MPa and 40-100° C temperature which justify the present findings [Zhou *et al.* 2008; Kayaki *et al.* 2009]. The most stable intermediate **18** in pathway VI may serve as the role of turnover frequency determining intermediate (TDI) and the subsequent transition state **TS$_{11}$** may act as the turnover frequency determining transition state (TDTS) [Stegelmann *et al.* 2009; Kozuch and Shaik 2011]. However, **TS$_6$** and **TS$_8$** are the respective distinctly different transition states for NHC-CO_2 mediated and free NHC mediated reaction pathways which have the prime role to determine the course of reaction. The ter molecular pathway suggested for this reaction provides the role of free NHC and CO_2 in the reaction mechanism and thus contributes toward the improved design and application of this reaction.

Summary

The part A of this chapter deals with the NHC catalyzed intermolecular Stetter reaction between benzaldehyde and cyclopropene. The mechanistic study presented herein clearly reveals that water or bases such as DBU or TBD play an important role in the proton transfer process to form the Breslow intermediate for the NHC catalyzed Stetter reaction to occur at room temperature where these species significantly lower the activation barriers which otherwise will be quite high. The nucleophilic attack of Breslow intermediate on the cyclopropene with simultaneous proton transfer is the stereocontrolling step of the reaction. The zwitterionic intermediate formed after the C-C bond formation is found to be turnover frequency determining intermediate (TDI) and subsequent transition state for regeneration of the catalyst is identified as turnover frequency determining transition state (TDTS).

The part B of this chapter deals with the NHC-mediated CO_2 transformation reaction of epoxide to cyclic carbonate. A detailed analysis of six different pathways reveals a ter molecular pathway of the reaction mechanism. The nucleophilic attack of NHC on the least substituted carbon of the epoxide can take place with the assistance from a CO_2 to the developing alkoxide moiety. The ter molecular pathway suggested for this reaction provides the role of free NHC and CO_2 in the reaction mechanism.

Stereoelectronic Features of NHC Ligands and Rational Design of Multi-topic NHCs

NHC-CO$_2$ adducts

$$NHC + CO_2 \rightleftharpoons NHC\text{-}CO_2$$

Electronic

Electronic

Electronic

Electronic

Steric

Steric
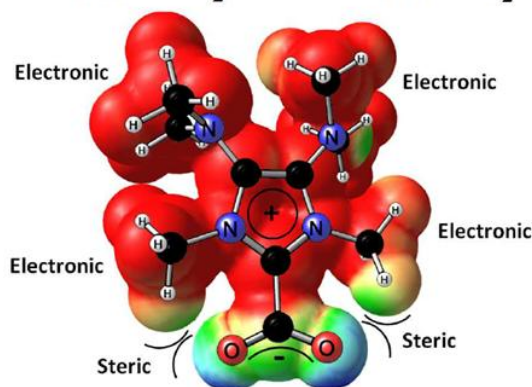
$E_{b1} = 18.0 \text{ kcal/mol}$

Multitopic NHCs
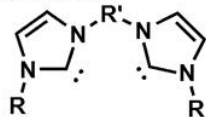
Ditopic NHC
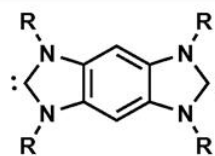
Janus type ditopic NHC
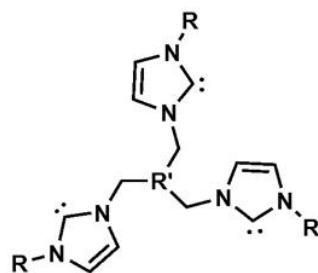
Tritopic NHC
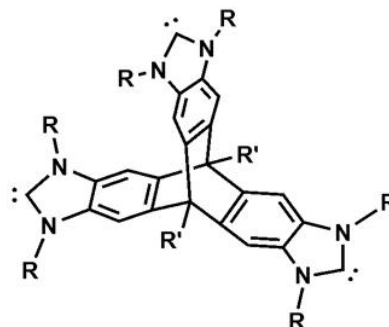
Cerberus type tritopic NHC

Abstract

In Part A of this chapter, the CO_2 fixation ability of N-heterocyclic carbenes (NHC) has been assessed on the basis of electronic and steric properties of the N- and C- substituents, measured in terms of molecular electrostatic potential minimum, observed at the carbene lone pair region of NHC (V_{min1}) as well as at the carboxylate region of NHC-CO_2 adduct (V_{min2}). Both V_{min1} and V_{min2} are found to be simple and efficient descriptors of the stereoelectronic effect of NHCs. The V_{min} based analysis also proved that the stereoelectronic effect of N- and C- substituents is additive. When only C-substituents are present in NHC, its CO_2 affinity solely depends on the electronic effect while if N-center bears the substituents, steric factor plays a major role in the carboxylation/decarboxylation process. For standard substituents, maximum CO_2 binding energy of 18.0 kcal/mol is observed for the most electron donating combination of -NMe_2 as the C-substituent and -Me as the N-substituent. Introduction of ring strain through five-membered ring fusion at the NC bond slightly increased the electron rich character of the carbene lone pair and also enhanced the CO_2 binding energy to 20.9 kcal/mol. To further improve the CO_2 fixing ability of NHCs, we have proposed the use of -CH_2OH, -$CH_2NHCOMe$, -CH_2NHPh as N-substituents as they participate in intramolecular hydrogen bond interaction with the carboxylate. With the new strategy, considerable improvement in the CO_2 binding energy (26.5 to 33.0 kcal/mol) is observed.

In part B of this chapter, rational design of multi-topic NHC ligands has been described. According to structural, thermodynamic, and magnetic criteria, it has been recognized that the imidazol-2-ylidenes possess substantial aromatic character which gives stability to the ring system. Several multi-topic NHC ligands with up to four carbene centres are designed on the basis of Clar's aromatic sextet theory. The aromatic stabilization energy, NICS and HOMA based measures of aromaticity, MESP based measure of lone pair strength, proton affinity, and binding energy with CuCl have indicated their stability as well as powerful coordination behaviour. Use of some of them in designing metal-organic framework with 1 – 1.5 nm cage/pore size is also demonstrated.

Part A: Assessment of Stereoelectronic Features of NHC Ligands

4.1 Introduction

A number of attempts have been carried out in the past to characterize reliable steric and electronic parameters for *N*-heterocyclic carbenes [Tolman 1977; Lever 1990; Lever 1991; Fielder *et al.* 1995; Hillier *et al.* 2003; Chianese *et al.* 2003; Peris and Crabtree 2004; Dorta *et al.* 2005; Scott *et al.* 2005; Díez-González and Nolan 2007; Fürstner *et al.* 2007; Leuthäußer *et al.* 2007; Kelly III *et al.* 2008; Huynh *et al.* 2009; Vorfait *et al.* 2009; Wolf and Plenio 2009; Gusev 2009; Mathew and Suresh 2010; Clavier and Nolan 2010; Fey 2010]. Huynh and co-workers proposed that the ^{13}C chemical shift of the carbene carbon in NHC complexes are useful to characterize the donor strength of NHC ligands in Palladium(II)-benzimidazolylidene complexes [Huynh *et al.* 2009]. Lever and co-workers used electrochemical E_0 value (Lever electronic parameter, LEP) for various redox couples in a series of Ru^{III}/Ru^{II} complexes containing the ligands of interest [Lever 1990; Lever 1991; Fielder *et al.* 1995]. Tolman electronic parameter (TEP) which measures the fundamental CO stretching frequencies of $Ni(CO)_3(NHC)$ complexes is a widely used parameter to evaluate the electron donor ability of the NHC ligands [Tolman 1977]. The TEP approach was built upon the pioneering work by Strohmeier and co-workers [Strohmeier and Muller 1967] and Bigorgne and co-workers [Bouquet *et al.* 1968] which makes use of the fact that the electron density from the ligand not only passed on to the metal but also to the antibonding orbital of CO ligands. Further, a large quantity of structural data have been generated by various groups in order to correlate the TEP values obtained for a large

variety of NHCs in different metal carbonyl complexes [Chianese *et al.* 2003; Peris and Crabtree 2004; Fürstner *et al.* 2007; Leuthäußer *et al.* 2007; Vorfait *et al.* 2009; Wolf and Plenio 2009]. Gusev used a diverse group of representative NHC ligands to quantify electron-donor properties by means of TEP and steric properties by a parameter called "repulsiveness" which is a measure of direct repulsive interaction between the NHC and carbonyl ligands of $Ni(CO)_3(NHC)$ [Gusev 2009]. Herrmann and co-workers examined and classified the relative σ-donor/π-acceptor quality of various NHC ligands by means of IR spectroscopy at the corresponding $Rh(CO)_2I(NHC)$ complexes [Herrmann *et al.* 2006]. A systematic investigation of the electronic and steric properties of various 4,5-dialkylated NHCs was reported by Glorius' group [Urban *et al.* 2009]. Recently studies from our laboratory [Mathew and Suresh 2010] showed that molecular electrostatic potential (MESP) at the carbene lone pair or at the nucleus of the carbene carbon can be used as a simple and efficient electronic parameter of NHCs and showed good correlation with TEP. Though the core of the NHC is largely planar, bulky substituents on the *N*-centers can exert large steric effect upon coordination to a metal and the proper quantification of such an effect is of great interest in catalyst design. An approach based on the critical features of the molecular electrostatic potential is also developed for the quantification of steric and electronic properties of NHCs in Grubbs second-generation olefin metathesis catalysts [Mathew and Suresh 2011]. Liu and co-workers studied NHC steric contours to understand the effects of NHC ligands on the reversal of regioselectivity in Ni-catalyzed reductive couplings of alkynes and aldehydes [Liu *et al.* 2011]. The buried volume method developed by cavallo and co-workers quantifies the steric demand of various NHCs by means of a single parameter called percent buried volume ($\%V_{bur}$) which is defined as the percent of the total volume of a sphere of definite radius occupied by a ligand with a metal center at its core [Hillier *et al.* 2003; Dorta *et al.* 2005; Scott *et al.* 2005; Cavallo *et al.* 2005; Kelly III *et al.* 2008]. The bond dissociation

energy of NHC ligands in metal complexes reflects the relative strength of metal–NHC bond which can also be dependent on the steric properties of the NHC ligands [Hillier *et al.* 2003; Scott *et al.* 2005; Singh *et al.* 2005].

Interestingly, all the previous quantifications of structural and electronic parameter of NHCs are based on treating NHC as a ligand in various metal complexes. Because NHCs are also used as versatile catalysts for organic transformations, to describe the stereoelectronic properties of the 'NHC catalyst', an organic model could be more useful than an organometallic model. Therefore, we propose that the formation of NHC-CO_2 adduct offers a simple and elegant model to describe and quantify the electronic and steric properties of NHC catalyst. Louie and co-workers studied factors influencing the decarboxylation of 1,3-disubstituted-2-imidazolium carboxylates and their results indicate that the steric bulkiness on the *N*-substituent increases the ability of NHC-CO_2 to decarboxylate and extra electron density on the imidazolium ring enhances the stability of NHC-CO_2 adducts [Van Ausdall *et al.* 2009]. The usefulness of NHC-CS_2 adducts had also been proposed by Delaude and co-workers for assessing the steric and electronic properties of NHC ligands [Delaude *et al.* 2009]. Most of the NHC mediated organocatalysis includes the formation of covalent, active intermediates by their addition to double bonds as the key step, leading to nucleophilic incorporation of the carbonyl functional group [Nair *et al.* 2004; Nair *et al.* 2008; Nair *et al.* 2010]. Such a σ-donor character of NHCs has also been applied to CO_2 capture, and the resulting imidazolium-2-carboxylates are identified as the typical NHC-CO_2 adducts [Zhou *et al.* 2008; Riduan *et al.* 2009; Kayaki *et al.* 2009]. It is assumed that a dynamic equilibrium of NHC-CO_2 adduct, free CO_2, and the corresponding NHCs exists in the organic solution of NHC-CO_2 adducts. Hence, the dissociation energy, E_{b1} of NHC-CO_2 adduct can serve as a good energetic parameter to describe the nucleophilic behavior of NHCs in organic transformations. Further, the CO_2 capture reaction by NHC enables us to

understand the atmospheric CO_2 fixation by various NHCs. This in turn can help in the designing of distinct NHC architectures of desirable electronic and steric demand for new organocatalytic transformations.

4.2 Computational Methods

We have selected four sets of unsaturated NHCs for the present study in which some NHCs are structurally characterized compounds and some others are possessing features that can be of interest for future investigation. Set A includes NHCs with substituents only on the carbon atoms, set B includes substituents only on the nitrogen atoms, set C includes substituents on both carbon and nitrogen atoms and set D consists of some miscellaneous NHCs with ring fusions (Figure 4.1 and Figure 4.2).
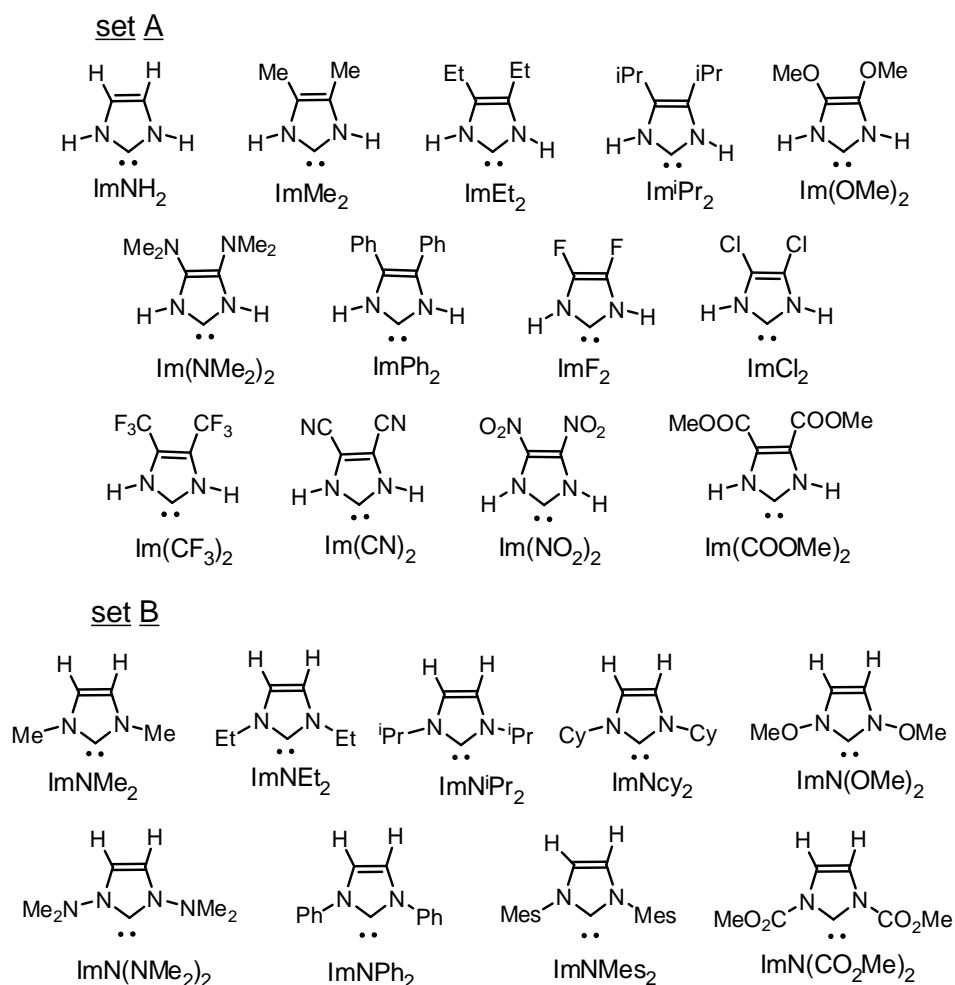
Figure 4.1 The selected NHCs for set A and set B with typical abbreviations [Gusev 2009].

set <u>C</u>

Im(NO$_2$)$_2$NMe$_2$ Im(CF$_3$)$_2$NMe$_2$ Im(NMe$_2$)$_2$NMe$_2$ ImCl$_2$NMe$_2$ Im(CN)$_2$NMe$_2$

Im(CO$_2$Me)$_2$NMe$_2$ ImF$_2$NMe$_2$ ImMe$_2$NMe$_2$ ImMe$_2$N(OMe)$_2$

ImMe$_2$N(NMe$_2$)$_2$ ImEt$_2$N(OMe)$_2$ ImEt$_2$N(NMe$_2$)$_2$ ImCl$_2$N^{i}Pr$_2$

Im(NO$_2$)$_2$N^{i}Pr$_2$ ImF$_2$NPh$_2$ ImPh$_2$N(OMe)$_2$ ImPh$_2$N(NMe$_2$)$_2$

set <u>D</u>

ImBicar   ImCyIm   ImPhen   ImPhenPh$_2$

ImDpyIm   BImNMe$_2$ BImNEt$_2$ Py[b]ImNMe$_2$ Py[c]ImNMe$_2$
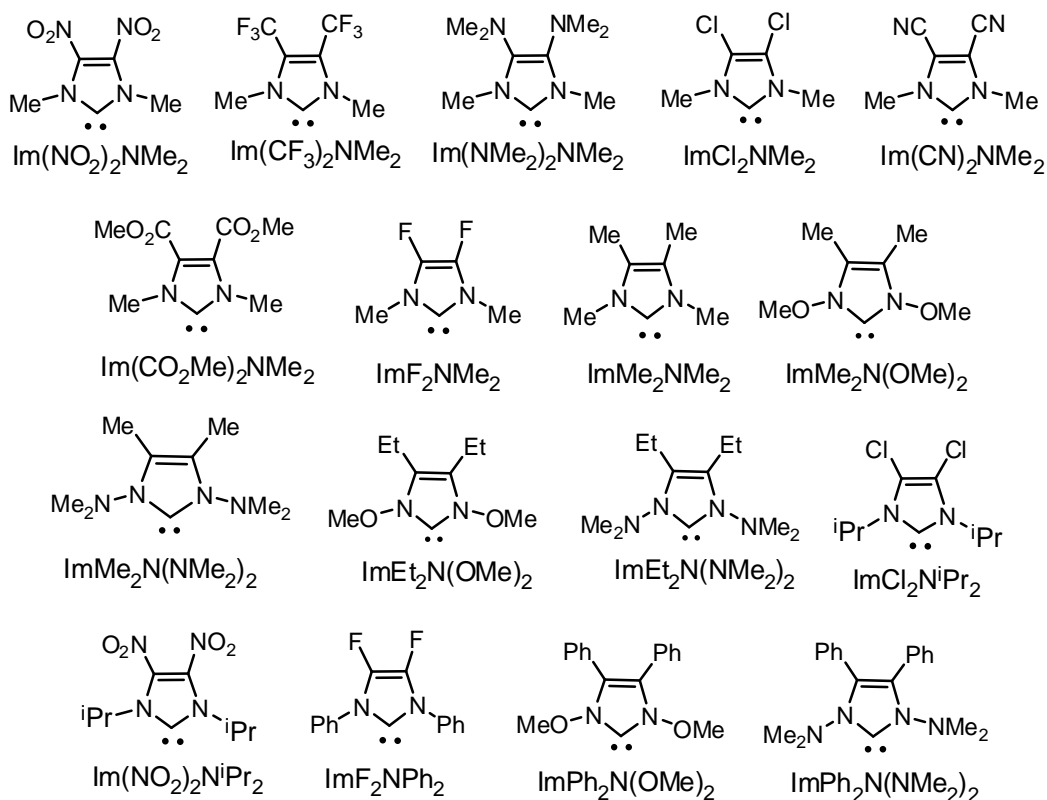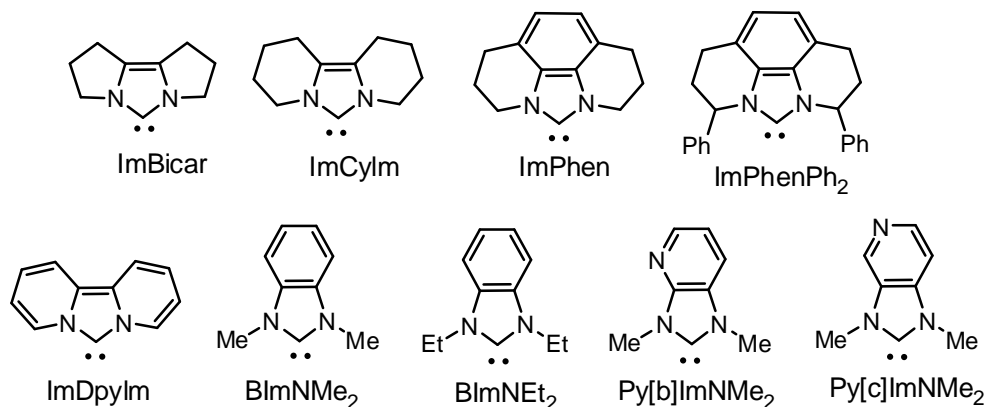
Figure 4.2 The selected NHCs for set C and set D with typical abbreviations [Gusev 2009].

All the NHC geometries and their CO$_2$ adducts were optimized using density functional theory at the MPWB1K/6-31++G(d,p) level [Lynch *et al.* 2000; Lynch *et al.* 2003; Mohan *et al.* 2010] using Gaussian03 suite of programs [Frisch *et al.* 2004] and the wave function generated from the same method is used for the Molecular Electrostatic Potential analysis [Politzer and Truhlar 1981; Gadre and Shirsat 2000]. MESP at the

carbene lone pair region (V_{min1}) and the MESP at the carboxylate moiety of the NHC-CO_2 adduct (V_{min2}) are calculated by the cube calculation in Gaussian 03. MESP has been widely used as an efficient electronic descriptor to quantify substituent effects in several organic systems [Gadre and Suresh 1997; Suresh and Gadre 1998; Gross *et al.* 2001; Politzer and Murray 2002; Galabov *et al.* 2006; Suresh 2006; Suresh and Gadre 2007; Mathew *et al.* 2007; Deshmukh *et al.* 2008; Pinjari and Gejji 2008; Sayyed and Suresh 2009; Sayyed *et al.* 2010]. The energy released due to the bonding interaction between NHC and CO_2 (E_{b1}) is calculated using the supermolecular approach. According to the supermolecular approach, E_{b1} is evaluated as the difference between the energy of NHC-CO_2 adducts and sum of the energies of its subsystems (NHC and CO_2).

4.3 Assessment of Stereoelectronic Factors that Influence the CO_2 Fixation Ability of *N*-Heterocyclic Carbenes

All the NHCs show a negative-valued MESP minimum, V_{min1} at the lone pair region while the NHC-CO_2 adducts show a negative-valued V_{min2} at the oxygen lone pair region. Considering ImNH$_2$ as the unsubstituted reference system (all N- and C-substituents are H; V_{min1}= -83.1 kcal/mol), the difference between the V_{min1} of a ligand and V_{min1} of the reference system (ΔV_{min1}) is used as a measure of the combined effect of the C- and N- substituents. In the case of ligands in set A, ΔV_{min1} gives the combined effect of the C$_4$ and C$_5$ substituents. For instance, the V_{min1} values -87.2, -87.5 and -52.5 kcal/mol calculated respectively for ImEt$_2$, Im(NMe$_2$)$_2$ and Im(NO$_2$) suggest that the effects of C-substituents Et, NMe$_2$, and NO$_2$ are -4.1, -4.4, and 30.7 kcal/mol, respectively (Table 4.1). In the case of NHC-CO_2 adducts, the relative value of the V_{min2} with respect to the reference system (ΔV_{min2}) is useful to assess the substituent effect. Both V_{min1} and V_{min2} (Table 4.1) follow almost the same trend in the relative order of the

values and show a strong linear correlation between them, indicating that the substituents exert almost the same stereoelectronic effect in both free and the complexed NHCs.

Table 4.1 V_{min1} of free NHCs and V_{min2}, E_{b1}, d_{cc}, and θ of NHC-CO_2 adducts of set A and set B NHCs.

system	V_{min1} (kcal/mol)	V_{min2} (kcal/mol)	E_{b1} (kcal/mol)	d_{cc} (Å)	θ (°)
$ImNH_2$	-83.1	-82.3	16.4	1.532	0.0
$ImMe_2$	-87.2	-86.0	18.9	1.528	0.0
$ImEt_2$	-87.2	-86.3	19.4	1.527	0.0
Im^iPr_2	-87.5	-87.1	19.9	1.527	0.0
$Im(OMe)_2$	-83.8	-84.7	17.3	1.522	0.0
$Im(NMe_2)_2$	-87.5	-88.5	21.0	1.522	1.3
$ImPh_2$	-81.6	-85.8	17.1	1.529	0.4
ImF_2	-71.1	-74.4	11.3	1.537	0.0
$ImCl_2$	-70.4	-76.4	11.1	1.538	0.0
$Im(CF_3)_2$	-62.6	-71.1	7.3	1.542	0.5
$Im(CN)_2$	-54.8	-66.1	4.2	1.546	0.0
$Im(NO_2)_2$	-52.5	-64.1	1.9	1.553	0.0
$Im(CO_2Me)_2$	-72.9	-78.7	11.4	1.538	1.8
$ImNMe_2$	-84.8	-85.8	16.3	1.540	0.0
$ImNEt_2$	-85.0	-84.3	18.2	1.544	18.6
$ImNiPr_2$	-86.0	-84.0	17.2	1.543	32.6
$ImNcy_2$	-86.8	-85.5	17.5	1.544	34.3
$ImN(OMe)_2$	-69.7	-79.8	6.0	1.559	45.4
$ImN(NMe_2)_2$	-75.6	-78.4	10.2	1.545	45.1
$ImNPh_2$	-75.5	-82.0	7.9	1.545	90.7
$ImNMes_2$	-83.9	-84.8	15.6	1.536	80.7
$ImN(CO_2Me)_2$	-57.4	-68.7	0.8	1.568	89.9

The MESP painted on the van der Waals surface is presented in Figure 4.3 for a representative set of NHC-CO_2 adducts which shows strong charge separation in the

systems, the carboxylate moiety is negatively charged while the rest of the molecule is positively charged. These pictures also indicate that the carbene lone pair is donated to the CO_2 carbon and the bonding is very similar to a ligand-metal 2e coordination bond observed in organometallic complexes. In NHC-CO_2 adduct, the negative charge is delocalized on the CO_2 moiety while the positive charge is delocalized on the NHC ring. Figure 4.4 shows V_{min1} of a representative set of NHC ligands taken from set A and set B as well as the V_{min2} of the corresponding CO_2 adducts. For set A and set B ligands, Table 4.1 also depicts the energy released due to the coordinate bonding interaction between NHC and CO_2 (E_{b1}), the distance between carbene carbon and the carbonyl carbon (d_{cc}), and angle between the plane of NHC and CO_2 of NHC-CO_2 adduct (θ).

ImNH2-CO2 **ImMe2-CO2** **ImBicar-CO2**

-50.0 kcal ▮▮▮ +50.0 kcal
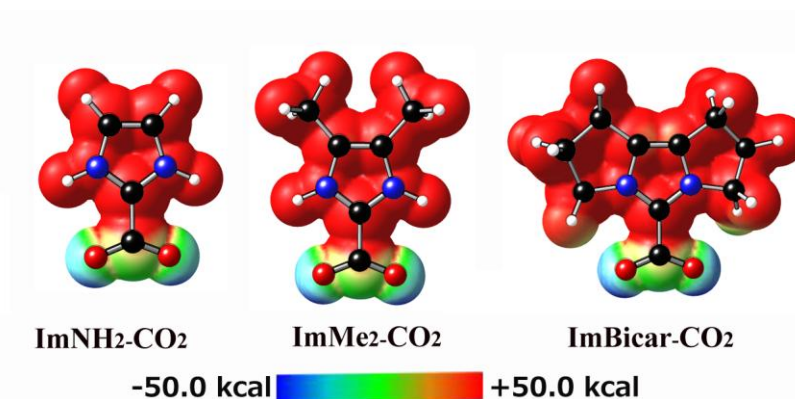
Figure 4.3 The MESP mapped on to the van der Waals surface of a representative set of NHC-CO_2 adducts.

In general, when V_{min1} is more negative, more energy (E_{b1}) is released during NHC-CO_2 adduct formation. Electron donating C-substituents always show high value for E_{b1}, the highest being 21.0 kcal/mol for Im(NMe$_2$)$_2$. On the other hand, CO_2 binding is weak when C-substituent is electron withdrawing, the lowest value of E_{b1} (1.9 kcal/mol) is obtained for Im(NO$_2$)$_2$. A good correlation between V_{min1} and E_{b1} (correlation coefficient is 0.99) exists for set A systems (Figure 4.5). This suggests that the CO_2 binding energy of set A systems solely depends on the electronic effects of the
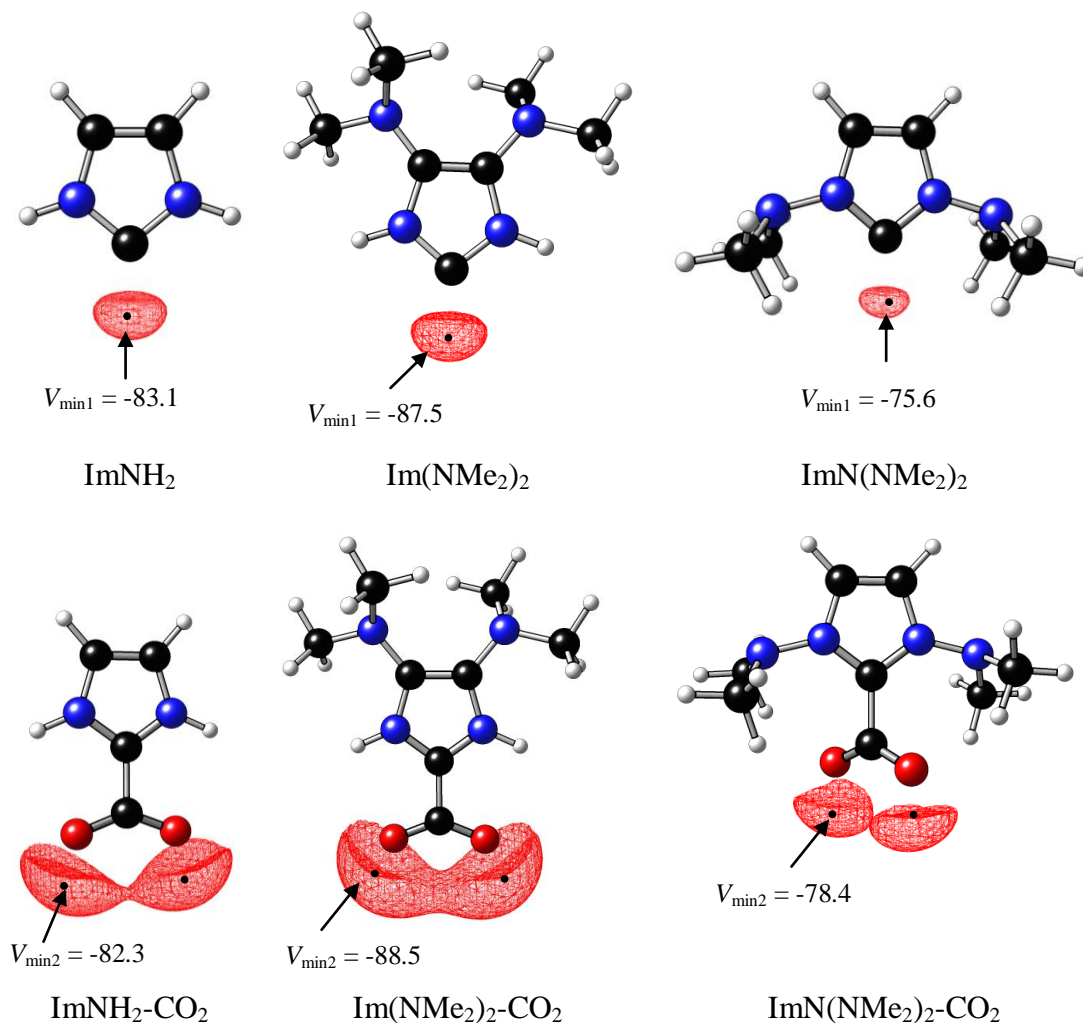
Figure 4.4 Representation of the MESP isosurface of some set A and set B NHCs. V_{min1} and V_{min2} are in kcal/mol.

C-substituents. The value of θ is zero or close to zero for set A systems, which also indicates that the CO_2 binding is not sterically affected by the C_4 and C_5 substituents. Hence, V_{min1} can be treated as a convenient electronic parameter to describe the substituent effect in NHCs which in turn can explain the binding efficiency of CO_2 though a 2e coordination bond from the carbene. The more electron rich is the carbene, the stronger is the coordination bond. This fact is also reflected in the CC bond distance (d_{cc}) of NHC-adduct (Table 4.1). The shortening of the CC bond occurs with increase in the electron donating nature of the NHC and results in weakening of the CO bond.
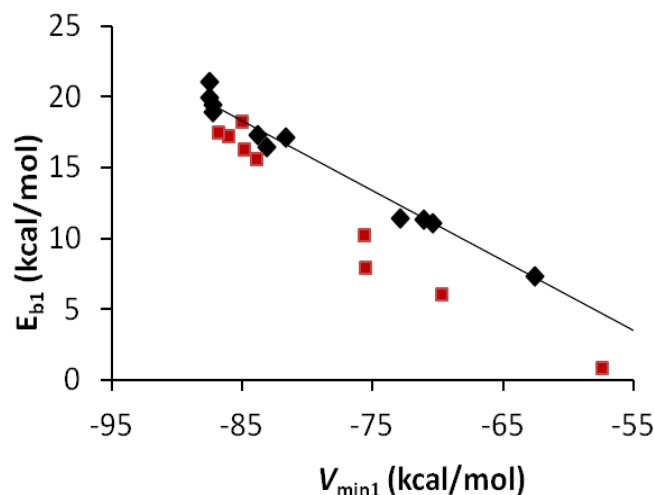
Figure 4.5 Correlation between V_{min1} and E_{b1} of the NHCs given in set A (black) and set B (red).

It is believed that the substituents at the nitrogen atoms significantly contribute to the steric demand of the carbene carbon and also they affect the stability of the NHC-CO_2 adducts. Both V_{min1} and V_{min2} show less negative values for set B systems than set A systems. This suggests that electronically, substitution at the N-positions is less effective for making electron rich carbene than substitution at C-positions. The binding distance of CO_2 with NHC (d_{cc}) is also increased in the case of N-substituted systems compared to C-substituted systems. This can be attributed to a decrease in the electron rich character of set B systems as well as increase in the steric effect. The θ values give a good indication of the steric effect which falls in the range of $18 - 90^o$ for all the N-substituted systems except the $ImNMe_2$-CO_2. In the case of $ImNMe_2$-CO_2, θ observed for the crystal structure [Van Ausdall *et al.* 2009] is $29.0°$ whereas the calculated structure showed a value of 0.0^o. Calculation also showed that $ImNMe_2$-CO_2 can exist in a twisted conformation ($\theta = 26.4°$) which is less stable than the planar conformation by 0.8 kcal/mol. These results suggest that N-substituents significantly hinder the co-planarity of carboxylate moiety and imidazolium ring. The V_{min1} of set B systems are significantly deviated from the correlation line obtained for set A systems (Figure 4.5). Since the

correlation line of set A systems is free from steric influence, the deviation of V_{min1}

points of set B systems from set A line is considered as due to steric influence of the N-

substituents. From the analysis of V_{min1} of set A and set B systems, it is clear that alkyl

substitution at the C- and N- positions can significantly increase the negative MESP

around the carbene lone pair. The C-substitution with NMe_2 is also very effective for

making an electron rich carbene while the same at N-positions will not be effective.

Set C and set D systems carry both N-and C-substituents wherein the former has

well defined substituents while the latter has saturated/unsaturated ring fusions at the C-

N bonds. Figure 4.6 shows the V_{min1} of a representative set of NHC ligands of set C and

D and V_{min2} of the corresponding CO_2 adduct. The V_{min1} of free NHCs and V_{min2}, E_{b1}, d_{cc},

$V_{min1} = -88.4$
Im(NMe$_2$)$_2$NMe$_2$

$V_{min1} = -90.3$
ImBicar

$V_{min2} = -88.0$
Im(NMe$_2$)$_2$NMe$_2$-CO$_2$

$V_{min2} = -91.0$
ImBicar-CO$_2$
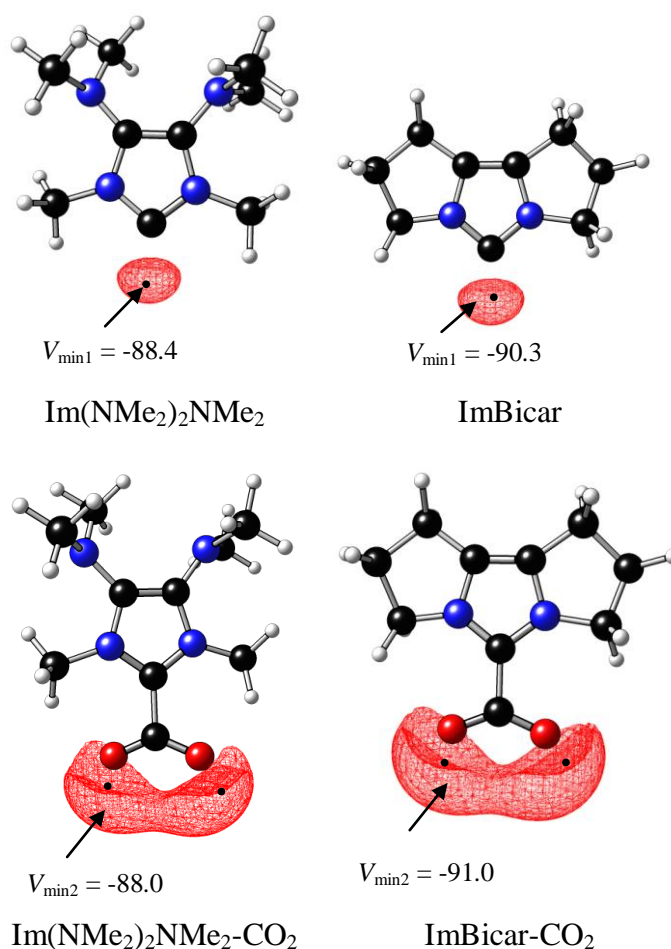
Figure 4.6 Representation of the MESP isosurface of set C and set D NHCs. V_{min1} and

V_{min2} are in kcal/mol.

and θ of   NHC-CO_2 adducts of set C and D systems are given in Table 4.2.

Table 4.2 V_{min1} of free NHCs and V_{min2}, E_{b1}, d_{cc}, and θ of NHC-CO_2 adducts of set C and set D NHCs.

system	V_{min1} (kcal/mol)	V_{min2} (kcal/mol)	E_{b1} (kcal/mol)	d_{cc} (Å)	θ (°)
Im(NO$_2$)$_2$NMe$_2$	-54.7	-65.6	1.8	1.569	33.7
Im(CF$_3$)$_2$NMe$_2$	-66.6	-73.5	7.1	1.557	29.3
Im(NMe$_2$)$_2$NMe$_2$	-88.4	-88.0	18.0	1.549	27.8
ImCl$_2$NMe$_2$	-72.9	-77.4	10.7	1.561	26.2
Im(CN)$_2$NMe$_2$	-58.4	-67.1	4.8	1.567	30.0
Im(CO$_2$Me)$_2$NMe$_2$	-75.1	-79.9	10.0	1.557	35.4
ImF$_2$NMe$_2$	-73.7	-76.8	11.0	1.56	18.5
ImMe$_2$NMe$_2$	-88.2	-86.5	17.7	1.55	26.4
ImMe$_2$N(OMe)$_2$	-73.6	-83.3	8.4	1.555	45.5
ImMe$_2$N(NMe$_2$)$_2$	-78.5	-80.8	12.5	1.542	45.7
ImEt$_2$N(OMe)$_2$	-73.3	-83.4	8.3	1.555	45.4
ImEt$_2$N(NMe$_2$)$_2$	-77.4	-80.8	12.3	1.543	50.4
ImPh$_2$N(OMe)$_2$	-73.7	-82.9	7.1	1.556	48.5
ImPh$_2$N(NMe$_2$)$_2$	-73.4	-79.6	10.5	1.542	53.3
ImCl$_2$N^{i}Pr$_2$	-74.2	-78.3	10.6	1.553	45.9
Im(NO$_2$)$_2$N^{i}Pr$_2$	-56.9	-67.6	4.2	1.558	42.7
ImF$_2$NPh$_2$	-67.7	-77.7	4.4	1.552	90.6
ImBicar	-90.3	-91.0	20.9	1.530	0.6
ImCylm	-89.9	-90.0	20.1	1.540	14.9
ImPhen	-83.3	-86.7	17.5	1.540	5.8
IMPhenPh$_2$	-83.7	-87.1	14.7	1.540	34.8
ImDpylm	-77.9	-85.9	17.6	1.530	0.0
BImNMe$_2$	-79.3	-80.8	13.2	1.552	34.0
BImNEt$_2$	-79.4	-81.5	14.9	1.547	30.9
Py[b]ImNMe$_2$	-75.9	-80.6	11.8	1.551	25.6
Py[c]ImNMe$_2$	-73.2	-76.7	10.8	1.554	35.7

In Figure 4.7, (V_{min1}, E_{b1}) points are plotted for set C and D systems along with V_{min1} versus E_{b1} correlation line for set A systems. This plot shows that set C and D systems agree with the general observation that CO_2 binding energy increases with increase in the electron rich character of the carbene lone pair. Since the correlation line for set A systems occupy steric free area, the deviation of (V_{min1}, E_{b1}) points from this line can be attributed to the steric effect. In general, steric effect decreases the affinity of NHC towards CO_2. The trends observed in d_{cc}, and θ are very similar to that observed in the cases of set A and set B systems. Sterically demanding substituents increase both θ and d_{cc}.
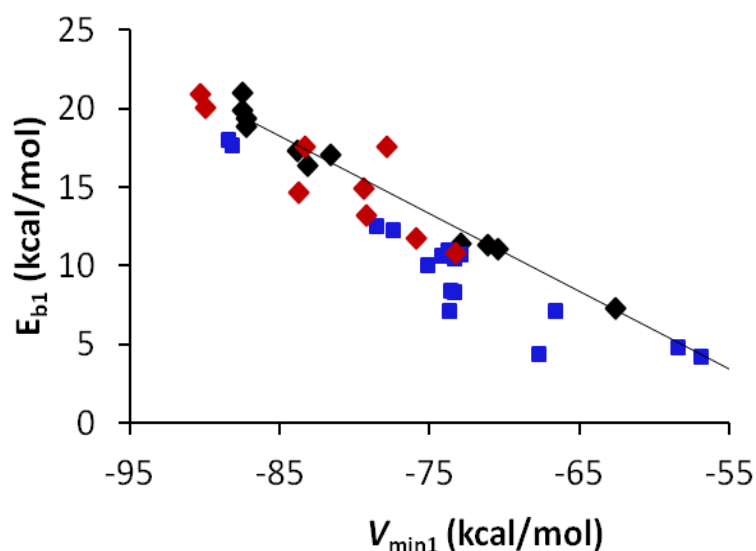
Figure 4.7 Correlation between V_{min1} and E_{b1} of the NHCs given in set A (black), set C (blue) and set D (red).

Since substituent effects are mostly additive in organic systems, the ligands in set C with substituents on both the ring nitrogen atoms and ring carbon atoms are expected to show the combined effect on the MESP at the carbene lone pair. Applying additivity of substituent effect, V_{min1} or V_{min2} of set C systems can be predicted by adding the contributions (ΔV_{min} values) of the C- substituents from set A systems and N-substituents

from set B systems to the corresponding V_{min1} or V_{min2} of the unsubstituted $ImNH_2$ system. All the systems follow additivity to a large extent (Figure 4.8) as the predicted V_{min1} and V_{min2} values are approximately $\pm3\%$ deviated from the actual values for most of the systems. However, the ImF_2NPh_2 and $ImPh_2N(OMe)_2$ systems show a deviation of 6.3 and 7.6 %, respectively for V_{min1} and the $ImF_2NPh_2-CO_2$ systems shows a deviation of 4.7% for V_{min2}. The most electron rich NHC is $Im(NMe_2)_2NMe_2$ as it contains the most donating $N(Me_2)$ substituent at the C-position and Me at the N-position.
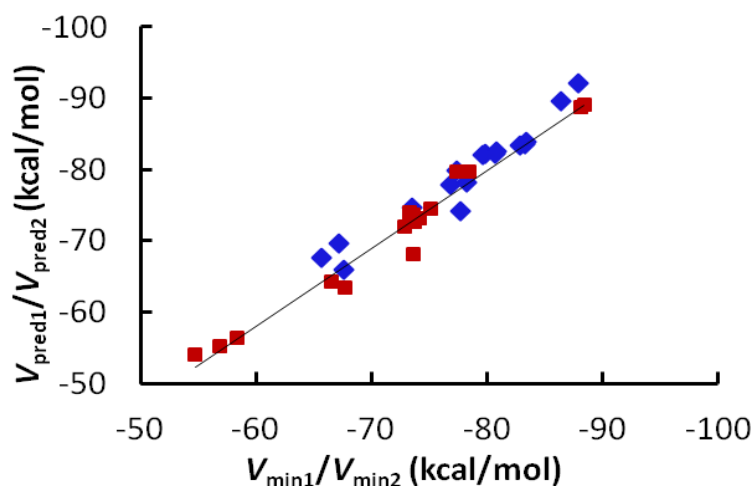
Figure 4.8 Correlation between actual V_{min} and predicted V_{min} using additivity of substituent effect. Red squares correspond to V_{min1} and V_{pred1} and blue squares correspond to V_{min2} and V_{pred2}.

Substitution in ImBicar can be compared with the $ImMe_2NMe_2$ given in set C because the C- and N- positions of both systems are connected to saturated hydrocarbon moieties. Importantly, V_{min1} (-90.3 kcal/mol) and V_{min2} (-91.0 kcal/mol) of ImBicar are respectively 2.1 kcal/mol and 4.5 kcal/mol more negative than $ImMe_2NMe_2$. This means that the ring fusion and the ring strain associated with the additional five-membered ring in ImBicar can enhance the electron density at the carbene lone pair. Very similar observation of V_{min} is observed for ImCylm where the N- and C- substitutions are filled

with saturated hydrocarbon portions. Among all the NHC systems studied herein, MESP features suggest that the most electron rich systems are ImBicar and ImCylm and they show the highest CO_2 binding affinity of 20.9 and 20.1 kcal/mol, respectively. The C- and N- positions of ImPhen, IMPhenPh$_2$, BImNMe$_2$, BImNEt$_2$, Py[b]ImNMe$_2$, and Py[c]ImNMe$_2$ are connected to sp^2 and sp^3 hybridized carbon atoms, respectively and therefore the V_{min} of these systems can be compared with ImPh$_2$NMe$_2$. Similarly, V_{min} of ImDpylm can be assessed on the basis of the V_{min} of ImPh$_2$NPh$_2$ system. These comparisons clearly indicate that, the ring fused structures show slightly more negative character for V_{min} in both free and CO_2 complexed systems. A connection to sp^2 carbon will decrease the electron density on the carbene. In general, ring fusion at the CC and CN bonds of the NHC system as well as ring strain due to additional five-membered ring is good for increasing the electron rich character of the carbene lone pair as well as its CO_2 affinity.

On the basis of the MESP-based analysis of the carbene center of NHC, we can see that the combined effect of alkyl and -NMe$_2$ substitution can at the most increase the binding energy to a value of 18.0 kcal/mol which is 1.6 kcal/mol more than unsubstituted NHC (16.4 kcal/mol). For standard experimental conditions, even the most negative E_{b1} value (20.9 kcal/mol) observed for ImBicar is not enough to make stable NHC-CO_2 complexes. Therefore, to enhance the binding energy, we propose the use of N-substituents with hydrogen bond formation ability with the incoming CO_2 moiety and such systems (set E) are presented in Figure 4.9. The selected N-substituents are -CH$_2$OH, -CH$_2$NHCOMe, -CH$_2$NHPh, and related ring-fused substituents. The incorporation of amino/amido groups on the N-positions is already reported in the literature [Spencer and Fryzuk 2005; Li *et al.* 2011]. All the systems in set E show considerable improvement (6 - 14 kcal/mol) in the binding energy from the most stable ImBicar-CO_2 system.
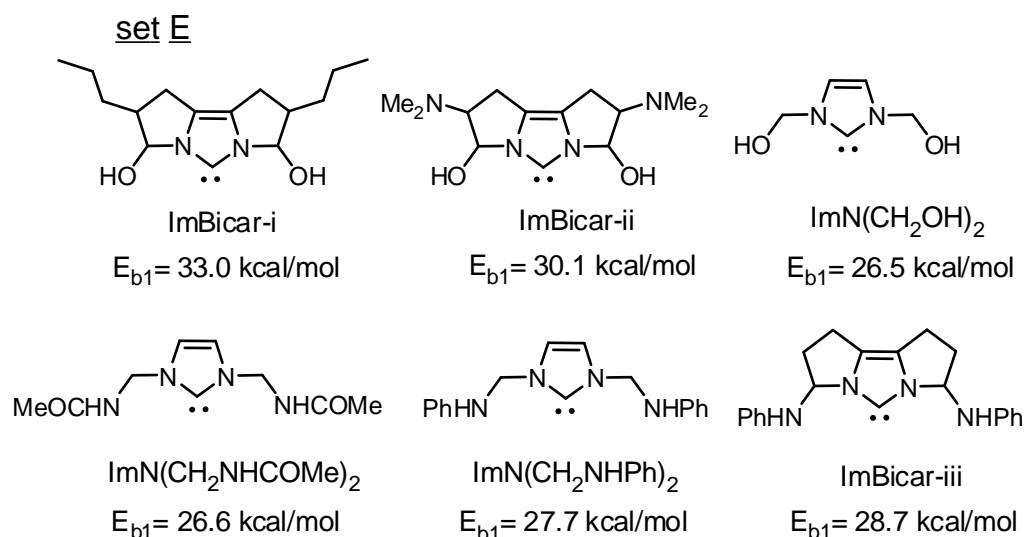
Figure 4.9 Selected new designs of NHCs. The CO_2 binding energy is also depicted.

ImBicar-i and ImBicar-ii show good binding affinity (33.0 and 30.1 kcal/mol respectively) due to the combined effect of electron donating substituents, ring strain, and hydrogen bonding interactions (Table 4.3). Substitution of *N*-amino group also stabilizes the NHC-CO_2 adduct *via* hydrogen bonding interactions. ImN(CH$_2$NHCOMe)$_2$ shows a binding affinity (E$_{b1}$) of 26.6 kcal/mol whereas ImN(CH$_2$NHPh)$_2$ and ImBicar-iii shows 27.7 and 28.7 kcal/mol respectively.

Table 4.3 V_{min1} of free NHCs and V_{min2}, E_{b1}, d_{cc}, and θ of NHC-CO_2 adducts of set E NHCs.

system	V_{min1} (kcal/mol)	V_{min2} (kcal/mol)	E_{b1} (kcal/mol)	d_{cc} (Å)	θ (°)
ImBicar-i	-69.3	-73.6	33.0	1.515	0.2
ImBicar-ii	-70.5	-74.0	30.1	1.516	0.4
ImN(CH$_2$OH)$_2$	-72.2	-68.7	26.5	1.529	0.5
ImN(CH$_2$NHCOMe)$_2$	-75.0	-71.2	26.6	1.531	17.3
ImN(CH$_2$NHPh)$_2$	-64.8	-73.9	27.7	1.535	6.7
ImBicar-iii	-79.2	-80.0	28.7	1.517	10.4

Part B: Rational Design of Multi-topic NHCs

4.4 Introduction

N-heterocyclic carbenes (NHCs) are well known for their unique reactivity and strong coordination behavior with transition metals in various oxidation states [Arduengo III 1999; Peris and Crabtree 2004; Hahn and Jahnke 2008; De Frémont *et al.* 2009; Poyatos *et al.* 2009; Diez-Gonzalez *et al.* 2009] and a large variety of stable NHCs with different structural and electronic properties are already available for numerous applications in chemistry [Fürstner *et al.* 2001; Trnka and Grubbs 2001; Connor *et al.* 2002; Enders *et al.* 2007; De Frémont *et al.* 2009; Crees *et al.* 2010; Oisaki *et al.* 2010]. Most of the NHCs function as monodendate ligands through the utilization of the carbene lone pair while recent research has yielded a variety of multi-topic ligands that can act as bischelating, pincer, tripodal, or bridging mode of complexation with the metal [Arduengo *et al.* 1992; Rasika Dias and Jin 1994; Hu *et al.* 2003; Boydston *et al.* 2005; Khramov *et al.* 2006; Bedford *et al.* 2006; Scheele *et al.* 2006; Mata *et al.* 2007; Liu *et al.* 2007; Edworthy *et al.* 2007; Normand and Cavell 2008; Poyatos *et al.* 2008; Raynal *et al.* 2008; Morgan *et al.* 2009; Varnado Jr *et al.* 2009; Dominique *et al.* 2009; Corberan *et al.* 2009 ; Williams and Bielawski 2010; Tennyson *et al.* 2010; Prades *et al.* 2011; Mercs *et al.* 2011]. Recently Bielawski and co-workers reported a Janus-type NHC (benzobis(imidazolylidene)) which was the first annelated system with two carbene centers arranged facially opposite [Khramov *et al.* 2006]. They also synthesized a Cerberus-type annelated tritopic NHC from a triptycene derivative (**13** in Figure 4.10) [Williams and Bielawski 2010]. Apart from **3** and **13**, no other annelated multi-topic architectures are reported yet. NHC based chemistry is expected to grow from their early

adolescent stage to a mature stage with the synthesis of multitopic ligands [Poyatos *et al.* 2009] as they offer rapid advancement in homogeneous catalysis, organocatalysis, organometallic polymers, molecular electronics, metal-based drug molecules, metal organic and covalent-organic frameworks *etc*.

Several experimental and theoretical studies aimed at quantifying the stereoelectronic properties of NHCs as well as understanding the nature of metal-carbon bonding have contributed immensely to the development of novel ligands for catalysis [Dorta *et al.* 2005; Cavallo *et al.* 2005; Herrmann *et al.* 2006; Tonner *et al.* 2007; Fürstner *et al.* 2007; Leuthaeusser *et al.* 2007; Kelly III *et al.* 2008; Song *et al.* 2008; Khramov *et al.* 2008; Huynh *et al.* 2009; Gusev 2009; Hirano *et al.* 2009]. According to structural, thermodynamic, and magnetic criteria, it has been recognized that the imidazol-2-ylidene, the core constituent of a typical NHC, possesses substantial aromatic character due to the delocalization of six-π electron (sextet) within the *N*-heterocyclic ring [Heinemann *et al.* 1996; Boehme and Frenking 1996; Lehmann *et al.* 1999]. For instance, the aromatic stabilization of imidazol-2-ylidene is 27.8 kcal/mol, which is comparable to that of benzene (26-37 kcal/mol) [Schleyer and Pühlhofer 2002; Suresh and Koga 2002; Mo and Schleyer 2006; Suresh and Koga 2006].

In the case of polycyclic aromatic hydrocarbons (PAHs), Clar's sextet theory is used to describe and compare their aromatic character. A Kekule resonance structure having the largest number of disjoint aromatic π-sextets (benzene-like moieties; Figure 4.10A) is the most aromatic and the most suitable to describe a PAH [Clar 1972; Suresh and Gadre 1999; Chai and Head-Gordon 2008]. For instance, tetracene, a linear polyacene having only one sextet is less aromatic than chrysene as the latter possesses two sextets. Similarly, triphenylene with three aromatic sextets is more aromatic than its isomers tetracene and chrysene.

(A)

benzene naphthalene anthracene phenanthrene tetracene chrysene

triphenylene pentacene benzo[*k*]tetraphene tribenzo[*f*,*k*,*m*]tetraphene

(B)

1   2   3   4   5   6

7   8   9   10

11   12   13   14
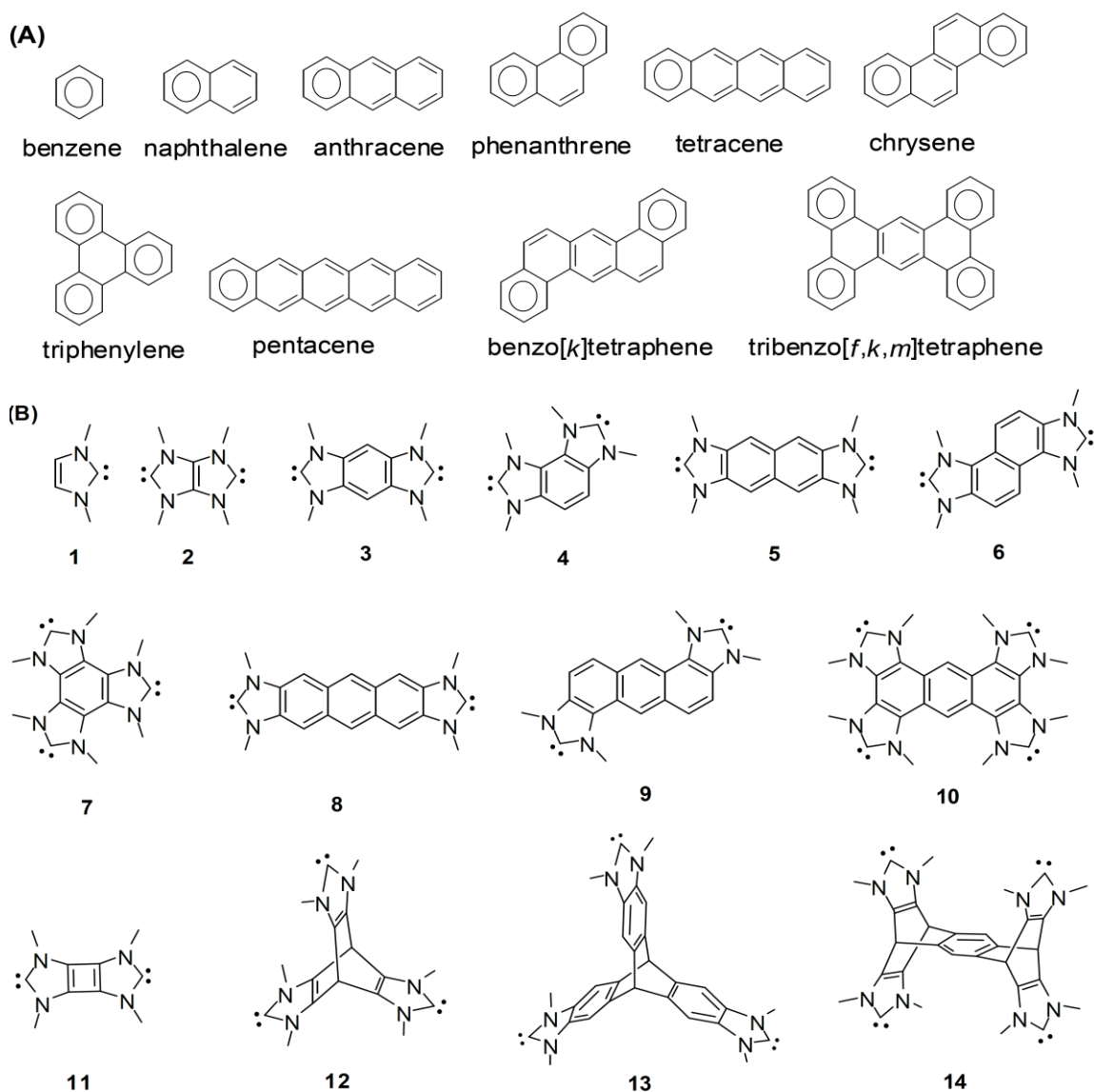
Figure 4.10 (A) Clar's 'sextet' structures of benzenoid hydrocarbons. (B) Proposed NHC systems. **1**, **3**, and **13** are known.

Extending Clar's sextet theory to heterocyclic five membered NHC systems is not straight forward because this theory is centered on delocalization of a sextet of electrons within a six-membered ring. Since one NHC ring possesses one full 'sextet' of electrons, the ring fusion at the CC bond may lead to the formation of a naphthalene analogue, **2** – a bisimidazolinylidene. Though **2** is not yet reported, the saturated analogue of **2** (tetraazabicyclooctane) is recently synthesized by Peris and co-workers and also showed its conversion into a biscarbene iridium complex [Prades *et al.* 2011]. Expansion of **2** to

higher analogues, *viz.* anthracene, phenanthrene, and other PAH topologies using only imidazole carbene moieties are impossible because a second CC bond for ring fusion is not available. In order to bypass this disadvantage and also to follow Clar's sextet theory, NHC system can be fused with benzenoid moieties to produce multiple ring multi-topic structures. The Janus type di-topic NHC synthesized by Bielawski and co-workers gives a good example for the application of such a strategy [Khramov *et al.* 2006]. Hence, multi-topic NHC structures that are analogues to Clar's benzenoid hydrocarbons can be designed (Figure 4.10B). In such systems, the number of π-electrons are identical to the corresponding PAH. A structure **11** analogues to the strained biphenylene is also possible by joining two NHCs *via* two formal C_{sp2}-C_{sp2} single bonds.

Ring fusions can yield only two dimensional NHC architectures. For three dimensional structures, the CC bond of an NHC can be connected to C_{sp3} atoms as in **12**. The Cerberus type architecture **13** of Bielawski and co-workers is the only known example for this [Williams and Bielawski 2010] and in this ligand, the NHCs annelated to benzenoid moieties are connected to the C_{sp3} atoms. A variety of multi-topic NHC systems with architecture similar to **13** can be made by substituting its benzenoid part with various other PAH moieties. Further, we propose that molecular architecture incorporating four NHC moieties as in **14** could be feasible if two di-topic NHC moieties can be connected *via* an aromatic spacer moiety. By changing the spacer to different PAH moieties as well as by the use of annelated NHC systems as branches from C_{sp3} links, further expansion of this architecture is possible.

4.5 Computational Methods

The M06-L/6-311++G(d,p) level DFT method [Zhao and Truhlar 2006] as implemented in Gaussian 09 [Frisch 2009] is used for geometry optimization and frequency calculation. For the design of large metal organic complexes, PM6 method is

used [Stewart 2007]. This study will reveal that all the linear, angular, two dimensional and three dimensional multi-topic designs of NHCs given in Figure 4.10 can exist as stable molecules. The assessment on stability as well as reactivity will be made by studying the aromaticity, proton affinity, lone pair strength of the carbene and the coordination reaction of the ligand with CuCl.

4.6 Designing Multi-topic *N*-Heterocyclic Carbenes

Hydrogenation of the carbene carbon can remove aromatic conjugation in the NHC ring. On the basis of this, the homodesmotic reaction of the type given in Scheme 4.1 is designed for all the NHCs. Since the number, nature and type of bonds are conserved in the reaction except the aromatic conjugation, the energy of the reaction will give a good quantitative estimate of the aromatic stabilization (E_{Aroma}) of an NHC. E_{Aroma} 25.7 kcal/mol is estimated for **1** which is very close to the value 27.8 kcal/mol reported by Boehme and Frenking [Boehme and Frenking 1996] for imidazol-2-ylidene. E_{Aroma} values (Table 4.4) show that **1** is the most stabilized NHC while the Janus type (**3**) and Cerberus type (**13**) have E_{Aroma} 18.7 and 19.2 kcal/mol, respectively. Since **3** and **13** are known, we expect that NHCs showing E_{Aroma} around 18 kcal/mol could be stable. Thus **2**, **4**, **6**, **9**, **10**, **12**, and **14** are recommended as stable multi-topic carbenes. **5**, **7**, **8**, and **11** also could be stable as they show appreciable E_{Aroma} values (> 12 kcal/mol). In general, angular systems are more stable than linear systems (**5** and **6**; **8** and **9**) while **3** and **4** are exceptions because the latter experiences some steric effect from the adjacent *N*-methyl substituents. Aromaticity decreased along the linear polyacene analogues **3**, **5**, and **8**. **2** is an exception to this trend as it experiences larger strain effect from two fused five-membered rings.
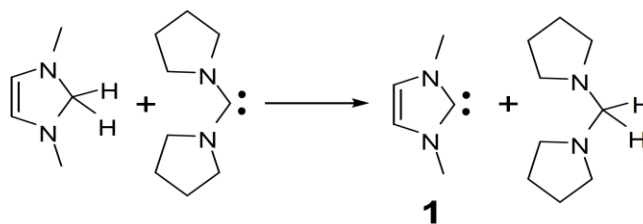
Scheme 4.1 Homodesomitc reaction to measure aromatization Energy.

Table 4.4. Aromatic properties, MESP minimum (V_{min}), proton affinity (PA), and CuCl binding energy (E_{CuCl}) for NHCs. E_{Aroma}, V_{min}, PA, and E_{CuCl} in kcal/mol.

NHC	E_{Aroma}	NICS(0)	HOMA	V_{min}	PA	E_{CuCl}
1	25.7	-11.8	0.784	-82.3	259.3	67.7
2	17.3	-9.1	0.666	-76.5	260.5	67.3
3	18.7	-9.9	0.846	-77.1	261.6	67.4
4	17.2	-10.3	0.853	-75.3	260.2	67.2
5	14.3	-8.7	0.818	-75.7	261.9	67.3
6	18.2	-10.8	0.876	-76.4	262.9	67.4
7	14	-10.4	0.852	-72.9	260.1	66.2
8	12.2	-8.1	0.783	-74.7	262.3	67.2
9	19.4	-10.8	0.873	-76.7	264.4	67.5
10	17.8	-10.3	0.891	-72.4	262.6	66.7
11	13.9	-5.7	0.672	-75.4	260.7	66.9
12	21.6	-9.1	0.727	-78.3	264.9	67.8
13	19.2	-10.1	0.763	-77.6	264.2	67.6
14	21.3	-10	0.705	-78.9	267.4	68.3

Aromatic character of NHC systems are also measured using nucleus independent chemical shift at the ring center (NICS(0)) [Schleyer *et al.* 1996] as well as the geometry based harmonic oscillator model of aromaticity (HOMA) [Krygowski 1993; Cyrañski *et al.* 1998]. Both show very similar trend (Table 4.4) and suggest that all the recommended systems possess good aromatic character. NICS(0) is the most negative in
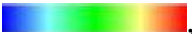
1 (-11.8) and the least negative in biphenylene analogue **11** (-5.7) while the rest show values close to that of **1** (-8.1 – -10.8). Though HOMA value of **1** is high, many of the NHCs annelated to benzenoid moieties (**3**, **4**, **5**, **6**, **7**, **9**, and **10**) show larger HOMA values. The NHC analogous to tribenzo[f,k,m]tetraphene (**10**) has four carbene centers and it shows good aromatic stabilization energy (17.8 kcal/mol) as well as high aromatic character (NICS(0) = -10.3; HOMA = 0.891).

Recently we have shown that molecular electrostatic potential (MESP) minimum (V_{min}) at the carbene lone pair is an efficient descriptor for the electron donating power of an NHC system [Mathew and Suresh 2010]. V_{min} of all the carbenes are depicted in Table 4.4. The MESP distribution is also shown in Figure 4.11 which shows the electron rich carbene lone pair region as well as the delocalized electron distribution over the annelated aromatic rings (V_{min} for carbene lone pair is located in the dark blue region). **1** shows the most negative V_{min} (-82.3 kcal/mol) and suggests its strong electron donating power for coordination bonds while **3** (-76.9 kcal/mol) and **13** (-77.6 kcal) show slightly higher V_{min} values. V_{min} of all the other NHCs too fall in the narrow range -72.4 – -78.8 kcal/mol. This means that annelation as well as branching through C_{sp3} carbon atoms only slightly affect the electron rich character of the carbene center of a multi-topic NHC system and they all must behave as strong electron donating ligands. In general, an increase in E_{Aroma} shows a decrease in the negative character of V_{min}.

The gas phase proton affinity (PA) values are reported in Table 4.4. The PA 259.3 kcal/mol obtained for **1** is in good agreement with the value 258.3 kcal/mol reported by Yates and co-workers using the high accuracy CBS-QB3 method [Magill *et al.* 2004]. Compared to **1**, all other NHC show slightly higher PA values (260.1 - 267.4 kcal/mol), the smallest for **1** and the highest for **14**. PA has been shown to correlate directly with pKa and hence the former is used to assess the pKa of carbenes [Kovacevic and Maksic 2001; Magill *et al.* 2004]. Between **1** and **14**, the difference in PA is only
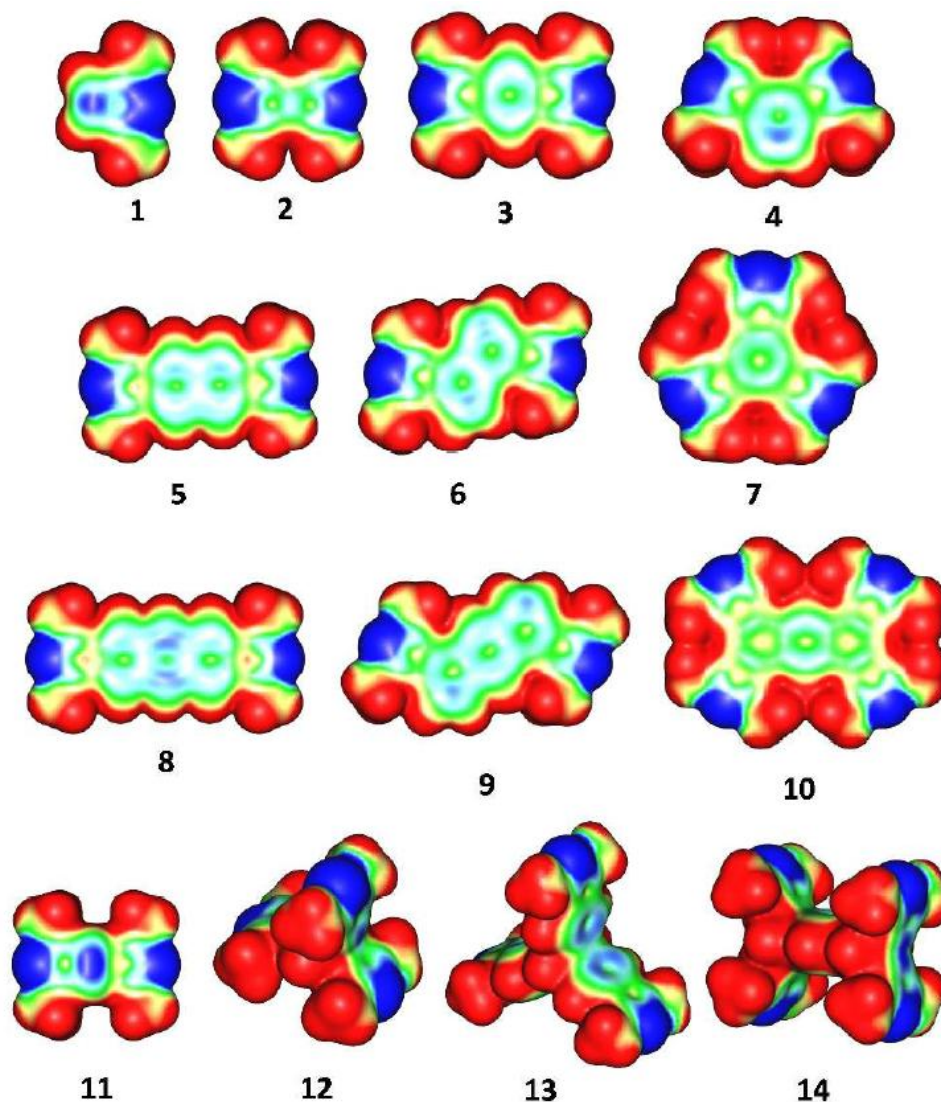
Figure 4.11 Molecular electrostatic potential mapped on to 0.003 a.u. electron density surface. Color coding ▬▬▬▬▬▬, blue -0.02 a.u. to red 0.02 a.u.

7.1 kcal/mol. To make a comparison, we consider the PA difference 6.6 kcal/mol reported by Yates and co-workers for **1** (1,3-dimethylimidazol-2-ylidene) and its higher derivative 1,2,3,4-tetramethylimidazol-2-ylidene [Magill *et al.* 2004]. The pKa of **1** was 21.1 while that of the higher derivative was 23.8. It means that for all the new designs of NHCs presented herein, pKa value will fall very close to that of **1**.

Since well-defined (NHC)CuCl complexes can be easily prepared from the imidazolium salt and copper(I) chloride [Diez-Gonzalez *et al.* 2010], we have estimated the binding energy of CuCl with NHC (E_{CuCl}) to assess the coordinating power of these

ligands. E_{CuCl} also measures the metal-carbon bond energy. Geometric parameters of **1**-CuCl showed excellent agreement to a recently reported X-ray structure of (1,3-diadamantylimidazol-2-ylidene)-CuCl [Diez-Gonzalez *et al.* 2010]. For instance the (calculated, X-ray) values in Å for C_1-Cu, Cu-Cl, C_1-N, C_2-N, and C_2-C_3 are respectively (1.883,1.894), (2.107, 2.111), (1.364, 1.361), (1.380, 1.383), and (1.355, 1.355). The E_{CuCl} is nearly same for all the ligands, the smallest being 66.2 kcal/mol for **7** and the highest being 68.2 kcal/mol for **14**. This indicates that the annelation and branching strategies are highly useful to preserve the coordination power of the carbene in multi-topic systems. We also found a linear correlation (correlation coefficient = 0.941) between V_{min} and E_{CuCl} (**1** is an exception) which agrees with the earlier finding that V_{min} of the carbene lone pair gives a good measure of the electron donating power of the NHC ligands. The present V_{min} data is highly sensitive considering the fact that E_{CuCl} values fall in a very narrow range 66.2 − 68.3 kal/mol.

Among the fourteen systems given in Figure 4.10B, **14** is perhaps the most interesting to design a metal organic framework because it consists of two pairs of carbene centers, one angling in the upward and the other in the downward directions (Figure 4.10B). This orientation of carbene centers will enable the formation of compact cage/pore structures through metal coordination. To illustrate this, $(\mathbf{14})_2(CuCl)_2$ and $(\mathbf{14})_3(CuCl)_4$ are modeled (Figures 4.12a and 4.12b). The cages formed are hexagonal in shape and they show ~1 nm size width and length. In the case of the complex given in Figure 4.12c, the ligand (**15**) has a naphthyl spacer which will enable the cage to expand more lengthwise. A cage structure with ~1.5 nm size for width and length is possible if the ligand (**16**) has a naphthyl spacer and annelated carbene centers on a benzenoid moiety (Figure 4.12d). On the basis of M06-L/6-311++G(d,p)//PM6 calculation, C-Cu bond energy is estimated to be 41.7, 42.0, 42.0, and 43.3 kcal/mol for $(\mathbf{14})_2(CuCl)_2$, $(\mathbf{14})_3(CuCl)_4$, $(\mathbf{15})_2(CuCl)_2$, and $(\mathbf{16})_2(CuCl)_2$, respectively.
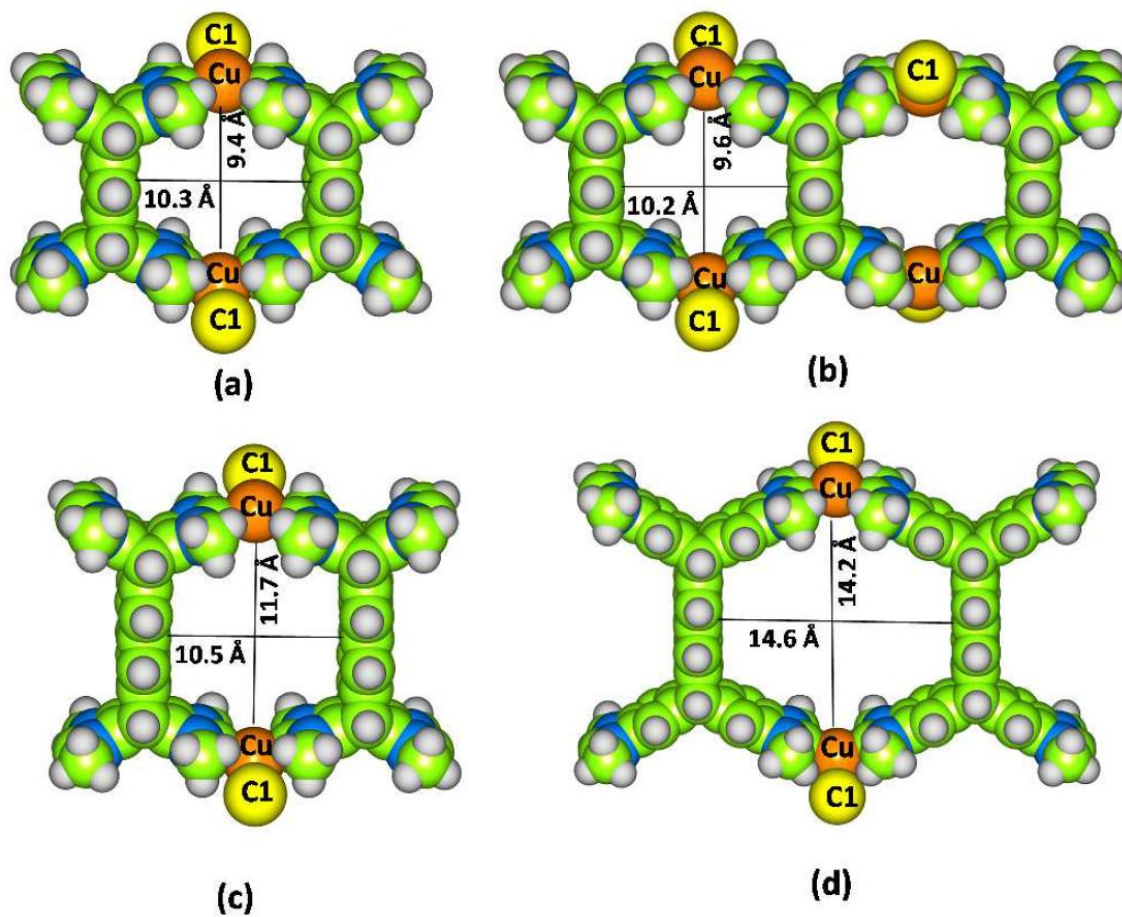
Figure 4.12 Optimized geometries at PM6 level for association complexes of multi-topic

ligands with CuCl.

Summary

The topological features of MESP to evaluate the stereoelectronic properties of NHC as well as the NHC−CO$_2$ adduct are presented in the first part of this chapter. In general, the electron-rich character of the carbene center is well reflected on the V_{min1} value observed for the carbene lone pair. The C-substituents exert electronic effect on the carbene center while N-substituents contribute significantly through steric effects. For the combination of standard substituents given in set C, the most electron-rich NHC is Im(NMe$_2$)$_2$NMe$_2$, as it contains the most electron donating NMe$_2$ substituent at the C-position and Me at the N position. V_{min1} or V_{min2} of set C systems can be predicted by applying the additivity of substituent effect. It is also observed that the ring fusion at the CC and CN bonds of the NHC system and the associated ring strain in the structure is good for increasing the electron-rich character of the carbene lone pair. In addition, the use of an N-substituent such as CH$_2$OH, CH$_2$NHCOMe, and CH$_2$NHPh substantially improve the CO$_2$ fixing ability of NHCs.

We have also designed and characterized theoretically several multi-topic NHC systems based on Clar's sextet theory and is summarized in the second part of this chapter. Annelation of NHC to a benzenoid moiety as well as branching through C$_{sp3}$ linkage is highly recommended for the synthesis of stable multi-topic architectures. Though synthesis of these systems is a challenge for experiment, the recently established synthetic methodology by Peris and co-workers [Prades *et al.* 2011] on double C-H bond activation of CH$_2$ groups for the preparation bisimidazolinylidene complexes as well as the synthetic methods developed by Bielawski and co-workers [Neilson *et al.* 2012] for accessing di-topic NHCs could provide breakthroughs.

List of publications

A) Articles in Journals

1. A Higher Energy Conformer of (S)-proline is the Active Catalyst in Intermolecular Aldol Reaction: Evidence from DFT Calculations: **Manjaly J. Ajitha** and Cherumuttathu H. Suresh, *J. Mol. Catal. A*, **2011**, 345, 37.

2. Role of Stereoelectronic Features of Imine and Enamine in (S)-Proline Catalyzed Mannich Reaction of Acetaldehyde: An in Silico Study: **Manjaly J. Ajitha** and Cherumuttathu H. Suresh, *J. Comp. Chem.,* **2011**, 32, 1962.

3. Mechanism of Epoxide Hydrolysis in Microsolvated Nucleotide Bases Adenine, Guanine and Cytosine: A DFT Study: Kunduchi P. Vijayalakshmi, Neetha Mohan, **Manjaly J. Ajitha** and Cherumuttathu H. Suresh, *Org. Biomol. Chem.,* **2011**, 9, 5115.

4. NHC Catalyzed CO_2 Fixation with Epoxides: Probable Mechanisms Reveal Ter Molecular Pathway: **Manjaly J. Ajitha** and Cherumuttathu H. Suresh, *Tetrahedron Lett.,* **2011**, 52, 5403.

5. Assessment of Stereoelectronic Factors that Influence the CO_2 Fixation Ability of *N*-Heterocyclic Carbenes: A DFT Study: **Manjaly J. Ajitha** and Cherumuttathu H. Suresh, *J. Org. Chem.,* **2012**, 77, 1087.

6. DPPH Radical Scavenging Activity of Tricin and its Conjugates Isolated from 'Njavara' Rice Bran: A DFT Study: **Manjaly J. Ajitha**, Smitha Mohanlal, Cherumuttathu H. Suresh and Ananthasankaran Jayalekshmy, *J. Agric. Food Chem.*, 2012, 60, 3693.

B) Published contributions to academic conferences

7. Presented a poster entitled "Role of Stereoelectronic Features of Imine and Enamine in (*S*)-proline Catalyzed Mannich Reaction of Acetaldehyde: An *in-Silico* Study" in the "Theoretical Chemistry Symposium (TCS)" held at IIT, Kanpur during 8-12 December 2010.

8. Presented a poster entitled "NHC Catalyzed CO_2 Fixation with Epoxides: Probable Mechanisms Reveal Ter Molecular Pathway" in the International Conference on "Applied Theory on Molecular Systems (ATOMS)" held at Indian Institute of Chemical Technology, Pune, during 2-5 November 2011.

References

Adamo, C.; Barone, V. "Exchange functionals with improved long-range behavior and adiabatic connection methods without adjustable parameters: The mPW and mPW1PW models", *J. Chem. Phys.* 1080, **1998**, 664.

Adamo, C.; Barone, V. "Toward Reliable Density Functional Methods without Adjustable Parameters: The PBE0 Model", *J. Chem. Phys.* 110, **1999**, 6158.

Agami, C.; Levisalles, J.; Puchot, C. "A New Diagnostic Tool for Elucidating the Mechanism of Enantioselective Reactions. Application to the Hajos-Parrish Reaction", *J. Chem. Soc., Chem. Commun.*, **1985**, 441.

Agami, C.; Puchot, C.; Sevestre, H. "Is the Mechanism of the Proline-Catalyzed Enantioselective Aldol Reaction Related to Biochemical Processes?", *Tetrahedron Lett.* 27, **1986**, 1501.

Ahrendt, K. A.; Borths, C. J.; MacMillan, D. W. C. "New Strategies for Organic Catalysis: The First Highly Enantioselective Organocatalytic Diels-Alder Reaction", *J. Am. Chem. Soc.* 122, **2000**, 4243.

Akiyama, T.; Itoh, J.; Yokota, K.; Fuchibe, K. "Enantioselective Mannich-Type Reaction Catalyzed by a Chiral Brønsted Acid", *Angew. Chem. Int. Ed.* 43, **2004**, 1566.

Alcaide, B.; Almendros, P. "Organocatalytic Reactions with Acetaldehyde", *Angew. Chem. Int. Ed.* 47, **2008**, 4632.

Alcarazo, M.; Stork, T.; Anoop, A.; Thiel, W.; Fürstner, A. "Steering the Surprisingly Modular π-Acceptor Properties of N-Heterocyclic Carbenes: Implications for Gold Catalysis", *Angew. Chem. Int. Ed.* 49, **2010**, 2542.

Allemann, C.; Gordillo, R.; Clemente, F. R.; Cheong, P. H. Y.; Houk, K. N. "Theory of Asymmetric Organocatalysis of Aldol and Related Reactions: Rationalizations and Predictions", *Acc. Chem. Res.* 37, **2004**, 558.

Allen, L. C.; Karo, A. M. "Basis Functions for *Ab initio* Calculations", *Rev. Modern Phys.* 32, **1960**, 275.

Arduengo, A. J.; Dias, H. V. R.; Harlow, R. L.; Kline, M. "Electronic Stabilization of Nucleophilic Carbenes", *J. Am. Chem. Soc.* 114, **1992**, 5530.

Arduengo III, A. J. "Looking for Stable Carbenes: The Difficulty in Starting a New", *Acc. Chem. Res.* 32, **1999**, 913.

Aresta, M.; Dibenedetto, A. "Utilisation of CO_2 as a Chemical Feedstock: Opportunities and Challenges", *Dalton Trans.* **2007**, 2975.

Arno, M.; Domingo, L. R. "Density Functional Theory Study of the Mechanism of the Proline-Catalyzed Intermolecular Aldol Reaction", *Theor. Chem. Acc.* 108, **2002**, 232.

Bahmanyar, S.; Houk, K. N. "Origins of Opposite Absolute Stereoselectivities in Proline-Catalyzed Direct Mannich and Aldol Reactions", *Org. Lett.* 5, **2003**, 1249.

[a]Bahmanyar, S.; Houk, K. N. "The Origin of Stereoselectivity in Proline-Catalyzed Intramolecular Aldol Reactions", *J. Am. Chem. Soc.* 123, **2001**, 12911.

[b]Bahmanyar, S.; Houk, K. N. "Transition States of Amine-Catalyzed Aldol Reactions Involving Enamine Intermediates: Theoretical Studies of Mechanism, Reactivity, and Stereoselectivity", *J. Am. Chem. Soc.* 123, **2001**, 11273.

Bahmanyar, S.; Houk, K. N.; Martin, H. J.; List, B. "Quantum Mechanical Predictions of the Stereoselectivities of Proline-Catalyzed Asymmetric Intermolecular Aldol Reactions", *J. Am. Chem. Soc.* 125, **2003**, 2475.

Ban, F.; Rankin, K. N.; Gauld, J. W.; Boyd, R. J. "Recent Applications of Density Functional Theory Calculations to Biomolecules", *Theor. Chem. Acc.* 108, **2002**, 1.

Banerjee, R.; Phan, A.; Wang, B.; Knobler, C.; Furukawa, H.; O'Keeffe, M.; Yaghi, O. M. "High-Throughput Synthesis of Zeolitic Imidazolate Frameworks and Application to CO_2 Capture", *Science* 319, **2008**, 939.

Barbas III, C. F. "Organocatalysis Lost: Modern Chemistry, Ancient Chemistry, and an Unseen Biosynthetic Apparatus", *Angew. Chem. Int. Ed.* 47, **2008**, 42.

Barone, V.; Cossi, M.; Tomasi, J. "A New Definition of Cavities for the Computation of Solvation Free Energies by the Polarizable Continuum Model", *J. Chem. Phys.* 107, **1997**, 3210.

Barone, V.; Orlandini, L.; Adamo, C. "Proton Transfer in Model Hydrogen-Bonded Systems by a Density Functional Approach", *Chem. Phys. Lett.* 231, **1994**, 295.

Bartlett, R. J.; Silver, D. M. "Many-Body Perturbation Theory Applied to Electron Pair Correlation Energies. I. Closed-Shell First-Row Diatomic Hydrides", *J. Chem. Phys.* 62, **1975**, 3258.

Becke, A. D. "Density-Functional Exchange-Energy Approximation with Correct Asymptotic Behavior", *Phys. Rev.* A 38, **1988**, 3098.

Becke, A. D. "Density-Functional Thermochemistry. III. The Role of Exact Exchange", *J. Chem. Phys.* 98, **1993**, 5648.

Becke, A. D. "Density-functional thermochemistry. IV. A new dynamical correlation functional and implications for exact-exchange mixing", *J. Chem. Phys.* 104 **1996**, 1040.

Bedford, R. B.; Betham, M.; Bruce, D. W.; Danopoulos, A. A.; Frost, R. M.; Hird, M. "Iron-Phosphine, -Phosphite, -Arsine and Carbene Catalysts for the Coupling of Primary and Secondary Alkyl Halides with Aryl Grignard Reagents", *J. Org. Chem.* 71, **2006**, 1104.

Berkessel, A.; Elfert, S.; Etzenbach-Effers, K.; Teles, J. H. "Aldehyde Umpolung by N-Heterocyclic Carbenes: NMR Characterization of the Breslow Intermediate in its Keto Form, and a Spiro-Dioxolane as the Resting State of the Catalytic System", *Angew. Chem. Int. Ed.* 49, **2010**, 7120.

Berkessel, A.; Gröger, H. "*Asymmetric Organocatalysis*", Wiley-VCH, Weinheim, Germany, **2005**.

Bertelsen, S.; Jørgensen, K. A. "Organocatalysis - after the Gold Rush", *Chem. Soc. Rev.* 38, **2009**, 2178.

Bhanage, B. M.; Fujita, S. I.; Ikushima, Y.; Arai, M. "Synthesis of Dimethyl Carbonate and Glycols from Carbon Dioxide, Epoxides, and Methanol Using Heterogeneous Basic Metal Oxide Catalysts with High Activity and Selectivity", *Appl. Catal., A* 219, **2001**, 259.

Bickelhaupt, F. M.; Baerends, E. J. "Kohn-Sham Density Functional Theory: Predicting and Understanding Chemistry," *Rev. Comput. Chem.*, 15, **2000**, 1.

Bickelhaupt, F. M.; Baerends, E. J. "The Case for Steric Repulsion Causing the Staggered Conformation of Ethane", *Angew. Chem. Int. Ed.* 42, **2003**, 4183.

Biju, A. T.; Kuhl, N.; Glorius, F. "Extending NHC-Catalysis: Coupling Aldehydes with Unconventional Reaction Partners", *Acc. Chem. Res.* 44, **2011**, 1182.

Biju, A. T.; Padmanaban, M.; Wurz, N. E.; Glorius, F. "N-Heterocyclic Carbene Catalyzed Umpolung of Michael Acceptors for Intermolecular Reactions", *Angew. Chem. Int. Ed.* 50, **2011**, 8412.

Binkley, J. S.; Pople, J.; Hehre, W. J. "Self-Consistent Molecular Orbital Methods. 21. Small Split-Valence Basis Sets for First-Row Elements", *J. Am. Chem. Soc.* 102, **1980**, 939.

Blackmond, D. G.; Moran, A.; Hughes, M.; Armstrong, A. "Unusual Reversal of Enantioselectivity in the Proline-Mediated α-Amination of Aldehydes Induced by Tertiary Amine Additives", *J. Am. Chem. Soc.* 132, **2010**, 7598.

Bock, D. A.; Lehmann, C. W.; List, B. "Crystal Structures of Proline-Derived Enamines", *Proc. Natl. Acad. Sci. U. S. A* 107, **2010**, 20636.

Boehme, C.; Frenking, G. "Electronic Structure of Stable Carbenes, Silylenes, and Germylenes", *J. Am. Chem. Soc.* 118, **1996**, 2039.

Boese, A. D.; Klopper, W.; Martin, J. M. L. "Assessment of Various Density Functionals and Basis Sets for the Calculation of Molecular Anharmonic Force Fields", *Int. J. Quantum Chem.* 104, **2005**, 830.

Bøgevig, A.; Juhl, K.; Kumaragurubaran, N.; Zhuang, W.; Jørgensen, K. A. "Direct Organo-Catalytic Asymmetric α-Amination of Aldehydes - a Simple Approach to Optically Active α-Amino Aldehydes, α-Amino Alcohols, and α-Amino Acids", *Angew. Chem. Int. Ed.* 41, **2002**, 1790.

Bøgevig, A.; Sundén, H.; Córdova, A. "Direct Catalytic Enantioselective α-Aminoxylation of Ketones: A Stereoselective Synthesis of α-Hydroxy and α,α′-Dihydroxy Ketones", *Angew. Chem. Int. Ed.* 43, **2004**, 1109.

Bolli, M.; Micura, R.; Eschenmoser, A. "Pyranosyi-RNA: Chiroselective Self-Assembly of Base Sequences by Ligative Oligomerization of Tetranucleotide-2',3'-Cyclophosphates (with a Commentary Concerning the Origin of Biomolecular Homochirality)", *Chem. Biol.* 4, **1997**, 309.

Born, M.; Oppenheimer, J. R. "The quantum theory of molecules", *Ann. Phys.* 84, **1927**, 457.

Bouquet, G.; Loutellier, A.; Bigorgne, M. "Spectroscopic study of vibrations M-C, M-CO and its nickel carbonyl derivatives", *J. Mol. Struct.* 1, **1968**, 211.

Bourissou, D.; Guerret, O.; Gabbaï, F. P.; Bertrand, G. "Stable Carbenes", *Chem. Rev.* 100, **2000**, 39.

Bowen, J. P.; Allinger, N. L. "Molecular Mechanics: The Art and Science of Parameterization", *Rev. Comp. Chem.* 2, **1991**, 81.

Boyd, D. B.; Lipkowitz, K. B. "Molecular Mechanics: The Method and its Underlying Philosophy", *J. Chem. Educ.* 59, **1982**, 269.

Boydston, A. J.; Williams, K. A.; Bielawski, C. W. "A Modular Approach to Main-Chain Organometallic Polymers", *J. Am. Chem. Soc.* 127, **2005**, 12496.

[a]Boys, S. F. "Electronic Wave Functions. I. A General Method of Calculation for the Stationary States of any Molecular System", *Proc. Roy. Soc. (London)* 200, **1950**, 542.

[b]Boys, S. F. "Electronic Wave Functions. II. A Calculation for the Ground State of the Beryllium Atom", *Proc. Roy. Soc. (London)* 201, **1950**, 125.

Bredig, G.; Balcom, R. W. "The kinetics of carbon dioxide removal from Campho-carbonicacid ", *Ber. Deutsch. Chem. Ger.* 41, **1908**, 740.

Bredig, G.; Fajans, K. "The stereochemistry of the catalysis ", *Ber. Deutsch. Chem. Ger.* 41, **1908**, 752.

Bredig, G.; Fiske, P. S. *Biochem. Z.* 46, **1913**, 7.

Bremeyer, N.; Smith, S. C.; Ley, S. V.; Gaunt, M. J. "An Intramolecular Organocatalytic Cyclopropanation Reaction", *Angew. Chem. Int. Ed.* 43, **2004**, 2681.

Breslow, R. "On the Mechanism of Thiamine Action. IV. Evidence from Studies on Model Systems", *J. Am. Chem. Soc.* 80, **1958**, 3719.

Brillouin, L. "Fields Self-consistents and Hartree Fock ", *Actualities Sci. Ind.* 159, **1934**, 37.

Brochu, M. P.; Brown, S. P.; MacMillan, D. W. C. "Direct and Enantioselective Organocatalytic α-Chlorination of Aldehydes", *J. Am. Chem. Soc.* 126, **2004**, 4108.

Brown, S. P.; Brochu, M. P.; Sinz, C. J.; MacMillan, D. W. C. "The Direct and Enantioselective Organocatalytic α-Oxidation of Aldehydes", *J. Am. Chem. Soc.* 125, **2003**, 10808.

Bugaut, X.; Liu, F.; Glorius, F. "N-Heterocyclic Carbene (NHC)-Catalyzed Intermolecular Hydroacylation of Cyclopropenes", *J. Am. Chem. Soc.* 133, **2011**, 8130.

Bui, T.; Barbas III, C. F. "A Proline-Catalyzed Asymmetric Robinson Annulation Reaction", *Tetrahedron Lett.* 41, **2000**, 6951.

Burgi, H. B.; Dunitz, J. D. "From Crystal Statics to Chemical Dynamics", *Acc. Chem. Res.* 16, **1983**, 153.

Burgi, H. B.; Dunitz, J. D.; Lehn, J. M.; Wipff, G. "Stereochemistry of Reaction Paths at Carbonyl Centres", *Tetrahedron* 30, **1974**, 1563.

Burgi, H. B.; Dunitz, J. D.; Shefter, E. "Geometrical Reaction Coordinates. II. Nucleophilic Addition to a Carbonyl Group", *J. Am. Chem. Soc.* 95, **1973**, 5065.

Burroughs, L.; Clarke, P. A.; Forintos, H.; Gilks, J. A. R.; Hayes, C. J.; Vale, M. E.; Wade, W.; Zbytniewski, M. "Asymmetric Organocatalytic Formation of Protected and Unprotected Tetroses under Potentially Prebiotic Conditions", *Org. Biomol. Chem.* 10, **2012**, 1565.

Burroughs, L.; Vale, M. E.; Gilks, J. A. R.; Forintos, H.; Hayes, C. J.; Clarke, P. A. "Efficient Asymmetric Organocatalytic Formation of Erythrose and Threose under Aqueous Conditions", *Chem. Commun.* 46, **2010**, 4776.

Burstein, C.; Glorius, F. "Organocatalyzed Conjugate Umpolung of α,β-Unsaturated Aldehydes for the Synthesis of γ-Butyrolactones", *Angew. Chem. Int. Ed.* 43, **2004**, 6205.

Cabrera, S.; Reyes, E.; Alemán, J.; Milelli, A.; Kobbelgaard, S.; Jørgensen, K. A. "Organocatalytic Asymmetric Synthesis of α,α-Disubstituted α-Amino Acids and Derivatives", *J. Am. Chem. Soc.* 130, **2008**, 12031.

Calderon, F.; Doyaguez, E. G.; Cheong, P. H.-Y.; Fernandez-Mayoralas, A.; Houk, K. N. "Origins of the Double Asymmetric Induction on Proline-Catalyzed Aldol Reactions", *J. Org. Chem.* 73, **2008**, 7916.

Calter, M. A.; Orr, R. K.; Song, W. "Catalytic, Asymmetric Preparation of Ketene Dimers from Acid Chlorides", *Org. Lett.* 5, **2003**, 4745.

Cardinal-David, B.; Raup, D. E. A.; Scheidt, K. A. "Cooperative N-Heterocyclic Carbene/Lewis Acid Catalysis for Highly Stereoselective Annulation Reactions with Homoenolates", *J. Am. Chem. Soc.* 132, **2010**, 5345.

Cavallo, L.; Correa, A.; Costabile, C.; Jacobsen, H. "Steric and Electronic Effects in the Bonding of N-Heterocyclic Ligands to Transition Metals", *J. Organomet. Chem.* 690, **2005**, 5407.

Chandler, C.; Galzerano, P.; Michrowska, A.; List, B. "The Proline-Catalyzed Double Mannich Reaction of Acetaldehyde with *N*-Boc Imines", *Angew. Chem. Int. Ed.* 48, **2009**, 1978.

Cheong, P. H. Y.; Houk, K. N. "Origins of Selectivities in Proline-Catalyzed α-Aminoxylations", *J. Am. Chem. Soc.* 126, **2004**, 13912.

Cheong, P. H. Y.; Houk, K. N. "Origins and Predictions of Stereoselectivity in Intramolecular Aldol Reactions Catalyzed by Proline Derivatives", *Synthesis*, **2005**, 1533.

Cheong, P. H. Y.; Legault, C. Y.; Um, J. M.; Çelebi-Ölçüm, N.; Houk, K. N. "Quantum Mechanical Investigations of Organocatalysis: Mechanisms, Reactivities, and Selectivities", *Chem. Rev.* 111, **2011**, 5042.

Cheong, P. H. Y.; Zhang, H.; Thayumanavan, R.; Tanaka, F.; Houk, K. N.; Barbas III, C. F. "Pipecolic acid-Catalyzed Direct Asymmetric Mannich Reactions", *Org. Lett* 8, **2006**, 811.

Chianese, A. R.; Li, X.; Janzen, M. C.; Faller, J. W.; Crabtree, R. H. "Rhodium and Iridium Complexes of N-Heterocyclic Carbenes *via* Transmetalation: Structure and Dynamics", *Organometallics* 22, **2003**, 1663.

Chiang, P. C.; Bode, J. W. "On the Role of CO_2 in NHC-Catalyzed Oxidation of Aldehydes", *Org. Lett.* 13, **2011**, 2422.

Chiang, P. C.; Kaeobamrung, J.; Bode, J. W. "Enantioselective, Cyclopentene-Forming Annulations *via* NHC-Catalyzed Benzoin-Oxy-Cope Reactions", *J. Am. Chem. Soc.* 129, **2007**, 3520.

Čizek, J. "On the Correlation Problem in Atomic and Molecular Systems. Calculation of Wavefunction Components in Ursell-Type Expansion Using Quantum-Field Theoretical Methods", *J. Chem. Phys.* 45, **1966**, 4256.

Clar, E. "*The Aromatic Sextet*", Wiley: New York, **1972**.

Clavier, H.; Nolan, S. P. "Percent Buried Volume for Phosphine and N-Heterocyclic Carbene Ligands: Steric Properties in Organometallic Chemistry", *Chem. Commun.* 46, **2010**, 841.

Clemente, F. R.; Houk, K. N. "Computational Evidence for the Enamine Mechanism of Intramolecular Aldol Reactions Catalyzed by Proline", *Angew. Chem. Int. Ed.* 43, **2004**, 5766.

Clemente, F. R.; Houk, K. N. "Theoretical Studies of Stereoselectivities of Intramolecular Aldol Cyclizations Catalyzed by Amino Acids", *J. Am. Chem. Soc.* 127, **2005**, 11294.

Clementi, E. "Simple Basis Set for Molecular Wavefunctions Containing First- and Second-Row Atoms", *J. Chem. Phys.* 40, **1964**, 1944.

Cohen, D. T.; Cardinal-David, B.; Scheidt, K. A. "Lewis Acid Activated Synthesis of Highly Substituted Cyclopentanes by the N-Heterocyclic Carbene Catalyzed Addition of Homoenolate Equivalents to Unsaturated Ketoesters", *Angew. Chem. Int. Ed.* 50, **2011**, 1678.

Connor, E. F.; Nyce, G. W.; Myers, M.; Möck, A.; Hedrick, J. L. "First Example of N-Heterocyclic Carbenes as Catalysts for Living Polymerization: Organocatalytic Ring-Opening Polymerization of Cyclic Esters", *J. Am. Chem. Soc.* 124, **2002**, 914.

Corberan, R.; Mas-Marza, E.; Peris, E. "Mono-, Bi-, and Tridentate N-Heterocyclic Carbene Ligands for the Preparation of Transition-Metal-Based Homogeneous Catalysts", *Eur. J. Inorg. Chem.* **2009**, 1700.

Córdova, A. "The Direct Catalytic Asymmetric Cross-Mannich Reaction: A Highly Enantioselective Route to 3-Amino Alcohols and α-Amino Acid Derivatives", *Chem. Eur. J.* 10, **2004**, 1987.

[a]Córdova, A.; Engqvist, M.; Ibrahem, I.; Casas, J.; Sundén, H. "Plausible Origins of Homochirality in the Amino Acid Catalyzed Neogenesis of Carbohydrates", *Chem. Commun.* **2005**, 2047.

[b]Córdova, A.; Ibrahem, I.; Casas, J.; Sundén, H.; Engqvist, M.; Reyes, E. "Amino Acid Catalyzed Neogenesis of Carbohydrates: A Plausible Ancient Transformation", *Chem. Eur. J.* 11, **2005**, 4772.

Córdova, A.; Notz, W.; Barbas III, C. F. "Proline-Catalyzed One-Step Asymmetric Synthesis of 5-Hydroxy-(2E)-Hexenal from Acetaldehyde", *J. Org. Chem.* 67, **2002**, 301.

Córdova, A.; Zou, W.; Dziedzic, P.; Ibrahem, I.; Reyes, E.; Xu, Y. "Direct Asymmetric Intermolecular Aldol Reactions Catalyzed by Amino Acids and Small Peptides", *Chem. Eur. J.* 12, **2006**, 5383.

Corey, E. J.; Grogan, M. J. "Enantioselective Synthesis of α-Amino Nitriles from N-Benzhydryl Imines and HCN with a Chiral Bicyclic Guanidine as Catalyst", *Org. Lett.* 1, **1999**, 157.

Cossi, M.; Scalmani, G.; Rega, N.; Barone, V. "New Developments in the Polarizable Continuum Model for Quantum Mechanical and Classical Calculations on Molecules in Solution", *J. Chem. Phys.* 117, **2002**, 43.

Cramer, C. J. "*Essentials of Computational Chemistry*", John Wiley & Sons, Chichester, **2004**.

Crees, R. S.; Cole, M. L.; Hanton, L. R.; Sumby, C. J. "Synthesis of a Zinc(II) Imidazolium Dicarboxylate Ligand Metal-Organic Framework (MOF): A Potential Precursor to MOF-Tethered N-Heterocyclic Carbene Compounds", *Inorg. Chem.* 49, **2010**, 1712.

Curci, R.; D'Accolti, L.; Fiorentino, M.; Rosa, A. "Enantioselective Epoxidation of Unfunctionalized Alkenes Using Dioxiranes Generated *in Situ*", *Tetrahedron Lett.* 36, **1995**, 5831.

Curci, R.; Fiorentino, M.; Serio, M. R. "Asymmetric Epoxidation of Unfunctionalized Alkenes by Dioxirane Intermediates Generated from Potassium Peroxomonosulphate and Chiral Ketones", *J. Chem. Soc., Chem. Commun.*, **1984**, 155.

Cutler, A. R.; Hanna, P. K.; Vites, J. C. "Carbon Monoxide and Carbon Dioxide Fixation: Relevant C_1 and C_2 Ligand Reactions Emphasizing $(\eta^5\text{-}C_5H_5)$Fe-Containing Complexes", *Chem. Rev.* 88, **1988**, 1363.

Cyrañski, M. K.; Krygowski, T. M.; Wisiorowski, M.; Van Eikema Hommes, N. J. R.; Von Ragué Schleyer, P. "Global and Local Aromaticity in Porphyrins: An

Analysis Based on Molecular Geometries and Nucleus-Independent Chemical Shifts", *Angew. Chem., Int. Ed.* 37, **1998**, 177.

Dalko, P. I. "*Enantioselective Organocatalysis*", Wiley-VCH, Weinheim, Germany, **2007**.

Dalko, P. I.; Moisan, L. "Enantioselective Organocatalysis", *Angew. Chem. Int. Ed.* 40, **2001**, 3726.

Dalko, P. I.; Moisan, L. "In the Golden Age of Organocatalysis", *Angew. Chem. Int. Ed.* 43, **2004**, 5138.

Dapprich, S.; Komaromi, I.; Byun, K. S.; Morokuma, K.; Frisch, M. J. "A New ONIOM Implementation in Gaussian 98. Part I. The Calculation of Energies, Gradients, Vibrational Frequencies and Electric Field Derivatives", *J. Mol. Struct. (Theochem)* 462, **1999**, 1.

De Frémont, P.; Marion, N.; Nolan, S. P. "Carbenes: Synthesis, Properties, and Organometallic Chemistry", *Coord. Chem. Rev.* 253, **2009**, 862.

Delaude, L.; Demonceau, A.; Wouters, J. "Assessing the Potential of Zwitterionic NHC-CS$_2$ Adducts for Probing the Stereoelectronic Parameters of N-Heterocyclic Carbenes", *Eur. J. Inorg. Chem.* **2009**, 1882.

Denmark, S. E.; Forbes, D. C.; Hays, D. S.; DePue, J. S.; Wilde, R. G. "Catalytic Epoxidation of Alkenes with Oxone", *J. Org. Chem.* 60, **1995**, 1391.

Deshmukh, M. M.; Gadre, S. R.; Tonner, R.; Frenking, G. "Molecular Electrostatic Potentials of Divalent Carbon(0) Compounds", *Phys. Chem. Chem. Phys.* 10, **2008**, 2298.

Diez-Gonzalez, S.; Marion, S.; Nolan, S. P. "N-Heterocyclic Carbenes in Late-Transition Metals Catalysis", *Chem. Rev.* 109, **2009**, 3612.

Diez-Gonzalez, S.; Escudero-Adan, E. C.; Benet-Buchholz, J.; Stevens, E. D.; Slawin, A. M. Z.; Nolan, S. P. "[(NHC)CuX] Complexes: Synthesis, Characterization and Catalytic Activities in Reduction Reactions and Click Chemistry. On the Advantage of Using Well-Defined Catalytic Systems", *Dalton Trans.* 39, **2010**, 7595.

Díez-González, S.; Marion, N.; Nolan, S. P. "N-Heterocyclic Carbenes in Late Transition Metal Catalysis", *Chem. Rev.* 109, **2009**, 3612.

Díez-González, S.; Nolan, S. P. "Stereoelectronic Parameters Associated with N-Heterocyclic Carbene (NHC) Ligands: A Quest for Understanding", *Coord. Chem. Rev.* 251, **2007**, 874.

Dinur, U.; Hagler, A. T. "New Approaches to Empirical Force Fields", *Rev. Comp. Chem.* 2, **1991**, 99.

Dirac, P. A. M. "Quantum Mechanics of Many-Electron Systems", *Proc. Roy. Soc. (London)* A 123, **1929**, 714.

Ditchfield, R.; Hehre, W. J.; Pople, J. "Self-Consistent Molecular-Orbital Methods. Ix. An Extended Gaussian-Type Basis for Molecular-Orbital Studies of Organic Molecules", *J. Chem. Phys.* 54, **1971**, 724.

Doll, J.; Freeman, D. L. "Monte Carlo Methods in Chemistry", *IEEE Comput. Sci. Eng.* 1, **1994**, 22.

Dolling, U. H.; Davis, P.; Grabowski, E. J. J. "Efficient Catalytic Asymmetric Alkylations. 1. Enantioselective Synthesis of (+)-Indacrinone *via* Chiral Phase-Transfer Catalysis", *J. Am. Chem. Soc.* 106, **1984**, 446.

Dominique, F. J.-B. d.; Gornitzka, H.; Sournia-Saquet, A.; Hemmert, C. "Dinuclear Gold(I) and Gold(III) Complexes of Bridging Functionalized Bis (N-Heterocyclic

Carbene) Ligands: Synthesis, Structural, Spectroscopic and Electrochemicak Characterizations", *Dalton Trans.* **2009**, 340.

Dondoni, A.; Massi, A. "Asymmetric Organocatalysis: From Infancy to Adolescence", *Angew. Chem. Int. Ed.* 47, **2008**, 4638.

Dorta, R.; Scott, N. M.; Costabile, C.; Cavallo, L.; Hoff, C. D.; Nolan, S. P. "Steric and Electronic Properties of N-Heterocyclic Carbenes (NHC): A Detailed Study on Their Interaction with $Ni(CO)_4$", *J. Am. Chem. Soc.* 127, **2005**, 2485.

Dröge, T.; Glorius, F. "The Measure of All Rings: N-Heterocyclic Carbenes", *Angew. Chem. Int. Ed.* 49, **2010**, 6940.

Ducháčková, L.; Kadlčíková, A.; Kotora, M.; Roithová, J. "Oxygen Superbases as Polar Binding Pockets in Nonpolar Solvents", *J. Am. Chem. Soc.* 132, **2010**, 12660.

Dunning Jr., T. H. "Gaussian Basis Functions for Use in Molecular Calculations. I. Contraction of (9s5p) Atomic Basis Sets for the First-Row Atoms", *J. Chem. Phys.* 53, **1970**, 2823.

Dunning Jr, T. H. "Gaussian Basis Functions for Use in Molecular Calculations. III. Contraction of (10s6p) Atomic Basis Sets for the First-Row Atoms", *J. Chem. Phys.* 55, **1971**, 716.

Dunning Jr, T. H. "Gaussian Basis Sets for Use in Correlated Molecular Calculations. I. The Atoms Boron through Neon and Hydrogen", *J. Chem. Phys.* 90, **1989**, 1007.

Duong, H. A.; Tekavec, T. N.; Arif, A. M.; Louie, J. "Reversible Carboxylation of N-Heterocyclic Carbenes", *Chem. Commun.* 10, **2004**, 112.

Dykstra, C. E. "*Ab initio Calculation of the Structures and Properties of Molecules*", Elsevier, Amsterdam, **1988**.

Eder, U.; Sauer, G.; Wiechert, R. "New Type of Asymmetric Cyclization to Optically Active Steroid CD Partial Structures", *Angew. Chem. Int. Ed.* 10, **1971**, 496.

Edworthy, I. S.; Blake, A. J.; Wilson, C.; Arnold, P. L. "Synthesis and NHC Lability of d0 Lithium, Ytrium, Titanium and Zirconium Amido Bis(N-Heterocyclic Carbene) Complexes", *Organometallics* 26, **2007**, 3684.

Enders, D.; Balensiefer, T. "Nucleophilic Carbenes in Asymmetric Organocatalysis", *Acc. Chem. Res.* 37, **2004**, 534.

Enders, D.; Grondal, C.; Hüttl, M. R. M. "Asymmetric Organocatalytic Domino Reactions", *Angew. Chem. Int. Ed.* 46, **2007**, 1570.

Enders, D.; Grondal, C.; Vrettou, M.; Raabe, G. "Asymmetric Synthesis of Selectively Protected Amino Sugars and Derivatives by a Direct Organocatalytic Mannich Reaction", *Angew. Chem. Int. Ed.* 44, **2005**, 4079.

Enders, D.; Kallfass, U. "An Efficient Nucleophilic Carbene Catalyst for the Asymmetric Benzoin Condensation", *Angew. Chem. Int. Ed.* 41, **2002**, 1743.

Enders, D.; Narine, A. A. "Lessons from Nature: Biomimetic Organocatalytic Carbon-Carbon Bond Formations", *J. Org. Chem.* 73, **2008**, 7857.

Enders, D.; Niemeier, O.; Henseler, A. "Organocatalysis by N-Heterocyclic Carbenes", *Chem. Rev.* 107, **2007**, 5606.

Esterhuysen, C.; Frenking, G. "The Nature of the Chemical Bond Revisited. An Energy Partitioning Analysis of Diatomic Molecules E_2 (E=N-Bi, F-I), CO and BF", *Theoret. Chem. Acc.* 111, **2004**, 381.

Feller, D.; Davidson, E. R. "Basis Sets for *Ab initio* Molecular Orbital Calculations and Intermolecular Interactions", *Rev. Comp. Chem.* 1, **1990**, 1.

[a]Fernandez, I.; Frenking, G.; Uggerud, E. "Response to the Comment on "the Interplay between Steric and Electronic Effects in S_N2 Reactions", *Chem. Eur. J.* 16, **2010**, 5542.

[b]Fernandez, I.; Frenking, G.; Uggerud, E. "Rate-Determining Factors in Nucleophilic Aromatic Substitution Reactions", *J. Org. Chem.* 75, **2010**, 2971.

Fey, N. "The Contribution of Computational Studies to Organometallic Catalysis: Descriptors, Mechanisms and Models", *Dalton Trans.* 39, **2010**, 296.

Field, M. J.; Bash, P. A.; Karplus, M. "A Combined Quantum Mechanical and Molecular Mechanical Potential for Molecular Dynamics Simulations", *J. Comput. Chem.* 11, **1990**, 700.

Fielder, S. S.; Osborne, M. C.; Lever, A. B. P.; Pietro, W. J. "First-Principles Interpretation of Ligand Electrochemical ($E_L(L)$) Parameters. Factorization of the σ and π Donor and π Acceptor Capabilities of Ligands", *J. Am. Chem. Soc.* 117, **1995**, 6990.

Fock, V. "Approximation method to solve quantum mechanical many-body problem", *Z. Phys.* 61, **1930**, 126.

Fonseca, M. T. H.; List, B. "Catalytic Asymmetric Intramolecular Michael Reaction of Aldehydes", *Angew. Chem. Int. Ed.* 43, **2004**, 3958.

Foresman, J. B.; Frisch, A. "*Exploring Chemistry with Electronic Structure Methods*", Gaussian, Inc., Pittsburgh, PA., **1996**.

Foresman, J. B.; Head-Gordon, M.; Pople, J. A.; Frisch, M. J. "Toward a Systematic Molecular Orbital Theory for Excited States", *J. Phys. Chem.* 96, **1992**, 135.

France, S.; Weatherwax, A.; Taggi, A. E.; Lectka, T. "Advances in the Catalytic, Asymmetric Synthesis of β-Lactams", *Acc. Chem. Res.* 37, **2004**, 592.

Frenking, G.; Wichmann, K.; Frohlich, N.; Loschen, C.; Lein, M.; Frunzke, J.; Rayon, V. M. "Towards a Rigorously Defined Quantum Chemical Analysis of the Chemical Bond in Donor-Acceptor Complexes", *Coord. Chem. Rev.* 238, **2003**, 55.

Frisch, M. J.; Trucks, G. W.; Schlegel, H. B.; Scuseria, G. E.; Robb, M. A.; Cheeseman, J. R.; Montgomery, J. A.; Vreven Jr., T.; Kudin, K. N.; Burant, J. C.; Millam, J. M.; Iyengar, S. S.; Tomasi, J.; Barone, V.; Mennucci, B.; Cossi, M.; Scalmani, G.; Rega, N.; Petersson, G. A.; Nakatsuji, H.; Hada, M.; Ehara, M.; Toyota, K.; Fukuda, R.; Hasegawa, J.; Ishida, M.; Nakajima, T.; Honda, Y.; Kitao, O.; Nakai, H.; Klene, M.; Li, X.; Knox, J. E.; Hratchian, H. P.; Cross, J. B.; Bakken, V.; Adamo, C.; Jaramillo, J.; Gomperts, R.; Stratmann, R. E.; Yazyev, O.; Austin, A. J.; Cammi, R.; Pomelli, C.; Ochterski, J. W.; Ayala, P. Y.; Morokuma, K.; Voth, G. A.; Salvador, P.; Dannenberg, J. J.; Zakrzewski, V. G.; Dapprich, S.; Daniels, A. D.; Strain, M. C.; Farkas, O.; Malick, D. K.; Rabuck, A. D.; Raghavachari, K.; Foresman, J. B.; Ortiz, J. V.; Cui, Q.; Baboul, A. G.; Clifford, S.; Cioslowski, J.; Stefanov, B. B.; Liu, G.; Liashenko, A.; Piskorz, P.; Komaromi, I.; Martin, R. L.; Fox, D. J.; Keith, T.; Al-Laham, M. A.; Peng, C. Y.; Nanayakkara, A.; Challacombe, M.; Gill, P. M. W.; Johnson, B.; Chen, W.; Wong, M. W.; Gonzalez, C.; Pople, J. A.*Gaussian 03, Revision E.01,Gaussian, Inc., Wallingford CT,* , **2004**.

Frisch, M. J.; Trucks, G. W.; Schlegel, H. B.; Scuseria, G. E.; Robb, M. A.; Cheeseman, J. R.; Scalmani, G. B., V.; Mennucci, B.; Petersson, G. A.; Nakatsuji, H.; Caricato, M.; Li, X.; Hratchian, H. P.; Izmaylov, A. F.; Bloino, J.; Zheng, G.; Sonnenberg, J. L.; Hada, M.; Ehara, M.; Toyota, K.; Fukuda, R.; Hasegawa, J.; Ishida, M.; Nakajima, T.; Honda, Y.; Kitao, O.; Nakai, H.; Vreven, T.; Montgomery, J. A.; A., J.; Peralta, J. E.; Ogliaro, F.; Bearpark, M.; Heyd, J. J.;

Brothers, E.; Kudin, K. N.; Staroverov, V. N.; Kobayashi, R.; Normand, J.; Raghavachari, K.; Rendell, A.; Burant, J. C.; Iyengar, S. S.; Tomasi, J.; Cossi, M.; Rega, N.; Millam, N. J.; Klene, M.; Knox, J. E.; Cross, J. B.; Bakken, V.; Adamo, C.; Jaramillo, J.; Gomperts, R.; Stratmann, R. E.; Yazyev, O.; Austin, A. J.; Cammi, R.; Pomelli, C.; Ochterski, J. W.; Martin, R. L.; Morokuma, K.; Zakrzewski, V. G.; Voth, G. A.; Salvador, P.; Dannenberg, J. J.; Dapprich, S.; Daniels, A. D.; Farkas, Ö.; Foresman, J. B.; Ortiz, J. V.; Cioslowski, J.; Fox, D. J.*Gaussian 09, Revision A.1, Gaussian, Inc., Wallingford CT*, **2009**.

Fu, A.; Li, H.; Si, H.; Yuan, S.; Duan, Y. "Theoretical Studies of Stereoselectivities in the Direct syn- and anti-Mannich Reactions Catalyzed by Different Amino Acids", *Tetrahedron: Asymmetry* 19, **2008**, 2285.

Fürstner, A.; Ackermann, L.; Gabor, B.; Goddard, R.; Lehmann, C. W.; Mynott, R.; Stelzer, F.; Thiel, O. R. "Comparative Investigation of Ruthenium-Based Metathesis Catalysts Bearing N-Heterocyclic Carbene (NHC) Ligands", *Chem. Eur. J.* 7, **2001**, 3236.

Fürstner, A.; Alcarazo, M.; Krause, H.; Lehmann, C. W. "Effective Modulation of the Donor Properties of N-Heterocyclic Carbene Ligands by "through-Space" Communication within a Planar Chiral Scaffold", *J. Am. Chem. Soc.* 129, **2007**, 12676.

Gadre, S. R.; Bhadane, P. K.; Pundlik, S. S.; Pingale, S. S. "*Molecular Electrostatic Potential: Concepts and Applications*", eds. J. S. Murray and K. D. Sen, Elsevier, Amsterdam, **1996**.

Gadre, S. R.; Kulkarni, S. A.; Shrivastava, I. H. "Molecular Electrostatic Potentials: A Topographical Study", *J. Chem. Phys.* 96, **1992**, 5253.

Gadre, S. R.; Pathak, R. K. "Maximal and Minimal Characteristics of Molecular Electrostatic Potentials", *J. Chem. Phys.* 93, **1990**, 1770.

Gadre, S. R.; Shirsat, R. N. "*Electrostatics of Atoms and Molecules*", Universities Press: Hyderabad, India, **2000**.

Gadre, S. R.; Shrivastava, I. H. "Topography Driven Electrostatic Charge Models for Molecules", *Chem. Phys. Lett.* 205, **1993**, 350.

Gadre, S. R.; Suresh, C. H. "Electronic Perturbations of the Aromatic Nucleus: Hammett Constants and Electrostatic Potential Topography", *J. Org. Chem.* 62, **1997**, 2625.

Galabov, B.; Ilieva, S.; Schaefer III, H. F. "An Efficient Computational Approach for the Evaluation of Substituent Constants", *J. Org. Chem.* 71, **2006**, 6382.

Gao, J. "Methods and Applications of Combined Quantum Mechanical and Molecular Mechanical Potentials", *Rev. Comp. Chem.* 7, **1996**, 119.

Garber, S. B.; Kingsbury, J. S.; Gray, B. L.; Hoveyda, A. H. "Efficient and Recyclable Monomeric and Dendritic Ru-Based Metathesis Catalysts", *J. Am. Chem. Soc.* 122, **2000**, 8168.

Gaunt, M. J.; Johansson, C. C. C.; McNally, A.; Vo, N. T. "Enantioselective Organocatalysis", *Drug Discovery Today* 12, **2007**, 8.

Glorius, F. "*N-Heterocyclic Carbenes in Transition Metal Catalysis*", Springer-Verlag, Berlin, Germany, **2007**.

Gonzalez, C.; Schlegel, H. B. "An Improved Algorithm for Reaction Path Following", *J. Chem. Phys.* 90, **1989**, 2154.

Gonzalez, C.; Schlegel, H. B. "Reaction Path Following in Mass-Weighted Internal Coordinates", *J. Phys. Chem. 94*, **1990**, 5523.

Gonzalez, J.; Anglada, J. M.; Buszek, R. J.; Francisco, J. S. "Impact of Water on the OH + HOCl Reaction", *J. Am. Chem. Soc. 133*, **2011**, 3345.

Green, J. C.; Scurr, R. G.; Arnold, P. L.; Cloke, F. G. N. "An Experimental and Theoretical Investigation of the Electronic Structure of Pd and Pt Bis(Carbene) Complexes", *Chem. Commun.* **1997**, 1963.

Grimme, S. "Semiempirical GGA-Type Density Functional Constructed with a Long-Range Dispersion Correction", *J. Comput. Chem. 27*, **2006**, 1787.

Gross, K. C.; Seybold, P. G.; Peralta-Inga, Z.; Murray, J. S.; Politzer, P. "Comparison of Quantum Chemical Parameters and Hammett Constants in Correlating pka Values of Substituted Anilines", *J. Org. Chem. 66*, **2001**, 6919.

Gruttadauria, M.; Giacalone, F.; Noto, R. "Supported Proline and Proline-Derivatives as Recyclable Organocatalysts", *Chem. Soc. Rev. 37*, **2008**, 1666.

Gu, L.; Zhang, Y. "Unexpected CO_2 Splitting Reactions to Form CO with N-Heterocyclic Carbenes as Organocatalysts and Aromatic Aldehydes as Oxygen Acceptors", *J. Am. Chem. Soc. 132*, **2010**, 914.

Guo, H. C.; Ma, J. A. "Catalytic Asymmetric Tandem Transformations Triggered by Conjugate Additions", *Angew. Chem. Int. Ed. 45*, **2006**, 354.

Gusev, D. G. "Electronic and Steric Parameters of 76 N-Heterocyclic Carbenes in $Ni(CO)_3(NHC)$", *Organometallics 28*, **2009**, 6458.

Guthrie, J. P.; Jordan, F. "Amine-Catalyzed Decarboxylation of Acetoacetic Acid. The Rate Constant for Decarboxylation of a β-Imino Acid", *J. Am. Chem. Soc. 94*, **1972**, 9136.

Hahn, B. T.; Fröhlich, R.; Harms, K.; Glorius, F. "Proline-Catalyzed Highly Enantioselective and anti-Selective Mannich Reaction of Unactivated Ketones: Synthesis of Chiral α-Amino Acids", *Angew. Chem. Int. Ed.* 47, **2008**, 9985.

Hahn, F. E.; Jahnke, M. C. "Heterocyclic Carbenes: Synthesis and Coordination Chemistry", *Angew. Chem., Int. Ed.* 47, **2008**, 3122.

Hajos, Z. G.; Parrish, D. R., German Patent DE 2102623, **1971**.

Hajos, Z. G.; Parrish, D. R. "Asymmetric Synthesis of Bicyclic Intermediates of Natural Product Chemistry", *J. Org. Chem.* 39, **1974**, 1615.

Hall, G. G. "The Molecular Orbital Theory of Chemical Valency. VIII. A Method of Calculating Ionization Potentials", *Proc. Roy. Soc. (London)* A205, **1951**, 541.

Halland, N.; Aburel, P. S.; Jørgensen, K. A. "Highly Enantio- and Diastereoselective Organocatalytic Asymmetric Domino Michael-Aldol Reaction of β-Ketoesters and α,β-Unsaturated Ketones", *Angew. Chem. Int. Ed.* 43, **2004**, 1272.

Halland, N.; Braunton, A.; Bachmann, S.; Marigo, M.; Jørgensen, K. A. "Direct Organocatalytic Asymmetric α-Chlorination of Aldehydes", *J. Am. Chem. Soc.* 126, **2004**, 4790.

[a]Hayashi, Y.; Tsuboi, W.; Ashimine, I.; Urushima, T.; Shoji, M.; Sakai, K. "The Direct and Enantioselective, One-Pot, Three-Component, Cross-Mannich Reaction of Aldehydes", *Angew. Chem. Int. Ed.* 42, **2003**, 3677.

[b]Hayashi, Y.; Tsuboi, W.; Shoji, M.; Suzuki, N. "Application of High Pressure Induced by Water-Freezing to the Direct Catalytic Asymmetric Three-Component List-Barbas-Mannich Reaction", *J. Am. Chem. Soc.* 125, **2003**, 11208.

[c]Hayashi, Y.; Yamaguchi, J.; Hibino, K.; Shoji, M. "Direct Proline Catalyzed Asymmetric α-Aminooxylation of Aldehydes", *Tetrahedron Lett.* 44, **2003**, 8293.

Hayashi, Y. "Recent Progress in the Asymmetric Organocatalysis", *J. Synth. Org. Chem. Jpn.* 63, **2005**, 464.

Hayashi, Y.; Matsuzawa, M.; Yamaguchi, J.; Yonehara, S.; Matsumoto, Y.; Shoji, M.; Hashizume, D.; Koshino, H. "Large Nonlinear Effect Observed in the Enantiomeric Excess of Proline in Solution and That in the Solid State", *Angew. Chem. Int. Ed.* 45, **2006**, 4593.

Hayashi, Y.; Okano, T.; Itoh, T.; Urushima, T.; Ishikawa, H.; Uchimaru, T. "Direct Organocatalytic Mannich Reaction of Acetaldehyde: An Improved Catalyst and Mechanistic Insight from a Computational Study", *Angew. Chem. Int. Ed.* 47, **2008**, 9053.

Hayashi, Y.; Yamaguchi, J.; Sumiya, T.; Shoji, M. "Direct Proline-Catalyzed Asymmetric α-Aminoxylation of Ketones", *Angew. Chem. Int. Ed.* 43, **2004**, 1112.

Hehre, W. J.; Ditchfield, R.; Pople, J. "Self-Consistent Molecular Orbital Methods. XII. Further Extensions of Gaussian-Type Basis Sets for Use in Molecular Orbital Studies of Organic Molecules", *J. Chem. Phys.* 56, **1972**, 2257.

Hehre, W. J.; Stewart, R. F.; Pople, J. A. "Self-Consistent Molecular-Orbital Methods. I. Use of Gaussian Expansions of Slater-Type Atomic Orbitals", *J. Chem. Phys.* 51, **1969**, 2657.

Hein, J. E.; Burés, J.; Lam, Y. H.; Hughes, M.; Houk, K. N.; Armstrong, A.; Blackmond, D. G. "Enamine Carboxylates as Stereodetermining Intermediates in Prolinate Catalysis", *Org. Lett.* 13, **2011**, 5644.

Heinemann, C.; Müller, T.; Apeloig, Y.; Schwarz, H. "On the Question of Stability, Conjugation, and "Aromaticity" in Imidazol-2-Ylidenes and Their Silicon Analogs", *J. Am. Chem. Soc.* 118, **1996**, 2023.

Herrmann, W. A. "N-Heterocyclic Carbenes: A New Concept in Organometallic Catalysis", *Angew. Chem. Int. Ed.* 41, **2002**, 1290.

Herrmann, W. A.; Schütz, J.; Frey, G. D.; Herdtweck, E. "N-Heterocyclic Carbenes: Synthesis, Structures, and Electronic Ligand Properties", *Organometallics* 25, **2006**, 2437.

Hillier, A. C.; Sommer, W. J.; Yong, B. S.; Petersen, J. L.; Cavallo, L.; Nolan, S. P. "A Combined Experimental and Theoretical Study Examining the Binding of N-Heterocyclic Carbenes (NHC) to the Cp*Rucl (Cp* = η^5-C$_5$Me$_5$) Moiety: Insight into Stereoelectronic Differences between Unsaturated and Saturated NHC Ligands", *Organometallics* 22, **2003**, 4322.

Hirano, K.; Urban, S.; Wang, C.; Glorius, F. "A Modular Synthesis of Highly Substituted Imidazolium Salts", *Org. Lett.* 11, **2009**, 1019.

Hoang, L.; Bahmanyar, S.; Houk, K. N.; List, B. "Kinetic and Stereochemical Evidence for the Involvement of Only One Proline Molecule in the Transition States of Proline-Catalyzed Intra- and Intermolecular Aldol Reactions", *J. Am. Chem. Soc.* 125, **2003**, 16.

Hoffmann, T.; Zhong, G.; List, B.; Shabat, D.; Anderson, J.; Gramatikova, S.; Lerner, R. A.; Barbas III, C. F. "Aldolase Antibodies of Remarkable Scope", *J. Am. Chem. Soc.* 120, **1998**, 2768.

Hohenberg, P.; Kohn, W. "Inhomogeneous Electron Gas", *Phys. Rev.* 136, **1964**, B864.

Holbrey, J. D.; Reichert, W. M.; Tkatchenko, I.; Bouajila, E.; Walter, O.; Tommasi, I.; Rogers, R. D. "1,3-Dimethylimidazolium-2-Carboxylate: The Unexpected Synthesis of an Ionic Liquid Precursor and Carbene-CO_2 Adduct", *Chem. Commun.* 9, **2003**, 28.

Hopffgarten, M. V.; Frenking, G. "Energy Decomposition Analysis", *WIREs Comput. Mol. Sci.* 2, **2012**, 43.

Houk, K. N.; Cheong, P. H. Y. "Computational Prediction of Small-Molecule Catalysts", *Nature* 455, **2008**, 309.

Hu, X. L.; Castro-Rodriguez, I.; Meyer, K. "A Bis-Carbenealkenyl Copper(I) Complex from a Tripodal Carbene Ligand", *Organometallics* 22, **2003**, 3016.

Huang, F.; Lu, G.; Zhao, L.; Li, H.; Wang, Z. X. "The Catalytic Role of N-Heterocyclic Carbene in a Metal-Free Conversion of Carbon Dioxide into Methanol: A Computational Mechanism Study", *J. Am. Chem. Soc.* 132, **2010**, 12388.

Huang, Y.; Walji, A. M.; Larsen, C. H.; MacMillan, D. W. C. "Enantioselective Organo-Cascade Catalysis", *J. Am. Chem. Soc.* 127, **2005**, 15051.

Hughes, D. L.; Dolling, U. H.; Ryan, K. M.; Schoenewaldt, E. F.; Grabowski, E. J. J. "Efficient Catalytic Asymmetric Alkylations. 3. A Kinetic and Mechanistic Study of the Enantioselective Phase-Transfer Methylation of 6,7-Dichloro-5-Methoxy-2-Phenyl-1-Indanone", *J. Org. Chem.* 52, **1987**, 4745.

Humbel, S.; Sieber, S.; Morokuma, K. "The Imomo Method: Integration of Different Levels of Molecular Orbital Approximations for Geometry Optimization of Large Systems: Test for *N*-Butane Conformation and S_N2 Reaction: Rcl^+Cl^-", *J. Chem. Phys.* 105, **1996**, 1959.

Huynh, H. V.; Han, Y.; Jothibasu, R.; Yang, J. A. "^{13}C NMR Spectroscopic Determination of Ligand Donor Strengths Using N-Heterocyclic Carbene Complexes of Palladium(II)", *Organometallics* 28, **2009**, 5395.

Huzinaga, S. "Gaussian-Type Functions for Polyatomic Systems. I", *J. Chem. Phys.* 42, **1965**, 1293.

Ishikawa, H.; Suzuki, T.; Hayashi, Y. "High-Yielding Synthesis of the anti-Influenza Neuramidase Inhibitor (-)-Oseltamivir by Three "One-Pot" Operations", *Angew. Chem. Int. Ed.* 48, **2009**, 1304.

Ishikawa, T.; Araki, Y.; Kumamoto, T.; Seki, H.; Fukuda, K.; Isobe, T. "Modified Guanidines as Chiral Superbases: Application to Asymmetric Michael Reaction of Glycine Imine with Acrylate or Its Related Compounds", *Chem. Commun.* **2001**, 245.

Iwabuchi, Y.; Nakatani, M.; Yokoyama, N.; Hatakeyama, S. "Chiral Amine-Catalyzed Asymmetric Baylis-Hillman Reaction: A Reliable Route to Highly Enantiomerically Enriched (α-Methylene-β-Hydroxy)Esters [5]", *J. Am. Chem. Soc.* 121, **1999**, 10219.

Iyer, M. S.; Gigstad, K. M.; Namdev, N. D.; Lipton, M. "Asymmetric Catalysis of the Strecker Amino Acid Synthesis by a Cyclic Dipeptide", *J. Am. Chem. Soc.* 118, **1996**, 4910.

Jacobsen, E. N.; MacMillan, D. W. C. "Organocatalysis", *Proc. Natl. Acad. Sci. U. S. A* 107, **2010**, 20618.

Jacobsen, E. N.; Pfalz, A.; Yamamoto, H. "*Comprehensive Asymmetric Catalysis*", eds. A. Mori and S. Inoue, Springer, Heidelberg, **1999**.

Jacobsen, H. "Bonding Aspects of P-Heterocyclic Carbene Transition Metal Complexes. A Computational Assessment", *J. Organomet. Chem.* 690, **2005**, 6068.

Jacobsena, E. N.; MacMillanb, D. W. C. "Organocatalysis", *Proc. Natl. Acad. Sci. U. S. A* 107, **2010**, 20618.

Jen, W. S.; Wiener, J. J. M.; MacMillan, D. W. C. "New Strategies for Organic Catalysis: The First Enantioselective Organocatalytic 1,3-Dipolar Cycloaddition", *J. Am. Chem. Soc.* 122, **2000**, 9874.

Jensen, F. "*Introduction to Computational Chemistry*", Wiley, Chichester, **1999**.

Johnson, J. S. "Catalyzed Reactions of Acyl Anion Equivalents", *Angew. Chem. Int. Ed.* 43, **2004**, 1326.

Joly, G. D.; Jacobsen, E. N. "Thiourea-Catalyzed Enantioselective Hydrophosphonylation of Imines: Practical Access to Enantiomerically Enriched α-Amino Phosphonic Acids", *J. Am. Chem. Soc.* 126, **2004**, 4102.

Jørgensen, P.; Simons, J., and North Atlantic Treaty Organization, Scientific Affairs Division "*Geometrical Derivatives of Energy Surfaces and Molecular Properties*", Reidel, Dordrecht, **1986**.

Jousseaume, T.; Wurz, N. E.; Glorius, F. "Highly Enantioselective Synthesis of α-Amino Acid Derivatives by an NHC-Catalyzed Intermolecular Stetter Reaction", *Angew. Chem., Int. Ed.* 50, **2011**, 1410.

Joyce, G. F.; Visser, G. M.; Van Boeckel, C. A. A. "Chiral Selection in Poly(C)-Directed Synthesis of Oligo(G)", *Nature* 310, **1984**, 602.

Juliá, S.; Guixer, J.; Masana, J.; Rocas, J.; Colonna, S.; Annuziata, R.; Molinari, H. "Synthetic Enzymes. Part 2. Catalytic Asymmetric Epoxidation by Means of

Polyamino-Acids in a Triphase System", *J. Chem. Soc., Perkin Trans. 1*, **1982**, 1317.

Juliá, S.; Masana, J.; Vega, J. C. ""Synthetic Enzymes". Highly Stereoselective Epoxidation of Chalcone in a Triphasic Toluene-Water-Poly[(*S*)-Alanine] System", *Angew. Chem. Int. Ed.* 19, **1980**, 929.

Jung, M. E. "A Review of Annulation", *Tetrahedron* 32, **1976**, 3.

Kadlčíková, A.; Valterová, I.; Ducháčková, L.; Roithová, J.; Kotora, M. "Lewis Base Catalyzed Enantioselective Allylation of α,β- Unsaturated Aldehydes", *Chem. Eur. J.* 16, **2010**, 9442.

Kagan, H. B.; Riant, O. "Catalytic Asymmetric Diels-Alder Reactions", *Chem. Rev.* 92, **1992**, 1007.

Kamioka, S.; Ajami, D.; Rebek Jr, J. "Autocatalysis and Organocatalysis with Synthetic Structures", *Proc. Natl. Acad. Sci. U. S. A* 107, **2010**, 541.

Kaneko, S.; Yoshino, T.; Katoh, T.; Terashima, S. "Synthetic Studies of Huperzine a and Its Fluorinated Analogues. 1. Novel Asymmetric Syntheses of an Enantiomeric Pair of Huperzine A", *Tetrahedron* 54, **1998**, 5471.

Kayaki, Y.; Yamamoto, M.; Ikariya, T. "N-Heterocyclic Carbenes as Efficient Organocatalysts for CO_2 Fixation Reactions", *Angew. Chem. Int. Ed.* 48, **2009**, 4194.

Kayaki, Y.; Yamamoto, M.; Ikariya, T. "N-Heterocyclic Carbenes as Efficient Organocatalysts for CO_2 Fixation Reactions", *Angew. Chem. Int. Ed.* 48, **2009**, 4194.

Kayaki, Y.; Yamamoto, M.; Ikariya, T. "N-Heterocyclic Carbenes as Efficient Organocatalysts for CO_2 Fixation Reactions", *Angew. Chem., Int. Ed. Engl.* 48, **2009**, 4194.

Kelly, H. P. "*Advances in Chemical Physics*", John Wiley & Sons, New York, **1969**.

Kelly III, R. A.; Clavier, H.; Giudice, S.; Scott, N. M.; Stevens, E. D.; Bordner, J.; Samardjiev, I.; Hoff, C. D.; Cavallo, L.; Nolan, S. P. "Determination of N-Heterocyclic Carbene (NHC) Steric and Electronic Parameters Using the [(NHC)Ir(CO)$_2$Cl] System", *Organometallics* 27, **2008**, 202.

Kerr, M. S.; De Alaniz, J. R.; Rovis, T. "A Highly Enantioselective Catalytic Intramolecular Stetter Reaction", *J. Am. Chem. Soc.* 124, **2002**, 10298.

Kerr, M. S.; Rovis, T. "Effect of the Michael Acceptor in the Asymmetric Intramolecular Stetter Reaction", *Synlett*, **2003**, 1934.

Khramov, D. M.; Boydston, A. J.; Bielawski, C. W. "Synthesis and Study of Janus Bis(Carbene)S and Their Transition-Metal Complexes", *Angew. Chem. Int. Ed.* 45, **2006**, 6186.

Khramov, D. M.; Rosen, E. L.; Er, J. A.; Vu, P. D.; Lynch, V. M.; Bielawski, C. W. "N-Heterocyclic Carbenes: Deducing σ- and π-Contributions in Rh-Mediated Hydroboration and Pd-Mediated Coupling Reactions", *Tetrahedron* 64, **2008**, 6853.

Kirmse, W. "The Beginnings of N-Heterocyclic Carbenes", *Angew. Chem. Int. Ed.* 49, **2010**, 8798.

Klussmann, M.; Iwamura, H.; Mathew, S. P.; Wells Jr, D. H.; Pandya, U.; Armstrong, A.; Blackmond, D. G. "Thermodynamic Control of Asymmetric Amplification in Amino Acid Catalysis", *Nature* 441, **2006**, 621.

Kofoed, J.; Nielsen, J.; Reymond, J. L. "Discovery of New Peptide-Based Catalysts for the Direct Asymmetric Aldol Reaction", *Bioorg. Med. Chem. Lett.* 13, **2003**, 2445.

Kohn, W.; Sham, L. J. "Self-Consistent Equations Including Exchange and Correlation Effects", *Phys. Rev.* 140, **1965**, A1133.

[a]Kotsuki, H.; Ikishima, H.; Okuyama, A. "Organocatalytic Asymmetric Synthesis Using Proline and Related Molecules. Part 1", *Heterocycles* 75, **2008**, 493.

[b]Kotsuki, H.; Ikishima, H.; Okuyama, A. "Organocatalytic Asymmetric Synthesis Using Proline and Related Molecules. Part 2", *Heterocycles* 75, **2008**, 757.

Kovacevic, B.; Maksic, Z. B. "Basicity of Some Organic Superbases in Acetonitrile", *Org. Lett.* 3, **2001**, 1523.

Kovacs, A.; Esterhuysen, C.; Frenking, G. "The Nature of the Chemical Bond Revisited: An Energy-Partitioning Analysis of Nonpolar Bonds", *Chem. Eur. J.* 11, **2005**, 1813.

Kozuch, S.; Shaik, S. "How to Conceptualize Catalytic Cycles? The Energetic Span Model", *Acc. Chem. Res.* 44, **2011**, 101.

Krapp, A.; Bickelhaupt, F. M.; Frenking, G. "Orbital Overlap and Chemical Bonding", *Chem. Eur. J.* 12, **2006**, 9196.

Krishnan, K. S.; Kuthanappillil, J. M.; John, J.; Suresh, C. H.; Suresh, E.; Radhakrishnan, K. V. "Stereocontrolled Synthesis of Novel Spirocyclic Oxa-Bridged Cyclooctanoids through Sequential Transformations of Pentafulvenes", *Synthesis*, **2008**, 2134.

Krishnan, R.; Pople, J. A. "Approximate Fourth-Order Perturbation Theory of the Electron Correlation Energy", *Int. J. Quantum Chem.* 14, **1978**, 91.

Krygowski, T. M. "Crystallographic Studies of Inter- and Intramolecular Interactions Reflected in Aromatic Character Of π-Electron Systems", *J. Chem. Inf. Comput. Sci.* 33, **1993**, 70.

Kümmel, H. G. "*A Biography of the Coupled Cluster Method*", eds. R. F. Bishop, T. Brandes, K. A. Gernoth, N. R. Walet and Y. Xian, World Scientific Publishing, Singapore, **2002**.

Kumaragurubaran, N.; Juhl, K.; Zhuang, W.; Bøgevig, A.; Jørgensen, K. A. "Direct L-Proline-Catalyzed Asymmetric α-Amination of Ketones", *J. Am. Chem. Soc.* 124, **2002**, 6254.

Lacoste, E. "Proline: An Essential Amino Acid as Effective Chiral Organocatalyst", *Synlett.* **2006**, 1973.

Langenbeck, W. "By similarities in the catalytic action of enzymes and organic substances defined", *Angew. Chem.* 41, **1928**, 740.

Langenbeck, W. "Fermentproblem and organic catalysis", *Angew. Chem.* 45, **1932**, 97.

Langenbeck, W. "*The organic catalysts And your relationship to the enzymes*", 2nd ed., Springer, Berlin, **1949**.

Lee, C.; Yang, W.; Parr, R. G. "Development of the Colle-Salvetti Correlation-Energy Formula into a Functional of the Electron Density", *Phys. Rev. B* 37, **1988**, 785.

Lehmann, J. F.; Urquhart, S. G.; Ennis, L. E.; Hitchcock, A. P.; Hatano, K.; Gupta, S.; Denk, M. K. "Core Excitation Spectroscopy of Stable Cyclic Diaminocarbenes, -Silylenes, and -Germylenes", *Organometallics* 18, **1999**, 1862.

Lein, M.; Frenking, G. "*Theory and Applications of Computational Chemistry: The First 40 Years*", eds. C. E. Dykstra, G. Frenking, K. S. Kim and G. E. Scuseria, Elsevier, Amsterdam, 2005.

Lein, M.; Szabo, A.; Kovacs, A.; Frenking, G. "Theoretical Studies of Inorganic Compounds. Part XXVIII. Energy Decomposition Analysis of the Chemical Bond in Main Group and Transition Metal Compounds", *Faraday Discuss.* 124, **2003**, 365.

Lesarri, A.; Mata, S.; Cocinero, E. J.; Blanco, S.; López, J. C.; Alonso, J. L. "The Structure of Neutral Proline", *Angew. Chem., Int. Ed.* 41, **2002**, 4673.

Leuthaeusser, S.; Schwarz, D.; Plenio, H. "Tuning the Electronic Properties of N-Heterocyclic Carbenes", *Chem. Eur. J.* 13, **2007**, 7195.

Lever, A. B. P. "Electrochemical Parametrization of Metal Complex Redox Potentials, Using the Ruthenium(III)/Ruthenium(II) Couple to Generate a Ligand Electrochemical Series", *Inorg. Chem.* 29, **1990**, 1271.

Lever, A. B. P. "Electrochemical Parametrization of Rhenium Redox Couples", *Inorg. Chem.* 30, **1991**, 1980.

Li, C. Y.; Kuo, Y. Y.; Tsai, J. H.; Yap, G. P. A.; Ong, T. G. "Amine-Linked N-Heterocyclic Carbenes: The Importance of an Pendant Free-Amine Auxiliary in Assisting the Catalytic Reaction", *Chem. Asian J.* 6, **2011**, 1520.

Li, H.; Fu, A.; Shi, H. "Theoretical Studies of Stereoselectivities in the Direct Organocatalytic Mannich Reactions Involving Ketimine", *J. Mol. Catal. A: Chem.* 303, **2009**, 1.

Li, Y.; Paddon-Row, M. N.; Houk, K. N. "Transition Structures of Aldol Reactions", *J. Am. Chem. Soc.* 110, **1988**, 3684.

List, B. "The Direct Catalytic Asymmetric Three-Component Mannich Reaction", *J. Am. Chem. Soc.* 122, **2000**, 9336.

List, B. "Asymmetric Aminocatalysis", *Synlett*, **2001**, 1675.

List, B. "Direct Catalytic Asymmetric α-Amination of Aldehydes", *J. Am. Chem. Soc.* 124, **2002**, 5656.

List, B. "Proline-Catalyzed Asymmetric Reactions", *Tetrahedron* 58, **2002**, 5573.

List, B. "Enamine Catalysis is a Powerful Strategy for the Catalytic Generation and Use of Carbanion Equivalents", *Acc. Chem. Res.* 37, **2004**, 548.

List, B.; Hoang, L.; Martin, H. J. "New Mechanistic Studies on the Proline-Catalyzed Aldol Reaction", *Proc. Natl. Acad. Sci. U. S. A* 101, **2004**, 5839.

List, B.; Lerner, R. A.; Barbas III, C. F. "Proline-Catalyzed Direct Asymmetric Aldol Reactions", *J. Am. Chem. Soc.* 122, **2000**, 2395.

List, B.; Pojarliev, P.; Biller, W. T.; Martin, H. J. "The Proline-Catalyzed Direct Asymmetric Three-Component Mannich Reaction: Scope, Optimization, and Application to the Highly Enantioselective Synthesis of 1,2-Amino Alcohols", *J. Am. Chem. Soc.* 124, **2002**, 827.

List, B.; Pojarliev, P.; Castello, C. "Proline-Catalyzed Asymmetric Aldol Reactions between Ketones and α-Unsubstituted Aldehydes", *Org. Lett.* 3, **2001**, 573.

Liu, B.; Chen, W.; Jin, S. "Synthesis, Characterization and Luminescence of New Silver Aggregates Containing Short Ag-Ag Bonds Stabilized by Bis(N-Heterocyclic Carbene) Ligands", *Organometallics* 26, **2007**, 3660.

Liu, F.; Bugaut, X.; Schedler, M.; Fröhlich, R.; Glorius, F. "Designing N-Heterocyclic Carbenes: Simultaneous Enhancement of Reactivity and Enantioselectivity in the

Asymmetric Hydroacylation of Cyclopropenes", *Angew. Chem., Int. Ed.* 50, **2011**, 12626.

Liu, P.; Montgomery, J.; Houk, K. N. "Ligand Steric Contours to Understand the Effects of N-Heterocyclic Carbene Ligands on the Reversal of Regioselectivity in Ni-Catalyzed Reductive Couplings of Alkynes and Aldehydes", *J. Am. Chem. Soc.* 133, **2011**, 6956.

Luinstra, G. A.; Haas, G. R.; Molnar, F.; Bernhart, V.; Eberhardt, R.; Rieger, B. "On the Formation of Aliphatic Polycarbonates from Epoxides with Chromium(III) and Aluminum(III) Metal-Salen Complexes", *Chem. Eur. J.* 11, **2005**, 6298.

Luque, F. J.; Orozco, M.; Bhadane, P. K.; Gadre, S. R. "Effect of Solvation on the Shapes, Sizes and Anisotropies of Polyatomic Anions *via* Molecular Electrostatic Potential Topology: An *Ab initio* Self Consistent Reaction Field Approach", *J. Chem. Phys.* 100, **1994**, 6718.

Lynch, B. J.; Fast, P. L.; Harris, M.; Truhlar, D. G. "Adiabatic Connection for Kinetics", *J. Phys. Chem. A* 104, **2000**, 4813.

Lynch, B. J.; Zhao, Y.; Truhlar, D. G. "Effectiveness of Diffuse Basis Functions for Calculating Relative Energies by Density Functional Theory", *J. Phys. Chem. A* 107, **2003**, 1384.

Ma, J.; Zhang, X.; Zhao, N.; Al-Arifi, A. S. N.; Aouak, T.; Al-Othman, Z. A.; Xiao, F.; Wei, W.; Sun, Y. "Theoretical Study of TBD-Catalyzed Carboxylation of Propylene Glycol with CO_2", *J. Mol. Catal. A: Chem.* 315, **2010**, 76.

MacMillan, D. W. C. "The Advent and Development of Organocatalysis", *Nature* 455, **2008**, 304.

Magill, A. M.; Cavell, K. J.; Yates, B. F. "Basicity of Nucleophilic Carbenes in Aqueous and Nonaqueous Solvents - Theoretical Predictions", *J. Am. Chem. Soc.* 126, **2004**, 8717.

Mahatthananchai, J.; Zheng, P.; Bode, J. W. "α,β-Unsaturated Acyl Azoliums from N-Heterocyclic Carbene Catalyzed Reactions: Observation and Mechanistic Investigation", *Angew. Chem. Int. Ed.* 50, **2011**, 1673.

Marion, N.; Díez-González, S.; Nolan, S. P. "N-Heterocyclic Carbenes as Organocatalysts", *Angew. Chem.. Int. Ed.* 46, **2007**, 2988.

Maruoka, K.; Ooi, T. "Enantioselective Amino Acid Synthesis by Chiral Phase-Transfer Catalysis", *Chem. Rev.* 103, **2003**, 3013.

Maseras, F.; Morokuma, K. "Imomm: A New Integrated *Ab initio* + Molecular Mechanics Geometry Optimization Scheme of Equilibrium Structures and Transition States", *J. Comput. Chem.* 16, **1995**, 1170.

Mata, J. A.; Poyatos, M.; Peris, E. "Structural and Catalytic Properties of Chelating Bis- and Tris-N-Heterocyclic Carbenes", *Coord. Chem. Rev.* 251, **2007**, 841.

Mata, S.; Vaquero, V.; Cabezas, C.; Pena, I.; Perez, C.; Lopez, J. C.; Alonso, J. L. "Observation of Two New Conformers of Neutral Proline", *Phys. Chem. Chem. Phys.* 11, **2009**, 4141.

Mathew, J.; Suresh, C. H. "Use of Molecular Electrostatic Potential at the Carbene Carbon as a Simple and Efficient Electronic Parameter of N-Heterocyclic Carbenes", *Inorg. Chem.* 49, **2010**, 4665.

Mathew, J.; Suresh, C. H. "Assessment of Steric and Electronic Effects of N-Heterocyclic Carbenes in Grubbs Olefin Metathesis Using Molecular Electrostatic Potential", *Organometallics* 30, **2011**, 3106.

Mathew, J.; Thomas, T.; Suresh, C. H. "Quantitative Assessment of the Stereoelectronic Profile of Phosphine Ligands", *Inorg. Chem.* 46, **2007**, 10800.

Meierhenrich, U. J.; Muñoz Caro, G. M.; Schutte, W. A.; Barbier, B.; Segovia, A. A.; Rosenbauer, H.; Thiemann, W. H. P.; Brack, A. "The Prebiotic Synthesis of Amino Acids - Interstellar *Vs.* Atmospheric Mechanisms", *Exo-Astrobiology , ESA SP-518*, **2002**, 25.

Meinert, C.; de Marcellus, P.; Le Sergeant d'Hendecourt, L.; Nahon, L.; Jones, N. C.; Hoffmann, S. V.; Bredehöft, J. H.; Meierhenrich, U. J. "Photochirogenesis: Photochemical Models on the Absolute Asymmetric Formation of Amino Acids in Interstellar Space", *Phys. Life Rev.* 8, **2011**, 307.

Melchiorre, P.; Marigo, M.; Carlone, A.; Bartoli, G. "Asymmetric Aminocatalysis - Gold Rush in Organic Chemistry", *Angew. Chem. Int. Ed.* 47, **2008**, 6138.

Mennucci, B.; Cammi, R.; Tomasi, J. "Analytical Free Energy Second Derivatives with Respect to Nuclear Coordinates: Complete Formulation for Electrostatic Continuum Solvation Models", *J. Chem. Phys.* 110, **1999**, 6858.

Mercs, L.; Neels, A.; Stoeckli-Evans, H.; Albrecht, M. "Probing Intermetallic Coupling in Dinuclear N-Heterocyclic Carbeneruthenium(II) Complexes", *Inorg. Chem.* 50, **2011**, 8188.

Miller, S. J. "In Search of Peptide-Based Catalysts for Asymmetric Organic Synthesis", *Acc. Chem. Res.* 37, **2004**, 601.

Mitsumori, S.; Zhang, H.; Cheong, P. H. Y.; Houk, K. N.; Tanaka, F.; Barbas, C. F. "Direct Asymmetric anti-Mannich-Type Reactions Catalyzed by a Designed Amino Acid", *J. Am. Chem. Soc.* 128, **2006**, 1040.

Mo, Y.; Schleyer, P. V. R. *Chem. Eur. J.* 12, **2006**, 2009.

Mohan, N.; Vijayalakshmi, K. P.; Koga, N.; Suresh, C. H. "Comparison of Aromatic NH···π, OH···π, and CH···π Interactions of Alanine Using MP2, CCSD, and DFT Methods", *J. Comput. Chem.* 31, **2010**, 2874.

Molines, H.; Wakselman, C. "From annelated fluorinating Carbonyls Compounds to the Fluoro-1 Vinyl Methyl Ketone", *Tetrahedron* 32, **1976**, 2099.

Mordasini, T. Z.; Thiel, W. "Combined Quantum Mechanical and Molecular Mechanical Approaches", *Chimia* 52, **1998**, 288.

Morgan, B. P.; Galdamez, G. A.; Gilliard Jr, R. J.; Smith, R. C. "Canopied Trans-Chelating Bis(N-Heterocyclic Carbene) Ligand: Synthesis, Structure and Catalysis", *Dalton Trans.* **2009**, 2020.

Morokuma, K. "Why Do Molecules Interact? The Origin of Electron Donor-Acceptor Complexes, Hydrogen Bonding, and Proton Affinity", *Acc. Chem. Res.* 10, **1977**, 294.

Moss, R. A.; Wang, L.; Odorisio, C. M.; Krogh-Jespersen, K. "A Carbene-Carbene Complex Equilibrium", *J. Am. Chem. Soc.* 132, **2010**, 10677.

Mukherjee, S.; Yang, J. W.; Hoffmann, S.; List, B. "Asymmetric Enamine Catalysis", *Chem. Rev.* 107, **2007**, 5471.

Muñoz Caro, G. M.; Melerhenrich, U. J.; Schutte, W. A.; Barbier, B.; Arcones Segovia, A.; Rosenbauer, H.; Thiemann, W. H. P.; Brack, A.; Greenberg, J. M. "Amino Acids from Ultraviolet Irradiation of Interstellar Ice Analogues", *Nature* 416, **2002**, 403.

Nair, V.; Bindu, S.; Sreekumar, V. "N-Heterocyclic Carbenes: Reagents, Not Just Ligands!", *Angew. Chem. Int. Ed. Engl.* 43, **2004**, 5130.

Nair, V.; Menon, R. S.; Biju, A. T.; Sinu, C. R.; Paul, R. R.; Jose, A.; Sreekumar, V. "Employing Homoenolates Generated by NHC Catalysis in Carbon-Carbon Bond-Forming Reactions: State of the Art", *Chem. Soc. Rev.* 40, **2011**, 5336.

Nair, V.; Varghese, V.; Paul, R. R.; Jose, A.; Sinu, C. R.; Menon, R. S. "NHC Catalyzed Transformation of Aromatic Aldehydes to Acids by Carbon Dioxide: An Unexpected Reaction", *Org. Lett.* 12, **2010**, 2653.

Nair, V.; Vellalath, S.; Babu, B. P. "Recent Advances in Carbon-Carbon Bond-Forming Reactions Involving Homoenolates Generated by NHC Catalysis", *Chem. Soc. Rev.* 37, **2008**, 2691.

Neilson, B. M.; Tennyson, A. G.; Bielawski, C. W. "Advances in Bis(N-Heterocyclic Carbene) Chemistry: New Classes of Structurally Dynamic Materials", *J. Phys. Org. Chem.* 25, **2012**, 531.

Nemcsok, D.; Wichmann, K.; Frenking, G. "The Significance of π Interactions in Group 11 Complexes with N-Heterocyclic Carbenes", *Organometallics* 23, **2004**, 3640.

Nolan, S. P. "*N-Heterocyclic Carbenes in Synthesis*", Wiley-VCHM, Weinheim, Germany, **2006**.

Normand, A. T.; Cavell, K. J. "Donor-Functionalised N-Heterocyclic Carbene Complexes of Group 9 and 10 Metals in Catalysis: Trends and Directions", *Eur. J. Inorg. Chem.*, **2008**, 2781.

Northrup, A. B.; MacMillan, D. W. C. "Two-Step Synthesis of Carbohydrates by Selective Aldol Reactions", *Science* 305, **2004**, 1752.

Notz, W.; List, B. "Catalytic Asymmetric Synthesis of anti-1,2-Diols", *J. Am. Chem. Soc.* 122, **2000**, 7386.

Notz, W.; Tanaka, F.; Barbas III, C. F. "Enamine-Based Organocatalysis with Proline and Diamines: The Development of Direct Catalytic Asymmetric Aldol, Mannich, Michael, and Diels-Alder Reactions", *Acc. Chem. Res.* 37, **2004**, 580.

Notz, W.; Tanaka, F.; Watanabe, S. I.; Chowdari, N. S.; Turner, J. M.; Thayumanavan, R.; Barbas III, C. F. "The Direct Organocatalytic Asymmetric Mannich Reaction: Unmodified Aldehydes as Nucleophiles", *J. Org. Chem.* 68, **2003**, 9624.

Nyberg, A. I.; Usano, A.; Pihko, P. M. "Proline-Catalyzed Ketone-Aldehyde Aldol Reactions Are Accelerated by Water", *Synlett.* **2004**, 1891.

Oberhuber, M.; Joyce, G. F. "A DNA-Templated Aldol Reaction as a Model for the Formation of Pentose Sugars in the RNA World", *Angew. Chem. Int. Ed.* 44, **2005**, 7580.

Öfele, K. "1,3-dimethyl-4-Imidazolinyliden-(2)-A New Pentacarbonylchromium transition metal-carbene complex", *J. Organomet. Chem.* 12, **1968**, P42.

Öfele, K. "Dichlor(2,3-Diphenylcyclopropenyliden)Palladium(II)", *J. Organomet. Chem.* 22, **1970**, C9.

Oisaki, K.; Li, Q.; Furukawa, H.; Czaja, A. U.; Yaghi, O. M. "A Metal-Organic Framework with Covalently Bound Organometallic Complexes", *J. Am. Chem. Soc.* 132, **2010**, 9262.

[a]Ooi, T.; Doda, K.; Maruoka, K. "Designer Chiral Quaternary Ammonium Bifluorides as an Efficient Catalyst for Asymmetric Nitroaldol Reaction of Silyl Nitronates with Aromatic Aldehydes", *J. Am. Chem. Soc.* 125, **2003**, 2054.

[b]Ooi, T.; Doda, K.; Maruoka, K. "Highly Enantioselective Michael Addition of Silyl Nitronates to α,β-Unsaturated Aldehydes Catalyzed by Designer Chiral

Ammonium Bifluorides: Efficient Access to Optically Active γ-Nitro Aldehydes and Their Enol Silyl Ethers", *J. Am. Chem. Soc.* 125, **2003**, 9022.

Ooi, T.; Kameda, M.; Maruoka, K. "Molecular Design of a C_2-Symmetric Chiral Phase-Transfer Catalyst for Practical Asymmetric Synthesis of α-Amino Acids [12]", *J. Am. Chem. Soc.* 121, **1999**, 6519.

Ooi, T.; Maruoka, K. "Asymmetric Organocatalysis of Structurally Well-Defined Chiral Quaternary Ammonium Fluorides", *Acc. Chem. Res.* 37, **2004**, 526.

Ooi, T.; Taniguchi, M.; Kameda, M.; Maruoka, K. "Direct Asymmetric Aldol Reactions of Glycine Schiff Base with Aldehydes Catalyzed by Chiral Quaternary Ammonium Salts", *Angew. Chem. Int. Ed.* 41, **2002**, 4542.

Orgel, L. E. "Prebiotic Chemistry and the Origin of the RNA World", *Crit. Rev. Biochem. Mol. Biol.* 39, **2004**, 99.

Padmanaban, M.; Biju, A. T.; Glorius, F. "Efficient Synthesis of Benzofuranones: N-Heterocyclic Carbene (NHC)/Base-Catalyzed Hydroacylation-Stetter-Rearrangement Cascade", *Org. Lett.* 13, **2011**, 5624.

Papageorgiou, C. D.; Cubillo De Dios, M. A.; Ley, S. V.; Gaunt, M. J. "Enantioselective Organocatalytic Cyclopropanation *via* Ammonium Ylides", *Angew. Chem. Int. Ed.* 43, **2004**, 4641.

Parasuk, W.; Parasuk, V. "Theoretical Investigations on the Stereoselectivity of the Proline Catalyzed Mannich Reaction in Dmso", *J. Org. Chem.* 73, **2008**, 9388.

Parr, R. G.; Yang, W. "*Density Functional Theory of Atoms and Molecules*", Oxford University Press, New York, **1989**.

Pasteur, M. L. "Memory on The Fermentation of Tartaric acid", *Compt. Rend. Acad. Sc.i Paris* 46, **1858**, 615.

Pathak, R. K.; Gadre, S. R. "Nonexistence of Local Maxima in Molecular Electrostatic Potential Maps", *Proc. Ind Acad. Sci. (Chem. Sci.)* 102, **1990**, 189.

Pauli, J. W. "In Conclusion about the Relationship of Groups of Electrons in the Atom with the Complex Structure of the Spectra ", *Z. Phys.* 31, **1925**, 765.

Pellissier, H. "Asymmetric Organocatalysis", *Tetrahedron* 63, **2007**, 9267.

Peng, C. Y.; Ayala, P. Y.; Schlegel, H. B.; Frisch, M. J. "Using Redundant Internal Coordinates to Optimize Equilibrium Geometries and Transition States", *J. Comput. Chem.* 17, **1996**, 49.

Peng, C. Y.; Schlegel, H. B. "Combining Synchronous Transit and Quasi-Newton Methods to Find Transition-States", *Isr. J. Chem.* 33, **1993**, 449.

Perdew, J. P. "Density-Functional Approximation for the Correlation Energy of the Inhomogeneous Electron Gas", *Phys. Rev. B* 33, **1986**, 8822.

Perdew, J. P.; Burke, K.; Ernzerhof, M. "Generalized Gradient Approximation Made Simple", *Phys. Rev. Lett.* 77, **1996**, 3865.

Perdew, J. P.; Chevary, J. A.; Vosko, S. H.; Jackson, K. A.; Pederson, M. R.; Singh, D. J.; Fiolhais, J. C. "Atoms, Molecules, Solids, and Surfaces: Applications of the Generalized Gradient Approximation for Exchange and Correlation", *Phys. Rev. B* 46, **1992**, 6671.

Peris, E.; Crabtree, R. H. "Recent Homogeneous Catalytic Applications of Chelate and Pincer N-Heterocyclic Carbenes", *Coord. Chem. Rev.* 248, **2004**, 2239.

Peverati, R.; Baldridge, K. K. "Implementation and Performance of DFT-D with Respect to Basis Set and Functional for Study of Dispersion Interactions in Nanoscale Aromatic Hydrocarbons", *J. Chem. Theory Comput.* 4, **2008**, 2030.

Phan, A.; Doonan, C. J.; Uribe-Romo, F. J.; Knobler, C. B.; Okeeffe, M.; Yaghi, O. M. "Synthesis, Structure, and Carbon Dioxide Capture Properties of Zeolitic Imidazolate Frameworks", *Acc. Chem. Res.* 43, **2010**, 58.

Pidathala, C.; Hoang, L.; Vignola, N.; List, B. "Direct Catalytic Asymmetric Enolexo Aldolizations", *Angew. Chem. Int. Ed.* 42, **2003**, 2785.

Pidun, U.; Frenking, G. "[HRh(CO)4]-Catalyzed Hydrogenation of Co: A Systematic *Ab initio* Quantum-Chemical Investigation of the Reaction Mechanism", *Chem. Eur. J.* 4 **1998**, 522.

Piel, I.; Steinmetz, M.; Hirano, K.; Fröhlich, R.; Grimme, S.; Glorius, F. "Highly Asymmetric NHC-Catalyzed Hydroacylation of Unactivated Alkenes", *Angew. Chem. Int. Ed.* 50, **2011**, 4983.

Pihko, P. M. "Activation of Carbonyl Compounds by Double Hydrogen Bonding: An Emerging Tool in Asymmetric Catalysis", *Angew. Chem. Int. Ed.* 43, **2004**, 2062.

Pihko, P. M.; Laurikainen, K. M.; Usano, A.; Nyberg, A. I.; Kaavi, J. A. "Effect of Additives on the Proline-Catalyzed Ketone-Aldehyde Aldol Reactions", *Tetrahedron* 62, **2006**, 317.

Pillai, A. N.; Suresh, C. H.; Nair, V. "Pyridine-Catalyzed Stereoselective Addition of Acyclic 1,2-Diones to Acetylenic Esters: Synthetic and Theoretical Studies of an Unprecedented Rearrangement", *Chem. Eur. J.* 14, **2008**, 5851.

Pinjari, R. V.; Gejji, S. P. "Electronic Structure, Molecular Electrostatic Potential, and NMR Chemical Shifts in Cucurbit[n]Urils (n = 5-8), Ferrocene, and Their Complexes", *J. Phys. Chem. A* 112, **2008**, 12679.

Pizzarello, S.; Weber, A. L. "Prebiotic Amino Acids as Asymmetric Catalysts", *Science* 303, **2004**, 1151.

Pizzarello, S.; Weber, A. L. "Stereoselective Syntheses of Pentose Sugars under Realistic Prebiotic Conditions", *Origins Life Evol. Biosph.* 40, **2010**, 3.

Politzer, P.; Murray, J. S. "The Fundamental Nature and Role of the Electrostatic Potential in Atoms and Molecules", *Theor. Chem. Acc.* 108, **2002**, 134.

Politzer, P.; Parr, R. G. "Some New Energy Formulas for Atoms and Molecules", *J. Chem. Phys.* 61, **1974**, 4258.

Politzer, P.; Truhlar, D. G. "*Chemical Applications of Atomic and Molecular Electrostatic Potentials : Reactivity, Structure, Scattering, and Energetics of Organic, Inorganic, and Biological Systems*", Plenum Press: New York, **1981**.

Pople, J. A.; Beveridge, D. L. "*Approximate Molecular Orbital Theory*", McGraw-Hill, New York, **1970**.

Pople, J. A.; Binkley, J. S.; Seeger, R. "Theoretical Models Incorporating Electron Correlation", *Int. J. Quantum Chem. Symp.* 10, **1976**, 1.

Poyatos, M.; Mata, J. A.; Peris, E. "Complexes with Poly(N-Heterocyclic Carbene) Ligands: Structural Features and Catalytic Applications", *Chem. Rev.* 109, **2009**, 3677.

Poyatos, M.; McNamara, W.; Incarvito, C.; Clot, E.; Peris, E.; Crabtree, R. H. "A Weak Donor Planar Chelating Bitriazole N-Heterocyclic Carbene Ligand for Ruthenium(II), Palladium(II), and Rhodium", *Organometallics* 27, **2008**, 2128.

Pracejus, H. "Organic catalysts, LXI. Asymmetric Synthesis with ketenes, I. Alkaloid Catalyzed Asymmetric Synthesis of α-phenyl-propionic acid esters ", *Justus Liebigs Ann. Chem.* 634, **1960**, 9.

Prades, A.; Poyatos, M.; Mata, J. A.; Peris, E. "Double C-H Bond Activation of C(Sp^3)H$_2$ Groups for the Preparation of Complexes with Back-to-Back Bisimidazolinylidenes", *Angew. Chem. Int. Ed.* 50, **2011**, 7666.

Prelog, V.; Wilhelm, M. "The reaction mechanism and He Steric course of the asymmetric synthesis of cyanohydrins", *Helv. Chim. Acta* 192, **1954**, 1634.

Pulay, P. "*Modern Electronic Structure Theory*", World Scientific, Singapore, **1995**.

Pulkkinen, J.; Aburel, P. S.; Halland, N.; Jørgensen, K. A. "Highly Enantio- and Diastereoselective Organocatalytic Domino Michael-Aldol Reactions of β-Diketone and β-Ketosulfone Nucleophiles with α,β-Unsaturated Ketones", *Adv. Synth. Catal.* 346, **2004**, 1077.

Radius, U.; Bickelhaupt, F. M. "Bonding Capabilities of Imidazol-2-Ylidene Ligands in Group-10 Transition-Metal Chemistry", *Coord. Chem. Rev.* 253, **2009**, 678.

Ramachary, D. B.; Kishor, M.; Reddy, G. B. "Development of Drug Intermediates by Using Direct Organocatalytic Multi-Component Reactions", *Org. Biomol. Chem.* 4, **2006**, 1641.

Ramasastry, S. S. V.; Zhang, H.; Tanaka, F.; Barbas III, C. F. "Direct Catalytic Asymmetric Synthesis of anti-1,2-Amino Alcohols and syn-1,2-Diols through Organocatalytic anti-Mannich and syn-Aldol Reactions", *J. Am. Chem. Soc.* 129, **2007**, 288.

Rankin, K. N.; Gauld, J. W.; Boyd, R. J. "Density Functional Study of the Proline-Catalyzed Direct Aldol Reaction", *J. Phys. Chem. A* 106, **2002**, 5155.

Rapaport, D. C. "*The Art of Molecular Dynamics Simulation*", Cambridge University Press, Cambridge, **2004**.

Rasika Dias, H. V.; Jin, W. "A Stable Tridentate Carbene Ligand", *Tetrahedron Lett.* 35, **1994**, 1365.

Raynal, M.; Cazin, C. S. J.; Vallee, C.; Olivier-Bourbigou, H.; Braunstein, P. "An Unprecedented, Figure-of-Eight, Dinuclear Iridium(I) Dicarbene and New Iridium (III) "Pincer" Complexes", *Chem. Commun.* 34, **2008**, 3983.

Riduan, S. N.; Zhang, Y.; Ying, J. Y. "Conversion of Carbon Dioxide into Methanol with Silanes over N-Heterocyclic Carbene Catalysts", *Angew. Chem. Int. Ed.* 48, **2009**, 3322.

Roothaan, C. C. J. "New Developments in Molecular Orbital Theory", *Rev. Mod. Phys.* 23, **1951**, 69.

Rothlisberger, D.; Khersonsky, O.; Wollacott, A. M.; Jiang, L.; DeChancie, J.; Betker, J.; Gallaher, J. L.; Althoff, E. A.; Zanghellini, A.; Dym, O.; Albeck, S.; Houk, K. N.; Tawfik, D. S.; Baker, D. "Kemp Elimination Catalysts by Computational Enzyme Design", *Nature* 453, **2008**, 190.

Rueping, M.; Antonchick, A. P.; Theissmann, T. "A Highly Enantioselective Brønsted Acid Catalyzed Cascade Reaction: Organocatalytic Transfer Hydrogenation of Quinolines and Their Application in the Synthesis of Alkaloids", *Angew. Chem. Int. Ed.* 45, **2006**, 3683.

Sakakura, T.; Choi, J. C.; Yasuda, H. "Transformation of Carbon Dioxide", *Chem. Rev.* 107, **2007**, 2365.

Sakthivel, K.; Notz, W.; Bui, T.; Barbas III, C. F. "Amino Acid Catalyzed Direct Asymmetric Aldol Reactions: A Bioorganic Approach to Catalytic Asymmetric Carbon-Carbon Bond-Forming Reactions", *J. Am. Chem. Soc.* 123, **2001**, 5260.

Sayyed, F. B.; Suresh, C. H. "Quantification of Substituent Effects Using Molecular Electrostatic Potentials: Additive Nature and Proximity Effects", *New J. Chem.* 33, **2009**, 2465.

Sayyed, F. B.; Suresh, C. H.; Gadre, S. R. "Appraisal of through-Bond and through-Space Substituent Effects *via* Molecular Electrostatic Potential Topography", *J. Phys. Chem. A* 114, **2010**, 12330.

Scheele, U. J.; Dechert, S.; Meyer, F. "Bridged Dinucleating N-Heterocyclic Carbene Ligands and Their Double Helical Mercury(II) Complexes", *Inorganica Chimica Acta* 359, **2006**, 4891.

Schleyer, P. V. R.; Maerker, C.; Dransfeld, A.; Jiao, H.; Van Eikema Hommes, N. J. R. "Nucleus-Independent Chemical Shifts: A Simple and Efficient Aromaticity Probe", *J. Am. Chem. Soc.* 118, **1996**, 6317.

Schleyer, P. V. R.; Pühlhofer, F., "Recommendations for the Evaluation of Aromatic Stabilization Energies", *Org. Lett.* 4, **2002**, 2873.

Schlick, T. "*Molecular Modeling and Simulation*", Springer-Verlag, New York, **2002**.

Schmid, M. B.; Zeitler, K.; Gschwind, R. M. "The Elusive Enamine Intermediate in Proline-Catalyzed Aldol Reactions: NMR Detection, Formation Pathway, and Stabilization Trends", *Angew. Chem. Int. Ed.* 49, **2010**, 4997.

Schmid, M. B.; Zeitler, K.; Gschwind, R. M. "NMR Investigations on the Proline-Catalyzed Aldehyde Self-Condensation: Mannich Mechanism, Dienamine Detection, and Erosion of the Aldol Addition Selectivity", *J. Org. Chem.* 76, **2011**, 3005.

Schreiner, P. R. "Metal-Free Organocatalysis through Explicit Hydrogen Bonding Interactions", *Chem. Soc. Rev.* 32, **2003**, 289.

Schrödinger, E. "Quantization as an eigenvalue problem", *Ann. Phys. Chem., Ser. 2.* 79, **1926**, 361.

Scott, N. M.; Dorta, R.; Stevens, E. D.; Correa, A.; Cavallo, L.; Nolan, S. P. "Interaction of a Bulky N-Heterocyclic Carbene Ligand with Rh(I) and Ir(I). Double C-H Activation and Isolation of Bare 14-Electron Rh(III) and Ir(III) Complexes", *J. Am. Chem. Soc.* 127, **2005**, 3516.

Seayad, J.; List, B. "Asymmetric Organocatalysis", *Org. Biomol. Chem.* 3, **2005**, 719.

Seebach, D.; Beck, A. K.; Badine, D. M.; Limbach, M.; Eschenmoser, A.; Treasurywala, A. M.; Hobi, R.; Prikoszovich, W.; Linder, B. "Are Oxazolidinones Really Unproductive, Parasitic Species in Proline Catalysis? - Thoughts and Experiments Pointing to an Alternative View", *Helv. Chim. Acta* 90, **2007**, 425.

Sharma, A. K.; Sunoj, R. B. "Enamine Versus Oxazolidinone: What Controls Stereoselectivity in Proline-Catalyzed Asymmetric Aldol Reactions", *Angew. Chem. Int. Ed.* 49, **2010**, 6373.

Sharma, A. K.; Sunoj, R. B. "Stereocontrol in Proline-Catalyzed Asymmetric Amination: A Comparative Assessment of the Role of Enamine Carboxylic Acid and Enamine Carboxylate", *Chem. Commun.* 47, **2011**, 5759.

Shavitt, I. "*Methods in Computational Physics*", Academic Press, New York, **1963**.

Sherman, M. P.; Grither, W. R.; McCulla, R. D. "Computational Investigation of the Reaction Mechanisms of Nitroxyl and Thiols", *J. Org. Chem.* 75, **2010**, 4014.

Shi, Y. "Organocatalytic Asymmetric Epoxidation of Olefins by Chiral Ketones", *Acc. Chem. Res.* 37, **2004**, 488.

Shinisha, C. B.; Sunoj, R. B. "Bicyclic Proline Analogues as Organocatalysts for Stereoselective Aldol Reactions: An in Silico DFT Study", *Org. Biomol. Chem.* 5, **2007**, 1287.

Shirsat, R. N.; Bapat, S. V.; Gadre, S. R. "Molecular Electrostatics: A Comprehensive Topographical Approach", *Chem. Phys. Lett.* 200, **1992**, 373.

Sigman, M. S.; Jacobsen, E. N. "Schiff Base Catalysts for the Asymmetric Strecker Reaction Identified and Optimized from Parallel Synthetic Libraries", *J. Am. Chem. Soc.* 120, **1998**, 4901.

Sigman, M. S.; Vachal, P.; Jacobsen, E. N. "A General Catalyst for the Asymmetric Strecker Reaction", *Angew. Chem. Int. Ed.* 39, **2000**, 1279.

Singh, S.; Kumar, S. S.; Jancik, V.; Roesky, H. W.; Schmidt, H. G.; Noltemeyer, M. "A Facile One-Step Synthesis of a Lipophilic Gold(I) Carbene Complex - X-Ray Crystal Structures of LAuCl and LAuC≡CH (L = 1,3-Di-Tert-Butyl Imidazol-2-Ylidene)", *Eur. J. Inorg. Chem.*, **2005**, 3057.

Singh, U. C.; Kollman, P. A. "A Combined *Ab initio* Quantum Mechanical and Molecular Mechanical Method for Carrying out Simulations on Complex Molecular Systems: Applications to the CH_3Cl + Cl- Exchange Reaction and Gas Phase Protonation of Polyethers", *J. Comput. Chem.* 7, **1986**, 718.

Slater, J. C. "Note on Hartree's Method", *Phys. Rev.* 35, **1930**, 210.

Slater, J. C. "A Simplification of the Hartree-Fock Method", *Phys. Rev.* 81, **1951**, 385.

Sohn, S. S.; Bode, J. W. "N-Heterocyclic Carbene Catalyzed C-C Bond Cleavage in Redox Esterifications of Chiral Formylcyclopropanes", *Angew. Chem. Int. Ed.* 45, **2006**, 6021.

Song, G.; Su, Y.; Periana, R. A.; Crabtree, R. H.; Han, K.; Zhang, H.; Li, X. "Anion-Exchange-Triggered 1,3-Shift of an NH Proton to Iridium in Protic N-Heterocyclic Carbenes: Hydrogen-Bonding and Ion-Pairing Effects", *Angew. Chem. Int. Ed.* 49, **2010**, 912.

Song, G.; Zhang, Y.; Li, X. "Rh and Ir Abnormal N-Heterocyclic Carbenes Derived from Imidazo[1,2-α]Pyridine", *Organometallics* 27, **2008**, 1936.

Spencer, L. P.; Fryzuk, M. D. "Synthesis and Reactivity of Zirconium and Hafnium Complexes Incorporating Chelating Diamido-N-Heterocyclic-Carbene Ligands", *J. Organomet. Chem.* 690, **2005**, 5788.

Spencer, T. A.; Neel, H. S.; Flechtner, T. W.; Zayle, R. A. "Observations on Amine Catalysis of Formation and Dehydration of Ketols", *Tetrahedron Lett.* 6, **1965**, 3889.

Stauffer, S. R.; Lee, S.; Stambuli, J. P.; Hauck, S. I.; Hartwig, J. F. "High Turnover Number and Rapid, Room-Temperature Amination of Chloroarenes Using Saturated Carbene Ligands", *Org. Lett.* 2, **2000**, 1423.

Stegelmann, C.; Andreasen, A.; Campbell, C. T. "Degree of Rate Control: How Much the Energies of Intermediates and Transition States Control Rates", *J. Am. Chem. Soc.* 131, **2009**, 8077.

Stewart, J. J. P. "Semiempirical Molecular Orbital Methods", *Rev. Comp. Chem.* 1, **1990**, 45.

Stewart, J. J. P. "Optimization of Parameters for Semiempirical Methods V: Modification of NDDO Approximations and Application to 70 Elements", *J. Mol. Model.* 13, **2007**, 1173.

Stewart, R. F. "Small Gaussian Expansions of Slater-Type Orbitals", *J. Chem. Phys.* 52, **1970**, 431.

Strohmeier, W.; Muller, F. *J. Chem. Ber.* 100, **1967**, 2812.

Suresh, C. H. "Molecular Electrostatic Potential Approach to Determining the Steric Effect of Phosphine Ligands in Organometallic Chemistry", *Inorg. Chem.* 45, **2006**, 4982.

Suresh, C. H.; Frenking, G. "Direct 1-3 Metal - Carbon Bonding and Planar Tetracoordinated Carbon in Group 6 Metallacyclobutadienes", *Organometallics* 29, **2010**, 4766.

Suresh, C. H.; Gadre, S. R. "A Novel Electrostatic Approach to Substituent Constants: Doubly Substituted Benzenes", *J. Am. Chem. Soc.* 120, **1998**, 7049.

Suresh, C. H.; Gadre, S. R. "Clar's Aromatic Sextet Theory Revisited *via* Molecular Electrostatic Potential Topography", *J. Org. Chem.* 64, **1999**, 2505.

Suresh, C. H.; Gadre, S. R. "Electrostatic Potential Minimum of the Aromatic Ring as a Measure of Substituent Constant", *J. Phys. Chem. A* 111, **2007**, 710.

Suresh, C. H.; Koga, N. "Accurate Calculation of Aromaticity of Benzene and Antiaromaticity of Cyclobutadiene: New Homodesmotic Reactions", *J. Org. Chem.* 67, **2002**, 1965.

Suresh, C. H.; Koga, N. "An Isodesmic Reaction Based Approach to Aromaticity of a Large Spectrum of Molecules", *Chem. Phys. Lett.* 419, **2006**, 550.

Suresh, C. H.; Mohan, N.; Vijayalakshmi, K. P.; George, R.; Mathew, J. M. "Typical Aromatic Noncovalent Interactions in Proteins: A Theoretical Study Using Phenylalanine", *J. Comput. Chem.* 30, **2009**, 1392.

Suresh, C. H.; Ramaiah, D.; George, M. V. "Rearrangement of 1,3-Dipolar Cycloadducts Derived from Bis(Phenylazo) Stilbene: A DFT Level Mechanistic Investigation", *J. Org. Chem.* 72, **2007**, 367.

[a]Svensson, M.; Humbel, S.; Froese, R. D. J.; Matsubara, T.; Sieber, S.; Morokuma, K. "ONIOM: A Multilayered Integrated MO + MM Method for Geometry Optimizations and Single Point Energy Predictions. A Test for Diels-Alder Reactions and $Pt(P(t-Bu)_3)_2 + H_2$ Oxidative Addition", *J. Phys. Chem.* 100, **1996**, 19357.

[b]Svensson, M.; Humbel, S.; Morokuma, K. "Energetics Using the Single Point Imomo (Integrated Molecular Orbital+Molecular Orbital) Calculations: Choices of Computational Levels and Model System", *J. Chem. Phys.* 105, **1996**, 3654.

Szabo, A.; Ostlund, N. S. "*Modern Quantum Chemistry Introduction to Advanced Electronic Structure Theory*", Dover, New York, **1996**.

Tanaka, S.; Oguma, Y.; Tanaka, Y.; Echizen, H.; Masu, H.; Yamaguchi, K.; Kishikawa, K.; Kohmoto, S.; Yamamoto, M. "Double Nitro-Mannich Reaction Utilizing in Situ Generated *N*-Trimethylsilylaldimines: Novel Four-Component One-Pot Synthesis of Nitroimines", *Tetrahedron* 64, **2008**, 1388.

Tao, J.; Perdew, J. P.; Staroverov, V. N.; Scuseria, G. E. "Climbing the Density Functional Ladder: Nonempirical Meta-Generalized Gradient Approximation Designed for Molecules and Solids", *Phys. Rev. Lett.* 91, **2003**.

Taylor, M. S.; Jacobsen, E. N. "Highly Enantioselective Catalytic Acyl-Pictet-Spengler Reactions", *J. Am. Chem. Soc.* 126, **2004**, 10558.

Teles, J. H.; Melder, J. P.; Ebel, K.; Schneider, R.; Gehrer, E.; Harder, W.; Brode, S.; Enders, D.; Breuer, K.; Raabe, G. "The Chemistry of Stable Carbenes: Part 2 -

Benzoin-Type Condensations of Formaldehyde Catalyzed by Stable Carbenes", *Helv. Chim. Acta* 79, **1996**, 61.

Tennyson, A. G.; Ono, R. J.; Hudnall, T. W.; Khramov, D. M.; Er, J. A. V.; Kamplain, J. W.; Lynch, V. M.; Sessler, J. L.; Bielawski, C. W. "Indirectly Connected Bis(N-Heterocyclic Carbenes)Bimetallic Complexes: Dependence of Metal-Metal Interaction on Linker Geometry", *Chem. Eur. J.* 16, **2010**, 304.

Tolman, C. A. "Steric Effects of Phosphorus Ligands in Organometallic Chemistry and Homogeneous Catalysis", *Chem. Rev.* 77, **1977**, 313.

Tommasi, I.; Sorrentino, F. "Utilisation of 1,3-Dialkylimidazolium-2-Carboxylates as CO_2-Carriers in the Presence of Na^+ and K^+: Application in the Synthesis of Carboxylates, Monomethylcarbonate Anions and Halogen-Free Ionic Liquids", *Tetrahedron Lett.* 46, **2005**, 2141.

Tonner, R.; Frenking, G. "Are Carbodiphosphoranes Better Ligands Than N-Heterocyclic Carbenes for Grubb's Catalysts?", *Chem. Commun.* **2008**, 1584.

Tonner, R.; Heydenrych, G.; Frenking, G. "Bonding Analysis of N-Heterocyclic Carbene Tautomers and Phosphine Ligands in Transition-Metal Complexes: A Theoretical Study", *Chem. Asian J.* 2, **2007**, 1555.

Trnka, T. M.; Grubbs, R. H. "The Development of $L_2X_2Ru=CHR$ Olefin Metathesis Catalysts: An Organometallic Success Story", *Acc. Chem. Res.* 34, **2001**, 18.

Trost, B. M. "*Comprehensive Organic Synthesis*", Vol. 2, ed. L. F. Tietze, Pergamon Press, New York, **1991**.

Uddin, J.; Frenking, G. "Energy Analysis of Metal-Ligand Bonding in Transition Metal Complexes with Terminal Group-13 Diyl Ligands $(Co)_4Fe-ER$, $Fe(EMe)_5$ and

Ni(EMe)$_4$ (E = B-Tl; R = Cp, N(SiH$_3$)$_2$, Ph, Me) Reveals Significant π Bonding in Homoleptical Molecules", *J. Am. Chem. Soc.* 123, **2001**, 1683.

Uraguchi, D.; Sorimachi, K.; Terada, M. "Organocatalytic Asymmetric Aza-Friedel-Crafts Alkylation of Furan", *J. Am. Chem. Soc.* 126, **2004**, 11804.

Uraguchi, D.; Terada, M. "Chiral Brønsted Acid-Catalyzed Direct Mannich Reactions *via* Electrophilic Activation", *J. Am. Chem. Soc.* 126, **2004**, 5356.

Urban, S.; Tursky, M.; Fröhlich, R.; Glorius, F. "Investigation of the Properties of 4,5-Dialkylated N-Heterocyclic Carbenes", *Dalton Trans.* **2009**, 6934.

Van Ausdall, B. R.; Glass, J. L.; Wiggins, K. M.; Aarif, A. M.; Louie, J. "A Systematic Investigation of Factors Influencing the Decarboxylation of Imidazolium Carboxylates", *J. Org. Chem.* 74, **2009**, 7935.

Varnado Jr, C. D.; Lynch, V. M.; Bielawski, C. W. "1,1′-Bis(*N*-Benzimidazolylidene)Ferrocene: Synthesis and Study of a Novel Ditopic Ligand and Its Transition Metal Complexes", *Dalton Trans.* **2009**, 7253.

Velde, G. T.; Bickelhaupt, F. M.; Baerends, E. J.; Guerra, C. F.; Van Gisbergen, S. J. A.; Snijders, J. G.; Ziegler, T. "Chemistry with Adf", *J. Comput. Chem.* 22, **2001**, 931.

Verma, P.; Patni, P. A.; Sunoj, R. B. "Mechanistic Insights on N-Heterocyclic Carbene-Catalyzed Annulations: The Role of Base-Assisted Proton Transfers", *J. Org. Chem.* 76, **2011**, 5606.

Vignola, N.; List, B. "Catalytic Asymmetric Intramolecular α-Alkylation of Aldehydes", *J. Am. Chem. Soc.* 126, **2004**, 450.

von Liebig, J. "About The Education Of oxamide from Cyan", *Annalen der Chemie und Pharmacie* 113, **1860**, 246.

Vorfait, T.; Leuthäußer, S.; Plenio, H. "An [(NHC)(NHC(EWG))RuCl₂(CHPh)] Complex for the Efficient Formation of Sterically Hindered Olefins by Ring-Closing Metathesis", *Angew. Chem. Int. Ed.* 48, **2009**, 5191.

Vougioukalakis, G. C.; Grubbs, R. H. "Ruthenium-Based Heterocyclic Carbene-Coordinated Olefin Metathesis Catalysts", *Chem. Rev.* 110, **2010**, 1746.

Voutchkova, A. M.; Appelhans, L. N.; Chianese, A. R.; Crabtree, R. H. "Disubstituted Imidazolium-2-Carboxylates as Efficient Precursors to N-Heterocyclic Carbene Complexes of Rh, Ru, Ir, and Pd", *J. Am. Chem. Soc.* 127, **2005**, 17624.

Voutchkova, A. M.; Feliz, M.; Clot, E.; Eisenstein, O.; Crabtree, R. H. "Imidazolium Carboxylates as Versatile and Selective N-Heterocyclic Carbene Transfer Agents: Synthesis, Mechanism, and Applications", *J. Am. Chem. Soc.* 129, **2007**, 12834.

Vreven, T.; Mennucci, B.; da Silva, C. O.; Morokuma, K.; Tomasi, J. "The ONIOM-PCM Method: Combining the Hybrid Molecular Orbital Method and the Polarizable Continuum Model for Solvation. Application to the Geometry and Properties of a Merocyanine in Solution", *J. Chem. Phys.* 115, **2001**, 62.

Vreven, T.; Morokuma, K. "On the Application of the Imomo (Integrated Molecular Orbital + Molecular Orbital) Method", *J. Comput. Chem.* 21, **2000**, 1419.

Wanzlick, H. W. "Aspects of Nucleophilic Carbene Chemistry", *Angew. Chem. Int. Ed.* 1, **1962**, 75.

Wanzlick, H. W. "Nucleophilic Carbene Chemistry", *Angew. Chem.* 74, **1962**, 129.

Wanzlick, H. W.; Schönherr, H. J. "Direct Synthesis of a Mercury Salt-Carbene Complex", *Angew. Chem. Int. Ed.* 7, **1968**, 141.

Warshel, A.; Levitt, M. "Theoretical Studies of Enzymatic Reactions: Dielectric, Electrostatic and Steric Stabilization of the Carbonium Ion in the Reaction of Lysozyme", *J. Mol. Biol.* 103, **1976**, 227.

Weber, A. L.; Pizzarello, S. "The Peptide-Catalyzed Stereospecific Synthesis of Tetroses: A Possible Model for Prebiotic Molecular Evolution", *Proc. Natl. Acad. Sci. U. S. A* 103, **2006**, 12713.

Weiner, P. K.; Kollman, P. A. "AMBER: Assisted Model Building with Energy Refinement. A General Program for Modeling Molecules and Their Interactions", *J. Comput. Chem.* 2, **1981**, 287.

Wenzel, A. G.; Jacobsen, E. N. "Asymmetric Catalytic Mannich Reactions Catalyzed by Urea Derivatives: Enantioselective Synthesis of β-Aryl-β-Amino Acids", *J. Am. Chem. Soc.* 124, **2002**, 12964.

Williams, K. A.; Bielawski, C. W. "Cerberus-Type N-Heterocyclic Carbenes: Synthesis and Study of the First Tritopic Carbenes with D_3h-Symmetry", *Chem. Commun.* 46, **2010**, 5166.

Wodrich, M. D.; Corminboeuf, C.; Schleyer, P. V. R. "Systematic Errors in Computed Alkane Energies Using B3lyp and Other Popular DFT Functionals", *Org. Lett.* 8, **2006**, 3631.

Wolf, S.; Plenio, H. "Synthesis of (NHC)Rh(Cod)Cl and (NHC)RhCl(CO)$_2$ Complexes - Translation of the Rh- into the Ir-Scale for the Electronic Properties of NHC Ligands", *J. Organomet. Chem.* 694, **2009**, 1487.

Woon, D. E.; Dunning Jr., T. H. "Gaussian Basis Sets for Use in Correlated Molecular Calculations. III. The Atoms Aluminum through Argon", *J. Chem. Phys.* 98, **1993**, 1358.

Wynberg, H.; Staring, E. G. J. "Asymmetric Synthesis of (*S*)- and (*R*)-Malic Acid from Ketene and Chloral", *J. Am. Chem. Soc.* 104, **1982**, 166.

Wynberg, H.; Staring, E. G. J. "Catalytic Asymmetric Synthesis of Chiral 4-Substituted 2-Oxetanones", *J. Org. Chem.* 50, **1985**, 1977.

Xia, Y.; Liang, Y.; Chen, Y.; Wang, M.; Jiao, L.; Huang, F.; Liu, S.; Li, Y.; Yu, Z. X. "An Unexpected Role of a Trace Amount of Water in Catalyzing Proton Transfer in Phosphine-Catalyzed (3 + 2) Cycloaddition of Allenoates and Alkenes", *J. Am. Chem. Soc.* 129, **2007**, 3470.

Yang, D. "Ketone-Catalyzed Asymmetric Epoxidation Reactions", *Acc. Chem. Res.* 37, **2004**, 497.

Yang, G.; Yang, Z.; Zhou, L.; Zhu, R.; Liu, C. "A Revisit to Proline-Catalyzed Aldol Reaction: Interactions with Acetone and Catalytic Mechanisms", *J. Mol. Catal. A: Chem.* 316, **2010**, 112.

Yang, J. W.; Chandler, C.; Stadler, M.; Kampen, D.; List, B. "Proline-Catalysed Mannich Reactions of Acetaldehyde", *Nature* 452, **2008**, 453.

Yang, J. W.; Stadler, M.; List, B. "Practical Proline-Catalyzed Asymmetric Mannich Reaction of Aldehydes with *N*-Boc-Imines", *Nature Protocols* 2, **2007**, 1937.

Zachos, J.; Pagani, M.; Sloan, L.; Thomas, E.; Billups, K. "Trends, Rhythms, and Aberrations in Global Climate 65 Ma to Present", *Science* 292, **2001**, 686.

Zhang, H.; Mitsumori, S.; Utsumi, N.; Imai, M.; Garcia-Delgado, N.; Mifsud, M.; Albertshofer, K.; Cheong, P. H. Y.; Houk, K. N.; Tanaka, F.; Barbas III, C. F. "Catalysis of 3-Pyrrolidinecarboxylic Acid and Related Pyrrolidine Derivatives in Enantioselective anti-Mannich-Type Reactions: Importance of the 3-Acid Group on Pyrrolidine for Stereocontrol", *J. Am. Chem. Soc.* 130, **2008**, 875.

Zhao, Y.; Schultz, N. E.; Truhlar, D. G. "Exchange-Correlation Functional with Broad Accuracy for Metallic and Nonmetallic Compounds, Kinetics, and Noncovalent Interactions", *J. Chem. Phys.* 123, **2005**, 1.

Zhao, Y.; Truhlar, D. G. "Hybrid Meta Density Functional Theory Methods for Thermochemistry, Thermochemical Kinetics, and Noncovalent Interactions: The MPW1B95 and MPWB1K Models and Comparative Assessments for Hydrogen Bonding and van der Waals Interactions", *J. Phys. Chem. A* 108, **2004**, 6908.

Zhao, Y.; Truhlar, D. G. "A New Local Density Functional for Main-Group Thermochemistry, Transition Metal Bonding, Thermochemical Kinetics, and Noncovalent Interactions", *J. Chem. Phys.* 125, **2006**. 194101.

[a]Zhao, Y.; Truhlar, D. G. "Density Functionals with Broad Applicability in Chemistry", *Acc. Chem. Res.* 41, **2008**, 157.

[b]Zhao, Y.; Truhlar, D. G. "The M06 Suite of Density Functionals for Main Group Thermochemistry, Thermochemical Kinetics, Noncovalent Interactions, Excited States, and Transition Elements: Two New Functionals and Systematic Testing of Four M06 Functionals and 12 Other Functionals", *Theor. Chem. Acc.* 119, **2008**, 525.

Zhong, G. "A Facile and Rapid Route to Highly Enantiopure 1,2-Diols by Novel Catalytic Asymmetric α-Aminoxylation of Aldehydes", *Angew. Chem. Int. Ed.* 42, **2003**, 4247.

Zhou, H.; Zhang, W. Z.; Liu, C. H.; Qu, J. P.; Lu, X. B. "CO_2 Adducts of N-Heterocyclic Carbenes: Thermal Stability and Catalytic Activity toward the Coupling of CO_2 with Epoxides", *J. Org. Chem.* 73, **2008**, 8039.

Zhou, H.; Zhang, W. Z.; Wang, Y. M.; Qu, J. P.; Lu, X. B. "N-Heterocyclic Carbene Functionalized Polymer for Reversible Fixation-Release of CO_2", *Macromolecules* 42, **2009**, 5419.

Zhu, H.; Clemente, F. R.; Houk, K. N.; Meyer, M. P. "Rate Limiting Step Precedes C-C Bond Formation in the Archetypical Proline-Catalyzed Intramolecular Aldol Reaction", *J. Am. Chem. Soc.* 131, **2009**, 1632.

Zhu, J.; Bienayme, H. "*Multi-Component Reactions*", eds. J. Seayad and B. List, Wiley-VCH, Weinheim, Germany, **2004**.

Ziegler, T.; Rauk, A. "On the Calculation of Bonding Energies by the Hartree Fock Slater Method - I. The Transition State Method", *Theor. Chim. Acta* 46, **1977**, 1.

Zotova, N.; Broadbelt, L. J.; Armstrong, A.; Blackmond, D. G. "Kinetic and Mechanistic Studies of Proline-Mediated Direct Intermolecular Aldol Reactions", *Bioorg. Med. Chem. Lett.* 19, **2009**, 3934.